

ISSN 1881-7815 Online ISSN 1881-7823

BST

BioScience Trends

Volume 17, Number 2
April, 2023



www.biosciencetrends.com

BST

BioScience Trends



ISSN: 1881-7815
Online ISSN: 1881-7823
CODEN: BTIRCZ
Issues/Year: 6
Language: English
Publisher: IACMHR Co., Ltd.

BioScience Trends is one of a series of peer-reviewed journals of the International Research and Cooperation Association for Bio & Socio-Sciences Advancement (IRCA-BSSA) Group. It is published bimonthly by the International Advancement Center for Medicine & Health Research Co., Ltd. (IACMHR Co., Ltd.) and supported by the IRCA-BSSA.

BioScience Trends devotes to publishing the latest and most exciting advances in scientific research. Articles cover fields of life science such as biochemistry, molecular biology, clinical research, public health, medical care system, and social science in order to encourage cooperation and exchange among scientists and clinical researchers.

BioScience Trends publishes Original Articles, Brief Reports, Reviews, Policy Forum articles, Communications, Editorials, News, and Letters on all aspects of the field of life science. All contributions should seek to promote international collaboration.

Editorial Board

Editor-in-Chief:

Norihiro KOKUDO
National Center for Global Health and Medicine, Tokyo, Japan

Co-Editors-in-Chief:

Xishan HAO
Tianjin Medical University, Tianjin, China
Takashi KARAKO
National Center for Global Health and Medicine, Tokyo, Japan
John J. ROSSI
Beckman Research Institute of City of Hope, Duarte, CA, USA

Hongen LIAO
Tsinghua University, Beijing, China
Misao MATSUSHITA
Tokai University, Hiratsuka, Japan
Fanghua QI
Shandong Provincial Hospital, Ji'nan, China
Ri SHO
Yamagata University, Yamagata, Japan
Yasuhiko SUGAWARA
Kumamoto University, Kumamoto, Japan
Ling WANG
Fudan University, Shanghai, China

Senior Editors:

Tetsuya ASAKAWA
The Third People's Hospital of Shenzhen, Shenzhen, China
Yu CHEN
The University of Tokyo, Tokyo, Japan
Xunjia CHENG
Fudan University, Shanghai, China
Yoko FUJITA-YAMAGUCHI
Beckman Research Institute of the City of Hope, Duarte, CA, USA
Jianjun GAO
Qingdao University, Qingdao, China
Na HE
Fudan University, Shanghai, China

Proofreaders:

Curtis BENTLEY
Roswell, GA, USA
Thomas R. LEBON
Los Angeles, CA, USA

Editorial and Head Office

Pearl City Koishikawa 603,
2-4-5 Kasuga, Bunkyo-ku, Tokyo 112-0003, Japan
E-mail: office@biosciencetrends.com

BioScience Trends

Editorial and Head Office

Pearl City Koishikawa 603, 2-4-5 Kasuga, Bunkyo-ku,
Tokyo 112-0003, Japan

E-mail: office@biosciencetrends.com
URL: www.biosciencetrends.com

Editorial Board Members

Girdhar G. AGARWAL (Lucknow, India)	Sheng-Tao HOU (Guanzhou, China)	Michihiro Nakamura (Yamaguchi, Japan)	Usa C. THISYAKORN (Bangkok, Thailand)
Hirotsugu AIGA (Geneva, Switzerland)	Xiaoyang HU (Southampton, UK)	Munehiro NAKATA (Hiratsuka, Japan)	Toshifumi TSUKAHARA (Nomi, Japan)
Hidechika AKASHI (Tokyo, Japan)	Yong HUANG (Ji'ning, China)	Satoko NAGATA (Tokyo, Japan)	Mudit Tyagi (Philadelphia, PA, USA)
Moazzam ALI (Geneva, Switzerland)	Hirofumi INAGAKI (Tokyo, Japan)	Miho OBA (Odawara, Japan)	Kohjiro UEKI (Tokyo, Japan)
Ping AO (Shanghai, China)	Masamine JIMBA (Tokyo, Japan)	Xianjun QU (Beijing, China)	Masahiro UMEZAKI (Tokyo, Japan)
Hisao ASAMURA (Tokyo, Japan)	Chun-Lin JIN (Shanghai, China)	Carlos SAINZ-FERNANDEZ (Santander, Spain)	Junming WANG (Jackson, MS, USA)
Michael E. BARISH (Duarte, CA, USA)	Kimataka KAGA (Tokyo, Japan)	Yoshihiro SAKAMOTO (Tokyo, Japan)	Qing Kenneth WANG (Wuhan, China)
Boon-Huat BAY (Singapore, Singapore)	Michael Kahn (Duarte, CA, USA)	Erin SATO (Shizuoka, Japan)	Xiang-Dong WANG (Boston, MA, USA)
Yasumasa BESSHO (Nara, Japan)	Kazuhiro KAKIMOTO (Osaka, Japan)	Takehito SATO (Isehara, Japan)	Hisashi WATANABE (Tokyo, Japan)
Generoso BEVILACQUA (Pisa, Italy)	Kiyoko KAMIBEPPU (Tokyo, Japan)	Akihito SHIMAZU (Tokyo, Japan)	Jufeng XIA (Tokyo, Japan)
Shiuan CHEN (Duarte, CA, USA)	Haidong KAN (Shanghai, China)	Zhifeng SHAO (Shanghai, China)	Feng XIE (Hamilton, Ontario, Canada)
Yi-Li CHEN (Yiwu, China)	Bok-Luel LEE (Busan, Korea)	Xiao-Ou SHU (Nashville, TN, USA)	Jinfu XU (Shanghai, China)
Yue CHEN (Ottawa, Ontario, Canada)	Mingjie LI (St. Louis, MO, USA)	Sarah Shuck (Duarte, CA, USA)	Lingzhong XU (Ji'nan, China)
Naoshi DOHMAE (Wako, Japan)	Shixue LI (Ji'nan, China)	Judith SINGER-SAM (Duarte, CA, USA)	Masatake YAMAUCHI (Chiba, Japan)
Zhen FAN (Houston, TX, USA)	Ren-Jang LIN (Duarte, CA, USA)	Raj K. SINGH (Dehradun, India)	Aitian YIN (Ji'nan, China)
Ding-Zhi FANG (Chengdu, China)	Chuan-Ju LIU (New York, NY, USA)	Peipei SONG (Tokyo, Japan)	George W-C. YIP (Singapore, Singapore)
Xiao-Bin FENG (Beijing, China)	Lianxin LIU (Hefei, China)	Junko SUGAMA (Kanazawa, Japan)	Xue-Jie YU (Galveston, TX, USA)
Yoshiharu FUKUDA (Ube, Japan)	Xinqi LIU (Tianjin, China)	Zhipeng SUN (Beijing, China)	Rongfa YUAN (Nanchang, China)
Rajiv GARG (Lucknow, India)	Daru LU (Shanghai, China)	Hiroshi TACHIBANA (Isehara, Japan)	Benny C-Y ZEE (Hong Kong, China)
Ravindra K. GARG (Lucknow, India)	Hongzhou LU (Guanzhou, China)	Tomoko TAKAMURA (Tokyo, Japan)	Yong ZENG (Chengdu, China)
Makoto GOTO (Tokyo, Japan)	Duan MA (Shanghai, China)	Tadatoshi TAKAYAMA (Tokyo, Japan)	Wei ZHANG (Shanghai, China)
Demin HAN (Beijing, China)	Masatoshi MAKUUCHI (Tokyo, Japan)	Shin'ichi TAKEDA (Tokyo, Japan)	Wei ZHANG (Tianjin, China)
David M. HELFMAN (Daejeon, Korea)	Francesco MAROTTA (Milano, Italy)	Sumihito TAMURA (Tokyo, Japan)	Chengchao ZHOU (Ji'nan, China)
Takahiro HIGASHI (Tokyo, Japan)	Yutaka MATSUYAMA (Tokyo, Japan)	Puay Hoon TAN (Singapore, Singapore)	Xiaomei ZHU (Seattle, WA, USA)
De-Fei HONG (Hangzhou, China)	Qingyue MENG (Beijing, China)	Koji TANAKA (Tsu, Japan)	(as of January 2023)
De-Xing HOU (Kagoshima, Japan)	Mark MEUTH (Sheffield, UK)	John TERMINI (Duarte, CA, USA)	

Review

- 85-116** **Sequelae of long COVID, known and unknown: A review of updated information.**
Tetsuya Asakawa, Qingxian Cai, Jiayin Shen, Ying Zhang, Yongshuang Li, Peifen Chen, Wen Luo, Jiangguo Zhang, Jinfeng Zhou, Hui Zeng, Ruihui Weng, Feng Hu, Huiquan Feng, Jun Chen, Jie Huang, Xiaoyin Zhang, Yu Zhao, Liekui Fang, Rongqing Yang, Jia Huang, Fuxiang Wang, Yingxia Liu, Hongzhou Lu

Original Article

- 117-125** **Improving the sensitivity of liver tumor classification in ultrasound images via a power-law shot noise model.**
Kenji Karako, Yuichiro Mihara, Kiyoshi Hasegawa, Yu Chen
- 126-135** **Interaction with ERp57 is required for progranulin protection against Type 2 Gaucher disease.**
Yuzhao Liu, Xiangli Zhao, Jinlong Jian, Sadaf Hasan, Chuanju Liu
- 136-147** **FOXA2 plays a critical role in hepatocellular carcinoma progression and lenvatinib-associated drug resistance.**
Zhengxia Wang, Junyi Shen, Chuwen Chen, Tianfu Wen, Chuan Li
- 148-159** **Optimized concurrent hearing and genetic screening in Beijing, China: A cross-sectional study.**
Cheng Wen, Xiaozhe Yang, Xiaohua Cheng, Wei Zhang, Yichen Li, Jing Wang, Chuan Wang, Yu Ruan, Liping Zhao, Hongli Lu, Yingxin Li, Yue Bai, Yiding Yu, Yue Li, Jinge Xie, Bei-er Qi, Hui En, Hui Liu, Xinxing Fu, Lihui Huang, Demin Han
- 160-167** **2-4 weeks is the optimal time to operate on colorectal liver metastasis after neoadjuvant chemotherapy.**
Yurun Huang, Hang Jiang, Linwei Xu, Xitian Wu, Jia Wu, Yuhua Zhang

Correspondence

- 168-171** **Decrease in CD226 expression on CD4⁺ T cells in patients with endometriosis.**
Cui Li, Jing Zhou, Jun Shao, Lei Yuan, Qiang Cheng, Ling Wang, Zhongliang Duan
- 172-176** **Characteristics, scope of activity, and negative emotions in elderly women with urinary incontinence: Based on a longitudinal followup in Shanghai, China.**
Yunwei Zhang, Changying Wang, Xiaoyan Yu, Lingshan Wan, Wendi Cheng, Chunyan Xie, Duo Chen, Yifan Cao, Jia Xue, Yuhong Niu, Hansheng Ding
- 177-182** **A cross-sectional study on the need for and utilization of assistive walking devices by people age 55 and older in Shanghai.**
Wendi Cheng, Yifan Cao, Hua Wang, Xin Peng, Chunyan Xie, Changying Wang, Duo Chen, Lingshan Wan, Jia Xue, Yunwei Zhang, Hongyun Xin, Wei Zhuang, Hansheng Ding

Letter to the Editor

- 183-185** **Poor emotional status increases the risk of attempted suicide for the elderly age 55 and older in Shanghai, China: A longitudinal follow-up study.**
Lingshan Wan, Tingting Zhu, Jing Zhang, Wendi Cheng, Duo Chen, Hansheng Ding

Sequelae of long COVID, known and unknown: A review of updated information

Tetsuya Asakawa^{1,8,*}, Qingxian Cai^{2,8}, Jiayin Shen^{3,8}, Ying Zhang^{4,8}, Yongshuang Li^{5,8}, Peifen Chen^{6,8}, Wen Luo⁶, Jiangguo Zhang⁷, Jinfeng Zhou⁷, Hui Zeng⁸, Ruihui Weng⁹, Feng Hu¹⁰, Huiquan Feng¹¹, Jun Chen², Jie Huang⁵, Xiaoyin Zhang⁷, Yu Zhao⁹, Liekui Fang¹¹, Rongqing Yang⁵, Jia Huang¹², Fuxiang Wang¹³, Yingxia Liu^{13,*}, Hongzhou Lu^{1,13,*}

¹Institute of Neurology, National Clinical Research Center for Infectious Diseases, the Third People's Hospital of Shenzhen, Shenzhen, China;

²Department of Hepatology, National Clinical Research Center for Infectious Diseases, the Third People's Hospital of Shenzhen, Shenzhen, China;

³Department of Science and Education, National Clinical Research Center for Infectious Diseases, the Third People's Hospital of Shenzhen, Shenzhen, China;

⁴Department of Endocrinology, National Clinical Research Center for Infectious Diseases, the Third People's Hospital of Shenzhen, Shenzhen, China;

⁵Department of Dermatology, National Clinical Research Center for Infectious Diseases, the Third People's Hospital of Shenzhen, Shenzhen, China;

⁶Department of Respiratory Medicine, National Clinical Research Center for Infectious Diseases, the Third People's Hospital of Shenzhen, Shenzhen, China;

⁷Department of Gastroenterology, National Clinical Research Center for Infectious Diseases, the Third People's Hospital of Shenzhen, Shenzhen, China;

⁸Department of Cardiology, National Clinical Research Center for Infectious Diseases, the Third People's Hospital of Shenzhen, Shenzhen, China;

⁹Department of Neurology, National Clinical Research Center for Infectious Diseases, the Third People's Hospital of Shenzhen, Shenzhen, China;

¹⁰Department of Nephrology, National Clinical Research Center for Infectious Diseases, the Third People's Hospital of Shenzhen, Shenzhen, China;

¹¹Department of Urology, National Clinical Research Center for Infectious Diseases, the Third People's Hospital of Shenzhen, Shenzhen, China;

¹²Department of Intensive Care Unit, National Clinical Research Center for Infectious Diseases, the Third People's Hospital of Shenzhen, Shenzhen, China;

¹³Department of Infectious Diseases, National Clinical Research Center for Infectious Diseases, the Third People's Hospital of Shenzhen, Shenzhen, China.

SUMMARY Over three years have passed since the COVID-19 pandemic started. The dangerousness and impact of COVID-19 should definitely not be ignored or underestimated. Other than the symptoms of acute infection, the long-term symptoms associated with SARS-CoV-2 infection, which are referred to here as "sequelae of long COVID (LC)", are also a conspicuous global public health concern. Although such sequelae were well-documented, the understanding of and insights regarding LC-related sequelae remain inadequate due to the limitations of previous studies (the follow-up, methodological flaws, heterogeneity among studies, *etc.*). Notably, robust evidence regarding diagnosis and treatment of certain LC sequelae remain insufficient and has been a stumbling block to better management of these patients. This awkward situation motivated us to conduct this review. Here, we comprehensively reviewed the updated information, particularly focusing on clinical issues. We attempt to provide the latest information regarding LC-related sequelae by systematically reviewing the involvement of main organ systems. We also propose paths for future exploration based on available knowledge and the authors' clinical experience. We believe that these take-home messages will be helpful to gain insights into LC and ultimately benefit clinical practice in treating LC-related sequelae.

Keywords COVID-19, SARS-CoV-2, sequelae, long COVID, follow-up

1. Introduction

Over three years have passed since the COVID-19 pandemic started. At present, Omicron and its subvariants are the predominant variants, but they are less likely to cause severe illness. However, the dangerousness and impact of COVID-19 should definitely not be ignored or underestimated (1). Other than the symptoms of acute infection, the long-term symptoms associated with SARS-CoV-2 infection are also a conspicuous global public health concern. The term "long COVID (LC)"

is used to describe the post-acute sequelae of SARS-CoV-2 infection. According to estimates, there are approximately 65 million people globally suffering from LC (2). Huang *et al.* conducted a one-year follow-up of 1,276 COVID-19 survivors and found that although 88% of patients recovered and returned to work at 12 months, their health status remained poorer than that of controls not infected with SARS-CoV-2 (3). In an online survey of patients with COVID-19, Davis *et al.* found that the most common symptoms during follow-up (7 months) were fatigue, post-exertional malaise, and

cognitive dysfunction. Eighty-five-point-nine percent of participants experienced relapses triggered by exercise, physical or mental activity, and stress; of those, 86.7% had fatigue at the time of survey (*vs.* 44.7% in recovered patients). Forty-five-point-two percent of participants reduced their working time, and 22.3% did not work during the survey due to illness. Cognitive impairments and memory loss were common across all age groups (4). Recently, Hedin *et al.* conducted a prospective study of adult outpatients with COVID-19. They found that of 270 outpatients, 52% developed LC and 32% had post-COVID-syndrome. Fatigue was the most common symptom during follow-up. Sports and household activities markedly affect lingering symptoms. LC and post-COVID-syndrome are also not rare in outpatients. Thirty-two percent of patients took over 12 weeks to return to their usual health (5). Lopez-Leon *et al.* performed a meta-analysis of 15 studies investigating LC sequelae in 47,910 patients with SARS-CoV-2 infection, and they identified 55 LC sequelae. Approximately 80% of patients with COVID-19 developed one or more LC sequelae. The top 5 symptoms were fatigue (58%), headaches (44%), attention disorder (27%), hair loss (25%), and dyspnea (24%) (6). Recently, Davis *et al.* reviewed that the incidence of LC is approximately 50-70% in hospitalized patients, 10-30% in non-hospitalized patients, and 10-12% in vaccinated patients (7). The clinical characteristics of LC include: *i*) Multisystemic involvement: COVID-19 was originally regarded as a respiratory disease, but evidence indicates that SARS-CoV-2 infection may cause multisystemic abnormalities. Thus far, over 200 LC-related symptoms have been documented, in which multiple organs and whole-body systems are involved, including the respiratory system, circulatory system, central nervous system (CNS), digestive system, urinary system, and the reproductive system, along with the immune system and the vascular system (7). *ii*) Complicated and multifaceted mechanisms: The mainstream view is that the tissue damage throughout the body is mainly due to COVID-19-related abnormal immune response and inflammation rather than direct viral infection of the tissues and subsequent cytopathic effects (7,8). Moreover, damage to the immune system and blood vessel system may influence the other organs and systems and then cause secondary damage throughout the body (9). The complicated interaction among organs results in multifaceted and intricate pathophysiological mechanisms of LC. A patient seems to "recover" from SARS-CoV-2 infection, but the subsequent clinical manifestations of LC might be diverse and particular. Disorders in all systems might develop, such as cardiovascular disease in the circulatory system (10), diabetes (11), and cognitive impairment and myalgic encephalomyelitis/chronic fatigue syndrome (ME/CFS) in the CNS (12,13). Noticeably, such illnesses seldom "resolve" with "recovery" from acute infection.

They might persist for several years (14), of those, the problems of ME/CFS even potentially be lifelong (15). *iii*) Nonspecific and uncertain: Many reported LC-related symptoms are also common in the general public (16). These so-called nonspecific "LC-related symptoms", such as ME/CFS and cardiovascular disorders, can also develop and deteriorate in people with or without SARS-CoV-2 infection. In some cases, identifying whether a certain symptom is indeed attributed to COVID-19 or to a certain variant in patients with recurrent infection is quite difficult. In addition, most of the available evidence is derived from studies in hospitalized patients whereas information on a large amount of non-hospitalized patients remains unknown. The nature of selection bias might increase the uncertainty of LC-related symptoms. In this regard, knowledge of and insights concerning LC, particularly for the diagnosis and treatment of LC, are quite limited so far.

Currently, many reviews have discussed LC from different angles. Davis *et al.* provided a panoramic overview regarding LC-related key findings, mechanisms, symptoms, LC in children, and the role of vaccination on the basis of the latest literature available. They pointed out that the diagnostic and therapeutic options for LC remain insufficient. This situation might be improved by conducting clinical trials addressing leading hypotheses, enhancing LC-related studies by avoiding potential biases, designing viral-onset studies, *etc.* (7). Rabaan *et al.* summarized the effects of SARS-CoV-2 infection on multiple organs and systems. They attempted to elucidate the wide range of atypical COVID-19-related symptoms to improve clinical practice (17). Oronsky *et al.* reviewed persistent LC-related symptoms (syndromes) along with their underlying mechanisms. They raised awareness and alarm regarding the persistent post-COVID syndrome from the view of dysfunction of the immune system (18). Yong *et al.* systematically reviewed six LC-related inflammatory and serum biomarkers. They found that levels of C-reactive protein, D-dimer, lactate dehydrogenase, and leukocytes were greater in patients with LC. According to sensitivity analyses, levels of lymphocytes and interleukin-6 remained significantly elevated in patients with LC (19). Nalbandian *et al.* summarized the available information on epidemiological and clinical trends and predominant clinical manifestations of a post-COVID-19 condition. They suggested that standardization of the case definition and research methods would improve LC-related studies (20). Ma *et al.* systematically reviewed long-term sequelae in individuals with an asymptomatic SARS-CoV-2 infection. They found that patients with an asymptomatic SARS-CoV-2 infection may have long-term symptoms, such as loss of taste or smell, fatigue, coughing, and that the risk of those symptoms was significantly lower than that of symptomatic individuals (21). Zanini *et al.* contended that vascular pathologies after SARS-CoV-2 infection should be

seriously considered and treated since they were observed in patients with LC and because they markedly affected endothelial dysfunction, worsened pre-existing atherosclerotic plaques, and caused thrombo-embolic arterial or venous complications (9). In addition, there are numerous reviews focusing on endocrine disorders (22), the respiratory system (23), the cardiovascular system (24), anxiety and depression (25), cognitive fatigue (26), *etc.* These informative studies enriched the understanding and knowledge of and the insights regarding LC. However, studies particularly focusing on clinical issues are limited.

Accordingly, the current work has reviewed clinical issues based on the latest available literature (Table 1, online data: <http://www.biosciencetrends.com/action/getSupplementalData.php?ID=140>) as well as the authors' clinical experience. Clinical practice regarding LC in the major organ systems will be discussed. This work will increase the knowledge of and insights into LC and ultimately benefit clinical practice.

2. The respiratory system

Initially, COVID-19 was identified as a respiratory disease, so the respiratory sequelae therefore received a great deal of attention and emphasis. The most commonly reported persistent respiratory symptoms (illnesses) include a chronic cough, shortness of breath, dyspnea, chest pain, decreased ability to exercise, acute respiratory diseases, fibrosis and lung disease, bronchiectasis, and pulmonary vascular disease (BOX 1). These conditions commonly develop three months after diagnosis and persist at least two months. Some may even persist over one year. Studies have reported that persistent abnormalities in lung function, such as a reduction in diffusion capacity, commonly develop in patients with initial severe lung involvement and pneumonia (27-29). The most common sequelae were reduced diffusion capacity, restrictive ventilatory defects (28), and persistent abnormalities on computed tomography (CT) imaging (30). Huang *et al.* reported that approximately 22% of patients with reduced diffusion (out of 1,733 patients) scored 3 on a severity scale (do not need supplemental oxygen), 29% scored 4 (requiring supplemental oxygen), and 56% scored 5-6 (requiring a high-flow nasal cannula or ventilation) (28). CT imaging is the most commonly used diagnostic tool for COVID-19. Roughly two types of abnormal CT findings might be observed in patients with COVID-19, namely pneumonia-related changes (inflammatory changes) and changes in COVID-19-related pulmonary fibrosis (CRPF, fibrotic changes). Fabbri *et al.* performed a meta-analysis to investigate persistent respiratory LC-related symptoms using CT scans and a pulmonary function test (PFT). They found that during a median 3-month follow-up, 50% of patients had inflammatory changes, whereas 29% of patients had fibrotic changes.

The duration of follow-up was significantly associated with inflammatory changes and not significantly associated with fibrotic changes. Impaired gas exchange was more prevalent than restrictive impairment (38% vs. 17%) (31). Another meta-analysis also reported LC-related sequelae using CT scans and the PFT, and it found that the most common abnormality on the PFT was reduced diffusion capacity during the 6- and 12-month follow-up. The prevalence of restrictive impairment was lower at the 12-month follow-up (vs. 6-month). The pooled prevalence of persistent ground-glass opacities (GGO) was 34%, and that of pulmonary fibrosis was 32%. The prevalence did not decrease over the follow-up (32). Besutti *et al.* investigated CT abnormalities in surviving patients with severe COVID-19. They found that 55.6% of patients were normal and 37.5% of patients had non-fibrotic changes. Only 4.4% of patients had fibrotic abnormalities. The most common fibrotic abnormalities were subpleural reticulation (15/18), traction bronchiectasis (16/18), and GGO (14/18). After a 12-month follow-up, residual changes improved over time. They concluded that pneumonia might be the most common CT finding in patients after severe COVID-19 (33). Wu *et al.* conducted a 12-month follow-up in patients with severe COVID-19 who did not require mechanical ventilation. They found that their lung function improved over the follow-up. Accordingly, the prevalence of abnormal CT imaging decreased from 78% (three months) to 24% (12 months). Only 5% of patients reported dyspnea and 20% had persistent CT changes at 12 months during the follow-up (34). The aforementioned evidence indicated that a certain proportion of COVID patients will develop persistent diminishment of lung function and/or abnormal CT findings. The most common abnormality in CT imaging is pneumonia-related changes, which improve over follow-up. Only a minority of patients will develop fibrotic changes and dyspnea, indicating a poor clinical outcome. The risk factors for developing CRPF still require further identification and verification.

Box 1: Commonly reported persistent respiratory symptoms

i) Airway disease: COVID-19 related airway disease and obstructive lung diseases have been documented, and interstitial lung disease has garnered a great deal of attention. Air trapping may persist as long as 200 days after the initial SARS-CoV-2 infection in some patients. Cho *et al.* observed 100 patients with post-acute sequelae of COVID-19 infected over 30 days using a quantitative chest CT (35). They found that 13.2% of patients in hospital and 28.7% of patients in the ICU had GGO, rates which were significantly higher than that in ambulatory patients (3.7%). The total lung affected by air trapping was 25.4%, 34.6%, and 27.3% in the ambulatory, hospitalized, and ICU patients, respectively, but 7.2% in healthy controls.

ii) Pulmonary vascular disease: COVID-19 related coagulation dysfunction is well documented. The incidence of thromboembolism is reported to range from 20-70% (36-39). Attention should be paid to chronic thromboembolism or micro-occlusions triggered by inflammatory responses in patients with LC. COVID-19 related pulmonary hypertension was seldom reported, so it might be underestimated. Tudoran et al. indicated that the prevalence of pulmonary hypertension and right ventricular dysfunction in patients with mild to moderate COVID-19 was 7.69 and 10.28%, respectively, two months after hospitalization (40).

iii) Persistent cough: Chronic cough is reported in 7-10% of patients with LC, which is independent of the pulmonary pathology (41,42). Viral invasion of the vagal sensory neurons, along with the neuroinflammatory response, might be involved in the mechanisms of persistent cough (43). Treatments for a persistent cough include corticosteroids or antimuscarinic drugs, neuromodulatory agents, and language therapy (44).

iv) Dyspnea: Dyspnea, along with fatigue, is the most common LC-related symptom. Mechanisms of LC-related dyspnea might be multifaceted, including dysfunctional breathing with or without hyperventilation deconditioning, subclinical myocardial disease, and peripheral limitations on exercise due to microcirculatory dysfunction (45-47). Cardiopulmonary exercise testing (CPET) is commonly used to evaluate unexplained dyspnea as well as to identify the cause of dyspnea and exercise intolerance in these patients (48). Treatments for LC-related dyspnea including hyperbaric oxygen therapy, nebulized administration of S-1126, antileukotrienes, sodium pyruvate nasal spray, and pulmonary rehabilitation should be selected according to the pathophysiological state of the patient.

There is no specific treatment for respiratory LC sequelae. Other than symptomatic treatments, corticosteroids, antifibrotics, and lung transplantation have been considered and verified (BOX 2). However, no treatment has been rigorously verified and can thereby be recommended. Another important issue is the role of rehabilitation. Thus far, rehabilitation seems to be an emerging effective therapy against LC-related respiratory symptoms, which needs to be further verified.

Box 2: Available evidence regarding treatments for respiratory LC sequelae

i) Corticosteroids: Oral administration of prednisolone has been a treatment for LC. Myall et al. conducted an observational study to verify the efficacy of corticosteroids in treating respiratory LC sequelae. Thirty patients received prednisolone treatment (the maximum initial dose of 0.5 mg/kg for 61 ± 19 days) and experienced significant symptomatic and radiological amelioration (49). Dhooria et al. conducted a randomized trial to verify the efficacy of prednisolone in low (10 mg) and high (40 mg) doses.

They found that both radiologic response functional capacity improved significantly and that dyspnea was significantly alleviated, but there were no significant differences between the low and high dose of prednisolone (50). These trials indicated the efficacy of oral administration of prednisolone, but evidence from a large, multi-center randomized controlled trial is needed.

ii) Antifibrotics: Thus far (Feb 2023), nintedanib (identifier: NCT04541680) and pirfenidone (identifier: NCT04607928) have been submitted for verification (51), and no more newer evidence has been reported.

iii) Lung transplantation: Lung transplantation seems to be the "last resort" to treat lung diseases. Bharat et al. verified the early outcomes after lung transplantation in patients with severe COVID-19 who had developed acute respiratory distress syndrome (ARDS). They found that all patients were weaned off extracorporeal support and survived in the short term. They concluded that lung transplantation is the only option for survival in patients with severe, unresolving COVID-19-associated ARDS (52).

3. The circulatory system

LC-related damage to the circulatory system is also highlighted because such damage commonly causes severe illnesses and can even be life-threatening. LC-related damage to the circulatory system commonly includes LC-related thrombosis (including vein thrombosis), endothelial dysfunction (along with its downstream damage), and pulmonary embolism and bleeding events *sensu stricto*; they should also include SARS-CoV-2 infection-related heart injury *sensu lato*, such as myocarditis, myocardial involvement, arrhythmia, and heart failure. Xie *et al.* conducted a prospective cohort study involving 150,000 patients with COVID-19 who had survived over 30 days from their initial SARS-CoV2 infection. They found that SARS-CoV2 infection significantly increased the risk of development of cardiovascular complications such as ischemic heart disease, arrhythmia, myocarditis, pericarditis, heart failure, and thromboembolic disease (10). SARS-CoV-2 may enter the host cells *via* ACE2. It can directly attack the myocardial cells and cause myocarditis. Moreover, it triggers abnormal inflammatory and immune responses, such as a cytokine storm, and further causes myocardial damage that may subsequently lead to arrhythmia and heart failure. Excessive release of cytokines like interleukin (IL)-6 and tumor necrosis factor (TNF)- α may contribute to endothelial dysfunction and cause various downstream injury, such as thrombosis and acute coronary syndrome. Thrombosis-associated pulmonary thromboembolism may cause lung injury, subsequently cause hypoxic pulmonary artery vasoconstriction, and finally increase pulmonary vascular resistance. In addition, SARS-CoV-2 infection may upregulate the expression of angiotensin II (Ang II) and downregulate the expression

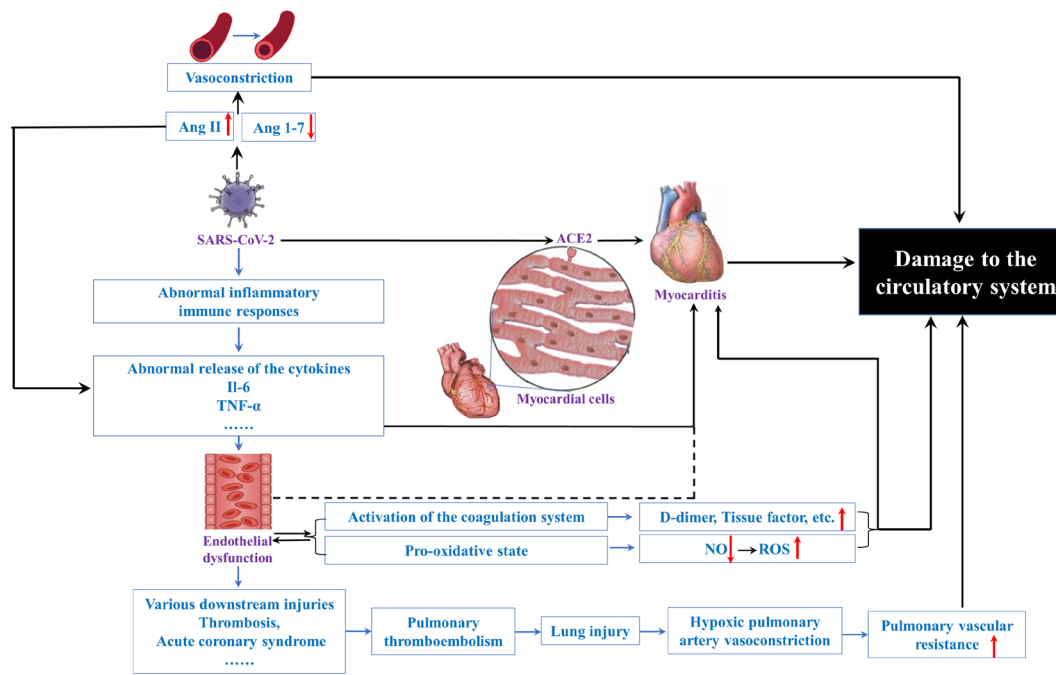


Figure 1. Mechanisms of COVID-19-related damage to the circulatory system.

of Ang 1-7 and lead to vasoconstriction. These complicated mechanisms contribute to damage to the circulatory system (Figure 1).

3.1. Thrombosis, vascular injury, and ischemic heart disease

Normal morphology and function of the vascular endothelium are protected and modulated by several anti-inflammatory cytokines and anti-clotting factors, such as nitric oxide (NO), prostaglandin I2 (PGI2), activated protein C, tissue factor pathway inhibitor, and Ang III. In a pathophysiological state, such as LC, obesity, or diabetes, induced oxidative stress may activate generation of reactive oxygen and pro-inflammatory cytokines, suppress activation of NO and PGI2, induce apoptosis of vascular endothelial cells, and finally induce dysfunction of the vascular endothelium. Moreover, release of pro-inflammatory cytokines and pro-clotting factors may cause vascular inflammation, platelet aggregation, and thrombosis. SARS-CoV-2 may directly infect the vascular endothelium and damage it. Since endothelial dysfunction plays a vital role in disturbance of the microcirculation, thrombosis and vascular injury may cause illnesses throughout the body. In addition, long-term bedrest, particularly by patients with severe COVID-19, may cause their condition to deteriorate. Piazza *et al.* reported the prevalence of thrombotic events in patients with COVID-19. They found that the frequency of major arterial or venous thromboembolism, major cardiovascular adverse events, and symptomatic venous thromboembolism was highest in patients in the ICU, followed by the hospitalized non-ICU patients,

while the frequency in outpatients was 0% for all (53). Their findings indicated that the risk of developing thrombosis is positively correlated with the severity of COVID-19. Interestingly, the prevalence of thrombotic events in hospitalized patients with COVID-19 is reported to be higher than that in patients with other critical diseases and other respiratory viral infections (such as influenza). Hence, some researchers have coined the novel term "COVID-19-associated coagulopathy," suggesting early preventive anticoagulation (54,55). Although several observational studies have suggested a benefit of anticoagulation, robust evidence including optimal selection of anticoagulants, their dose, and the duration of treatment remains insufficient (54). Viecca *et al.* evaluated the efficacy of tirofiban, an antiplatelet agent, in treating severe COVID-19 with hypercoagulability (56). They found that tirofiban might be effective in improving the ventilation/perfusion ratio in patients with severe COVID-19 and respiratory failure. They proposed administration of an antiplatelet agent to prevent cardiovascular complications in patients with COVID-19 pneumonia. Liu *et al.* verified that dipyridamole, another antiplatelet agent, helped to improve the clinical outcomes of patients with severe COVID-19 (57).

3.2. Myocarditis and myocardial involvement

Two sorts of myocarditis, namely COVID-19-related myocarditis and COVID-19 vaccine-related myocarditis, have been reported. Most of the reported cases of myocarditis involve young patients who underwent mRNA vaccination (58). A few studies have documented

COVID-19-related myocarditis. The current review will only discuss LC-related myocarditis, which is reported to be very rare but potentially life-threatening (59). The underlying mechanisms of COVID-19-related myocarditis are shown in Figure 1. Commonly, progression of COVID-19-related myocarditis is very fast. It usually causes rapidly progressive cardiogenic shock and fulminant biventricular failure (60). In this regard, COVID-19-related myocarditis is quite dangerous and commonly requires sophisticated use of multiple extracorporeal devices such as veno-arterial extracorporeal membrane oxygenation (VA-ECMO) in the ICU.

Diagnosis of COVID-19-related myocarditis is difficult in current clinical practice. The gold standard diagnostic tool is an endomyocardial biopsy (EMB), which can also provide an etiological diagnosis (for example, identification of SARS-CoV-2 in the myocardium). However, EMB is seldom performed in patients without heart failure or ventricular arrhythmias, and particularly in young and/or low-risk patients, due to its invasiveness. Most of the cases are diagnosed based on symptoms (chest pain), an electrocardiogram (ECG), laboratory results (such as a troponin increase (61)), echocardiography, and cardiac magnetic resonance imaging. Ruling out obstructive coronary artery disease is also crucial. Due to the diagnostic difficulties, there are no compelling data on epidemiological characteristics. Thus far, only case reports and serial case reports with a small sample size are available.

Thus far, there is not much evidence for treatment of myocarditis. The American Heart Association recommends that treatments for cardiogenic shock fulminant myocarditis should include administration of inotropes and/or vasopressors and mechanical ventilation and using mechanical circulatory support for long-term management (62). Some researchers suggest using high-dose steroids (63,64) and intravenous immunoglobulins (IVIG) (61) to treat COVID-19-related myocarditis. However, using high-dose steroids is a double-edged sword that might cause adverse effects. Russell *et al.* reported that high-dose steroids might lead to a reduction in viral clearance and an increased mortality for all causes (65). Nonsteroidal anti-inflammatory drugs (NSAID) are not recommended for myocarditis due to their adverse effects (62). The efficacy of antivirals against COVID-19-related myocarditis remains unclear.

3.3. Heart failure

Heart failure is a final outcome of various heart diseases, such as myocarditis, arrhythmias, acute coronary syndrome, myocardial infarction, Takotsubo syndrome, and acute pulmonary embolism (66). Hence, many pathological factors in the context of COVID-19 can finally cause heart failure, or rather, LC can induce heart failure directly or indirectly. COVID-19-related heart

failure is associated with abnormal inflammatory and immune reactions (Figure 1). Aging, arrhythmias, and chronic kidney disease were identified as independent predictors of mortality in COVID-19 patients with heart failure. Nevertheless, elucidating the actual etiology causing heart failure, which might be a comprehensive result of interactions among these complex pathological factors, is sometimes very difficult. For hospitalized patients with heart failure, SARS-CoV-2 infection plays a role as an independent predictor of mortality. Moreover, COVID-19 is associated with many adverse outcomes (increased in-hospital mortality, longer hospital stays, and higher cost of hospitalization) in patients with heart failure (67). Accordingly, management of heart failure in the context of COVID-19 is extremely important in clinical practice.

A knotty problem is how to make a differential diagnosis between COVID-19-related acute respiratory distress syndrome (ARDS) and acute heart failure (AHF) because they share the same symptoms (dyspnea and fatigue). Sometimes, a patient can suffer from both ARDS and AHF, increasing the difficulty of differentiation. Palazzuoli *et al.* devised a method of distinguishing ARDS and AHF by comparing differences in their history, clinical manifestations, supplemental examinations, and laboratory results (66) (Table 2). Treatments for COVID-19 related heart failure should be selected to alleviate both COVID-19 and heart failure. The mainstay treatments for ARDS and AHF are also listed in Table 2. In addition, treatment with tocilizumab (TCZ), an IL-6 receptor antagonist, has also been reported. A meta-analysis indicated that the mortality of COVID-19 patients treated with TCZ was 12% lower than those not treated with TCZ (68). The efficacy and safety of TCZ treatment for COVID-19 were verified in several studies (69,70).

3.4. Arrhythmia

Arrhythmia (particularly atrial arrhythmias) is known to be one of the most common cardiovascular complications of COVID-19, whether in the acute phase of infection or LC (71,72). It is also the most significant factor causing new onset or deterioration of COVID-19-related heart failure (66). Commonly reported COVID-19-related atrial arrhythmias include atrial fibrillation (AF), flutter and supraventricular tachycardias (SVT), bradyarrhythmia, ventricular arrhythmias (VA), and sudden cardiac death (SCD). AF is the most common arrhythmia in patients with COVID-19 (71,73). Studies investigating arrhythmia in LC are limited. Xie *et al.* reported a significant increase in dysrhythmias and cardiac arrest between 30 days and 12 months after initial infection (10). AF, atrial flutter, and undefined ventricular arrhythmias increased in all patients with LC (74). Mechanisms of developing an arrhythmia are shown in Figure 1, but the long-term arrhythmic sequelae of

Table 2. Differential diagnosis between COVID-19-related acute respiratory distress syndrome (ARDS) and acute heart failure (AHF) and related treatments (Palazzuoli *et al.*, 2022)

Items	COVID-19-related ARDS	AHF
Differential diagnosis		
Clinical history of related risk factors	<ul style="list-style-type: none"> • High cardiovascular risk factors • COVID-19 contact history 	<ul style="list-style-type: none"> • High cardiovascular risk factors • History of recurrent heart failure • History of myocardial infarction
Symptoms	<ul style="list-style-type: none"> • Prone position alleviates dyspnea • Fever • Persistent cough • Loss of taste and smell • Gastrointestinal symptoms • Isolated pulmonary crackles or diffuse reduction in pulmonary ventilation 	<ul style="list-style-type: none"> • Orthopneic position alleviates dyspnea • Signs of pulmonary crackles • Systemic congestion • Murmur • Third heart sound
Laboratory results	<ul style="list-style-type: none"> • Mild increase in natriuretic peptides • Increased C-reactive protein and ferritin • Relative lymphopenia • Increased D-Dimer and fibrinogen 	<ul style="list-style-type: none"> • Marked increase in natriuretic peptides and troponin
Gas exchange	<ul style="list-style-type: none"> • Hypoxemia with hypocapnia or hypercapnia associated with SPO₂ < 90% • Respiratory acidosis 	<ul style="list-style-type: none"> • Hypoxemia with or without hypercapnia, mixed acidosis or respiratory alkalosis
Chest radiography	<ul style="list-style-type: none"> • Normal cardiac shape with minimal or patchy opacities 	<ul style="list-style-type: none"> • Enlarged cardiac shape with interstitial edema • Pulmonary venous congestion
Echocardiography	<ul style="list-style-type: none"> • No cardiac dilatation • Left ventricular hypertrophy • Normal or slight increase in pulmonary pressure 	<ul style="list-style-type: none"> • Right heart failure with an increase in pulmonary pressure • Heart failure with a reduced ejection fraction due to myocarditis or worsening of chronic heart failure • High score for heart failure with a preserved ejection fraction • Pericardial effusion
Lung CT	<ul style="list-style-type: none"> • Pulmonary interstitial involvement and fibrotic changes • Dilatation of the main pulmonary artery branches 	<ul style="list-style-type: none"> • Signs of post capillary hypertension and alveolar edema • Cardiac dilatation, hypertrophy • Distention of central vein
Magnetic resonance imaging	<ul style="list-style-type: none"> • Restrictive edema associated with mild pericardial effusion 	<ul style="list-style-type: none"> • Segmental and global reduction in myocardial contractility along with signs of diffuse extracellular matrix deposition
Treatments		
	<ul style="list-style-type: none"> • Oxygen therapy to increase oxygen levels • Mechanical ventilation with a low tidal volume • Veno-venous extracorporeal membrane oxygenation • Intravenous fluids • Antiviral therapies • Appropriate antibiotic therapy • Corticosteroids: dexamethasone • Anti-fibrotic therapies: pirfenidone, alteplase 	<ul style="list-style-type: none"> • IV vasoactive therapies, a combination of hydralazine and nitrate • Mechanical circulatory support: venous arterial extracorporeal membrane oxygenation, intra-aortic balloon pump, • Angiotensin-converting enzyme inhibitors/angiotensin receptor blockers • Optimization of beta-blockers and ivabradine • Angiotensin receptor neprilysin inhibitors: sacubitril/valsartan • Hemofiltration therapy

SARS-CoV-2 infection remain unclear. Like myocarditis mentioned earlier, determining whether arrhythmia is caused by SARS-CoV-2 infection is difficult. EBM is also the gold standard to answer this question but is seldom performed. In this regard, antiviral therapies have to be fully considered.

3.5. What about the future?

Current robust evidence for treatment of LC is quite limited. Over three years have passed since the start of the COVID-19 pandemic, allowing investigation of the effects of LC on the circulatory system. Indeed, many clinical trials investigating LC and cardiovascular sequelae are ongoing, including rehabilitation programs,

symptomatic therapies, metabolic modulators, immunomodulatory therapies, antifibrotic treatments, and anticoagulation (75). The results are eagerly anticipated. With advances in computer technology, studies based on mobile apps, artificial intelligence, big data, and machine learning are booming (76). Barrios *et al.* reported a telemedicine approach to manage anticoagulation in AF (77). Indeed, use of telemedicine in LC, and particularly in management of the patients with LC-related circulatory diseases, should have many advantages. It can reduce the exposure to SARS-CoV-2 infection and offer convenience to patients, caregivers, and clinicians. Other than management of the oral administration of medicines, remote but real-time monitoring of key indices, such as cardiac rhythm

(even remote ECG), is useful. Moreover, remote diagnosis, remote rehabilitation, remote robot-assistant rehabilitation, and remote diagnosis and treatment should be paths for future exploration, although at present there are still many technological and ethical concerns that need to be addressed. But what is needed first of all is a smart top-level design and reasonable development plan based on the pathophysiological nature of circulatory diseases in the context of LC.

4. The neurological system

Neurological and cognitive problems in LC are highly concerning because they are common in patients who have recovered from the acute phase of SARS-CoV-2 infection. Importantly, they may persist longer than three months after diagnosis (4) and might be long-term (even lifelong) sequelae of COVID-19 in some cases. Most of these neurologic symptoms are refractory and often relapsing. These features may greatly impact the quality of life (QOL) and activities of daily living (ADL) of patients. Nevertheless, understanding and knowledge regarding these neurologic symptoms are quite limited. Other than their mechanisms, the epidemiological features, clinical characteristics, diagnosis, effective treatment, and prognosis for these problems remains unclear due to the limitations of methodologies, the stage of the pandemic, and technology, all of which warrant further investigation in the future.

4.1. Symptomatology issues

Involvement of neurological and cognitive systems is a marked feature of LC, and it commonly includes a wide spectrum of symptoms, including non-specific symptoms (fatigue, headaches, dizziness, and vertigo), sensory impairment (paresthesia, hypogeusia or ageusia, hyposmia or anosmia, tinnitus, and hearing loss), neuropsychological symptoms (memory loss and cognitive impairment), and neuropsychiatric symptoms (insomnia, depression, anxiety, and post-traumatic stress disorder (PTSD)). Moreover, ataxia, epilepsy, disturbance of consciousness, skeletal muscular symptoms, peripheral nervous symptoms, and other stroke-like symptoms were also reported (78). Kamal *et al.* found that LC-related symptoms would present as late as 20 days after the onset of infection. They found that fatigue was the most common symptom (72.8%), and only 10.8% of patients had no LC-related sequelae. Importantly, the severity of the sequelae was closely associated the severity of acute infection (79). Taquet *et al.* conducted a retrospective study of electronic health records to investigate neurological and psychiatric sequelae of COVID-19 (80). They found that 33.63% of patients suffered from the neurological and psychiatric sequelae during a 6-month follow-up. Patients with more severe COVID-19 are prone to have more neurological

and psychiatric problems. Patel *et al.* conducted a meta-analysis investigating the long-term neurological sequelae in patients who recovered from severe COVID-19 (81). Their meta-analysis included seven studies involving 3,304 patients. They found that 20.20% of individuals had LC symptoms over two weeks after the acute phase, including headaches (27.8%), fatigue (26.7%), myalgia (23.14%), anosmia (22.8%), dysgeusia (12.1%), sleep disturbance (63.1%), confusion (32.6%), difficulty concentrating (22%), PTSD (31%), feeling depressed (20%), and suicidality (2%) Hugon *et al.* studied a cohort of 100 patients with COVID-19 and they found that 85% of patients had impaired ADL (82). The top 9 neurologic symptoms were cognitive impairment with brain fog (81%), headaches (68%), paresthesia (60%), ageusia (59%), anosmia (55%), myalgia (55%) dizziness (47%), pain (43%), and depression and anxiety (42%). Approximately 18% of patients had abnormal MRI imaging (white matter changes). However, the relevance between MRI changes and symptoms remains unknown.

Results from different studies display marked heterogeneity. The distribution of sequelae differs considerably among these studies. Most of these studies are single-center studies with a small sample size, so they might suffer from selection bias. Moreover, the different follow-up, criteria for inclusion/exclusion, and assessment tools used might contribute to this heterogeneity. Indeed, the distribution of LC symptoms is still puzzling.

Headaches are a common symptom presenting in both acute-phase COVID-19 and LC. Headaches are reported in approximately 11-34% of hospitalized patients. The characteristics of COVID-19-related headaches are that they are migraine-like, tend to recur, and intractable. Administration of common NSAIDs and/or anti-inflammatory medications seems to have little effect (81). Importantly, most of the patients who tend to develop headaches have not had migraines or their risk factors, indicating a close causal relationship between these headaches and SARS-CoV-2 infection (81,83).

Fatigue is also a common LC sequela reported in many studies. Approximately 34.0-72.8% of patients with COVID-19 reportedly suffered from fatigue (81,84). The duration of fatigue fell from 52% (at 6 months) to 20% (at 12 months) (3). LC-related fatigue is quite analogous to ME/CFS, which is closely associated with immune-inflammatory dysfunction (85). Davis *et al.* reviewed the similarities between LC and ME/CFS from the perspectives of etiology, symptomatology, mechanisms, disease distribution, diagnosis, and treatment, and they concluded that SARS-CoV-2 infection might cause ME/CFS, where fatigue is a keystone connecting both (7). However, fatigue in LC is reportedly not associated with either the level of pro-inflammatory markers and cytokines (84) or the severity of COVID-19 (81). A plausible explanation is that LC-related-fatigue is

influenced by many pathophysiological factors and not limited to viral infection (81).

Neuropsychiatric symptoms include depression, anxiety, PTSD, and other neuropsychiatric problems (obsessive-compulsive disorder, insomnia, *etc.*) that are reported to be closely associated with COVID-19. Patients with COVID-19 may have double the risk of developing mood disorders (86). Approximately 30-40% of patients are estimated to have such neuropsychiatric problems (87), and that number is markedly higher than only 10% to 35% in other non-COVID diseases (88,89). Females and adolescents and young adults are more vulnerable to mood disorders (90). Mazza *et al.* observed LC symptoms in 402 patients and found that prevalent neuropsychiatric symptoms were PTSD (28%), depression (31%), anxiety (42%), obsessive-compulsive disorder (20%), and insomnia (40%) (91). They contend that these symptoms were associated with immune-inflammatory dysfunction. A meta-analysis reported that the prevalence of depression, anxiety, and PTSD was 20%, 35% and 53%, respectively, in 113,285 individuals (92). Another meta-analysis presented a pooled prevalence of depression (45%) and anxiety (47%) in patients with COVID-19 (93). Certainly, negative emotions (apprehensions regarding health and unemployment, dread of medical treatment, isolation, hospitalization, *etc.*) may directly cause mood problems, yet several studies have demonstrated that the abnormal immune-inflammation reaction seems to play a non-negligible role in the initiation, development, and deterioration of these neuropsychiatric symptoms (91,94). Since such neuropsychiatric symptoms are closely associated with QOL for a long time, close attention should be paid to mental health after acute COVID-19 (90), along with inflammation in these patients (91).

Cognitive impairment, colloquially called "brain fog," is a notable neuropsychological symptom of LC, and particularly the domains of attention, memory, and executive functions (95). Almeria *et al.* found that approximately 34.4 % of patients had cognitive problem. Cognitive impairments can be found in patients with acute-stage COVID-19, and patients with severe disease readily develop cognitive problems (96). These cognitive impairments can last at least four months after COVID-19 (97). Commonly, females, patients who had respiratory problems at the onset of infection, and patients admitted to the ICU are more vulnerable to developing cognitive problems. Another noteworthy problem is that persisting cognitive impairments and emotional deficits can also be found in young adults who recovered from mild COVID-19. Manukyan *et al.* observed the neuropsychological state of 40 young patients (age 19.9 ± 2.06 , ranging from 18-27) who recovered from mild COVID-19 and found that performance on inhibition tasks and scores on depression subscale in these patients were worse than those of controls, even though there were no significant differences in anxiety and fatigue

(98). Hence, the neuropsychological problems in young patients with mild disease cannot be ignored. However, due to the complex nature of brain fog, the available studies display a high level of heterogeneity. Use of subjective self-report assessments might contribute to this heterogeneity.

Other neurologic symptoms are also reported. Insomnia is the most prominent sleep disturbance. COVID-19 may worsen existing sleep disorders or "cause" a new sleep disorder (99). Sensory impairments, such as hypogeusia, ageusia, hyposmia, and anosmia, are noticeable symptoms in the acute phase. Approximately 60% of patients suffered from olfactory dysfunction during the acute phase, and it regarded as a long-term symptom in LC. But identifying such ageusia or anosmia as an LC symptom in patients whose only COVID-19 symptoms were sensory loss is sometimes difficult because the history of SARS-CoV-2 infection is uncertain (100). Encephalitis/encephalopathy have been well-documented in the context of COVID-19, but a biopsy study ruled out active encephalitis as a feature of SARS-CoV-2 infection (101).

The available literature often focuses on the association between these symptoms and SARS-CoV-2 infection and it pays little attention to the interactions among LC-related symptoms. SARS-CoV-2 might play a background role in the long-term pathophysiology of LC. Instead, interactions among LC-related symptoms might play a more important role in the progression of diseases. For example, does a COVID-related sleep disturbance worsen cognitive impairment? Does COVID-related sensory loss influence cognition? These questions are still unanswered and warrant further investigation.

4.2. Potential mechanisms underlying neurologic involvement

Thus far, mechanisms underlying how SARS-CoV-2 infection affects the nervous system, and especially the CNS, are not fully understood. There are too many internal/external factors involved. Moreover, the complicated interactions among these factors complicate and confuse the story. Several hypotheses have been put forth but require further verification.

i) SARS-CoV-2 direct invasion hypothesis: This hypothesis contends that many neurologic changes in the nervous system are the direct result of invasion by SARS-CoV-2. SARS-CoV-2 is a neurotropic virus, and ACE2 plays a role as a docking gene for cellular entry. Along with other genes such as neuropilin-1, basigin (BSG; CD147), and transmembrane protease serine 2 (TMPRSS2), SARS-CoV-2 can enter the brain (102,103). In addition, SARS-CoV-2-related cytokines, such as IL-6, IL-1 β , IL-17, and TNF- α , may contribute to disruption of the blood-brain barrier (BBB) and allow entry of the virus (104). Other than the dysregulated BBB, another plausible route for neurologic entry of SARS-

CoV-2 is the olfactory system. The virus may invade nerve terminals by endocytosis, then be transported retrogradely, and trans-synaptically spread to other brain regions (104). Clinical evidence also corroborates this route, such as marked olfactory-related symptoms (hyposmia or anosmia) and abnormal MRI findings in the olfactory cortex (105) caused by SARS-CoV-2 infection. In addition, viruses can enter the brain carried by infected immune cells (104). However, this hypothesis remains controversial since direct evidence of viral invasion is insufficient. Bernard-Valnet *et al.* reported two cases of acute meningoencephalitis concomitant with COVID-19, but they found no evidence of SARS-CoV-2 infection in the patients' cerebrospinal fluid (CSF) (106). Pilotto *et al.* investigated 25 patients who suffered from SARS-CoV-2 related encephalitis and found that CSF samples were negative for SARS-CoV-2 RNA according to RT-PCR (107). Moreover, Kantonen *et al.* performed an autopsy on four patients with COVID-19 and found that all CNS samples tested with RT-PCR were negative for SARS-CoV-2 (108), which seems to rule out the direct infection of SARS-CoV-2 in the CNS. Another autopsy study in Germany also indicated that COVID-related changes in patients seemed to be mild, whereas marked neuroinflammatory changes in the brainstem were the most common finding (109). This refutes the contention that CNS damage is directly caused by SARS-CoV-2 infection. Hence, other than the effects of direct infection, abnormal immune-inflammatory reactions seem to play a more crucial role in LC-related symptoms in the CNS (25).

ii) Abnormal immune-inflammatory reactions hypothesis: This hypothesis contends that neurologic involvement is the result of abnormal immune-inflammatory reactions. In the context of COVID-19, the BBB might be disrupted (102). The circulating levels of pro-inflammatory cytokines, such as IL-6, and TNF- α , in patients are usually elevated (110). These cytokines, along with viral proteins and molecular complexes from damaged cells (such as nuclear protein high mobility group box 1) might enter the brain *via* the compromised BBB and trigger an innate immune response in macrophages in the brain and microglia, finally inducing brain dysfunction (104). This hypothesis has been verified by many bench (94,111) and bedside studies (109,112) and is therefore accepted by most researchers. SARS-CoV-2 infection may trigger excessive production of pro-inflammatory cytokines and cause many downstream pathological changes, such as headaches (113) and vascular and organ damage (7). Elevated inflammatory indices in patients with COVID-19 corroborate this hypothesis. Hyperinflammatory and hypercoagulable states, which affect all organ systems, might be a plausible explanation for LC symptoms (100). That said, involvement of the hypothalamic-pituitary-adrenocortical (HPA) axis is also possible. In the context of COVID-19, pro-inflammatory cytokines,

such as IL-6, and TNF- α , were upregulated, and these cytokines activate the HPA axis. The HPA axis can also be activated by BBB dysfunction and neurovascular inflammation (114). Once the HPA axis is activated, release of norepinephrine and glucocorticoids increases, further inducing splenic atrophy, T cell apoptosis, and NK cell deficiency, thereby reducing systemic immunity. These immune-inflammation-related mechanisms comprehensively act on the CNS and finally cause brain dysfunction. Hence, anti-inflammatory therapy can be considered as a strategy to treat LC symptoms.

iii) Dysautonomia hypothesis: Many studies attribute the symptoms in LC to dysautonomia (100,115,116). The main idea of this hypothesis is that many COVID-19-related pathogenic factors, like oxidative stress, immune dysfunction, and an inflammatory reaction, may cause dysautonomia. Dysautonomia is what plays a vital role in causing the subsequent multi-organic symptoms. DePace and Colombo even commented that LC symptoms can be interpreted as "a pro-inflammatory state with oxidative stress and parasympathetic and sympathetic (P&S) dysfunction" (100). This hypothesis is plausible since P&S dysfunction indeed triggers almost all reported LC symptoms. Colombo *et al.* used autonomic treatments to treat patients with COVID-19 and found that SARS-CoV-2 infection significantly worsened autonomic dysfunction and related symptoms, but this dysfunction and these symptoms were ameliorated by autonomic treatments (116).

iv) Dysbiosis of gut microbiota: Now there is direct evidence that COVID-19-related gut microbiota might play a role in the development of cognitive impairment in LC (117) (see the section discussing the digestive system).

4.3. Available treatments

Thus far, there is no specific treatment for neurologic symptoms in LC, and symptomatic treatment is the mainstay. Supportive therapy is a keystone for COVID-19. Treatments for underlying diseases (such as diabetes) are also crucial. The efficacy/safety of antiviral, anti-inflammatory, steroid, and autonomic treatment is still uncertain.

4.4 Paths for future exploration

So many methodological and technological flaws have been stumbling blocks holding back the progress of the bench and bedside studies of LC. First, due to the multidimensional nature of neurological involvement, multidisciplinary collaboration should be advocated to compensate for the limitations of a narrow view of a single discipline. Second, to reduce heterogeneity among the different studies, clinical criteria for and definitions of LC should be standardized. Third, large-scale, multi-

center studies involving international collaboration should be conducted. Fourth, health education regarding LC and the value of vaccination should be conducted. Fifth, clinical studies should be more closely tied to biopsy findings. A biopsy study is limited by many factors, but its findings are greatly helpful in providing clinical insights and correcting possible biases regarding LC.

4.4.1. For diagnosis

i) More sensitive, specific, and reliable biomarkers (with limited invasiveness, if possible) that can be actually used in clinical practice should be identified. This must rely on advances in basic research. Use of bioinformatic technology might be a path to explore more novel biomarkers.

ii) Commonly used self-reporting scales for neuropsychological symptoms might potentially have observation bias and cause heterogeneity among different studies. Hence, more administered scales/batteries specially for LC-related neuropsychological symptoms should be considered and developed. Next-generation neuropsychological assessments should be devised following the principle of OMS (objective, multi-purpose, and simple) as described in previous studies by the current authors (118-120). Importantly, the latest computer technology should be capitalized upon (76).

4.4.2. For treatment

i) Verification of the efficacy/safety of several antivirals, anti-inflammatories, antioxidant drugs, steroids, and monoclonal antibodies in treating neurologic symptoms is underway. Novel treatments like electrical neuro-prostheses stimulation should be developed. The results are eagerly anticipated.

ii) Psychological interventions should be highlighted for those who suffer from LC-related depression, anxiety, PTSD, and suicidality. Family support and professional care are both important and therefore advocated for.

iii) Just as with other neurological diseases, the role of rehabilitation, and particularly the value of early rehabilitation (121), should be recognized and emphasized. Accordingly, novel technologies for and concepts of rehabilitation should also be devised and used to treat LC-induced disabilities, such as use of robot-assistant rehabilitation and remote rehabilitation.

5. The digestive system

Digestive system involvement is commonly reported with COVID-19 since ACE2 is widely expressed in the digestive system, including the gastrointestinal (GI) tract (esophagus, stomach, and small and large intestine), liver, and pancreas (122). Accordingly, symptoms in the

digestive system are commonly reported, both in acute COVID-19 and LC. Although these symptoms are non-specific for SARS-CoV-2 infection, they usually bring discomfort and markedly impact the QOL of patients, hence requiring medical intervention.

5.1. Involvement of the GI tract

Commonly reported COVID-19-related symptoms include diarrhea, constipation, acid reflux, abdominal pain, and altered smell/taste. However, LC-related GI symptoms are not well identified. Blackett *et al.* conducted a 6-month follow-up in hospitalized patients and an online survey of patients with COVID-19 and found that the symptoms at 6-month follow-up were abdominal pain (7.5%), constipation (6.8%), diarrhea (4.1%), and vomiting (4.1%) (123). In total, 16% reported at least one GI symptoms during this follow-up. A recent prospective follow-up cohort study investigated the LC sequelae of the GI tract in 320 patients with COVID-19 and found that 11.3% of patients developed GI disorders at 1-month follow-up (124). Persistent symptoms were 8.4% at 3 months and 6.6% at 6 months. Symptoms at 3 months were irritable bowel syndrome (2.5%), diarrhea (2.2%), dyspepsia (1.9%), constipation (0.9%), overlap of dyspepsia-irritable bowel syndrome (0.6%), and abdominal bloating/distention (0.3%). A meta-analysis by Choudhury *et al.* reported that abdominal pain, diarrhea, along with hypogeusia or ageusia, loss of appetite, nausea and vomiting, dyspepsia, and irritable bowel syndrome are LC-related GI symptoms (125). They found that the frequency of GI symptoms was 12% in patients with COVID-19 and 22% in patients with LC. Frequent LC-related symptoms were diarrhea (10%), abdominal pain (14%), hypogeusia or ageusia (17%), loss of appetite (20%), nausea and vomiting (6%), dyspepsia (20%), and irritable bowel syndrome (17%). Importantly, they found that GI symptoms are not associated with severity of COVID-19 and that many patients with mild disease also possibly develop GI symptoms (125). Accordingly, loss of appetite, dyspepsia, irritable bowel syndrome, hypogeusia or ageusia, and abdominal pain might be the most common GI symptoms in LC. A point to keep in mind is that all these symptoms are non-specific for disorders in GI tract, so they also can develop due to the dysfunction of other systems.

5.1.1. Mechanisms underlying dysfunction of the GI tract

Thus far, mechanisms underlying dysfunction of the GI tract due to COVID-19 are not fully understood, and particularly the long-term effects of SARS-CoV-2 infection. The GI tract is mainly controlled by the autonomic nerves system. Theoretically, all pathological factors in the body, such as direct viral infection, abnormal immune-inflammatory reactions, abnormal gut microbiota composition, and an abnormal gut-brain

axis, may directly or indirectly influence the GI tract and cause various symptoms.

i) Concept of PI-FGID: The term "post-infection functional gastrointestinal disorders (PI-FGID)" is used to describe newly developing GI symptoms following infection-related acute gastroenteritis that meet the Rome criteria (124). The characteristics of PI-FGID are that it is: *i*) infection-related; *ii*) new onset; *iii*) independent (onset, development, and progression are independent of the initial infection); and *iv*) persistent. LC sequelae can be partly included in PI-FGID since transient GI symptoms in LC can trigger long-lasting FGID despite the situation during the initial infection (126). Likewise, PI-FGID has its independent mechanisms (not directly related to COVID-19), such as genetic predisposition and a pre-existing psychological disturbance (depression and/or anxiety). PI-FGID contributes to dysregulation of gut motility, visceral hypersensitivity, dysbiosis, increased intestinal permeability, bile acid malabsorption, and modifications of enteroendocrine cell and serotonin metabolism, which can partly explain the onset of GI symptoms.

ii) Direct influence of viral infection: Several studies have confirmed the direct influence of SARS-CoV-2 infection on the GI tract. SARS-CoV-2 RNA was found in stool samples from patients with COVID-19 (127). Natarajan *et al.* found SARS-CoV-2 RNA in 12.7% of stool samples in patients at a 4-month follow-up and in 3.8% at a 7-month follow-up (128). Gaebler *et al.* found that persistence of the SARS-CoV-2 antigen in the GI tract was approximately four months (range: 2.8-5.7 months) after infection (129). Zollner *et al.* noted the persistence of the SARS-CoV-2 antigen in the gut mucosa of LC patients developing inflammatory bowel disease seven months after the initial SARS-CoV-2 infection (130). Goh *et al.* noted the persistence of the nucleocapsid protein of SARS-CoV-2 in the appendix of patients 426 days after symptom onset (131). Another ongoing work found persistent abnormalities of lymphoid and myeloid cells in the GI tract up to 10 months after initial infection (132). All of the aforementioned evidence seems to imply a prolonged persistence of SARS-CoV-2 in the GI tract. Goh *et al.* even pointed out the possibility of the GI tract serving as a reservoir for SARS-CoV-2 (131).

iii) Dysbiosis of gut microbiota is a noteworthy GI change in patients with COVID-19 (133,134). Yeoh *et al.* checked the gut microbiota in stool samples from patients who recovered 30 days after SARS-CoV-2 infection. The composition of gut microbiota changed significantly in patients with and without COVID-19. Several gut commensals with known immunomodulatory potential, such as *Faecalibacterium prausnitzii*, *Eubacterium rectale*, and *bifidobacteria*, were lower in patients and remained lower in the samples collected 30 days after recovery from disease (133). Liu *et al.* reported higher levels of *Ruminococcus gnavus* and *Bacteroides vulgatus*,

along with lower levels of *Faecalibacterium prausnitzii*, in patients with LC (vs. non-COVID-19 controls). This gut dysbiosis may persist at least 14 months. Low levels of butyrate-producing bacteria were closely associated with LC at a 6-month follow-up (134). These data prove the great impact of SARS-CoV-2 infection on the microecosystem. Dysbiosis of gut microbiota may affect not only the GI system but also the whole body. De Almeida *et al.* performed fecal bacteria transplantation (FMT) from patients with LC to healthy germ-free mice and they noted cognitive impairment and impaired lung defenses in these mice that were partly treated with the commensal probiotic bacterium *Bifidobacterium longum* (117). This study provides direct evidence that *i*) SARS-CoV-2 virus can remain in the GI tract for a long time even though the patient has recovered from acute infection and that *ii*) (3) dysbiosis of gut microbiota induced by COVID-19 plays a role in the development of COVID-19-related cognitive impairment.

Other than the aforementioned mechanisms, existence of inflammatory bowel disease indicated that abnormal immune-inflammatory reactions may play a role in the GI sequelae of LC (130). Mechanisms causing dysfunction in the GI tract might be complicated and multifaceted. Several bench studies have reported that crosstalk between neurons and intestinal epithelial cells might play a role in defense from infection, indicating the involvement of neuromodulation in GI immune-inflammatory regulation (135,136). The involvement of neuromodulation in LC sequelae requires further investigation.

5.1.2. Management of GI symptoms in LC and the future

Thus far, insights regarding selection of optimal treatments for GI sequelae in LC remain limited. Non-specific treatments such as supportive therapy and symptomatic therapy are the mainstay. Although there have been advances in the treatment of diseases like postinfection irritable bowel syndrome (137,138), whether those treatments can be used to treat SARS-CoV-2 infection remains unknown.

On the basis of known information, several paths may be considered for future research: *i*) Verification of exiting treatments for postinfection irritable bowel syndrome in patients with LC; *ii*) Previous studies indicated the possible long-term reserve of SARS-CoV-2 in the GI tract, so is administration of an antiviral to LC patients essential and effective? *iii*) Due to the involvement of dysautonomia, are neuroregulatory therapeutics, such as tricyclic antidepressants, or electrical neuro-prostheses stimulation of either the parasympathetic (vagus) or sympathetic nervous system, effective for LC patients? *iv*) Due to the gut microbial-related mechanisms, can FMT be effective in treating GI sequelae in LC? These issues should be addressed to explore optional treatments for the GI symptoms in LC

5.2. Involvement of the hepatobiliary system

Hepatic manifestations have been reported since early observational studies concerning COVID-19 (139-143), ranging from asymptomatic elevation of liver enzymes to decompensated hepatic function. A study has reported that approximately 14-53% of patients with COVID-19 developed abnormal liver function (144), whereas severe illness was associated with a higher incidence of liver dysfunction (145). In general, hepatic involvement in COVID-19 might be attributed to the direct cytopathic effects of SARS-CoV-2, drug-induced liver injury, hypoxia reperfusion injury, secondary infection, an auto-immune disorder, and a cytokine storm. COVID-19-related liver dysfunction was initially regarded as transient and was thought to recover along with the resolution of COVID-19. Recently, however, Liu *et al.* found that abnormal liver function was still observed in 11.2%, 9.5%, and 7.6% of LC patients at 3, 6, and 12 months after discharge, respectively (146). Liao *et al.* reported that abnormalities in a liver function test were observed in 25.1% of patients with COVID-19 at one month, 13.2% at three months, 16.7% at six months, and 13.2% at 12 months after discharge (147). These findings suggest that liver dysfunction might be a persistent LC sequela that is independent of recovery from acute COVID-19. Moreover, a novel entity known as post-COVID-19 cholangiopathy (PCC) has recently been reported occasionally (148-152). This syndrome usually manifests as cholestasis and jaundice during convalescence from COVID-19 and accompanied by marked increases in serum alkaline phosphatase and direct bilirubin, along with injury of the bile ducts on imaging. It is also referred to as "post COVID-19 sclerosing cholangitis." Hence, involvement of the hepatobiliary system is not rare and attention should be paid to it in clinical practice.

5.2.1. Underlying mechanisms of hepatobiliary dysfunction

Mechanisms underlying hepatobiliary dysfunction persisting after recovery from acute COVID-19 remain unclear. One plausible hypothesis is the persistent imbalance in immunity in LC (153). As described in the GI section, the GI tract might play a role as a reservoir for SARS-CoV-2 (131). This means that the virus will not disappear with recovery from acute infection. It might induce long-term abnormalities in the immune-inflammatory reactions and affect the whole body, certainly including the hepatobiliary system. Several current studies have reported a new-onset metabolic disorder during COVID-19 (154-159) that may increase the risk of developing metabolism-associated fatty liver disease (MAFLD). Milic *et al.* found that the prevalence of MAFLD increased from 37.3% on admission to 55.3% at follow-up (median 144.0 days (130.0-167.5))

in 235 patients with COVID-19 (160). A prospective cohort study by Liao *et al.* found that the prevalence of ultrasound-determined fatty liver disease increased from 18.5% at discharge to 71.4% after a 12-month follow-up (147). Accordingly, new-onset fatty liver disease also markedly contributes to the development of LC-related hepatobiliary dysfunction. Finally, cholangiocytes are known to exhibit a higher level of ACE2 expression than hepatocytes. This might trigger cytopathic and immunological effects during SARS-CoV-2 infection and ultimately induce cholangiopathy (148).

5.2.2. Treatment for hepatobiliary dysfunction

Most LC-related liver dysfunction is mild and requires no intervention. However, when patients present symptoms of liver injury, liver protective medication is recommended. Available evidence for PCC is rare so far. Ursodeoxycholic acid and obeticholic acid, which are mainly used to treat cholestatic diseases (161), are the medications most frequently used to treat PCC as an empiric therapy (149). When PCC develops into severe liver decompensation, liver transplantation is required. Faruqi *et al.* reported that 12 patients were definitively diagnosed with PCC; of those, five patients finally underwent liver transplantation due to persistent jaundice, liver failure and/or recurrent bacterial cholangitis (162). Durazo *et al.* reported a 47-year-old man who recovered from COVID-19-related ARDS and who subsequently developed end-stage liver disease from PCC (163). This patient underwent liver transplantation and survived at the 7-month follow-up.

5.2.3. Paths for future exploration

Liver injury after COVID-19 is not rare. However, most of the patients are asymptomatic. Hence, a regular liver function test and abdomen imaging screening are highly recommended for COVID-19 patients during convalescence. The prevalence of PCC is low but it is life-threatening, so careful attention should be paid to it in routine clinical practice. During the COVID-19 pandemic, PCC should be listed as a potential diagnosis for all patients suffering from cholestatic liver disease of an unknown cause.

6. The urinary system

Renal complications and lower urinary tract symptoms (LUTS) are commonly reported in the context of LC. Acute kidney injury (AKI) is the most significant kidney disease in LC. Other kidney diseases, such as chronic kidney disease (CKD), glomerular diseases, and end-stage kidney disease, can also develop or worsen as a result of SARS-CoV-2 infection. Patients with COVID-19 are known to have a high risk of adverse kidney outcomes (164). LUTS is not rare in patients

with COVID-19. In early studies, some patients with COVID-19 presented with LUTS, such as frequent urination, that were believed to be associated with viral cystitis after SARS-CoV-2 infection (165). Crete *et al.* systematically reviewed the LUTS in COVID-19 and found that approximately 3-5% of patients with COVID-19 developed LUTS (166). A recent study investigated the relationship between LUTS and COVID-19 and found that augmented frequent urination was the most common urological symptom (167). Of those patients with COVID-19, 3.4% had frequent urination, 1.0% had dysuria, and 1.0% had acute urinary retention. Dysfunction of the detrusor muscle in the bladder might be a cause of LUTS in the context of COVID-19 (168).

Kidney sequelae play a key role in LC-related urinary sequelae and therefore cannot be ignored. This section will focus on kidney involvement.

6.1. AKI, the most common form of LC-related renal dysfunction

AKI is common in hospitalized patients with COVID-19. As per the definition in Kidney Disease: Improving Global Outcomes (KDIGO), AKI is defined as any of the following issues: "increase in serum creatinine by ≥ 0.3 mg/dL (≥ 26.5 μ mol/L) within 48 hours; or increase in serum creatinine to ≥ 1.5 times baseline, which is known or presumed to have occurred within the prior seven days; or urine volume < 0.5 mL/kg/hour for 6 hours". (169). A recent meta-analysis found that the pooled prevalence of AKI was 28% among hospitalized patients; of those, 9% required dialysis (AKI in Stage 3D) (170). Stage 3D AKI is even more common in patients requiring admission to the ICU. Hsu *et al.* reported that 2,361 of 4,221 (56%) patients with COVID-19 in the ICU developed AKI; of those, 876 (21%) patients underwent kidney replacement therapy (KRT) (171). Hirsch *et al.* reviewed medical records of 5,449 hospitalized patients with COVID-19 and found that 36.6% of patients developed AKI; 46.5% had stage 1, 22.4% had stage 2, and 31.1% had stage 3; of those, 14.3% required KRT (172). In total, 89.7% of patients requiring ventilation developed AKI (*vs.* 21.7% of those who did not require ventilation), and 96.8% of patients requiring KRT also required mechanical ventilation. Approximately 52.2% of patients developed AKI within 24 hours of intubation. Finally, 26% of patients were discharged, 39% were hospitalized, and 35% unfortunately died. Later, Hirsch *et al.* observed the impact of AKI on clinical outcomes in hospitalized patients with COVID-19 and found that risk of in-hospital death was higher in patients with AKI 1-3 and AKI 3D (173). A previously cited study also indicated that patients with COVID-19 who developed AKI had a significantly higher mortality rate than those who did not develop AKI (38% *vs.* 13%) (171). The estimated glomerular filtration rate (eGFR) is significantly reduced

by COVID-19-related AKI (77,164,174-176). Bowe *et al.* reported that approximately 5% of non-hospitalized COVID-19 survivors suffered a 30% reduction in eGFR (164). A study in China conducted a retrospective and prospective follow-up to investigate the eGFR and reduced renal function in patients with COVID-19 and found that 8.3% of COVID-19 patients with AKI in acute phase suffered from decreased eGFR, which was significantly higher than the ratio in patients without AKI (174). These patients had worse renal function at follow-up. The frequency of a decreased eGFR in COVID-19 patients with AKI was 6.02% in patients with stage 1 AKI, 15.99% in patients with stage 2, and 17.79% in patients with stage 3, indicating that COVID-19 patients with AKI in the acute phase are prone to have worse renal function during follow-up. Several studies compared AKI in patients with and without COVID-19. Xu *et al.* found that AKI more frequently developed in patients with COVID-19 than those without COVID-19 (29% *vs.* 18%) (175). Patients with COVID-19 who developed AKI had a lower eGFR than that of patients without COVID-19. The risk of in-hospital death was greatest for patients with COVID-19 and AKI, followed by those with COVID-19 and without AKI, and then those without COVID-19 and with AKI. Nugent *et al.* also found that COVID-19-related AKI may involve a greater reduction in the eGFR than non-COVID-19-related AKI (176). Huang *et al.* reported that 35% of patients with COVID-19 developed AKI, a figure that was significantly higher in patients without COVID-19 (13%) (28). The findings of these studies indicate that AKI is common in hospitalized patients with COVID-19 and that it is closely associated with prognosis.

That said, studies have indicated that preexisting CKD is a key risk factor for AKI. A prospective cohort study including 701 patients with COVID-19 found that the incidence of AKI was significantly higher in those with increased baseline creatinine (*vs.* normal baseline creatinine) (11.9% *vs.* 4.0%) (177). Available evidence indicates that CKD is an independent predictor of severe AKI (178,179).

However, renal sequelae in LC are not fully understood and still require further investigation. Nowadays, CKD, the severity of initial respiratory symptoms, and not being vaccinated (180) are known to be possible risk factors for developing AKI in LC. Due to the non-specific nature of the symptoms (dyspnea, fatigue, weakness, *etc.*), investigation of long-term renal sequelae is challenging.

6.2. Potential pathogenic mechanisms underlying COVID-19-related AKI and renal dysfunction

Mechanisms of COVID-19 related AKI and renal dysfunction are multifactorial and not fully elucidated. Similarly, they are comprehensive results of the direct effects of SARS-CoV-2 infection, abnormal immune-

inflammatory reactions, the influence of other organs, and treatment-related injuries. A large spectrum of COVID-19-related pathological processes, including tubular injury, endothelial damage, release of inflammatory mediators, activation of complements, micro- and/or macrovascular injury, rhabdomyolysis, hypovolemia, hypotension or septic shock, pro-coagulant status, and activation of the renin-angiotensin-aldosterone system, may contribute to acute/long-term renal dysfunction (181-183).

Acute tubular injury is the most significant mechanism involved in COVID-19-related renal dysfunction. Many biopsy studies have reported marked tubular necrosis in patients with COVID-19 (184,185). Acute tubular injury is most likely directly caused by a local and/or systemic response to SARS-CoV-2 infection, which may lead to hypotension, activation of the renin-angiotensin system, endothelial injury, activation of coagulation pathways, and mitochondrial injury (184,186,187). It is also associated with several indirect factors such as hemodynamic abnormalities, ARDS, hyperuremia, nephrotoxin exposure, hypoxia, a cytokine storm, rhabdomyolysis, and secondary infections (176). The presence of SARS-CoV-2 in the kidneys of patients with COVID-19 further verified the possibility of direct viral toxicity (188).

Microcirculatory disturbances are also observed in many organs of patients with COVID-19 (189). Su *et al.* reported microvascular obstruction and segmental fibrin microthrombi in the glomeruli of patients with COVID-19 (190). The action of thrombocytes plays a key role in microvascular injury and disseminated intravascular coagulation in COVID-19 because SARS-CoV-2 might bind the ACE2 in the thrombocytes and activate them (191). In addition, activation of inflammatory pathways and complements *via* molecules (release of a pathogen-associated molecular pattern and damage-associated molecular pattern) may lead to the release of pro-coagulant substances and tissue factors involved in the activation of the extrinsic pathway of coagulation in COVID-19 (192). Emerging evidence suggests that excessive formation of neutrophil extracellular traps plays a key role in the pathophysiology of endothelial injury and immune-thrombosis in severe cases of COVID-19 (193,194).

Collapsing glomerulopathy is the most commonly reported glomerular disease in COVID-19 patients and is associated with polymorphisms of the APOL1 gene particularly in patients of African ancestry (195). A previous study indicated that viral infection may cause upregulation of the APOL1 gene, subsequent activation of interferon and toll-like receptors, and induce dysregulation of podocytes and glomeruli (196). However, evidence of SARS-CoV-2 infection is not available so far. Commonly signs of COVID-19-related collapsing glomerulopathy are AKI, heavy proteinuria, and hypoalbuminemia (197-199). Moreover, biopsy

findings of no collapsing features in some patients with focal segmental glomerulosclerosis suggest the involvement of podocytopathy in COVID-19-related glomerulopathy, a topic that requires further investigation.

In addition to the aforementioned pathogenic mechanisms, other hypotheses such as involvement of COVID-19-related tubulointerstitial fibrosis (176) warrant further investigation.

6.3. Insights into clinical practice

6.3.1. Biomarkers to predict prognosis

The aforementioned decrease in eGFR is regarded as a predictor of a worse prognosis for LC-related AKI. Chaudhri *et al.* reported that proteinuria and hematuria at admission and during hospitalization are associated with a worse prognosis in hospitalized patients with COVID-19 (200). In addition, many biomarkers, and particularly inflammation-related biomarkers, have been found to be closely associated with the prognosis for COVID-19 (201). In a meta-analysis evaluating the relationship between available biomarkers and the prognosis for hospitalized patients with COVID-19, the severity of COVID-19 was found to be associated with an increase in CRP, PCT, LDH, and D-dimer (202). More specific biomarkers of COVID-related AKI were evaluated, including urinary nephrin (203), IL-18 (204,205), neutrophil gelatinase-associated lipocalin (NGAL) (203,204,206), monocyte chemoattractant protein (MCP-1) (203,205), kidney injury molecule 1 (KIM-1) (203,205), epidermal growth factor (EGF) (205), plasma NGAL (204), NF α receptors in their soluble form (sTNFR 1 and 2) (207), YKL-40, KIM-1, IL-2, IL-10, IL-18, sFTL1, TNF- α , and Ang2 (208). The plasma sTNFR1 level was identified as a predictive factor of COVID-19 prognosis (207,208); high urinary levels of NGAL (203,204,206), KIM-1 (205), and MCP-1 (205) and a low urinary level of EGF (205) were associated with a worse prognosis for COVID-19-related AKI (203). However, these biomarkers require further investigation due to the limited available evidence.

6.3.2. Treatment for COVID-19-related renal dysfunction

A comprehensive strategy to treat COVID-19-related renal dysfunction should be promptly selected to avoid deterioration of the situation. Treatment for COVID-19-related AKI should include management of AKI along with treatment of COVID-19. The KDIGO guideline for AKI includes fluids and vasopressors, nutrition and glycemic control, diuretics, vasodilator therapy (such as dopamine, fenoldopam, and natriuretic peptides), and avoiding nephrotoxins (169). Available evidence in the context of COVID-19, however, is limited, so lung-kidney interactions should be seriously considered

(209). Several issues should be taken into account depending on the pathophysiological state of a given patient: *i*) Selection of appropriate ventilation (lung protective ventilation, or prone ventilation, or lung protective ventilation with a neuromuscular blockade, or spontaneous breathing during airway pressure release ventilation); *ii*) Fluid management (conservative fluid management, albumin, and diuretics); *iii*) Medications (antivirals, anti-inflammatory treatments such as glucocorticoids±mineralocorticoid, immunosuppressors such as cyclosporine, and antibiotics). Once all conservative treatments are unsuccessful, KRT and renal transplant should be considered for patients with volume overload and/or refractory hypoxemia.

6.4. Paths for future exploration

Thus far, insights into and understanding of COVID-19-related renal dysfunction are insufficient. Evidence regarding diagnosis and treatment remains limited. To better manage COVID-19-related renal dysfunction, several issues should be addressed:

i) Well-designed large-scale, multicenter RCTs on diagnostic and therapeutic strategies need to be conducted to obtain compelling evidence. Accordingly, a mechanism of transnational cooperation, an international surveillance system, and a databank of COVID-19-related renal dysfunction need to be established to promote international collaborative research and sharing of information.

ii) Renal dysfunction in LC lacks specific symptoms, so a renal function test should be performed routinely during follow-up for patients who recovered from acute COVID-19, and particularly for asymptomatic patients.

iii) A long-term follow-up prospective study should be conducted.

iv) Treatments for special populations, such as pregnant women, patients with diabetes, the elderly, children, and those who are undergoing surgery, should be considered.

7. The endocrine system

The endocrine system including the hypothalamus, pituitary, thyroid, pancreas, adrenal and reproductive glands plays a vital role in regulation of the physiological functions of the whole body. The nature of a wide distribution of ACE2 in endocrinal organs/glands indicates that such structures seem to be targeted by SARS-CoV-2 infection (210). Several known clinical characteristics of COVID-9, such as the relationship between susceptibility (and severity) of COVID-19 and diabetes/obesity, as well as the fact that males are likelier to develop a severe/life-threatening illness, confirm the involvement of the endocrine system. Accordingly, exploring the impacts of SARS-CoV-2 infection on the endocrine system, and particularly

the functioning of the endocrine glands, is extremely important in clinical practice. Unfortunately, due to the *status quo* of medical care during the pandemic, many indispensable tests of the functioning of the endocrine glands were not available, and this has been a stumbling block to better understanding the actual physiological state of the endocrine system. The mechanisms of endocrinal involvement, along with the long-term effects of COVID-19, have not been fully investigated and understood. Although direct viral invasion and viral toxicity to each organ might play a role, complicated systemic COVID-19-related mechanisms, such as abnormal immune-inflammatory reactions, dysautonomia, an abnormal hypothalamic-pituitary-glands axis, and particularly complex interactions among organs (glands) and among pathophysiological factors, might play a more crucial role in endocrinal involvement in the context of SARS-CoV-2 infection. The relationship between endocrine disorders and SARS-CoV-2 infection is reported to be bidirectional: On the one hand, preexisting endocrine disorders such as diabetes and obesity are known to negatively impact the severity and mortality of COVID-19. On the other hand, SARS-CoV-2 infection might trigger new endocrine disorders, such as diabetes, hypopituitarism, and primary adrenal insufficiency (22). Importantly, some endocrinal symptoms triggered by acute infection do not resolve with recovery from acute infection and might be persistent or even lifelong (22). This issue warrants particular concern and further investigation.

7.1. Pituitary involvement

Due to the uncommon nature of pituitary disorders, recognition of and knowledge regarding pituitary involvement is still limited and uncertain. COVID-19 related hypopituitarism might be a result of pituitary apoplexy and/or hypophysitis (22). A number of risk factors, such as hypertension, hyperglycemia, obesity, vertebral fractures, and preexisting pituitary disorders, are reported to be associated with COVID-19-related hypopituitarism (211,212). However, ACE2 expression in pituitary is reported to be low in a healthy pituitary gland (213). Hence, some authors have contended that the involvement of the pituitary might be attributed to an emerging endocrine phenotype that is closely associated with the severity of and prognosis for COVID-19 (211,214). Thus far, available evidence remains limited. Carosi *et al.* found that pituitary hormonal deficiencies were present in 85.8% of patients with adrenal insufficiency and that hypopituitarism did not seem to significantly affect COVID-19 outcomes (215). Urhan *et al.* found that cortisol and growth hormone (GH) measured in a pituitary function test were lower in patients who recovered from acute COVID-19. They concluded that pituitary function, and particularly the HPA and GH axes, might be influenced

by SARS-CoV-2 infection (216). Yoshimura *et al.* reported a 65-year male patient with COVID-19 but with no history of endocrinopathy who suffered from multiple endocrine deficiencies affecting the HPA axis, GH-IGF-I axis, and testes (217). Acute respiratory symptoms improved, but the patient suddenly developed hypotension and a decrease in circulating ACTH and cortisol levels. After administration of hydrocortisone, hypotension was alleviated but the pituitary hormonal deficiencies persisted. An insulin tolerance test three months later indicated combined hypopituitarism. The GH response recovered completely, whereas the ACTH response recovered partly at 12 months after discharge. At 15 months after discharge, the basal ACTH and cortisol levels returned to normal, and hydrocortisone replacement was discontinued without a deterioration in symptoms. However, hypogonadism persisted. The GH and ACTH deficiency lasted for more than a year and finally disappeared, but hypogonadism did not disappear during the 15-month follow-up. This case indicates the existence of COVID-19-related hypopituitarism. All of the above findings suggest that hypopituitarism might be triggered by the initial SARS-CoV-2 infection and persist for a long time after recovery from acute infection. Some of the hormonal deficiencies may disappear during a long follow-up whereas some may not, and this topic requires further investigation. Hyponatremia is the most common electrolyte abnormality in patients with COVID-19. It occurs in approximately 20-60% of hospitalized patients (218). However, the *status quo* of hyponatremia in LC remains unclear. Oguz and Yildiz commented that hypopituitarism seems to not be associated with development of severe illness, whereas hyponatremia and hypocalcemia seem to be associated with the severity of COVID-19 (22).

7.2. Adrenal involvement

The abundant expression of ACE2 in the adrenal glands indicates that the adrenal glands are targets of SARS-CoV-2 infection. Adrenal dysfunction may be a comprehensive effect of direct viral toxicity, an abnormal HPA axis, microthrombi in small adrenal vessels (219), and adrenalitis (219,220). The involvement of the adrenal glands has been well-documented in acute COVID-19 (215,221,222), but a study has reported that adrenal involvement, and particularly adrenal insufficiency (AI), seldom affects the clinical outcomes of COVID-19 (22). Several previous studies have indicated that most adrenal dysfunction commonly occurs in the acute stage of SARS-CoV-2 infection, it lasts several months, and then it finally disappears after a long follow-up (217,223). Thus far, limited available data seem to imply that SARS-CoV-2 infection does not have long-term effects on the adrenal glands (22), though this topic requires further investigation.

7.3. Thyroid involvement

Thyroid involvement is quite analogous to adrenal involvement. The abundant expression of ACE2 in the thyroid gland indicates that both the thyroid gland and the hypothalamic-pituitary-thyroid (HPT) axis are targets of SARS-CoV-2 infection (224). The underlying mechanisms are direct viral effects, an abnormal HPT axis, and abnormal immune-inflammatory reactions (17). Thyroid impairment, such as abnormal thyroid function test results (225), non-thyroidal illness syndrome (NTIS) (226), and subacute thyroiditis (227), might develop both in the acute phase and recovery phase (17). NTIS is common in hospitalized patients with COVID-19, but it tends to resolve upon recovery (22). Lisco *et al.* indicated that COVID-19 might be associated with short-term and reversible thyroid impairment (228). Available evidence does not indicate the long-term effects of COVID-19 on the thyroid (22).

7.4. Obesity and COVID-19

The prominent role of obesity in COVID-19 has been well-documented. The close association between obesity and the worse clinical outcomes of COVID-19 is widely recognized. Obese people are susceptible to SARS-CoV-2 infection. Abdominal obesity is regarded as a risk factor for COVID-19, and a high body mass index (BMI) and increased visceral adipose tissue have been cited as predictors of COVID-19 severity (229). Another study based on the American Heart Association COVID-19 Cardiovascular Disease Registry indicated that obesity is an independent risk factor for the severity and mortality of COVID-19 (230).

The effects of obesity on SARS-CoV-2 infection are still not fully understood. Several hypotheses were put forth based on the available findings. As direct effects, *i*) Obesity may cause respiratory difficulties (such as atelectasis or a ventilation-perfusion mismatch) and subsequently cause hypoxemia (231); *ii*) Obesity is prone to cause a microcirculatory disturbance, such as increased blood viscosity, elevated prothrombotic markers, and suppressed fibrinolytic activity (232), and *iii*) Obese patients have more adipocytes and enlarged adipose tissue that abundantly express ACE2 and that might serve as a SARS-CoV-2 reservoir (232,233). As indirect effects, *i*) Obesity may induce immune dysfunction. Cytokines and adipokine secreted by adipose tissues induce a pro-inflammatory state in obese people (232) that might be associated with systemic abnormal immune-inflammatory reactions in the context of COVID-19, *ii*) Obesity is closely associated with a battery of metabolic-related comorbidities, such as hypertension, insulin resistance, and type 2 diabetes (T2B, see the next section), and secondarily affect the clinical outcomes of COVID-19, and *iii*) Obesity can induce mood disorders (depression, anxiety, and

stress) (234), which are also associated with the clinical outcomes of COVID-19. Accordingly, obesity results in a worse clinical outcome for COVID-19, in males and females of all ages.

Available findings and knowledge regarding LC sequelae are limited. Evidence in children and adolescents has indicated that obesity is associated with the severity of LC sequelae (235). LC-related symptoms were associated with a change in body weight that was independent of the patient's initial COVID-19 status (236). Hedin *et al.* found that obese patients infected with SARS-CoV-2 took twice as much time (*vs.* non-obesity patients) to return to usual health (5). A recent study analyzed the risk of post-acute sequelae of COVID-19 associated with the continuous spectrum of BMI in 11,296 patients with COVID-19 and found that a BMI of 22.1 in men and 21.6 in women may result in the best recovery (237). A higher BMI was associated with fatigue, neurocognitive impairment, and chest symptoms. Both high and low BMIs are associated with impaired recovery after COVID-19. Those findings seem to indicate that obesity and emaciation are not beneficial for recovery from COVID-19. The underlying mechanisms and the roles of exercise in recovery from LC sequelae need to be investigated further.

7.5. Diabetes and COVID-19

Diabetes, and particularly T2D, is the most significant

endocrine/metabolic disease. It is also the most significant COVID-19-related disease, playing a comprehensive role (risk factor for/predictor of infection, severe illness, and death; a comorbidity; a sign of the effects of many diseases, *etc.*) in the pathophysiological mechanisms of COVID-19. The complicated association between diabetes and COVID-19 has been well-documented. In the past, the association between T2D and COVID-19 was considered to be bidirectional (238). On the one hand, once glycemic control in pre-existing T2D is inappropriate, it can render the patient susceptible to infection, enhance the severity of COVID-19, or be independently associated with many adverse outcomes (238). On the other hand, SARS-CoV-2 infection *per se* can trigger a battery of metabolic abnormalities, including insulin resistance and hyperglycemia, finally inducing the onset of T2D (239). Many individuals with prediabetes that progressed to diabetes during the pandemic can be partly attributed to the viral infection (certainly, epidemic control measures such as "lockdowns" and "isolation at home" may have changed the lifestyles of some people, which might be an indirect cause of this issue). However, the association between T2D and COVID-19 appears to be multidirectional (Figure 2). First, both T2D and SARS-CoV-2 infection may affect the whole body. Second, almost all of the pathophysiological factors involved in SARS-CoV-2 infection are also associated/interact with T2D. Hence, rather than being "bidirectional," the

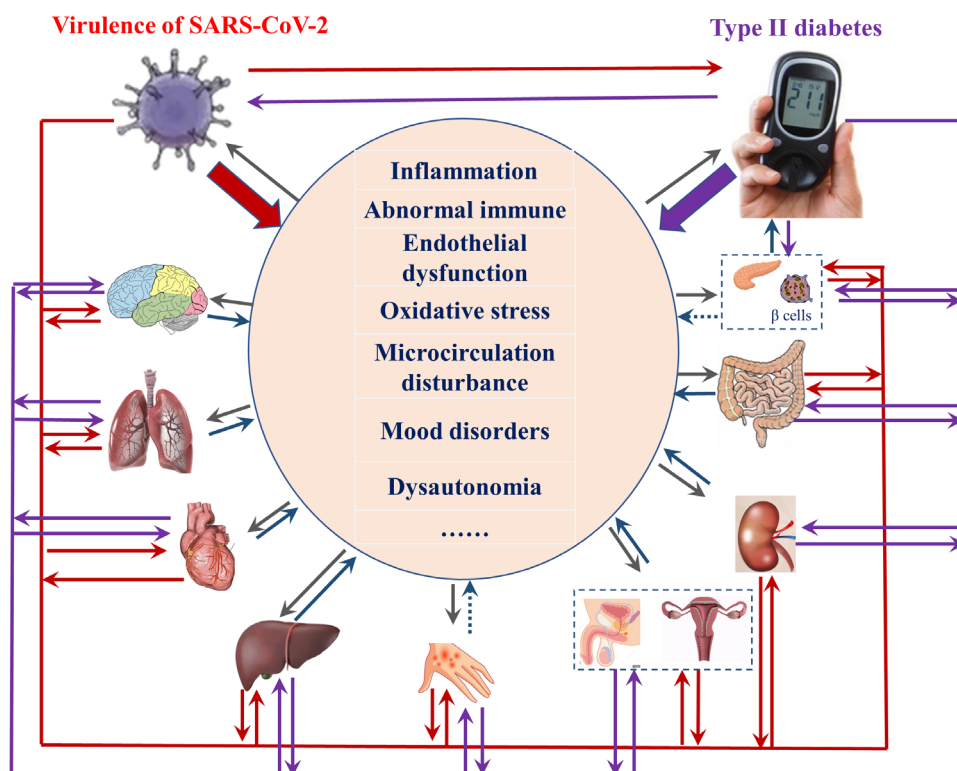


Figure 2. The multidirectional interactions between SARS-CoV-2 and type 2 diabetes. Red arrows/lines represent the influence of a SARS-CoV-2 infection. Purple arrows/lines represent the influence of type 2 diabetes. Gray arrows represent the influence of pathophysiological factors. Blue arrows represent the direct influence of the organs on pathophysiological factors, and a dotted line represents an uncertain influence.

association/interaction between T2D and COVID-19 is extremely complicated and intricate, and almost all organs and all pathophysiological factors might be involved (Figure 2). Thus, mechanisms between T2D and COVID-19 are far from clarified. ACE2 is expressed in the pancreas, so direct invasion of SARS-CoV-2 might be a plausible explanation for impaired insulin secretion. In addition to pancreatic injury, the essential question is whether beta cells are destroyed by the viral infection. Several clinical (154) and experimental (240) studies have found that rather than direct damage to beta cells, hyperstimulation of the beta cells by viral infection-related insulin resistance may cause exhaustion of beta cells and worsen diabetes (241). Alternatively, abnormal immune-inflammatory reactions (241), endothelial dysfunction (240), and other pathophysiological factors like dysautonomia and mood disorders more or less contribute to COVID-related insulin resistance and beta cell dysfunction (242). Nonetheless, T2D certainly appears to "connive" with SARS-CoV-2 to induce a worse clinical outcome. This contention is supported by a study in India, which indicated that T2D patients diagnosed during the COVID-19 pandemic had more severe glycemia than those diagnosed before the pandemic (154). What should be kept in mind is that impaired beta cell function and insulin resistance cannot recover as soon as the body recovers from acute infection. Those effects might be persistent (241) and even lifelong sequelae of COVID-19.

7.5.1. Diabetes in LC

Box 3. Particular concerns regarding diabetes in LC

- The prognosis for COVID-19-related hyperglycemia or diabetes
- Whether the incidence of diabetes remains higher in patients with LC
- What is the difference between T2D patients with and without a history of SARS-CoV-2 infection during a long-term follow-up?

Several particular concerns regarding diabetes in LC are listed in Box 3.

The available evidence is inadequate, but several clinical studies have helped to address these concerns. Montefusco *et al.* found that 46% of patients with COVID-19-related hyperglycemia were still hyperglycemic whereas 27% were normoglycemic (241). Even in those normoglycemic patients, abnormal glycometabolic control and a cytokine profile, along with insulin resistance, were still observed. Glycemic abnormalities can persist at least two months after recovery from acute infection. However, a study in Italy obtained the opposite results. The study observed 589 patients with COVID-19; 19.6% had preexisting T2D, 6.7% had new-onset T2D, 43.7% had hyperglycemia not in the diabetes range, and 30% were normoglycemic (243). After recovery from acute infection, the incidence

of dysglycemia returned to its level pre-admission. The study therefore ruled out COVID-19-related disruption of glycometabolic control as a long-term sequela. Accordingly, more rigorous trials need to be conducted to observe the long-term prognosis for COVID-19-related hyperglycemia or diabetes.

Xie and Al-Aly conducted a cohort study to observe the risks and burdens of incident diabetes in people with LC, and they found that patients with COVID-19 had a higher risk and excess burden of incident T2D and antihyperglycemic agent use during a 12-month follow-up (11). Another large cohort study investigating the long-term effects of COVID-19 on cardiometabolic outcomes found that the net incidence of T2D increased in the first four weeks after COVID-19 and remained high for 5-12 weeks but did not increase for 13-52 weeks. Hence, the incidence of T2D increased for at least 12 weeks after COVID-19 (244). These findings indicate that patients with COVID-19 had an increased risk of developing T2D during a long-term follow-up.

Fernández-de-Las-Peñas *et al.* conducted a case-control study to compare LC sequelae between COVID-19 patients with and without T2D and they found that the most common LC symptoms were fatigue, dyspnea on exertion, and pain (245). There were no differences in LC symptoms and reduction of ADL between COVID-19 patients with and without T2D. They wondered if T2D might be not a risk factor for developing LC symptoms. In another case-control study, Mittal *et al.* found that COVID-19 patients with T2D had more fatigue than those without T2D during an average 92-day follow-up (246).

Altogether, the heterogeneity of the limited available literature cannot provide compelling evidence to address the concerns in Box 3. The effects of diabetes in LC warrants further investigation because it may greatly impact the QOL of and prognosis for these patients.

7.5.2. Prospects for the future

In light of the limitations of the available studies and based on the authors' clinical experience, there are several recommendations to improve the management, diagnosis, and treatment of LC-related diabetes.

Management: T2D is a lifestyle-related disease, which means that it is associated with many unhealthy lifestyles. Indeed, T2D and COVID-19 share many common risk factors. Management of risk factors such as blood pressure, dyslipidemia and glucose, along with lifestyle improvements, can benefit T2D as well as LC. There is robust evidence regarding the beneficial effects of multifactorial-risk-factor-interventions on T2D (247). A future study should focus on verification of these multifactorial-risk-factor-interventions in LC, and particularly for controversial interventions such as exercise.

Diagnosis: Standardization of the diagnostic protocol

for T2D in the context of LC, including laboratory tests and timing, is important. Other than simple fasting blood glucose, more specific examinations such as oral glucose tolerance tests, multiple point insulin, C-peptides, pancreatic and hepatic ectopic fat, body composition, and a hyperglycemic clamp test should be considered and conducted (248). This will help to explore the association between LC and T2D (insulin resistance). Moreover, attention should be paid to the timing of the examination. Thus far, there is no robust evidence on the optimal timing for a T2D examination. In light of the authors' experience, three months after recovery from acute COVID-19 might be a good time given glycosylated hemoglobin levels and exclusion of hyperglycemia caused by steroids or stress. This topic needs to be investigated further.

Treatment: Several studies evaluated the efficacy/safety of mainstream anti-diabetic agents for treatment of patients with T2D and COVID-19 (249-252). One of those studies reported that dipeptidyl peptidase-4 inhibitor (DPP-4i) was related to increased mortality (249) and two reported adverse reactions to insulin (249,250). No study reported adverse reactions to glucagon-like peptide-1 receptor agonists (GLP1RA), sodium-glucose cotransporter-2 inhibitors (SGLT2i), or metformin. Moreover, GLP1RA, followed by SGLT2i and metformin, exhibited the best protective effects against death (250). GLP1RA and SGLT2i are also reported to help reduce body weight, facilitate glycemic control, reduce cardiovascular events, and improve renal outcomes (253). Administration of GLP1RA and SGLT2i is also associated with a better prognosis for COVID-19. Accordingly, GLP1RA and SGLT2i are most likely to be recommended for treating diabetes in LC, and this topic requires further verification by rigorously designed RCTs.

8. The reproductive system

SARS-CoV-2 infection may cause long-term sequelae in the reproductive systems of both males and females. ACE2 is widely expressed in the testes (254) and ovarian and endometrial tissue (255), hence unsurprisingly, SARS-CoV-2 infection can involve the male and female reproductive systems. Impairment of the HPA axis in the context of COVID-19 (described in the neurological section) also contributes to disorders in the reproductive system due to the dysfunction of the neuroendocrine system. Moreover, the abnormal immune-inflammation-related changes due to COVID-19, such as dysautonomia (100), ME/CFS (7,256), and mood disorders (257,258), may indirectly affect the reproductive system, thereby inducing many specific and non-specific symptoms. However, available studies regarding the long-term effects of SARS-CoV-2 infection on the reproductive system are quite limited thus far.

8.1. Involvement of the male reproductive system

Erectile dysfunction (ED) is the most common reported reproductive symptom in male patients with COVID-19. A study in Italy reported that the prevalence of ED was 28% in patients with COVID-19, which was significantly higher than that in individuals without COVID-19 (9.33%) (259). In an observational study in Thailand, Harirugsakul *et al.* reported that the prevalence of COVID-19-related ED was 64.7%; most ED was mild in severity (257). ED in these patients was associated with mental disorders. ED is affected by many factors. In addition to pathological factors, it is also influenced by other factors such as culture, education, religion, and attitude towards sex. This is understandable given the great heterogeneity among different countries. However, what is clear is that the prevalence of ED is higher in patients with COVID-19. Kresch *et al.* noted the prolonged presence of SARS-CoV-2 in penile tissue, which can induce vascular dysfunction or endothelial dysfunction and obstruct the blood supply to penile tissues thereby causing ED (260). In addition, direct testicular injury and COVID-19-related mood disorders (such as depression and anxiety due to SARS-CoV-2 infection) may also contribute to the development of ED (261).

Maleki *et al.* noted problems with sperm count, semen volume, motility, sperm morphology and sperm concentration in patients with LC and found that they were associated with increased cytokines and the presence of caspase 8, caspase 9 and caspase 3 in seminal fluid (262). These findings confirmed testicular injury in LC. Due to the abundance of ACE2 in the testes, testicular injury might be induced by SARS-CoV-2 infection-related oxidative stress and inflammation and further cause abnormal sperm motility, DNA breakage, and male infertility (263). Moreover, invasion by SARS-CoV-2 might cause orchitis and epididymitis of the testis (264). However, this hypothesis is controversial since no inflammatory markers associated with predicting testicular pain or orchitis were found in patients with COVID-19 (265). In addition, more cases of testicular torsion were reported during the COVID-19 pandemic, and those mechanisms remain unclear (266).

8.2. Involvement of the female reproductive system

ACE2 is well distributed in ovarian and endometrial tissue (267). A plausible hypothesis is that SARS-CoV-2 infection could greatly influence the production of ovarian hormones and endometrial response during menses (255). Ding *et al.* reported that ovarian damage, including diminished ovarian reserve and a reproductive endocrine disorder, were observed in female patients with COVID-19 (268). Menstrual changes are commonly reported during the COVID-19 pandemic. Li *et al.* found that in 237 female patients with COVID-19, frequent

menstrual dysfunctions were changes in menstrual volume (25%), changes in the menstrual cycle (28%), decreased volume (20%), and a prolonged cycle (19%). Concentrations of sex hormones and ovarian reserve did not change. These changes might be associated with systemic dysfunction rather than specific to the female reproductive system. The endocrine and ovarian systems seem not to be seriously affected by SARS-CoV-2 infection (269). Takmaz *et al.* found that the prevalence of a menstrual cycle irregularity increased due to COVID-19 pandemic-induced depression, anxiety, and stress in healthy female caregivers (258). In a large-scale retrospective cohort study involving 18,076 smartphone app users, Nguyen *et al.* found that the COVID-19 pandemic did not affect population-level changes in ovulation and menstruation in the women who participated (270). The results of these studies seem to imply that menstrual changes in COVID-19 are more associated with secondary changes in COVID-19 (e.g., mood disorders) rather than the direct impact of SARS-CoV-2 infection. Many researchers have argued that the problem of menstrual changes in COVID-19 seems to be "neglected" or "underestimated" so that long-term sequelae involving the female reproductive system are not well investigated (271-273). Medina-Perucha *et al.* conducted a cross-sectional online survey study investigating menstrual changes in LC and found that patients with LC had a higher risk of developing menstrual changes in comparison to those who did not have COVID-19 or those who had COVID-19 but not LC (273).

8.3. Paths for future exploration

In light of the available literature, the long-term effects of COVID-19 on the reproductive system, either male or female, remain uncertain. Other than the possible direct influence of viral invasion, interactions between the reproductive organs and other systems might be important, and particularly bidirectional interaction with mood disorders (4). This means that dysfunction of the reproductive system might adversely affect other systems and increase their dysfunction. Davis *et al.* reported that menstruation and the week before menstruation might play an inciting role in the relapse of LC symptoms (4). Hence, reproductive involvement in the context of COVID-19, and especially long-term effects, cannot be ignored. Aspects of reproductive involvement should be included in future follow-up studies.

9. Dermatologic involvement

Many dermatologic manifestations are reported in patients with COVID-19. Of those, acral chilblain-like or pernio-like lesions ("COVID toes," Figure 3A) are reportedly the most common dermatologic symptoms in acute COVID-19. The other commonly reported



Figure 3. Common dermatologic manifestations of long COVID. A, pernio-like lesions; B, urticaria; C, papulosquamous eruptions; D, morbilliform-like eruptions; E, hair loss.

skin findings include morbilliform-like eruptions, papulosquamous eruptions, urticaria, and livedo reticularis (Figure 3). Most of these lesions spontaneously resolve within two weeks after onset (20). However, some authors reported persistent lesions such as chilblain lesions (274), pernio, and papulosquamous eruptions (275) that might fall under dermatologic sequelae of LC. In a meta-analysis, Mirza *et al.* found that the prevalence of chilblains/pernio-like lesions was 51.5%, that of an erythematous maculopapular rash was 13.3%, and that of viral exanthem was 7.7%. Latency from initiation of respiratory symptoms to dermatologic manifestations was an average of 1.5 days in children and 7.9 days in adults, ranging from -3-38 days. Approximately 10% of patients have only dermatologic manifestations, and 5.3-13.3% of patients initially developed cutaneous symptoms (276). An important study observed dermatologic involvement in patients with COVID-19 and found that the median duration of skin findings was 13 days (IQR 7-21) for all patients, and seven days (IQR 5-14) for patients with laboratory-confirmed COVID-19. Chilblains/pernio-like lesions persisted a median of 15 days (IQR 10-30) in patients with suspected COVID-19 and 12 days

(IQR 7-23) in confirmed cases. Morbilliform persisted a median of 7 days (IQR 5-10) and urticarial eruptions persisted a median of 4 days (IQR 2-10) in patients with confirmed COVID-19; the longest duration was 28 days. Papulosquamous eruptions persisted 20 days (IQR 14-28) in confirmed cases; one patient had a confirmed "long-hauler" eruption persisting 70 days. Seven of 103 patients (6.8%) with pernio were long-haulers whose pernio persisted over 60 days (275). This observational study drew a useful picture of common COVID-19-related skin findings. The mechanisms of these skin findings are not clear. Tamaro *et al.* hypothesized that these dermatologic manifestations in LC might be induced by prolonged abnormal immune-inflammatory reactions, along with psychological stress, and this topic requires further investigation (274). Nailfold capillaroscopy has therefore been recommended for identification of potential microcirculatory morphological alterations in these patients (20).

In addition to the aforementioned skin findings, hair loss was reported in approximately 20-25% of patients 3-6 months after recovery from COVID-19 (6,28,277). This is also regarded as an LC sequela (Figure 3E). However, a study in South Korean involving 226,737 patients with COVID-19 found no evidence of an association between COVID-19 and the development of alopecia areata (278). Lopez-Leon *et al.* believe that hair loss after COVID-19 might be regarded as a form of telogen effluvium that results from the transition of premature follicles from the anagen phase to the telogen phase due to systemic stress and/or infection (6).

However, due to the complex nature of SARS-CoV-2 infection, there is no compelling evidence whether these dermatologic manifestations are caused by or related to COVID-19. The underlying causal relationship should be determined.

10. Concluding Remarks

The current study comprehensively reviewed the sequelae of LC in main organ systems on the basis of the latest available literature prior to February 2023. This work has attempted to provide updated information to all COVID-19 researchers. The take-home messages should help to improve the insights into and understanding of the long-term effects of COVID-19. Based on the aforementioned knowledge and limitations of the available studies so far, several considerations/suggestions can be offered for future investigation:

i) Over three years have passed since the COVID-19 pandemic started. A study with a longer follow-up (over two years) would help to better understand LC sequelae. That said, the possible inadequacy of medical examinations during the pandemic might limit our understanding of the effects of SARS-CoV-2 infection on each organ as well as related pathophysiological states. This might be partly compensated for with a well-

designed follow-up. Indeed, we are now conducting a two-year follow-up investigating the risk factors for COVID-19-related pulmonary fibrosis. More studies with a longer follow-up should be conducted.

ii) Most of the included studies did not report the variant infecting patients (Table 1, online data: <http://www.biosciencetrends.com/action/getSupplementalData.php?ID=140>). Due to the heterogeneous nature of the different variants (epidemiological and clinical features), future studies should clearly report the variant involved. In addition, rigorous comparison of LC sequelae by variant might be interesting.

iii) Findings have revealed that many LC sequelae developed independently of the initial severity of COVID-19. This means many LC sequelae can develop in mild and even asymptomatic patients. Moreover, some LC sequelae, such as dysfunction of the kidneys and liver, potentially develop into severe illness and even life-threatening syndromes. However, such conditions often lack specific symptoms and might be ignored in the early stage. We therefore strongly recommend that patients with a history of SARS-CoV-2 infection, no matter the severity of the initial infection (including asymptomatic patients), should undergo a periodic physical examination to identify possible hepatic and/or renal damage.

iv) An abnormal immune-inflammation reaction and a mood disorder (anxiety, depression, and stress) might be common mechanisms involved in the dysfunction of organs throughout the body (Figure 2). Hence, anti-inflammatory agents and antivirals and treatments for mood disorders should be developed and verified in future clinical trials, and particularly their long-term effects on LC sequelae and adverse reactions they might cause.

v) Interactions of symptoms might be bidirectional or even multidirectional (Figure 2). A typical example is the interaction between the ED and a mood disorder. ED might develop from depression, while conversely ED can also lead to depression. The interaction between ED and depression may constitute a vicious cycle and finally lead to a worse outcome. Clinicians should investigate the potential formation of a vicious cycle and attempt to break this vicious cycle to achieve a better clinical outcome. Accordingly, future studies should be conducted with full consideration of the interaction/crosstalk among organs and symptoms (Figure 2).

vi) The latest computer technology, such as artificial intelligence, big data, and machine learning, should be used in future LC studies.

Taken together, COVID-19 is a complicated disease involving the whole body. We propose establishing mechanisms for multidisciplinary collaboration to fight against LC. These should include not only the medical disciplines but also a large spectrum of disciplines including chemistry, engineering, materials science, and computer science in order to combat LC.

Funding: This work was supported by the National Natural Science Foundation of China (no. 82070420), the Shenzhen Scientific and Technological Foundation (no. JSGG20220301090005007), and the Third People's Hospital of Shenzhen Foundation (nos. G2021027 and G2022062)

Conflict of Interest: The authors have no conflicts of interest to disclose.

References

- Asakawa T. Focusing on development of novel sampling approaches and alternative therapies for COVID-19: Are they still useful in an era after the pandemic? *Biosci Trends*. 2022; 16:386-388.
- Ballering AV, van Zon SKR, Olde Hartman TC, Rosmalen JGM, Lifelines Corona Research I. Persistence of somatic symptoms after COVID-19 in the Netherlands: An observational cohort study. *Lancet*. 2022; 400:452-461.
- Huang L, Yao Q, Gu X, *et al*. 1-year outcomes in hospital survivors with COVID-19: A longitudinal cohort study. *Lancet*. 2021; 398:747-758.
- Davis HE, Assaf GS, McCorkell L, Wei H, Low RJ, Re'em Y, Redfield S, Austin JP, Akrami A. Characterizing long COVID in an international cohort: 7 months of symptoms and their impact. *EClinicalMedicine*. 2021; 38:101019.
- Hedin K, van der Velden AW, Hansen MP, *et al*. Initial symptoms and three months follow-up after acute COVID-19 in outpatients: An international prospective cohort study. *Eur J Gen Pract*. 2023; 2154074.
- Lopez-Leon S, Wegman-Ostrosky T, Perelman C, Sepulveda R, Rebolledo PA, Cuapio A, Villapol S. More than 50 long-term effects of COVID-19: a systematic review and meta-analysis. *Sci Rep*. 2021; 11:16144.
- Davis HE, McCorkell L, Vogel JM, Topol EJ. Long COVID: Major findings, mechanisms and recommendations. *Nat Rev Microbiol*. 2023; 1-14.
- Pallotti F, Esteves SC, Faja F, Buonacquisto A, Conflitti AC, Hirsch MN, Lenzi A, Paoli D, Lombardo F. COVID-19 and its treatments: Lights and shadows on testicular function. *Endocrine*. 2023; 79:243-251.
- Zanini G, Selleri V, Roncati L, Coppi F, Nasi M, Farinetti A, Manenti A, Pinti M, Mattioli AV. Vascular "long COVID": A new vessel disease? *Angiology*. 2023; 33197231153204.
- Xie Y, Xu E, Bowe B, Al-Aly Z. Long-term cardiovascular outcomes of COVID-19. *Nat Med*. 2022; 28:583-590.
- Xie Y, Al-Aly Z. Risks and burdens of incident diabetes in long COVID: A cohort study. *Lancet Diabetes Endocrinol*. 2022; 10:311-321.
- Kedor C, Freitag H, Meyer-Arndt L, *et al*. Author Correction: A prospective observational study of post-COVID-19 chronic fatigue syndrome following the first pandemic wave in Germany and biomarkers associated with symptom severity. *Nat Commun*. 2022; 13:6009.
- Ceban F, Ling S, Lui LMW, *et al*. Fatigue and cognitive impairment in Post-COVID-19 Syndrome: A systematic review and meta-analysis. *Brain Behav Immun*. 2022; 101:93-135.
- Demko ZO, Yu T, Mullapudi SK, Varela Heslin MG, Dorsey CA, Payton CB, Tornheim JA, Blair PW, Mehta SH, Thomas DL, Manabe YC, Antar AAR, Out SST. Post-acute sequelae of SARS-CoV-2 (PASC) impact quality of life at 6, 12 and 18 months post-infection. *medRxiv*. 2022 (preprint).
- Cairns R, Hotopf M. A systematic review describing the prognosis of chronic fatigue syndrome. *Occup Med (Lond)*. 2005; 55:20-31.
- Nasserie T, Hittle M, Goodman SN. Assessment of the frequency and variety of persistent symptoms among patients with COVID-19: A systematic review. *JAMA Netw Open*. 2021; 4:e2111417.
- Rabaan AA, Smajlovic S, Tombuloglu H, Cordic S, Hajdarevic A, Kudic N, Al Mutai A, Turkistani SA, Al-Ahmed SH, Al-Zaki NA, Al Marshood MJ, Alfaraj AH, Alhumaid S, Al-Suhaimi E. SARS-CoV-2 infection and multi-organ system damage: A review. *Biomol Biomed*. 2023; 23:37-52.
- Oronsky B, Larson C, Hammond TC, Oronsky A, Kesari S, Lybeck M, Reid TR. A review of persistent post-COVID syndrome (PPCS). *Clin Rev Allergy Immunol*. 2023; 64:66-74.
- Yong SJ, Halim A, Halim M, *et al*. Inflammatory and vascular biomarkers in post-COVID-19 syndrome: A systematic review and meta-analysis of over 20 biomarkers. *Rev Med Virol*. 2023; e2424.
- Nalbandian A, Desai AD, Wan EY. Post-COVID-19 condition. *Annu Rev Med*. 2023; 74:55-64.
- Ma Y, Deng J, Liu Q, Du M, Liu M, Liu J. Long-term consequences of asymptomatic SARS-CoV-2 infection: A systematic review and meta-analysis. *Int J Environ Res Public Health*. 2023; 20:1613.
- Oguz SH, Yildiz BO. Endocrine disorders and COVID-19. *Annu Rev Med*. 2023; 74:75-88.
- Murphy MC, Little BP. Chronic pulmonary manifestations of COVID-19 infection: Imaging evaluation. *Radiology*. 2023; 222379.
- Ashton RE, Philips BE, Faghy M. The acute and chronic implications of the COVID-19 virus on the cardiovascular system in adults: A systematic review. *Prog Cardiovasc Dis*. 2023; Jan 20: S0033-0620(23)00004-X.
- Piva T, Masotti S, Raisi A, Zerbini V, Grazi G, Mazzoni G, Belvederi Murri M, Mandini S. Exercise program for the management of anxiety and depression in adults and elderly subjects: Is it applicable to patients with post-covid-19 condition? A systematic review and meta-analysis. *J Affect Disord*. 2023; 325:273-281.
- Linnhoff S, Koehler L, Haghikia A, Zaehle T. The therapeutic potential of non-invasive brain stimulation for the treatment of Long-COVID-related cognitive fatigue. *Front Immunol*. 2022; 13:935614.
- Ramani C, Davis EM, Kim JS, Provencio JJ, Enfield KB, Kadl A. Post-ICU COVID-19 outcomes: A case series. *Chest*. 2021; 159:215-218.
- Huang C, Huang L, Wang Y, *et al*. 6-month consequences of COVID-19 in patients discharged from hospital: A cohort study. *Lancet*. 2021; 397:220-232.
- Bellan M, Soddu D, Balbo PE, *et al*. Respiratory and psychophysical sequelae among patients with COVID-19 four months after hospital discharge. *JAMA Netw Open*. 2021; 4:e2036142.
- You J, Zhang L, Ni-Jia-Ti MY, Zhang J, Hu F, Chen L, Dong Y, Yang K, Zhang B, Zhang S. Anormal pulmonary function and residual CT abnormalities in rehabilitating COVID-19 patients after discharge. *J Infect*. 2020; 81:e150-e152.
- Fabbri L, Moss S, Khan FA, Chi W, Xia J, Robinson K, Smyth AR, Jenkins G, Stewart I. Parenchymal lung

- abnormalities following hospitalisation for COVID-19 and viral pneumonitis: A systematic review and meta-analysis. *Thorax*. 2023; 78:191-201.
32. Lee JH, Yim JJ, Park J. Pulmonary function and chest computed tomography abnormalities 6-12 months after recovery from COVID-19: A systematic review and meta-analysis. *Respir Res*. 2022; 23:233.
 33. Besutti G, Monelli F, Schiro S, Milone F, Ottone M, Spaggiari L, Facciolongo N, Salvarani C, Croci S, Pattacini P, Sverzellati N. Follow-Up CT Patterns of residual lung abnormalities in severe COVID-19 pneumonia survivors: A multicenter retrospective study. *Tomography*. 2022; 8:1184-1195.
 34. Wu X, Liu X, Zhou Y, *et al*. 3-month, 6-month, 9-month, and 12-month respiratory outcomes in patients following COVID-19-related hospitalisation: A prospective study. *Lancet Respir Med*. 2021; 9:747-754.
 35. Cho JL, Villacreses R, Nagpal P, Guo J, Pezzulo AA, Thurman AL, Hamzeh NY, Blount RJ, Fortis S, Hoffman EA, Zabner J, Comellas AP. Quantitative chest CT assessment of small airways disease in post-acute SARS-CoV-2 infection. *Radiology*. 2022; 304:185-192.
 36. Cui S, Chen S, Li X, Liu S, Wang F. Prevalence of venous thromboembolism in patients with severe novel coronavirus pneumonia. *J Thromb Haemost*. 2020; 18:1421-1424.
 37. Hippensteel JA, Burnham EL, Jolley SE. Prevalence of venous thromboembolism in critically ill patients with COVID-19. *Br J Haematol*. 2020; 190:e134-e137.
 38. Llitjos JF, Leclerc M, Chochois C, Monsallier JM, Ramakers M, Auvray M, Merouani K. High incidence of venous thromboembolic events in anticoagulated severe COVID-19 patients. *J Thromb Haemost*. 2020; 18:1743-1746.
 39. Konstantinides SV, Meyer G, Becattini C, *et al*. 2019 ESC Guidelines for the diagnosis and management of acute pulmonary embolism developed in collaboration with the European Respiratory Society (ERS): The Task Force for the diagnosis and management of acute pulmonary embolism of the European Society of Cardiology (ESC). *Eur Respir J*. 2019; 54: 1901647.
 40. Tudoran C, Tudoran M, Lazureanu VE, Marinescu AR, Pop GN, Pescariu AS, Enache A, Cut TG. Evidence of pulmonary hypertension after SARS-CoV-2 infection in subjects without previous significant cardiovascular pathology. *J Clin Med*. 2021; 10:199.
 41. D'Cruz RF, Waller MD, Perrin F, *et al*. Chest radiography is a poor predictor of respiratory symptoms and functional impairment in survivors of severe COVID-19 pneumonia. *ERJ Open Res*. 2021; 7: 00655-2020.
 42. Mandal S, Barnett J, Brill SE, *et al*. 'Long-COVID': A cross-sectional study of persisting symptoms, biomarker and imaging abnormalities following hospitalisation for COVID-19. *Thorax*. 2021; 76:396-398.
 43. Song WJ, Hui CKM, Hull JH, Birring SS, McGarvey L, Mazzone SB, Chung KF. Confronting COVID-19-associated cough and the post-COVID syndrome: Role of viral neurotropism, neuroinflammation, and neuroimmune responses. *Lancet Respir Med*. 2021; 9:533-544.
 44. Esendagli D, Yilmaz A, Akcay S, Ozlu T. Post-COVID syndrome: Pulmonary complications. *Turk J Med Sci*. 2021; 51:3359-3371.
 45. Luchian ML, Motoc A, Lochy S, *et al*. Subclinical myocardial dysfunction in patients with persistent dyspnea one year after COVID-19-Why should screening for cardiovascular diseases be performed? Reply to Vankrunkelsven, P. Tendentious Paper-Titles and Wrong Conclusions Lead to Fear in the Population and Medical Overconsumption. Comment on "Luchian *et al*. Subclinical Myocardial Dysfunction in Patients with Persistent Dyspnea One Year after COVID-19. *Diagnostics* 2022, 12, 57". *Diagnostics (Basel)*. 2022; 12:1837.
 46. Motiejunaite J, Balagny P, Arnoult F, Mangin L, Bancal C, d'Ortho MP, Frija-Masson J. Hyperventilation: A possible explanation for long-lasting exercise intolerance in mild COVID-19 survivors? *Front Physiol*. 2020; 11:614590.
 47. Singh I, Joseph P, Heerdt PM, Cullinan M, Lutchmansingh DD, Gulati M, Possick JD, Systrom DM, Waxman AB. Persistent exertional intolerance after COVID-19: Insights from invasive cardiopulmonary exercise testing. *Chest*. 2022; 161:54-63.
 48. Mancini DM, Brunjes DL, Lala A, Trivieri MG, Contreras JP, Natelson BH. Use of cardiopulmonary stress testing for patients with unexplained dyspnea post-coronavirus disease. *JACC Heart Fail*. 2021; 9:927-937.
 49. Myall KJ, Mukherjee B, Castanheira AM, Lam JL, Benedetti G, Mak SM, Preston R, Thillai M, Dewar A, Molyneaux PL, West AG. Persistent post-COVID-19 interstitial lung disease. An observational study of corticosteroid treatment. *Ann Am Thorac Soc*. 2021; 18:799-806.
 50. Dhooria S, Chaudhary S, Sehgal IS, Agarwal R, Arora S, Garg M, Prabhakar N, Puri GD, Bhalla A, Suri V, Yaddanapudi LN, Muthu V, Prasad KT, Aggarwal AN. High-dose versus low-dose prednisolone in symptomatic patients with post-COVID-19 diffuse parenchymal lung abnormalities: An open-label, randomised trial (the COLDSTER trial). *Eur Respir J*. 2022; 59.
 51. Bazdyrev E, Rusina P, Panova M, Novikov F, Grishagin I, Nebolsin V. Lung fibrosis after COVID-19: Treatment prospects. *Pharmaceuticals (Basel)*. 2021; 14:807.
 52. Bharat A, Machuca TN, Querrey M, *et al*. Early outcomes after lung transplantation for severe COVID-19: A series of the first consecutive cases from four countries. *Lancet Respir Med*. 2021; 9:487-497.
 53. Piazza G, Campia U, Hurwitz S, Snyder JE, Rizzo SM, Pfeferman MB, Morrison RB, Leiva O, Fanikos J, Nauffal V, Almarzooq Z, Goldhaber SZ. Registry of arterial and venous thromboembolic complications in patients With COVID-19. *J Am Coll Cardiol*. 2020; 76:2060-2072.
 54. Farkouh ME, Stone GW, Lala A, *et al*. Anticoagulation in patients with COVID-19: JACC Review Topic of the Week. *J Am Coll Cardiol*. 2022; 79:917-928.
 55. Paranjpe I, Fuster V, Lala A, Russak AJ, Glicksberg BS, Levin MA, Charney AW, Narula J, Fayad ZA, Bagiella E, Zhao S, Nadkarni GN. Association of treatment dose anticoagulation with in-hospital survival among hospitalized patients with COVID-19. *J Am Coll Cardiol*. 2020; 76:122-124.
 56. Viecca M, Radovanovic D, Forleo GB, Santus P. Enhanced platelet inhibition treatment improves hypoxemia in patients with severe Covid-19 and hypercoagulability. A case control, proof of concept study. *Pharmacol Res*. 2020; 158:104950.
 57. Liu X, Li Z, Liu S, *et al*. Potential therapeutic effects of dipyridamole in the severely ill patients with COVID-19. *Acta Pharm Sin B*. 2020; 10:1205-1215.
 58. Kim HW, Jenista ER, Wendell DC, Azevedo CF, Campbell MJ, Darty SN, Parker MA, Kim RJ. Patients with acute

- myocarditis following mRNA COVID-19 vaccination. *JAMA Cardiol.* 2021; 6:1196-1201.
59. Noone S, Flinspach AN, Fichtlscherer S, Zacharowski K, Sonntagbauer M, Raimann FJ. Severe COVID-19-associated myocarditis with cardiogenic shock - management with assist devices - A case report & review. *BMC Anesthesiol.* 2022; 22:385.
 60. Mele D, Flamigni F, Rapezzi C, Ferrari R. Myocarditis in COVID-19 patients: Current problems. *Intern Emerg Med.* 2021; 16:1123-1129.
 61. Shi S, Qin M, Shen B, Cai Y, Liu T, Yang F, Gong W, Liu X, Liang J, Zhao Q, Huang H, Yang B, Huang C. Association of cardiac injury with mortality in hospitalized patients with COVID-19 in Wuhan, China. *JAMA Cardiol.* 2020; 5:802-810.
 62. Kociol RD, Cooper LT, Fang JC, Moslehi JJ, Pang PS, Sabe MA, Shah RV, Sims DB, Thiene G, Vardeny O, American Heart Association Heart F, Transplantation Committee of the Council on Clinical C. Recognition and initial management of fulminant myocarditis: A Scientific Statement From the American Heart Association. *Circulation.* 2020; 141:e69-e92.
 63. Hu H, Ma F, Wei X, Fang Y. Coronavirus fulminant myocarditis treated with glucocorticoid and human immunoglobulin. *Eur Heart J.* 2021; 42:206.
 64. Coyle J, Igbinomwanhia E, Sanchez-Nadales A, Danciu S, Chu C, Shah N. A recovered case of COVID-19 myocarditis and ARDS treated with corticosteroids, tocilizumab, and experimental AT-001. *JACC Case Rep.* 2020; 2:1331-1336.
 65. Russell CD, Millar JE, Baillie JK. Clinical evidence does not support corticosteroid treatment for 2019-nCoV lung injury. *Lancet.* 2020; 395:473-475.
 66. Palazzuoli A, Metra M, Collins SP, *et al.* Heart failure during the COVID-19 pandemic: Clinical, diagnostic, management, and organizational dilemmas. *ESC Heart Fail.* 2022; 9:3713-3736.
 67. Isath A, Malik A, Bandyopadhyay D, Goel A, Hajra A, Dhand A, Lanier GM, Fonarow GC, Lavie CJ, Gass AL. COVID-19, heart failure hospitalizations, and outcomes: A nationwide analysis. *Curr Probl Cardiol.* 2022; 48:101541.
 68. Malgie J, Schoones JW, Pijls BG. Decreased mortality in Coronavirus Disease 2019 patients treated with tocilizumab: A rapid systematic review and meta-analysis of observational studies. *Clin Infect Dis.* 2021; 72:e742-e749.
 69. Martinez-Sanz J, Muriel A, Ron R, Herrera S, Perez-Molina JA, Moreno S, Serrano-Villar S. Effects of tocilizumab on mortality in hospitalized patients with COVID-19: A multicentre cohort study. *Clin Microbiol Infect.* 2021; 27:238-243.
 70. Masia M, Fernandez-Gonzalez M, Padilla S, Ortega P, Garcia JA, Agullo V, Garcia-Abellan J, Telenti G, Guillen L, Gutierrez F. Impact of interleukin-6 blockade with tocilizumab on SARS-CoV-2 viral kinetics and antibody responses in patients with COVID-19: A prospective cohort study. *EBioMedicine.* 2020; 60:102999.
 71. Coromilas EJ, Kochav S, Goldenthal I, *et al.* Worldwide survey of COVID-19-associated arrhythmias. *Circ Arrhythm Electrophysiol.* 2021; 14:e009458.
 72. Khetpal V, Berkowitz J, Vijayakumar S, Choudhary G, Mukand JA, Rudolph JL, Wu WC, Erqou S. Long-term cardiovascular manifestations and complications of COVID-19: Spectrum and approach to diagnosis and management. *R I Med J (2013).* 2022; 105:16-22.
 73. Gopinathannair R, Merchant FM, Lakkireddy DR, Etheridge SP, Feigofsky S, Han JK, Kabra R, Natale A, Poe S, Saha SA, Russo AM. COVID-19 and cardiac arrhythmias: A global perspective on arrhythmia characteristics and management strategies. *J Interv Card Electrophysiol.* 2020; 59:329-336.
 74. Mitrani RD, Dabas N, Alfadhli J, Lowery MH, Best TM, Hare JM, Myerburg RJ, Goldberger JJ. Long-term cardiac surveillance and outcomes of COVID-19 patients. *Trends Cardiovasc Med.* 2022; 32:465-475.
 75. Raman B, Bluemke DA, Luscher TF, Neubauer S. Long COVID: Post-acute sequelae of COVID-19 with a cardiovascular focus. *Eur Heart J.* 2022; 43:1157-1172.
 76. Asakawa T, Sugiyama K, Nozaki T, Sameshima T, Kobayashi S, Wang L, Hong Z, Chen S, Li C, Namba H. Can the latest computerized technologies revolutionize conventional assessment tools and therapies for a neurological disease? The example of Parkinson's disease. *Neurol Med Chir (Tokyo).* 2019; 59:69-78.
 77. Barrios V, Cinza-Sanjurjo S, Garcia-Alegria J, Freixa-Pamias R, Llordachs-Marques F, Molina CA, Santamaria A, Vivas D, Suarez Fernandez C. Role of telemedicine in the management of oral anticoagulation in atrial fibrillation: A practical clinical approach. *Future Cardiol.* 2022; 18:743-754.
 78. Mao L, Jin H, Wang M, Hu Y, Chen S, He Q, Chang J, Hong C, Zhou Y, Wang D, Miao X, Li Y, Hu B. Neurologic manifestations of hospitalized patients with Coronavirus Disease 2019 in Wuhan, China. *JAMA Neurol.* 2020; 77:683-690.
 79. Kamal M, Abo Omirah M, Hussein A, Saeed H. Assessment and characterisation of post-COVID-19 manifestations. *Int J Clin Pract.* 2021; 75:e13746.
 80. Taquet M, Geddes JR, Husain M, Luciano S, Harrison PJ. 6-month neurological and psychiatric outcomes in 236 379 survivors of COVID-19: A retrospective cohort study using electronic health records. *Lancet Psychiatry.* 2021; 8:416-427.
 81. Patel UK, Mehta N, Patel A, Patel N, Ortiz JF, Khurana M, Urhoghide E, Parulekar A, Bhargavanshi A, Patel N, Mistry AM, Patel R, Arumathurai K, Shah S. Long-term neurological sequelae among severe COVID-19 patients: A systematic review and meta-analysis. *Cureus.* 2022; 14:e29694.
 82. Hugon J. Long-COVID: Cognitive deficits (brain fog) and brain lesions in non-hospitalized patients. *Presse Med.* 2022; 51:104090.
 83. Bolay H, Gul A, Baykan B. COVID-19 is a real headache! *Headache.* 2020; 60:1415-1421.
 84. Townsend L, Dyer AH, Jones K, *et al.* Persistent fatigue following SARS-CoV-2 infection is common and independent of severity of initial infection. *PLoS One.* 2020; 15:e0240784.
 85. Yang T, Yang Y, Wang D, Li C, Qu Y, Guo J, Shi T, Bo W, Sun Z, Asakawa T. The clinical value of cytokines in chronic fatigue syndrome. *J Transl Med.* 2019; 17:213.
 86. Herrman H, Patel V, Kieling C, *et al.* Time for united action on depression: A Lancet-World Psychiatric Association Commission. *Lancet.* 2022; 399:957-1022.
 87. Nalbandian A, Sehgal K, Gupta A, *et al.* Post-acute COVID-19 syndrome. *Nat Med.* 2021; 27:601-615.
 88. Rogers JP, Chesney E, Oliver D, Pollak TA, McGuire P, Fusar-Poli P, Zandi MS, Lewis G, David AS. Psychiatric and neuropsychiatric presentations associated with severe coronavirus infections: A systematic review and meta-

- analysis with comparison to the COVID-19 pandemic. *Lancet Psychiatry*. 2020; 7:611-627.
89. Sheng B, Cheng SK, Lau KK, Li HL, Chan EL. The effects of disease severity, use of corticosteroids and social factors on neuropsychiatric complaints in severe acute respiratory syndrome (SARS) patients at acute and convalescent phases. *Eur Psychiatry*. 2005; 20:236-242.
 90. Penninx B, Benros ME, Klein RS, Vinkers CH. How COVID-19 shaped mental health: From infection to pandemic effects. *Nat Med*. 2022; 28:2027-2037.
 91. Mazza MG, De Lorenzo R, Conte C, Poletti S, Vai B, Bollettini I, Melloni EMT, Furlan R, Ciceri F, Rovere-Querini P, group C-BOCS, Benedetti F. Anxiety and depression in COVID-19 survivors: Role of inflammatory and clinical predictors. *Brain Behav Immun*. 2020; 89:594-600.
 92. Lakhani R, Agrawal A, Sharma M. Prevalence of depression, anxiety, and stress during COVID-19 pandemic. *J Neurosci Rural Pract*. 2020; 11:519-525.
 93. Deng J, Zhou F, Hou W, Silver Z, Wong CY, Chang O, Huang E, Zuo QK. The prevalence of depression, anxiety, and sleep disturbances in COVID-19 patients: A meta-analysis. *Ann N Y Acad Sci*. 2021; 1486:90-111.
 94. Frere JJ, Serafini RA, Pryce KD, *et al*. SARS-CoV-2 infection in hamsters and humans results in lasting and unique systemic perturbations after recovery. *Sci Transl Med*. 2022; 14:eabq3059.
 95. Almeria M, Cejudo JC, Sotoca J, Deus J, Krupinski J. Cognitive profile following COVID-19 infection: Clinical predictors leading to neuropsychological impairment. *Brain Behav Immun Health*. 2020; 9:100163.
 96. Krishnan K, Lin Y, Prewitt KM, Potter DA. Multidisciplinary approach to brain fog and related persisting symptoms post COVID-19. *J Health Serv Psychol*. 2022; 48:31-38.
 97. Hampshire A, Trender W, Chamberlain SR, Jolly AE, Grant JE, Patrick F, Mazibuko N, Williams SC, Barnby JM, Hellyer P, Mehta MA. Cognitive deficits in people who have recovered from COVID-19. *EClinicalMedicine*. 2021; 39:101044.
 98. Manukyan P, Deviatierikova A, Velichkovsky BB, Kasatkin V. The impact of mild COVID-19 on executive functioning and mental health outcomes in young adults. *Healthcare (Basel)*. 2022; 10:1891.
 99. Pena Orbea C, Wang L, Shah V, Jehi L, Milinovich A, Foldvary-Schaefer N, Chung MK, Mashaqi S, Aboussouan L, Seidel K, Mehra R. Association of sleep-related hypoxia with risk of COVID-19 hospitalizations and mortality in a large integrated health system. *JAMA Netw Open*. 2021; 4:e2134241.
 100. DePace NL, Colombo J. Long-COVID syndrome and the cardiovascular system: A review of neurocardiologic effects on multiple systems. *Curr Cardiol Rep*. 2022; 24:1711-1726.
 101. Eschbacher KL, Larsen RA, Moyer AM, Majumdar R, Reichard RR. Neuropathological findings in COVID-19: An autopsy cohort. *J Neuropathol Exp Neurol*. 2022; 82:21-28.
 102. Krasemann S, Haferkamp U, Pfefferle S, *et al*. The blood-brain barrier is dysregulated in COVID-19 and serves as a CNS entry route for SARS-CoV-2. *Stem Cell Reports*. 2022; 17:307-320.
 103. Batchu S, Diaz MJ, Tran JT, Fadil A, Taneja K, Patel K, Lucke-Wold B. Spatial mapping of genes implicated in SARS-CoV-2 neuroinvasion to dorsolateral prefrontal cortex gray matter. *COVID*. 2023; 3:82-89.
 104. Iadecola C, Anrather J, Kamel H. Effects of COVID-19 on the nervous system. *Cell*. 2020; 183:16-27 e11.
 105. Politi LS, Salsano E, Grimaldi M. Magnetic resonance imaging alteration of the brain in a patient with Coronavirus Disease 2019 (COVID-19) and anosmia. *JAMA Neurol*. 2020; 77:1028-1029.
 106. Bernard-Valnet R, Pizzarotti B, Anichini A, Demars Y, Russo E, Schmidhauser M, Cerutti-Sola J, Rossetti AO, Du Pasquier R. Two patients with acute meningoencephalitis concomitant with SARS-CoV-2 infection. *Eur J Neurol*. 2020; 27:e43-e44.
 107. Pilotto A, Masciocchi S, Volonghi I, *et al*. Clinical presentation and outcomes of severe acute respiratory syndrome coronavirus 2-related encephalitis: The ENCOVID multicenter study. *J Infect Dis*. 2021; 223:28-37.
 108. Kantonen J, Mahzabin S, Mayranpaa MI, Tynnenen O, Paetau A, Andersson N, Sajantila A, Vapalahti O, Carpen O, Kekalainen E, Kantele A, Myllykangas L. Neuropathologic features of four autopsied COVID-19 patients. *Brain Pathol*. 2020; 30:1012-1016.
 109. Matschke J, Lutgehetmann M, Hagemel C, *et al*. Neuropathology of patients with COVID-19 in Germany: A post-mortem case series. *Lancet Neurol*. 2020; 19:919-929.
 110. Diao B, Wang C, Tan Y, *et al*. Reduction and functional exhaustion of T cells in patients with Coronavirus Disease 2019 (COVID-19). *Front Immunol*. 2020; 11:827.
 111. Fernandez-Castaneda A, Lu P, Geraghty AC, *et al*. Mild respiratory SARS-CoV-2 infection can cause multi-lineage cellular dysregulation and myelin loss in the brain. *bioRxiv*. 2022 (preprint).
 112. Calabrese LH. Cytokine storm and the prospects for immunotherapy with COVID-19. *Cleve Clin J Med*. 2020; 87:389-393.
 113. Caronna E, Ballve A, Llauro A, *et al*. Headache: A striking prodromal and persistent symptom, predictive of COVID-19 clinical evolution. *Cephalalgia*. 2020; 40:1410-1421.
 114. Dantzer R. Neuroimmune interactions: From the brain to the immune system and vice versa. *Physiol Rev*. 2018; 98:477-504.
 115. Jammoul M, Naddour J, Madi A, Reslan MA, Hatoum F, Zeineddine J, Abou-Kheir W, Lawand N. Investigating the possible mechanisms of autonomic dysfunction post-COVID-19. *Auton Neurosci*. 2023; 245:103071.
 116. Colombo J, Weintraub MI, Munoz R, Verma A, Ahmad G, Kaczmarek K, Santos L, DePace NL. Long COVID and the autonomic nervous system: The journey from dysautonomia to therapeutic neuro-modulation through the retrospective analysis of 152 patients. *Neurosci*. 2022; 3:300-310.
 117. de Almeida VM, Engel DF, Ricci MF, Cruz CS, Lopes IS, Alves DA, Auriol Md, Magalhães J, Zuccoli GS, Smith BJ. Gut microbiota from patients with mild COVID-19 cause alterations in mice that resemble post-COVID syndrome. 2022 (preprint).
 118. Asakawa T, Fang H, Sugiyama K, *et al*. Animal behavioral assessments in current research of Parkinson's disease. *Neurosci Biobehav Rev*. 2016; 65:63-94.
 119. Asakawa T, Fang H, Sugiyama K, Nozaki T, Kobayashi S, Hong Z, Suzuki K, Mori N, Yang Y, Hua F, Ding G, Wen G, Namba H, Xia Y. Human behavioral assessments in current research of Parkinson's disease. *Neurosci*

- Biobehav Rev. 2016; 68:741-772.
120. Asakawa T, Sugiyama K, Nozaki T, Sameshima T, Kobayashi S, Wang L, Hong Z, Chen SJ, Li CD, Ding D, Namba H. Current behavioral assessments of movement disorders in children. *CNS Neurosci Ther.* 2018; 24:863-875.
 121. Asakawa T, Zong L, Wang L, Xia Y, Namba H. Unmet challenges for rehabilitation after stroke in China. *Lancet.* 2017; 390:121-122.
 122. Hamming I, Timens W, Bulthuis ML, Lely AT, Navis G, van Goor H. Tissue distribution of ACE2 protein, the functional receptor for SARS coronavirus. A first step in understanding SARS pathogenesis. *J Pathol.* 2004; 203:631-637.
 123. Blackett JW, Li J, Jodorkovsky D, Freedberg DE. Prevalence and risk factors for gastrointestinal symptoms after recovery from COVID-19. *Neurogastroenterol Motil.* 2022; 34:e14251.
 124. Golla R, Vuyyuru S, Kante B, Kumar P, Thomas DM, Makharia G, Kedia S, Ahuja V. Long-term gastrointestinal sequelae following COVID-19: A prospective follow-up cohort study. *Clin Gastroenterol Hepatol.* 2022; 21:789-796.e1.
 125. Choudhury A, Tariq R, Jena A, Vesely EK, Singh S, Khanna S, Sharma V. Gastrointestinal manifestations of long COVID: A systematic review and meta-analysis. *Therap Adv Gastroenterol.* 2022; 15:17562848221118403.
 126. Schmulson M, Ghoshal UC, Barbara G. Managing the inevitable surge of post-COVID-19 functional gastrointestinal disorders. *Am J Gastroenterol.* 2021; 116:4-7.
 127. Zuo T, Liu Q, Zhang F, Lui GC, Tso EY, Yeoh YK, Chen Z, Boon SS, Chan FK, Chan PK, Ng SC. Depicting SARS-CoV-2 faecal viral activity in association with gut microbiota composition in patients with COVID-19. *Gut.* 2021; 70:276-284.
 128. Natarajan A, Zlitni S, Brooks EF, *et al.* Gastrointestinal symptoms and fecal shedding of SARS-CoV-2 RNA suggest prolonged gastrointestinal infection. *Med (N Y).* 2022; 3:371-387 e379.
 129. Gaebler C, Wang Z, Lorenzi JCC, *et al.* Evolution of antibody immunity to SARS-CoV-2. *Nature.* 2021; 591:639-644.
 130. Zollner A, Koch R, Jukic A, Pfister A, Meyer M, Rossler A, Kimpel J, Adolph TE, Tilg H. Postacute COVID-19 is characterized by gut viral antigen persistence in inflammatory bowel diseases. *Gastroenterology.* 2022; 163:495-506 e498.
 131. Goh D, Lim JCT, Fernandez SB, Joseph CR, Edwards SG, Neo ZW, Lee JN, Caballero SG, Lau MC, Yeong JPS. Case report: Persistence of residual antigen and RNA of the SARS-CoV-2 virus in tissues of two patients with long COVID. *Front Immunol.* 2022; 13:939989.
 132. Meringer H, Tokuyama M, Tankelevich M, Martinez-Delgado G, Jha D, Livanos AE, Canales-Herrerias P, Cossarini F, Mehandru S. 1161: Persistent immune cell abnormalities in the intestinal mucosa of patients after recovery from COVID-19 infection. *Gastroenterology.* 2022; 162:S-277.
 133. Yeoh YK, Zuo T, Lui GC, *et al.* Gut microbiota composition reflects disease severity and dysfunctional immune responses in patients with COVID-19. *Gut.* 2021; 70:698-706.
 134. Liu Q, Mak JWY, Su Q, Yeoh YK, Lui GC, Ng SSS, Zhang F, Li AYL, Lu W, Hui DS, Chan PK, Chan FKL, Ng SC. Gut microbiota dynamics in a prospective cohort of patients with post-acute COVID-19 syndrome. *Gut.* 2022; 71:544-552.
 135. Lai NY, Musser MA, Pinho-Ribeiro FA, *et al.* Gut-innervating nociceptor neurons regulate Peyer's patch microfold cells and SFB levels to mediate salmonella host defense. *Cell.* 2020; 180:33-49 e22.
 136. Ahrends T, Aydin B, Matheis F, Classon CH, Marchildon F, Furtado GC, Lira SA, Mucida D. Enteric pathogens induce tissue tolerance and prevent neuronal loss from subsequent infections. *Cell.* 2021; 184:5715-5727 e5712.
 137. Ghoshal UC. Postinfection irritable bowel syndrome. *Gut Liver.* 2022; 16:331-340.
 138. Zhou Q, Verne ML, Fields JZ, Lefante JJ, Basra S, Salameh H, Verne GN. Randomised placebo-controlled trial of dietary glutamine supplements for postinfectious irritable bowel syndrome. *Gut.* 2019; 68:996-1002.
 139. Huang C, Wang Y, Li X, *et al.* Clinical features of patients infected with 2019 novel coronavirus in Wuhan, China. *Lancet.* 2020; 395:497-506.
 140. Chen N, Zhou M, Dong X, Qu J, Gong F, Han Y, Qiu Y, Wang J, Liu Y, Wei Y, Xia J, Yu T, Zhang X, Zhang L. Epidemiological and clinical characteristics of 99 cases of 2019 novel coronavirus pneumonia in Wuhan, China: A descriptive study. *Lancet.* 2020; 395:507-513.
 141. Cai Q, Huang D, Yu H, *et al.* COVID-19: Abnormal liver function tests. *J Hepatology.* 2020; 73:566-574.
 142. Wang D, Hu B, Hu C, Zhu F, Liu X, Zhang J, Wang B, Xiang H, Cheng Z, Xiong Y, Zhao Y, Li Y, Wang X, Peng Z. Clinical characteristics of 138 hospitalized patients with 2019 Novel Coronavirus-infected pneumonia in Wuhan, China. *Jama.* 2020; 323:1061-1069.
 143. Sultan S, Altayar O, Siddique SM, Davitkov P, Feuerstein JD, Lim JK, Falck-Ytter Y, El-Serag HB. AGA Institute rapid review of the gastrointestinal and liver manifestations of COVID-19, meta-analysis of international data, and recommendations for the consultative management of patients with COVID-19. *Gastroenterology.* 2020; 159:320-334.e327.
 144. Jothimani D, Venugopal R, Abedin MF, Kaliamoorthy I, Rela M. COVID-19 and the liver. *J Hepatology.* 2020; 73:1231-1240.
 145. Kovalic AJ, Huang G, Thuluvath PJ, Satapathy SK. Elevated liver biochemistries in hospitalized Chinese patients with severe COVID-19: Systematic review and meta-analysis. *Hepatology (Baltimore, Md).* 2021; 73:1521-1530.
 146. Liu T, Wu D, Yan W, *et al.* Twelve-Month Systemic Consequences of Coronavirus Disease 2019 (COVID-19) in patients discharged from hospital: A prospective cohort study in Wuhan, China. *Clin Infect Dis.* 2022; 74:1953-1965.
 147. Liao X, Li D, Ma Z, Zhang L, Zheng B, Li Z, Li G, Liu L, Zhang Z. 12-month post-discharge liver function test abnormalities among patients with COVID-19: A single-center prospective cohort study. *Frontiers in Cellular and Infection Microbiology.* 2022; 12:864933.
 148. Caballero-Alvarado J, Zavaleta Corvera C, Merino Bacilio B, Ruiz Caballero C, Lozano-Peralta K. Post-COVID cholangiopathy: A narrative review. *Gastroenterologia y Hepatologia.* 2022;S0210-5705(22)00221-7.
 149. Yanny B, Alkhero M, Alani M, Stenberg D, Saharan A, Saab S. Post-Covid- 19 cholangiopathy: A systematic review. *J Clin Exper Hepatol.* 2022; Oct 30 Epub ahead of print.

150. Cesar Machado MC, Filho RK, El Bacha IAH, de Oliveira IS, Ribeiro CMF, de Souza HP, Parise ER. Post-COVID-19 secondary sclerosing cholangitis: A rare but severe condition with no treatment besides liver transplantation. *Amer J Case Reports*. 2022; 23:e936250.
151. Roth NC, Kim A, Vitkovski T, Xia J, Ramirez G, Bernstein D, Crawford JM. Post-COVID-19 cholangiopathy: A novel entity. *Am J Gastroenterol*. 2021; 116:1077-1082.
152. Lee A, Wein AN, Doyle MBM, Chapman WC. Liver transplantation for post-COVID-19 sclerosing cholangitis. *BMJ Case Reports*. 2021; 14:e244168.
153. Dufour JF, Marjot T, Becchetti C, Tilg H. COVID-19 and liver disease. *Gut*. 2022; 71:2350-2362.
154. Ghosh A, Anjana RM, Shanthi Rani CS, *et al*. Glycemic parameters in patients with new-onset diabetes during COVID-19 pandemic are more severe than in patients with new-onset diabetes before the pandemic: NOD COVID India Study. *Diabetes & Metabolic Syndrome*. 2021; 15:215-220.
155. Unsworth R, Wallace S, Oliver NS, Yeung S, Kshirsagar A, Naidu H, Kwong RMW, Kumar P, Logan KM. New-onset type 1 diabetes in children during COVID-19: Multicenter regional findings in the U.K. *Diabetes Care*. 2020; 43:e170-e171.
156. Li H, Tian S, Chen T, Cui Z, Shi N, Zhong X, Qiu K, Zhang J, Zeng T, Chen L, Zheng J. Newly diagnosed diabetes is associated with a higher risk of mortality than known diabetes in hospitalized patients with COVID-19. *Diabetes, Obesity & Metabolism*. 2020; 22:1897-1906.
157. Fadini GP, Morieri ML, Boscarì F, *et al*. Newly-diagnosed diabetes and admission hyperglycemia predict COVID-19 severity by aggravating respiratory deterioration. *Diabetes Res Clin Prac*. 2020; 168:108374.
158. Ebekozien OA, Noor N, Gallagher MP, Alonso GT. Type 1 Diabetes and COVID-19: Preliminary findings from a multicenter surveillance study in the U.S. *Diabetes Care*. 2020; 43:e83-e85.
159. Armeni E, Aziz U, Qamar S, Nasir S, Nethaji C, Negus R, Murch N, Beynon HC, Bouloux P, Rosenthal M, Khan S, Youssef A, Menon R, Karra E. Protracted ketonaemia in hyperglycaemic emergencies in COVID-19: A retrospective case series. *Lancet Diabetes Endocrinol*. 2020; 8:660-663.
160. Milic J, Barbieri S, Gozzi L, *et al*. Metabolic-associated fatty liver disease is highly prevalent in the postacute COVID syndrome. *Open Forum Infectious Diseases*. 2022; 9:ofac003.
161. Rodríguez Lugo DA, Coronado Tovar JJ, Solano Villamarín GA, Otero Regino W. [Primary biliary cholangitis. Part 2. State of the art, diagnosis, associated diseases, treatment and prognosis]. *Revista de Gastroenterología del Perú*. 2018; 38:64-71.
162. Faruqui S, Okoli FC, Olsen SK, *et al*. Cholangiopathy after severe COVID-19: Clinical features and prognostic implications. *Am J Gastroenterol*. 2021; 116:1414-1425.
163. Durazo FA, Kristbaum K, Miller J, Saeian K, Selim M, Hong JC. De novo autoimmune hepatitis after COVID-19 infection in an unvaccinated patient. *Case Reports Hepatol*. 2022; 2022:8409269.
164. Bowe B, Xie Y, Xu E, Al-Aly Z. Kidney outcomes in long COVID. *J Am Soc Nephrol*. 2021; 32:2851-2862.
165. Mumm JN, Osterman A, Ruzicka M, Stihl C, Vilsmaier T, Munker D, Khatamzas E, Giessen-Jung C, Stief C, Staehler M, Rodler S. Urinary frequency as a possibly overlooked symptom in COVID-19 patients: Does SARS-CoV-2 cause viral cystitis? *Eur Urol*. 2020; 78:624-628.
166. Creta M, Sagnelli C, Celentano G, *et al*. SARS-CoV-2 infection affects the lower urinary tract and male genital system: A systematic review. *J Med Virol*. 2021; 93:3133-3142.
167. Bani-Hani M, Alnifise M, Al-Zubi M, Albazee E, Al-Balawi M, Majeed H, Alhourri A. Evaluation of lower urinary tract symptoms among male COVID-19 patients during the second wave: An observational study. *Urol Ann*. 2022; 14:372-376.
168. Selvi I, Donmez MI, Ziyilan O, Oktar T. Urodynamically proven lower urinary tract dysfunction in children after COVID-19: A case series. *Low Urin Tract Symptoms*. 2022; 14:301-304.
169. Kellum JA, Lameire N, Group KAGW. Diagnosis, evaluation, and management of acute kidney injury: A KDIGO summary (Part 1). *Crit Care*. 2013; 17:204.
170. Silver SA, Beaubien-Souligny W, Shah PS, Harel S, Harel Z. The prevalence of acute kidney injury in patients hospitalized with COVID-19 infection: A systematic review and meta-analysis. *Kidney Medicine*. 2020; 3:83-98.
171. Hsu CM, Gupta S, Tighiouart H, Goyal N, Faugno AJ, Tariq A, Raichoudhury R, Sharma JH, Meyer L, Kshirsagar RK, Jose A, Leaf DE, Weiner DE, Investigators S-C. Kidney recovery and death in critically ill patients with COVID-19-associated acute kidney injury treated with dialysis: The STOP-COVID Cohort Study. *Am J Kidney Dis*. 2022; 79:404-416 e401.
172. Hirsch JS, Ng JH, Ross DW, Sharma P, Shah HH, Barnett RL, Hazzan AD, Fishbane S, Jhaveri KD, Northwell C-RC, Northwell Nephrology C-RC. Acute kidney injury in patients hospitalized with COVID-19. *Kidney Int*. 2020; 98:209-218.
173. Ng JH, Hirsch JS, Hazzan A, Wanchoo R, Shah HH, Malieckal DA, Ross DW, Sharma P, Sakhiya V, Fishbane S, Jhaveri KD, Northwell Nephrology C-RC. Outcomes among patients hospitalized with COVID-19 and acute kidney injury. *Am J Kidney Dis*. 2021; 77:204-215 e201.
174. Gu X, Huang L, Cui D, Wang Y, Wang Y, Xu J, Shang L, Fan G, Cao B. Association of acute kidney injury with 1-year outcome of kidney function in hospital survivors with COVID-19: A cohort study. *EBioMedicine*. 2022; 76:103817.
175. Xu H, Garcia-Ptacek S, Annetorp M, Bruchfeld A, Cederholm T, Johnson P, Kivipelto M, Metzner C, Religa D, Eriksdotter M. Acute kidney injury and mortality risk in older adults with COVID-19. *J Nephrol*. 2021; 34:295-304.
176. Nugent J, Aklilu A, Yamamoto Y, Simonov M, Li F, Biswas A, Ghazi L, Greenberg H, Mansour G, Moledina G, Wilson FP. Assessment of acute kidney injury and longitudinal kidney function after hospital discharge among patients with and without COVID-19. *JAMA Netw Open*. 2021; 4:e211095.
177. Cheng Y, Luo R, Wang K, Zhang M, Wang Z, Dong L, Li J, Yao Y, Ge S, Xu G. Kidney disease is associated with in-hospital death of patients with COVID-19. *Kidney Int*. 2020; 97:829-838.
178. Chaudhary K, Saha A. AKI in hospitalized patients with COVID-19. *J Amer Soc Nephrology*. 32:151-160.
179. Nadim MK, Forni LG, Mehta RL, Connor MJ, Kellum JA. Publisher Correction: COVID-19-associated acute kidney injury: Consensus report of the 25th Acute Disease Quality Initiative (ADQI) Workgroup. *Nature Reviews*

- Nephrology. 2020; 16:1-1.
180. Antonelli M, Penfold RS, Merino J, *et al.* Risk factors and disease profile of post-vaccination SARS-CoV-2 infection in UK users of the COVID Symptom Study app: A prospective, community-based, nested, case-control study. *Lancet Infect Dis.* 2022; 22:43-55.
 181. Copur S, Kanbay A, Afsar B, Elsurer Afsar R, Kanbay M. Pathological features of COVID-19 infection from biopsy and autopsy series. *Tuberk Toraks.* 2020; 68:160-167.
 182. Nadim MK, Forni LG, Mehta RL, *et al.* COVID-19-associated acute kidney injury: Consensus report of the 25th Acute Disease Quality Initiative (ADQI) Workgroup. *Nat Rev Nephrol.* 2020; 16:747-764.
 183. Long JD, Strohbahn I, Sawtell R, Bhattacharyya R, Sise ME. COVID-19 Survival and its impact on chronic kidney disease. *Transl Res.* 2022; 241:70-82.
 184. Santoriello D, Khairallah P, Bomback AS, Xu K, Kudose S, Batal I, Barasch J, Radhakrishnan J, D'Agati V, Markowitz G. Postmortem kidney pathology findings in patients with COVID-19. *J Am Soc Nephrol.* 2020; 31:2158-2167.
 185. Sharma P, Uppal NN, Wanchoo R, Shah HH, Yang Y, Parikh R, Khanin Y, Madireddy V, Larsen CP, Jhaveri KD, Bijol V, Northwell Nephrology C-RC. COVID-19-associated kidney injury: A case series of kidney biopsy findings. *J Am Soc Nephrol.* 2020; 31:1948-1958.
 186. Legrand M, Bell S, Forni L, Joannidis M, Koyner JL, Liu K, Cantaluppi V. Pathophysiology of COVID-19-associated acute kidney injury. *Nat Rev Nephrol.* 2021; 17:751-764.
 187. Golmai P, Larsen CP, DeVita MV, Wahl SJ, Weins A, Rennke HG, Bijol V, Rosenstock JL. Histopathologic and ultrastructural findings in postmortem kidney biopsy material in 12 patients with AKI and COVID-19. *J Am Soc Nephrol.* 2020; 31:1944-1947.
 188. Braun F, Lutgehetmann M, Pfefferle S, *et al.* SARS-CoV-2 renal tropism associates with acute kidney injury. *Lancet.* 2020; 396:597-598.
 189. Parra-Medina R, Herrera S, Mejia J. Systematic review of microthrombi in COVID-19 autopsies. *Acta Haematol.* 2021; 144:476-483.
 190. Su H, Yang M, Wan C, Yi LX, Tang F, Zhu HY, Yi F, Yang HC, Fogo AB, Nie X, Zhang C. Renal histopathological analysis of 26 postmortem findings of patients with COVID-19 in China. *Kidney Int.* 2020; 98:219-227.
 191. Zhang S, Liu Y, Wang X, Yang L, Hu L. SARS-CoV-2 binds platelet ACE2 to enhance thrombosis in COVID-19. *J Hematol & Oncol.* 2020; 13:120.
 192. Ng JH, Bijol V, Sparks MA, Sise ME, Izzedine H, Jhaveri KD. Pathophysiology and pathology of acute kidney injury in patients with COVID-19. *Advances in Chronic Kidney Disease.* 2020; 27.
 193. Ackermann M, Anders HJ, Bilyy R, *et al.* Patients with COVID-19: in the dark-NETs of neutrophils. *Cell Death Differ.* 2021; 28:3125-3139.
 194. Veras FP, Pontelli MC, Silva CM, *et al.* SARS-CoV-2-triggered neutrophil extracellular traps mediate COVID-19 pathology. *J Exp Med.* 2020; 217.
 195. Wu H, Larsen P, Hernandez-Arroyo C, Muner M, Caza T, Sharshir M, Chughtai A, Xie L, Gimenez J, Sandow T, Lusco M, Yang H, Acheampong E, Rosales I, Colvin R, Fogo A, Velez J. AKI and collapsing glomerulopathy associated with COVID-19 and APOL1 high-risk genotype. *J Amer Soc Nephrol.* 2020; 31.
 196. Nichols B, Jog P, Lee J, Blackler D, Wilmot M, D'Agati V, Markowitz G, Kopp J, Alper S, Pollack M, Friedman D. Innate immunity pathways regulate the nephropathy gene Apolipoprotein L1. *Kidney Int.* 2015; 87:332-342.
 197. Ferlicot S, Jamme M, Gaillard F, *et al.* The spectrum of kidney biopsies in hospitalized patients with COVID-19, acute kidney injury, and/or proteinuria. *Nephrol Dial Transplant.* 2021; Feb 12:gfab042.
 198. Peleg Y, Kudose S, D'Agati V, Siddall E, Ahmad S, Nickolas T, Kisselev S, Gharavi A, Canetta P. Acute kidney injury due to collapsing glomerulopathy following COVID-19 infection. *Kidney Int Rep.* 2020; 5:940-945.
 199. Nasr SH, Alexander MP, Cornell LD, Herrera LH, Fidler ME, Said SM, Zhang P, Larsen CP, Sethi S. Kidney biopsy findings in patients with COVID-19, kidney injury, and proteinuria. *Am J Kidney Dis.* 2021; 77:465-468.
 200. Chaudhri I, Moffitt R, Taub E, *et al.* Association of proteinuria and hematuria with acute kidney injury and mortality in hospitalized patients with COVID-19. *Kidney Blood Press Res.* 2020; 45:1018-1032.
 201. Menez S, Parikh CR. COVID-19 and the kidney: Recent advances and controversies. *Semin Nephrol.* 2022; 42:151279.
 202. Malik P, Patel U, Mehta D, Patel N, Kelkar R, Akrmah M, Gabrilove JL, Sacks H. Biomarkers and outcomes of COVID-19 hospitalisations: Systematic review and meta-analysis. *BMJ Evid Based Med.* 2021; 26:107-108.
 203. Bezerra GF, Meneses GC, Albuquerque PL, *et al.* Urinary tubular biomarkers as predictors of death in critically ill patients with COVID-19. *Biomark Med.* 2022; 16:681-692.
 204. Parikh CR, Coca SG, Thiessen-Philbrook H, *et al.* Postoperative biomarkers predict acute kidney injury and poor outcomes after adult cardiac surgery. *J Am Soc Nephrol.* 2011; 22:1748-1757.
 205. Menez S, Moledina DG, Thiessen-Philbrook H, *et al.* Prognostic significance of urinary biomarkers in patients hospitalized with COVID-19. *Am J Kidney Dis.* 2022; 79:257-267 e251.
 206. Xu K, Shang N, Levitman A, Corker A, Kudose S, Yaeh A, Neupane U, Stevens J, Sampogna R, Mills AM, D'Agati V, Mohan S, Kiryluk K, Barasch J. Elevated neutrophil gelatinase-associated lipocalin is associated with the severity of kidney injury and poor prognosis of patients with COVID-19. *Kidney Int Rep.* 2021; 6:2979-2992.
 207. Sancho Ferrando E, Hanslin K, Hultstrom M, Larsson A, Frithiof R, Lipcsey M, Uppsala Intensive Care C-RG. Soluble TNF receptors predict acute kidney injury and mortality in critically ill COVID-19 patients: A prospective observational study. *Cytokine.* 2022; 149:155727.
 208. Menez S, Coca S, Moledina D, Wen Y, Chan L, Philbrook H, Obeid W, Azeloglu E, Wilson F, Parikh C. Plasma TNFR1 predicts major adverse kidney events in hospitalized patients with COVID-19. *J Amer Soc Nephrol.* 2021; 59-60.
 209. Joannidis M, Forni LG, Klein SJ, *et al.* Lung-kidney interactions in critically ill patients: consensus report of the Acute Disease Quality Initiative (ADQI) 21 Workgroup. *Intensive Care Med.* 2020; 46:654-672.
 210. Parolin M, Parisotto M, Zanchetta F, Sartorato P, De Menis E. Coronaviruses and endocrine system: A systematic review on evidence and shadows. *Endocr Metab Immune Disord Drug Targets.* 2021; 21:1242-1251.
 211. Frara S, Loli P, Allora A, Santini C, di Filippo L, Mortini P, Fleseriu M, Giustina A. COVID-19 and hypopituitarism. *Rev Endocr Metab Disord.* 2022; 23:215-231.
 212. Frara S, Allora A, Castellino L, di Filippo L, Loli P,

- Giustina A. COVID-19 and the pituitary. *Pituitary*. 2021; 24:465-481.
213. Gu WT, Zhou F, Xie WQ, Wang S, Yao H, Liu YT, Gao L, Wu ZB. A potential impact of SARS-CoV-2 on pituitary glands and pituitary neuroendocrine tumors. *Endocrine*. 2021; 72:340-348.
214. Puig-Domingo M, Marazuela M, Yildiz BO, Giustina A. COVID-19 and endocrine and metabolic diseases. An updated statement from the European Society of Endocrinology. *Endocrine*. 2021; 72:301-316.
215. Carosi G, Morelli V, Del Sindaco G, *et al.* Adrenal insufficiency at the time of COVID-19: A retrospective study in patients referring to a tertiary center. *J Clin Endocrinol Metab*. 2021; 106:e1354-e1361.
216. Urhan E, Karaca Z, Unuvar GK, Gundogan K, Unluhizarci K. Investigation of pituitary functions after acute coronavirus disease 2019. *Endocr J*. 2022; 69:649-658.
217. Yoshimura K, Yamamoto M, Inoue T, Fukuoka H, Iida K, Ogawa W. Coexistence of growth hormone, adrenocorticotrophic hormone, and testosterone deficiency associated with coronavirus disease 2019: A case followed up for 15 months. *Endocr J*. 2022; 69:1335-1342.
218. Christ-Crain M, Hoorn EJ, Sherlock M, Thompson CJ, Wass J. Endocrinology in the time of COVID-19-2021 updates: The management of diabetes insipidus and hyponatraemia. *Eur J Endocrinol*. 2021; 185:G35-G42.
219. Kanczkowski W, Evert K, Stadtmuller M, *et al.* COVID-19 targets human adrenal glands. *Lancet Diabetes Endocrinol*. 2022; 10:13-16.
220. Zinserling VA, Semenova NY, Markov AG, Rybalchenko OV, Wang J, Rodionov RN, Bornstein SR. Inflammatory cell infiltration of adrenals in COVID-19. *Horm Metab Res*. 2020; 52:639-641.
221. Alzahrani AS, Mukhtar N, Aljomaiah A, Aljamei H, Bakhsh A, Alsudani N, Elsayed T, Alrashidi N, Fadel R, Alqahtani E, Raef H, Butt MI, Sulaiman O. The impact of COVID-19 viral infection on the hypothalamic-pituitary-adrenal axis. *Endocr Pract*. 2021; 27:83-89.
222. Tan T, Khoo B, Mills EG, Phylactou M, Patel B, Eng PC, Thurston L, Muzi B, Meeran K, Prevost AT, Comminos AN, Abbara A, Dhillo WS. Association between high serum total cortisol concentrations and mortality from COVID-19. *Lancet Diabetes Endocrinol*. 2020; 8:659-660.
223. Gonen MS, De Bellis A, Durcan E, Bellastella G, Cirillo P, Scappaticcio L, Longo M, Bircan BE, Sahin S, Sulu C, Ozkaya HM, Konukoglu D, Kartufan FF, Kelestimir F. Assessment of neuroendocrine changes and hypothalamo-pituitary autoimmunity in patients with COVID-19. *Horm Metab Res*. 2022; 54:153-161.
224. Scappaticcio L, Pitoia F, Esposito K, Piccardo A, Trimboli P. Impact of COVID-19 on the thyroid gland: An update. *Rev Endocr Metab Disord*. 2021; 22:803-815.
225. Khoo B, Tan T, Clarke SA, Mills EG, Patel B, Modi M, Phylactou M, Eng PC, Thurston L, Alexander EC, Meeran K, Comminos AN, Abbara A, Dhillo WS. Thyroid function before, during, and after COVID-19. *J Clin Endocrinol Metab*. 2021; 106:e803-e811.
226. Lui DTW, Lee CH, Chow WS, Lee ACH, Tam AR, Fong CHY, Law CY, Leung EKH, To KKW, Tan KCB, Woo YC, Lam CW, Hung IFN, Lam KSL. Role of non-thyroidal illness syndrome in predicting adverse outcomes in COVID-19 patients predominantly of mild-to-moderate severity. *Clin Endocrinol (Oxf)*. 2021; 95:469-477.
227. Trimboli P, Cappelli C, Croce L, Scappaticcio L, Chiovato L, Rotondi M. COVID-19-Associated Subacute Thyroiditis: Evidence-based data from a systematic review. *Front Endocrinol (Lausanne)*. 2021; 12:707726.
228. Lisco G, De Tullio A, Jirillo E, Giagulli VA, De Pergola G, Guastamacchia E, Triggiani V. Thyroid and COVID-19: A review on pathophysiological, clinical and organizational aspects. *J Endocrinol Invest*. 2021; 44:1801-1814.
229. Foldi M, Farkas N, Kiss S, Dembrovszky F, Szakacs Z, Balasko M, Eross B, Hegyi P, Szentesi A. Visceral adiposity elevates the risk of critical condition in COVID-19: A systematic review and meta-analysis. *Obesity (Silver Spring)*. 2021; 29:521-528.
230. Hendren NS, de Lemos JA, Ayers C, Das SR, Rao A, Carter S, Rosenblatt A, Walchok J, Omar W, Khera R, Hegde AA, Drazner MH, Neeland IJ, Grodin JL. Association of body mass index and age with morbidity and mortality in patients hospitalized with COVID-19: Results from the American Heart Association COVID-19 Cardiovascular Disease Registry. *Circulation*. 2021; 143:135-144.
231. Anderson MR, Shashaty MGS. Impact of obesity in critical illness. *Chest*. 2021; 160:2135-2145.
232. Aghili SMM, Ebrahimpur M, Arjmand B, Shadman Z, Pejman Sani M, Qorbani M, Larijani B, Payab M. Obesity in COVID-19 era, implications for mechanisms, comorbidities, and prognosis: A review and meta-analysis. *Int J Obes (Lond)*. 2021; 45:998-1016.
233. Stefan N, Birkenfeld AL, Schulze MB. Global pandemics interconnected - Obesity, impaired metabolic health and COVID-19. *Nat Rev Endocrinol*. 2021; 17:135-149.
234. De Rubeis V, Gonzalez A, de Groh M, Jiang Y, Erbas Oz U, Tarride JE, Basta NE, Kirkland S, Wolfson C, Griffith LE, Raina P, Anderson LN, Canadian Longitudinal Study on Aging T. Obesity and adverse childhood experiences in relation to stress during the COVID-19 pandemic: An analysis of the Canadian Longitudinal Study on Aging. *Int J Obes (Lond)*. 2023; 1-10.
235. Valenzuela G, Alarcon-Andrade G, Schulze-Schiapacasse C, *et al.* Short-term complications and post-acute sequelae in hospitalized paediatric patients with COVID-19 and obesity: A multicenter cohort study. *Pediatr Obes*. 2023; 18:e12980.
236. Berg SK, Birk NM, Thorsted AB, Rosenkilde S, Jensen LB, Nygaard U, Bundgaard H, Thygesen LC, Ersboll AK, Nielsen SD, Christensen AV. Risk of body weight changes among Danish children and adolescents during the COVID-19 pandemic. *Pediatr Obes*. 2023; e13005.
237. Peter RS, Nieters A, Brockmann SO, Gopel S, Kindle G, Merle U, Steinacker JM, Kern WV, Rothenbacher D, Group EPS. Association of BMI with general health, working capacity recovered, and post-acute sequelae of COVID-19. *Obesity (Silver Spring)*. 2023; 31:43-48.
238. Unnikrishnan R, Misra A. Diabetes and COVID19: A bidirectional relationship. *Nutr Diabetes*. 2021; 11:21.
239. Shin J, Toyoda S, Nishitani S, Onodera T, Fukuda S, Kita S, Fukuhara A, Shimomura I. SARS-CoV-2 infection impairs the insulin/IGF signaling pathway in the lung, liver, adipose tissue, and pancreatic cells *via* IRF1. *Metabolism*. 2022; 133:155236.
240. Paneni F, Patrono C. Increased risk of incident diabetes in patients with long COVID. *Eur Heart J*. 2022; 43:2094-2095.
241. Montefusco L, Ben Nasr M, D'Addio F, *et al.* Acute and long-term disruption of glycometabolic control after SARS-CoV-2 infection. *Nat Metab*. 2021; 3:774-785.

242. Lim S, Bae JH, Kwon HS, Nauck MA. COVID-19 and diabetes mellitus: From pathophysiology to clinical management. *Nat Rev Endocrinol.* 2021; 17:11-30.
243. Laurenzi A, Caretto A, Molinari C, Mercalli A, Melzi R, Nano R, Tresoldi C, Rovere Querini P, Ciceri F, Lampasona V, Bosi E, Scavini M, Piemonti L. No Evidence of long-term disruption of glycometabolic control after SARS-CoV-2 infection. *J Clin Endocrinol Metab.* 2022; 107:e1009-e1019.
244. Rezel-Potts E, Douiri A, Sun X, Chowieńczyk PJ, Shah AM, Gulliford MC. Cardiometabolic outcomes up to 12 months after COVID-19 infection. A matched cohort study in the UK. *PLoS Med.* 2022; 19:e1004052.
245. Fernandez-de-Las-Penas C, Guijarro C, Torres-Macho J, Velasco-Arribas M, Plaza-Canteli S, Hernandez-Barrera V, Arias-Navalon JA. Diabetes and the risk of long-term post-COVID symptoms. *Diabetes.* 2021; 70:2917-2921.
246. Mittal J, Ghosh A, Bhatt SP, Anoop S, Ansari IA, Misra A. High prevalence of post COVID-19 fatigue in patients with type 2 diabetes: A case-control study. *Diabetes & metabolic syndrome.* 2021; 15:102302.
247. Khunti K, Kosiborod M, Ray KK. Legacy benefits of blood glucose, blood pressure and lipid control in individuals with diabetes and cardiovascular disease: Time to overcome multifactorial therapeutic inertia? *Diabetes, obesity & metabolism.* 2018; 20:1337-1341.
248. Narayan KMV, Staimez LR. Rising diabetes diagnosis in long COVID. *Lancet Diabetes Endocrinol.* 2022; 10:298-299.
249. Nguyen NN, Ho DS, Nguyen HS, Ho DKN, Li HY, Lin CY, Chiu HY, Chen YC. Preadmission use of antidiabetic medications and mortality among patients with COVID-19 having type 2 diabetes: A meta-analysis. *Metabolism.* 2022; 131:155196.
250. Chen Y, Lv X, Lin S, Arshad M, Dai M. The association between antidiabetic agents and clinical outcomes of COVID-19 patients with diabetes: A Bayesian network meta-analysis. *Front Endocrinol (Lausanne).* 2022; 13:895458.
251. Kahkoska AR, Abrahamson TJ, Alexander GC, Bennett TD, Chute CG, Haendel MA, Klein KR, Mehta H, Miller JD, Moffitt RA, Sturmer T, Kvist K, Buse JB, Consortium NC. Association between glucagon-like peptide 1 receptor agonist and sodium-glucose cotransporter 2 inhibitor use and COVID-19 outcomes. *Diabetes Care.* 2021; 44:1564-1572.
252. Singh AK, Singh R, Saboo B, Misra A. Non-insulin anti-diabetic agents in patients with type 2 diabetes and COVID-19: A critical appraisal of literature. *Diabetes & Metabolic Syndrome.* 2021; 15:159-167.
253. Zelniker TA, Wiviott SD, Raz I, *et al.* Comparison of the effects of glucagon-like peptide receptor agonists and sodium-glucose cotransporter 2 inhibitors for prevention of major adverse cardiovascular and renal outcomes in type 2 diabetes mellitus. *Circulation.* 2019; 139:2022-2031.
254. Tipnis SR, Hooper NM, Hyde R, Karran E, Christie G, Turner AJ. A human homolog of angiotensin-converting enzyme. Cloning and functional expression as a captopril-insensitive carboxypeptidase. *J Biol Chem.* 2000; 275:33238-33243.
255. Sharp GC, Fraser A, Sawyer G, Kountourides G, Easey KE, Ford G, Olszewska Z, Howe LD, Lawlor DA, Alvergne A, Maybin JA. The COVID-19 pandemic and the menstrual cycle: Research gaps and opportunities. *Int J Epidemiol.* 2022; 51:691-700.
256. Thomas N, Gurvich C, Huang K, Gooley PR, Armstrong CW. The underlying sex differences in neuroendocrine adaptations relevant to Myalgic Encephalomyelitis Chronic Fatigue Syndrome. *Front Neuroendocrinol.* 2022; 66:100995.
257. Harirugsakul K, Wainipitapong S, Phannajit J, Paitoonpong L, Tantiwongse K. Erectile dysfunction among Thai patients with COVID-19 infection. *Transl Androl Urol.* 2021; 10:4376-4383.
258. Takmaz T, Gundogmus I, Okten SB, Gunduz A. The impact of COVID-19-related mental health issues on menstrual cycle characteristics of female healthcare providers. *J Obstet Gynaecol Res.* 2021; 47:3241-3249.
259. Sansone A, Mollaioli D, Ciocca G, Colonnello E, Limoncin E, Balercia G, Jannini EA. "Mask up to keep it up": Preliminary evidence of the association between erectile dysfunction and COVID-19. *Andrology.* 2021; 9:1053-1059.
260. Kresch E, Achua J, Saltzman R, Khodamoradi K, Arora H, Ibrahim E, Kryvenko ON, Almeida VW, Firdaus F, Hare JM, Ramasamy R. COVID-19 endothelial dysfunction can cause erectile dysfunction: Histopathological, immunohistochemical, and ultrastructural study of the human penis. *World J Mens Health.* 2021; 39:466-469.
261. Kaynar M, Gomes ALQ, Sokolakis I, Gul M. Tip of the iceberg: Erectile dysfunction and COVID-19. *Int J Impot Res.* 2022; 34:152-157.
262. Maleki BH, Tartibian B. COVID-19 and male reproductive function: A prospective, longitudinal cohort study. *Reproduction.* 2021; 161:319-331.
263. Haghpanah A, Masjedi F, Alborzi S, Hosseinpour A, Dehghani A, Malekmakan L, Roozbeh J. Potential mechanisms of SARS-CoV-2 action on male gonadal function and fertility: Current status and future prospects. *Andrologia.* 2021; 53:e13883.
264. Sun X, Lyu J. A short review of male genito-urinary lesions caused by coronavirus disease 2019. *Curr Urol.* 2022; 16:63-64.
265. Ediz C, Tavukcu HH, Akan S, Kizilkan YE, Alcin A, Oz K, Yilmaz O. Is there any association of COVID-19 with testicular pain and epididymo-orchitis? *Int J Clin Pract.* 2021; 75:e13753.
266. Shields LBE, Daniels MW, Peppas DS, White JT, Mohamed AZ, Canalichio K, Rosenberg S, Rosenberg E. Surge in testicular torsion in pediatric patients during the COVID-19 pandemic. *J Pediatr Surg.* 2022; 57:1660-1663.
267. Chadchan SB, Popli P, Maurya VK, Kommagani R. The SARS-CoV-2 receptor, angiotensin-converting enzyme 2, is required for human endometrial stromal cell decidualization. *Biol Reprod.* 2021; 104:336-343.
268. Ding T, Wang T, Zhang J, Cui P, Chen Z, Zhou S, Yuan S, Ma W, Zhang M, Rong Y, Chang J, Miao X, Ma X, Wang S. Analysis of ovarian injury associated with COVID-19 disease in reproductive-aged women in Wuhan, China: An observational study. *Front Med (Lausanne).* 2021; 8:635255.
269. Li K, Chen G, Hou H, Liao Q, Chen J, Bai H, Lee S, Wang C, Li H, Cheng L, Ai J. Analysis of sex hormones and menstruation in COVID-19 women of child-bearing age. *Reprod Biomed Online.* 2021; 42:260-267.
270. Nguyen BT, Pang RD, Nelson AL, Pearson JT, Benhar Nocchioli E, Reissner HR, Kraker von Schwarzenfeld A, Acuna J. Detecting variations in ovulation and

- menstruation during the COVID-19 pandemic, using real-world mobile app data. *PLoS One*. 2021; 16:e0258314.
271. Jahan N. Bleeding during the pandemic: The politics of menstruation. *Sex Reprod Health Matters*. 2020; 28:1801001.
272. Male V. Menstrual changes after covid-19 vaccination. *BMJ*. 2021; 374:n2211.
273. Medina-Perucha L, Lopez-Jimenez T, Holst AS, Jacques-Avino C, Munros-Feliu J, Martinez-Bueno C, Valls-Llobet C, Pinzon-Sanabria D, Vicente-Hernandez MM, Berenguera A. Self-reported menstrual alterations during the COVID-19 syndemic in Spain: A cross-sectional study. *Int J Womens Health*. 2022; 14:529-544.
274. Tammaro A, Parisella FR, Adebajo GAR. Cutaneous long COVID. *J Cosmet Dermatol*. 2021; 20:2378-2379.
275. McMahon DE, Gallman AE, Hruza GJ, Rosenbach M, Lipoff JB, Desai SR, French LE, Lim H, Cyster JG, Fox LP, Fassett MS, Freeman EE. Long COVID in the skin: A registry analysis of COVID-19 dermatological duration. *Lancet Infect Dis*. 2021; 21:313-314.
276. Mirza FN, Malik AA, Omer SB, Sethi A. Dermatologic manifestations of COVID-19: A comprehensive systematic review. *Int J Dermatol*. 2021; 60:418-450.
277. Garrigues E, Janvier P, Kherabi Y, *et al*. Post-discharge persistent symptoms and health-related quality of life after hospitalization for COVID-19. *J Infect*. 2020; 81:e4-e6.
278. Kim J, Hong K, Gomez RE, Kim S, Chun BC. Lack of evidence of COVID-19 being a risk factor of alopecia areata: Results of a national cohort study in South Korea. *Front Med (Lausanne)*. 2021; 8:758069.

Received February 12, 2023; Revised March 9, 2023; Accepted March 12, 2023.

§These authors contributed equally to this work.

*Address correspondence to:

Hongzhou Lu, Department of Infectious Diseases, National Clinical Research Center for Infectious Diseases, the Third People's Hospital of Shenzhen, 29 Bulan Road, Shenzhen, Guangdong 518112, China.
E-mail: luhongzhou@fudan.edu.cn

Yingxia Liu, Department of Infectious Diseases, National Clinical Research Center for Infectious Diseases, the Third People's Hospital of Shenzhen, 29 Bulan Road, Shenzhen, Guangdong 518112, China.
E-mail: szsy_lyx@szsy.sustech.edu.cn

Tetsuya Asakawa, Institute of Neurology, National Clinical Research Center for Infectious Diseases, the Third People's Hospital of Shenzhen, 29 Bulan Road, Shenzhen, Guangdong 518112, China.
E-mail: asakawat1971@gmail.com

Released online in J-STAGE as advance publication March 14, 2023.

Improving the sensitivity of liver tumor classification in ultrasound images *via* a power-law shot noise model

Kenji Karako¹, Yuichiro Mihara², Kiyoshi Hasegawa², Yu Chen^{1,*}

¹Department of Human and Engineered Environmental Studies, Graduate School of Frontier Sciences, The University of Tokyo, Chiba, Japan;

²Artificial Organ and Transplantation Surgery Division, Department of Surgery, Graduate School of Medicine, The University of Tokyo, Tokyo, Japan.

SUMMARY Power laws have been observed in various fields and help us understand natural phenomena. Power laws have also been observed in ultrasound images. This study used the power spectrum of the signal identified from the reflected ultrasound signal observed in ultrasonography based on the power-law shot noise (PLSN) model. The power spectrum follows a power law, which has a scaling factor that depends on the characteristics of the tissue in the region where the ultrasound wave propagates. To distinguish between a tumor and blood vessels in the liver, we propose a classification model that includes a scaling factor based on ResNet, a deep learning model for image classification. In a task to classify 6 types of tissue - a tumor, the inferior vena cava, the descending aorta, the Gleason sheath, the hepatic vein, and small blood vessels – tumor sensitivity increased 3.8% and the F-score for a tumor improved 2% while precision was maintained. The scaling factor obtained using the PLSN model was validated for classification of liver tumors.

Keywords ultrasonography, liver, deep learning, classification, power-law shot noise model

1. Introduction

Power laws occur and are observed in various scientific fields, and they are useful for understanding natural and man-made phenomena. The characteristics of power laws are used in economics and finance, and the scaling factors are used for prediction (1-3). The medical field is no exception, and power laws are also observed in ultrasonography.

Ultrasonography is a method widely used to image body tissues because it is relatively safe, versatile, low cost, and mobile. However, ultrasonography has the disadvantages of a low resolution and unclear images compared to other imaging methods such as X-rays, magnetic resonance imaging (MRI), and computerized tomography (CT) scans. One task for which ultrasonography is often used is to diagnose liver cancer. In Japanese guidelines for diagnosis of liver cancer, ultrasonography is the method of choice for screening at-risk patients (4). However, pathologists need experience and medical knowledge to accurately diagnose liver cancer. Factors such as contrast-based images, cross-sectional images, and changing shapes depending on the probe angle hamper the identification of parts of the liver in ultrasound images, even with medical knowledge. Experience helps to combine

medical knowledge with diverse structures in ultrasound images to correctly understand the intrahepatic region. Despite the convenience of ultrasonography, its drawback is that the examination can only be performed at a large hospital by a liver specialist.

Several studies have sought to determine the features of structures in ultrasound images in order to facilitate a diagnosis (5-7). Studies have sought to determine the characteristics of ultrasound waves propagated by a structure using the power-law shot noise (PLSN) model (8-10). An ultrasound image is obtained by converting the amplitude of the ultrasound waves emitted by the probe and reflected by structures scattering those waves in a given region into brightness. Previous studies have proposed that the amplitude of this reflected ultrasound wave can be represented by the PLSN model. Since the frequency characteristics of this amplitude follow a power law and the scaling factor of a power law differs depending on the characteristics of the structure propagating waves, they can presumably be used as a feature to distinguish between tissues. A previous study applied this PLSN model to ultrasound images of the breast, allowing breast cancer tissue to be distinguished from normal breast tissue. Such features can presumably be used to aid in diagnosis in areas such as liver cancer that require skill and experience.

At present, the PLSN model has not been applied to ultrasound images other than those of breast cancer.

The current study has focused on the fact that cancer tissue and normal tissue can be distinguished by the PLSN model and that this model can be used to diagnose ultrasound images of liver cancer, a task that requires skill for a precise diagnosis. First, in order to verify whether the PLSN model can be applied to ultrasound images of liver cancer, this study evaluated whether the frequency characteristics reveal the scaling factor according to the power law. Next, this study compared and evaluated whether liver cancer, blood vessels, and liver tissue can be distinguished based on scaling factors. In addition, this study constructed a neural network-based classifier using the scaling factors and it evaluated whether the scaling factors facilitate classification of structures.

The paper is organized as follows. Section 2.1 provides an overview of the PLSN model applied to ultrasonography. Section 2.2, 2.3 provides a method for determining scaling factors for ultrasound images of the liver using the PLSN model. Section 2.4 presents a configuration of a neural network-based classifier using scaling factors. Section 2.5 provides training and evaluation data for the neural network-based classifier. Section 3 provides an evaluation and results for classification of liver cancer, the inferior vena cava, the descending aorta, the Gleason sheath, the hepatic vein, and small blood vessels. Finally, concluding remarks are described in Section 4.

2. Materials and Methods

2.1. The PLSN model for ultrasonography

In ultrasonography, tissues in the body are usually modeled as regions containing randomly distributed structures that scatter ultrasound waves (scatterers), with each one independently affecting backscattering. In the PLSN model, the sum of all such backscattered signals that are received by the transducer is the reflected signal (10-13):

$$r(t) = \sum_i h(t, t_i, \mathbf{x}_i, \boldsymbol{\psi}_i), \quad (2.1)$$

where t is the time of observation; t_i are the times when independent backscattered pulses $h(\cdot)$ occur and are assumed to be random events taken from a non-homogeneous Poisson process with rate $\lambda(t)$; \mathbf{x}_i is the vector denoting the position of the i th scatterer from the transducer; and $\boldsymbol{\psi}_i$ is a random vector that characterizes the amplitude, phase, scale and duration of each backscattered pulse.

Let us focus on reflected signals generated from scatterers at approximately the same depth in tissue. We will also assume that the medium is stationary in the corresponding small segment of tissue and that the

scatterer's density, attenuation properties, and medium properties are constant. In addition, we will assume that there are no strong specular reflectors in the scattering region. Based on these assumptions, \mathbf{x}_i can be regarded as roughly constant, and the general model in (2.1) can be simplified as follows (10,12,13):

$$r(t) = \sum_i h(t - t_i, \boldsymbol{\psi}_i). \quad (2.2)$$

Because of the stationarity assumption, the t_i 's $h(\cdot)$ are random events from a homogeneous Poisson process with a constant rate λ . Moreover, since each pulse is a reflected pulse of the ultrasound signal from the probe, it can be assumed to be of the form (10):

$$\begin{aligned} h(t - t_i, \boldsymbol{\psi}_i) &= e(t - t_i, a_i) \cos(\omega_c(t - t_i) + \phi_i) \\ &= e_c(t - t_i, a_i) \cos(\omega_c t) - e_s(t - t_i, a_i) \sin(\omega_c t), \end{aligned} \quad (2.3)$$

where $e_c(t - t_i, a_i) = e(t - t_i, a_i) \cos(\phi_i - \omega_c t_i)$ and $e_s(t - t_i, a_i) = e(t - t_i, a_i) \sin(\phi_i - \omega_c t_i)$ are respectively the in-phase and quadrature components; ω_c is the center frequency of the ultrasound signal; $e(t - t_i, a_i)$ is the envelope of the backscattered pulse with a_i specifying its amplitude, and ϕ_i is a random phase. The sum of the scattered signals given by (2.2) is as follows (10):

$$\begin{aligned} r(t) &= r_c(t) \cos(\omega_c t) - r_s(t) \sin(\omega_c t), \\ r_c(t) &= \sum_i e(t - t_i, a_i) \cos(\phi_i - \omega_c t_i), \end{aligned} \quad (2.4)$$

$$r_s(t) = \sum_i e(t - t_i, a_i) \sin(\phi_i - \omega_c t_i). \quad (2.5)$$

Furthermore, we will assume that the envelope can be described by (10,14):

$$e(t - t_i, a_i) = a_i(t - t_i)^{-\nu} u(t - t_i), \quad (2.6)$$

where $u(t)$ is the unit step function; ϕ_i , a_i , and t_i are respectively assumed to be independent random variables with probability density functions uniform in $[0, 2\pi)$, $f_a(a) = f_a(-a)$, and the Poisson process; and ν is a parameter determined by the characteristics of the area of propagation.

For $0 < \nu \leq 0.5$, research has shown that the sample power spectrum $S(f)$ with regard to $r_c(t)$ or $r_s(t)$ exists and follows a $1/f^\beta$ -type behavior with $\beta = 2(1 - \nu)$ (14), as described by

$$S(f) = \lambda E[a^2] \Gamma^2(\beta/2) (2\pi f)^{-\beta}, \quad (2.7)$$

where $\Gamma(\cdot)$ is the gamma function (15), and $E[a^2]$ denotes the expected value of the square of the random amplitude a .

Let $|r(t)| = \sqrt{r_c^2(t) + r_s^2(t)}$ be the envelope of the backscattered signal. The power spectrum of the envelope was derived and has been shown to take a power-law form with exponent β_{env} based on numerical

evaluation (9).

In-phase and quadrature components can presumably be obtained from actual data $r(t)$ using a Hilbert transform as follows (9).

$$r_c(t) = \cos(\omega_c t) r(t) + \sin(\omega_c t) \bar{r}(t) \tag{2.8}$$

$$r_s(t) = \cos(\omega_c t) \bar{r}(t) + \sin(\omega_c t) r(t) \tag{2.9}$$

where $\bar{r}(t)$ is the Hilbert transform of $r(t)$. The envelope is obtained by

$$|r(t)| = \sqrt{r_c^2(t) + r_s^2(t)}. \tag{2.10}$$

The above calculation requires the center frequency ω_c of the ultrasound wave. The center frequency changes as the ultrasound wave propagates, and the exact value is not known. Therefore, the following method has been proposed (9).

$$\hat{\omega}_c = 2\pi \frac{\int f S_{nb}(f) df}{\int S_{nb}(f) df}, \tag{2.11}$$

Here, $S_{nb}(f)$ denotes the periodogram of the modulated ultrasound signal.

When applying the PLSN model to an actual ultrasound image, the reflected ultrasound signal $r(t)$ observed from the probe corresponds to the pixel values on the ultrasound signal path shown in Figure 1. The power spectrum can be obtained by calculating each component based on Equations 2.8-11 and performing a fast Fourier transform.

2.2. Calculation of scaling factors from ultrasound images of the liver

There are three steps in obtaining the scaling factor from the ultrasound image of the liver based on the PLSN model. The first step is the transformation of ultrasound images of the liver and the identification of reflected ultrasound signals. The second step is to calculate the power spectrum of reflected ultrasound signals and

to determine scaling factors from the power spectrum following the power law.

In the first step, to obtain the scaling factor based on the PLSN model, the reflected ultrasound signal has to be obtained from the region of propagation. This signal is a signal reflected back to the probe, and the pixel value on the ultrasound image represents the signal as shown in Figure 1. In the previous study that applied the PLSN to ultrasound images of the breast, the path of this reflected signal was in the vertical direction of the image, but in the ultrasound image of the liver, it radiates out from the top of image as shown in Figure 1. In order to determine the radial ultrasound signal, the signal is transformed vertically using piecewise affine transformation as shown in Figure 2. The scikit-image library is used for implementation (16). Specifically, the eight points in Figure 2 are correspondingly converted with piecewise affine transformation. The vertical pixel values of the transformed image are used as the reflected ultrasound signal $r(t)$ to calculate the scaling factor from step 2 onward.

In the second step, the vertical component is the ultrasound signal $r(t)$, and the cos component $r_c(t)$, sin component $r_s(t)$, and envelope component $|r(t)|$ of the ultrasound signal are calculated based on Equations 2.8-11. The power spectrum is calculated using the periodogram implemented by scipy (17) for these three components. Next, for each power spectrum and frequency, the logarithm is calculated. The slope is determined using linear regression provided by scikit-learn (18), and this is used as the scaling factor. A sample calculation based on the above is shown in Figure 3. In Figure 3, 300 pixels of continuous data in the direction of the y-axis are identified from the converted ultrasound image as the reflected ultrasound signal $r(t)$, and the power spectrum of the cos component, sin component, and envelope component are calculated and shown in a log-log graph. The slope of the graph is the scaling factor. Figure 3 shows that each component can be plotted as a straight line, although there is a lot of noise

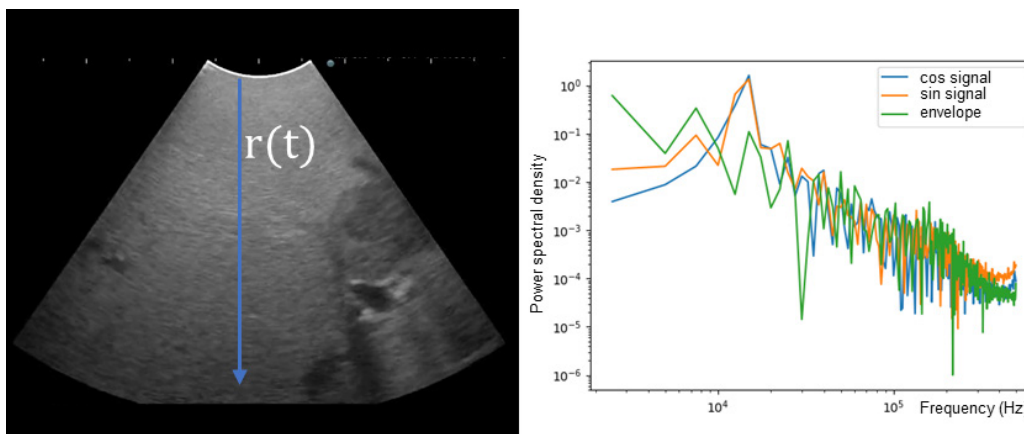


Figure 1. Power spectrum of the reflected ultrasound signal $r(t)$ in ultrasound images of the liver incorporating a power-law shot noise model. The power spectrum was calculated for the cos component, sin component, and envelope of the signal.

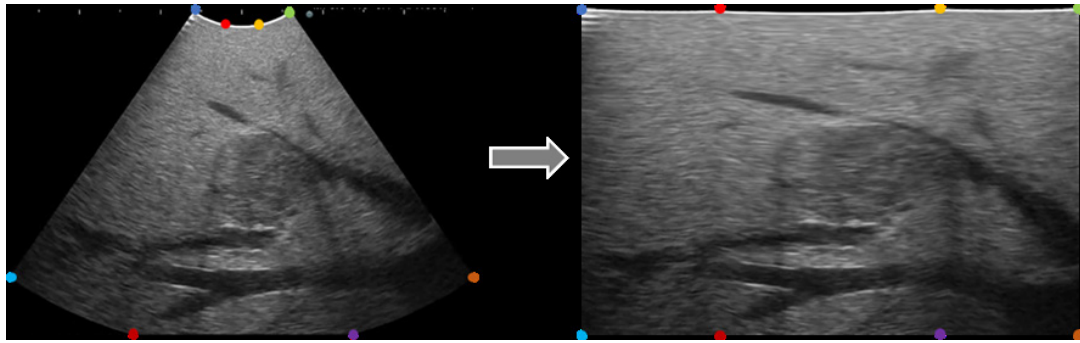


Figure 2. Ultrasound image of the liver transformed by piecewise affine transformation. The direction of signal propagation is unified vertically so that PLSN can be applied to the entire image.

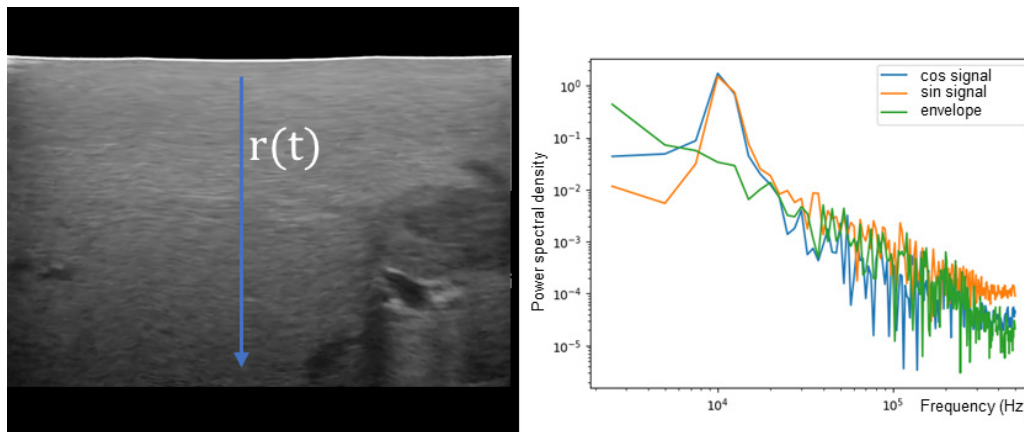


Figure 3. Example of the power spectrum for an image after application of a piecewise affine transformation.

at low and high frequencies, indicating that the power law is obeyed.

2.3. Evaluation of the possibility of distinguishing structures using scaling factors

This section will examine the possibility of distinguishing structures in the liver using scaling factors calculated from actual ultrasound images of the liver. In a previous study, the PLSN model was used to distinguish between cancer tissue and normal breast tissue. Unlike the breast, the liver can contain a tumor as well as the liver parenchyma many blood vessels and other organs. Therefore, the PLSN model has been applied to actual sample data and the frequency characteristics and scaling factors of the calculated reflected waves have been compared. The sample data was from the region indicated in Figure 4 using 3 images including liver cancer and blood vessels. All of the regions were cropped with a width of 50, and 50 reflected ultrasound signals $r(t)$ were included within the region. For each of the 50 signals, the scaling factors for the cos component $r_c(t)$, sin component $r_s(t)$, and envelope component $|r(t)|$ were calculated, and the average of the 50 signals is shown in the Table 1. This study was approved by the institutional review board of the Graduate School of Medicine and

Faculty of Medicine, The University of Tokyo (no. 2019166NI), and informed consent was obtained in the form of an opt-out on the website. All data were obtained from ultrasound images taken during an intraoperative ultrasound as part of liver cancer screening. All images used in this study were obtained from three patients with liver cancer and two donors with normal livers.

A comparison of the scaling factors for the cos and sin signals of the liver parenchyma in Table 1 to the scaling factors of other structures reveals that the liver parenchyma and other structures can be distinguished with a scaling factor less than 1.8. In contrast, tumors and blood vessels are difficult to distinguish with a scaling factor of 1.8 or higher. The large standard deviation indicates that the scaling factor obtained varies depending on the location of its acquisition.

2.4. A deep neural network model for ultrasound image classification using a scaling factor map

As shown in 2.3, the scaling factors obtained from the PLSN model were found to have some utility as discriminative indices. However, the scaling factors obtained vary greatly depending on the position, precluding their use alone to identify tumors and blood vessels. Therefore, a scaling factor map was generated

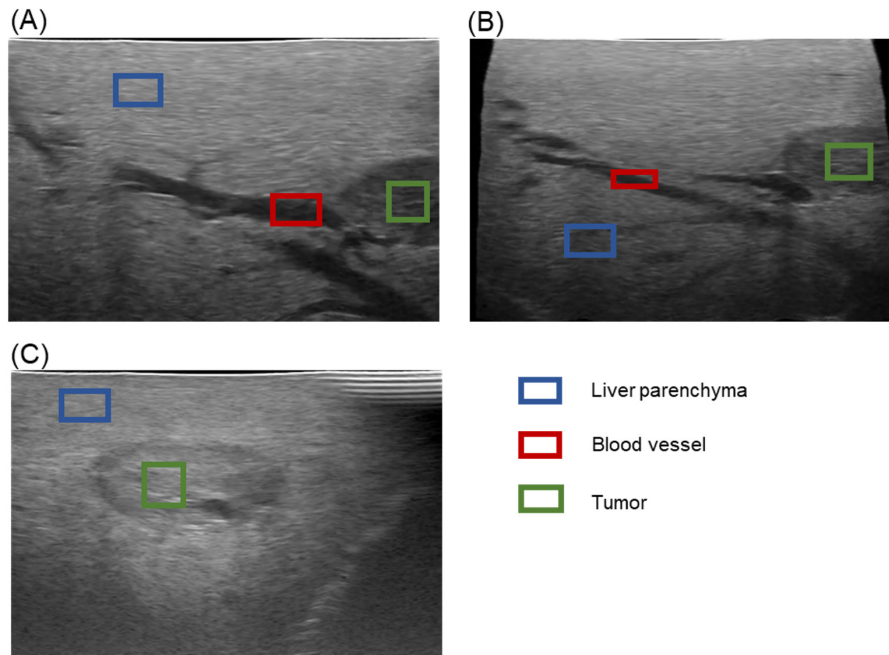


Figure 4. Regions of the liver parenchyma, blood vessels, and a tumor for scaling factor comparisons using the PLSN model. Vertical pixel information within each rectangle is used for comparison. Each region contains 50 ultrasound signals.

Table 1. Average of scaling factors calculated for the liver parenchyma, blood vessels, and tumors

Structure	Scaling factor		
	cos signal	sin signal	envelope
Blood vessel (A)	2.75 ± 0.83	2.11 ± 0.49	1.84 ± 0.55
Blood vessel (B)	2.21 ± 0.87	2.19 ± 0.84	2.34 ± 0.89
Tumor (A)	2.06 ± 0.66	1.93 ± 0.87	2.26 ± 0.47
Tumor (B)	1.94 ± 0.70	1.97 ± 0.63	2.00 ± 0.26
Tumor (C)	2.28 ± 0.55	2.09 ± 0.55	1.88 ± 0.41
Liver parenchyma (A)	1.32 ± 0.87	0.99 ± 0.56	1.28 ± 0.23
Liver parenchyma (B)	1.77 ± 0.67	1.36 ± 0.67	2.12 ± 0.39
Liver parenchyma (C)	1.72 ± 0.68	1.69 ± 0.67	1.28 ± 0.30

from ultrasound images in which local scaling factors were calculated for each coordinate. Proposed here is a model in which this scaling factor map and ultrasound images are combined to classify structures in the liver.

The scaling factor map is generated based on ultrasound images with the piecewise affine transformation described in 2.2. Let $r_{i,j}$ be the pixel value at coordinate (i,j) . The scaling factors for the cos component $r_c(t)$, sin component $r_s(t)$, and envelope component $|r(t)|$ are calculated using the value of $r_{i,j}$ to $r_{i,j+T}$ as the ultrasound signal $r_{i,j}(t)$, where T is the size of the clipping window. Each calculated scaling factor is used as a new pixel value ($\beta_{cos}, \beta_{sin}, \beta_{envelope}$) at (i,j) . Let the size of the original ultrasound image be $W \times H$. The scaling factor map is generated by performing this calculation in the region $W \times H - T$. A sample generated by this process is shown in Figure 5.

Image classification is accomplished by training an image classification deep neural network with both the scaling factor map obtained as described above and an original ultrasound image of size $W \times H - T$. ResNet-50

(19) has been used as the model of the deep neural network since it has exhibited excellent performance for the image classification involving 100 classes, known as CIFAR-100 (20). While ResNet-50 normally learns from normal images (images consisting of three types of information RGB: red, green, and blue), the proposed method uses 5 channels of RGB plus cos scaling factor β_{cos} and envelope scaling factor $\beta_{envelope}$. The reason why the sin component is not used here is that theoretically, the sin scaling factor β_{sin} and scaling factor β_{cos} are the same value, and the more information input in the neural network model, the more likely it is to become noise. The structure of the constructed model is shown in Figure 6. ResNet-50 is implemented using a model provided by PyTorch (21). A transfer learning method that utilizes a model that has previously been trained with CIFAR-100 in used during training. In this instance, the input layer is discarded because the learning model has 3 channels of RGB information in the input layer; the current model has been changed to receive 5 channels of information. Adam is used for learning, and a cross-entropy loss

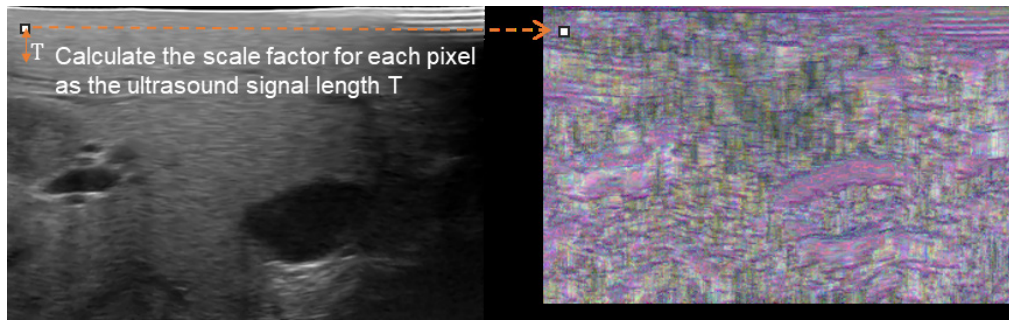


Figure 5. Conversion of an ultrasound image to a scaling factor map with a crop window size of $T=40$. The scaling factor map depicts the scaling factors for the cos, sin, and envelope components as a three-color image.

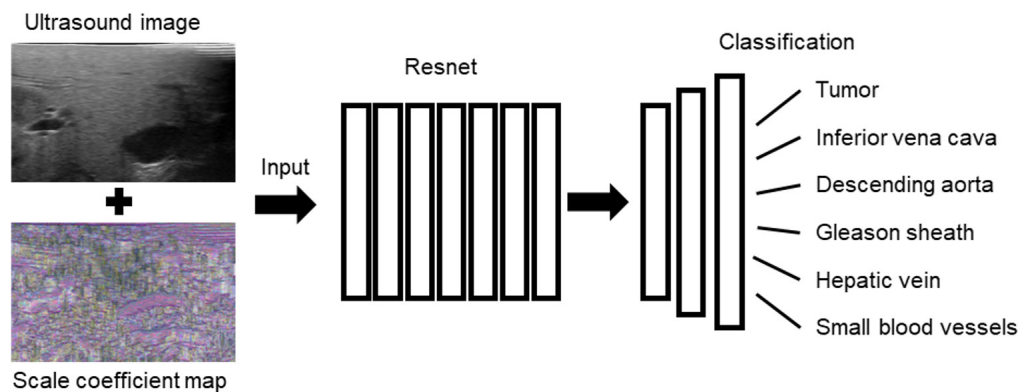


Figure 6. Configuration of a neural network for classification of structures in the liver, using ResNet-50 as a base model to identify features from the input ultrasound images and scaling factor maps. In the output layer, a feedforward neural network is used to predict 6 types of structures.

function is used as the loss function for classification.

2.5. Training and evaluation data from ultrasound images of the liver

To provide training and evaluation data for the proposed model, six types of structures in ultrasound images of the liver were labeled by an experienced physician based on the data described in 2.3: a tumor, the inferior vena cava, the descending aorta, the Gleason sheath, the hepatic vein, and small blood vessels. Sample images of the various structures are shown in Figure 7. For the training and evaluation data for the classification task, the image shown in Figure 7 is used instead of the entire image shown in Figure 5. In the cropped image, the region containing the structure is identified and only the target structure is included as much as possible. In addition, scaling factor maps are also used for learning and evaluation by cropping the ultrasound images according to their size. These sets of ultrasound images and scaling factor maps were obtained for each structure in the liver and their label information was used as learning and evaluation data. The training data obtained by the above method consisted of a total of 3,349 structures, including 251 tumors, 207 inferior vena cavas, 168 descending aortas, 1269 Gleason sheaths, 1145 hepatic veins, and 309 small blood vessels. Similarly, the data for evaluation

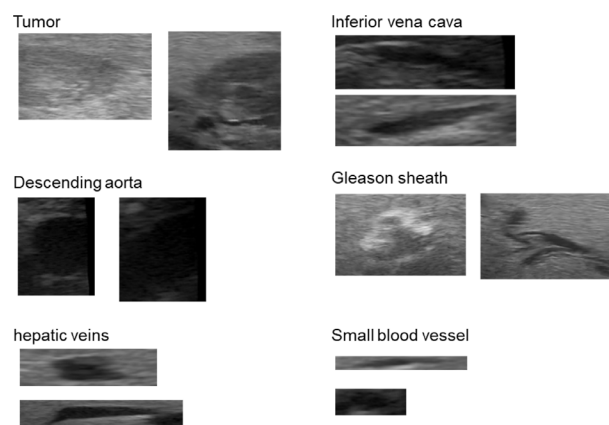


Figure 7. Sample images of a tumor, the inferior vena cava, the descending aorta, the Gleason sheath, the hepatic vein, and small blood vessels to be used as training and evaluation data. Scaling factor maps cropped to fit each image size are also used as input for the neural network.

consisted of a total of 770 structures, including 78 are tumors, 44 inferior vena cavas, 29 descending aortas, 264 Gleason sheaths, 277 hepatic veins, and 78 small blood vessels.

3. Results

To evaluate the performance of the proposed

classification model using scaling factors, the proposed model was trained using a classification task involving 6 types of structures in the liver using the training data described in 2.5. The proposed model was compared to a model trained on ultrasound images alone as input for the classification task. The evaluation data described in 2.5 were used to evaluate performance. To prevent overlearning of the data, noise addition, which is often used as a general method of data expansion, was used when training data for both models. The size of the cropping window T for the scaling factor map was 40, batch size during training was 128, total training epochs was 400, and Adam, a commonly used method of optimization, was used. Figures 8 show the changes in accuracy for all labels in each learning epoch. The performance index was calculated every 10 epochs.

The accuracy in Figure 8 indicates that learning is calmer after 300 epochs. The mean values of each performance indicator over 300 to 400 epochs are shown in Table 2. Table 2 shows that the overall accuracy decreased by 0.017 when ResNet-50 was compared to the proposed model. That said, the proposed model improved the sensitivity by 0.038 and it improved the F-score by 0.020 while maintaining precision with regard to tumor identification.

4. Discussion

The results in 2.3 demonstrate that the PLSN model can

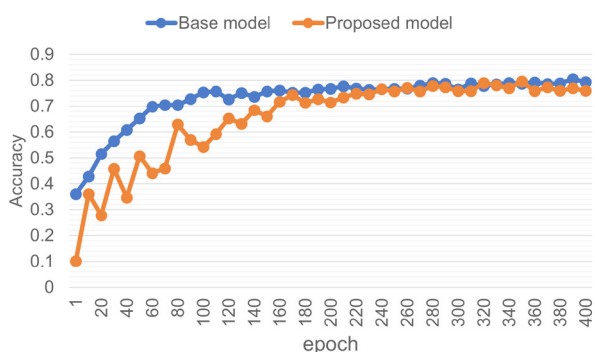


Figure 8. Accuracy per 10 epoch for all labels.

be used not only to distinguish cancer tissue from normal tissue in the breast, as reported in a previous study, but it can also distinguish between intrahepatic structures and the liver parenchyma, since the power law was observed in the ultrasound images of the liver. The scaling factor, which is expected to be an indicator with which to distinguish structures, can easily distinguish between the liver parenchyma and other structures (tumors and blood vessels), but it has difficulty clearly distinguishing between tumors and blood vessels because of the large variation in scaling factors depending on the location. One reason for the large variation is that the power spectrum of the reflected ultrasound signal calculated using the PLSN model contains a lot of noise at low and high frequencies, as shown in Figure 3. The scaling factor is the slope of the power spectrum, and its value is presumably greatly affected by noise. Due to this noise, there is a large standard deviation in the scaling factor for the same structure based on the ultrasound signal even though the regions used for verification in 2.3 were selected so that they all consisted of a single structure (a tumor, a blood vessel, or the liver parenchyma).

Since distinguishing between structures in the liver is difficult using scaling factors alone, a predictive model was constructed in 2.4 using a combination of ultrasound images and the scaling factor map. Its effectiveness was examined in 3, and the proposed model improved the sensitivity for a tumor, but the overall accuracy was lower than when only image data were used. The inclusion of a scaling factor improved sensitivity by 3.8% and the F-score by 2.0% for a tumor, and it improved precision by 6.7% and F-score by 2.8% for the inferior vena cava. For the descending aorta and Gleason sheath, precision and sensitivity improved but F-scores decreased. For the hepatic vein and small blood vessels, both precision and sensitivity and F-scores decreased. The detection of tumors is particularly important in ultrasonography. In this respect, the proposed model with scaling factors was effective at identifying intrahepatic tumors. Structures (a tumor, the inferior vena cava, the descending aorta, and the Gleason sheath) that were identified with increased precision or sensitivity had several features in common: they were circular in shape and larger than the hepatic

Table 2. Overall mean accuracy and precision, sensitivity, and F-score per epoch for each label averaged over 300 to 400 epochs. Superior values from the two models are shown in bold. The proposed model had improved tumor sensitivity while maintaining precision

	Base model			Proposed model		
	Precision	Sensitivity	F-score	Precision	Sensitivity	F-score
Overall accuracy		0.789			0.772	
Tumor	0.951	0.879	0.913	0.951	0.917	0.933
Inferior vena cava	0.879	0.980	0.925	0.946	0.961	0.953
Descending aorta	0.936	1.000	0.966	0.960	0.952	0.955
Gleason sheath	0.808	0.769	0.787	0.745	0.816	0.777
Hepatic vein	0.740	0.810	0.773	0.768	0.737	0.748
Small blood vessel	0.646	0.506	0.561	0.555	0.423	0.462

vein and small vessels. Currently, scaling factors are calculated by identifying ultrasound signals with a fixed length of 40 px in the vertical direction. When the structure is small, and especially when it has a short y-axis like the hepatic vein, the signal propagating through the structure and also the signal from the liver parenchyma and other structures are identified and the scaling factor is calculated, which adversely affects classification. Therefore, use of a particular method of ultrasound signal identification depending on the region would allow the exclusion of regions with different scaling factors during classification. Object detection models such as Faster R-CNN (22), Mask R-CNN (23), and YOLO (24) could be used to select the region. In fact, several studies have examined the detection of tumors in regions of ultrasound images (25,26), and a combination of this approach and scaling factors could further improve classification sensitivity with regard to tumors.

The PLSN model had previously been validated only for ultrasound images of breast cancer. However, the current study tested whether the PLSN model is also valid for ultrasound images of liver tumors. Results indicated that the liver parenchyma and other structures (tumor and blood vessels) can be distinguished based on the scaling factors calculated using the PLSN model. In addition, a classification model was proposed in which the scaling factor map is combined with a deep learning model to further distinguish intrahepatic structures. Validation with six types of structures (a tumor, the inferior vena cava, the descending aorta, the Gleason sheath, the hepatic vein, and small blood vessels) indicated that the sensitivity of tumor detection improved.

Funding: This study was supported by the Japan Society for the Promotion of Science (JSPS) KAKENHI Grant 20K20492 (Kumiko TANAKA-Ishii and Yu Chen).

Conflict of Interest: The authors have no conflicts of interest to disclose.

References

- Bouchaud JP. Power laws in economics and finance: Some ideas from physics. *Quant. Finance*. 2001; 1:105-112.
- Gabaix X. Power laws in economics and finance. *Annu. Rev. Econ.* 2009; 1:255-293.
- Gabaix X. Power laws in economics: An introduction. *J Econ Perspect*. 2016; 30:185-205.
- Kokudo N, Takemura N, Hasegawa K, Takayama T, Kubo S, Shimada M, *et al*. Clinical practice guidelines for hepatocellular carcinoma: The Japan Society of Hepatology 2017 (4th JSH-HCC guidelines) 2019 update. *Hepatol Res*. 2019; 49:1109-1113.
- Qi X, Yi F, Zhang L, Chen Y, Pi Y, Chen Y, Pi Y, Chen Y, Guo J, Wang J, Guo Q, Li J, Chen Y, Lv Q, Yi Z. Computer-aided diagnosis of breast cancer in ultrasonography images by deep learning. *Neurocomputing*. 2022; 472:152-165.
- Yi J, Kang HK, Kwon JH, Kim KS, Park MH, Seong YK, Kim DW, Ahn B, Ha K, Lee J, Hah Z, Bang WC. Technology trends and applications of deep learning in ultrasonography: image quality enhancement, diagnostic support, and improving workflow efficiency. *Ultrasonography*. 2021; 40:7-22.
- Ozaki J, Fujioka T, Yamaga E, Hayashi A, Kujiraoka Y, Imokawa T, Takahashi K, Okawa S, Yashima Y, Mori M, Kubota K, Oda G, Nakagawa T, Tateishi U. Deep learning method with a convolutional neural network for image classification of normal and metastatic axillary lymph nodes on breast ultrasonography. *Jpn J Radiol*. 2022; 40:814-822.
- Petropulu AP, Golas T, Vishwanathan G. Power-law shot noise and its application on modeling of ultrasound echoes. In: *Proceedings of the IEEE-SP International Symposium on Time-Frequency and Time-Scale Analysis*. 1998; 193-196.
- Kutay MA, Petropulu AP, Piccoli CW. On modeling biomedical ultrasound RF echoes using a power-law shot-noise model. *IEEE Trans Ultrason Ferroelectr Freq Control*. 2001; 48:953-968.
- Kutay MA, Petropulu AP, Piccoli CW. Breast tissue characterization based on modeling of ultrasonic echoes using the power-law shot noise model. *Pattern Recognit Lett*. 2003; 24:741-756.
- Wagner RF, Insana MF, Brown DG. Unified approach to the detection and classification of speckle texture in diagnostic ultrasound. *Opt Eng*. 1986; 25:256738-256738.
- Sleepe GE, Lele PP. Tissue characterization based on scatterer number density estimation. *IEEE Trans Ultrason Ferroelectr Freq Control*. 1988; 35:749-757.
- Chen JF, Zagzebski JA, Madsen EL. Non-Gaussian versus non-Rayleigh statistical properties of ultrasound echo signals. *IEEE Trans Ultrason Ferroelectr Freq Control*. 1994; 41:435-440.
- Lowen SB, Teich MC. Power-law shot noise. *IEEE Trans Inf Theory*. 1990; 36:1302-1318.
- Zwillinger D. 12 - Fourier, Laplace, and Mellin transforms. In: *Table of Integrals, Series, and Products* (Moll V, Gradshteyn IS, Ryzhik IM, eds.). Boston, 2014; pp. 1077-103.
- scikit-image, Piecewise Affine Transformation — skimage v0.20.0.dev0 docs. https://scikit-image.org/docs/dev/autodocs/examples/transform/plot_piecewise_affine.html (Accessed March 12, 2023).
- SciPy. scipy.signal.periodogram — SciPy v1.8.0 Manual. <https://docs.scipy.org/doc/scipy/reference/generated/scipy.signal.periodogram.html> (Accessed March 12, 2023).
- Scikit-learn. sklearn.linear_model.LinearRegression. https://scikit-learn.org/1.2/modules/generated/sklearn.linear_model.LinearRegression.html (Accessed March 12, 2023).
- He K, Zhang X, Ren S, Sun J. Deep residual learning for image recognition. In: *Proc. IEEE Comput Soc Conf Comput Vis Pattern Recognit*. 2016; 770-778. doi:10.1109/CVPR.2016.90.
- Krizhevsky A, Hinton G, others. Learning multiple layers of features from tiny images. 2009.
- PyTorch. ResNet | PyTorch. https://pytorch.org/hub/pytorch_vision_resnet/ (Accessed March 12, 2023).
- Ren S, He K, Girshick R, Sun J. Faster R-CNN: Towards real-time object detection with region proposal networks. *IEEE Trans Pattern Anal Mach Intell*. 2017; 39:1137-1149.

23. He K, Gkioxari G, Dollár P, Girshick R. Mask R-CNN. In: 2017 Proc IEEE Int Conf Comput Vis. 2017; 2980-2988.
24. Redmon J, Farhadi A. Yolov3: An incremental improvement. 2018, arXiv preprint. <https://doi.org/10.48550/arXiv.1804.02767>
25. Karako K, Mihara Y, Arita J, Ichida A, Bae SK, Kawaguchi Y, Ishizawa T, Akamatsu N, Kaneko J, Hasegawa K, Chen Y. Automated liver tumor detection in abdominal ultrasonography with a modified faster region-based convolutional neural networks (Faster R-CNN) architecture. *Hepatobiliary Surg Nutr.* 2022; 11:675-683.
26. Nakashima T, Tsutsumi I, Takami H, Doman K, Mekada Y, Nishida N, Kudo M. A study on liver tumor detection from an ultrasound image using deep learning. *Proceedings of*

the SPIE. 2020; 11515.

Received March 7, 2023; Revised March 31, 2023; Accepted April 5, 2023

**Address correspondence to:*

Yu Chen, Department of Human and Engineered Environmental Studies, Graduate School of Frontier Sciences, The University of Tokyo, 5-1-5 Kashiwanoha, Kashiwa Chiba 227-8568, Japan.

E-mail: chen@edu.k.u-tokyo.ac.jp

Released online in J-STAGE as advance publication April 13, 2023.

Interaction with ERp57 is required for progranulin protection against Type 2 Gaucher disease

Yuzhao Liu^{1,2,§}, Xiangli Zhao^{1,§}, Jinlong Jian¹, Sadaf Hasan¹, Chuanju Liu^{1,3,*}

¹Department of Orthopaedic Surgery, New York University Grossman School of Medicine, New York, New York, USA;

²Department of Endocrinology, the Affiliated Hospital of Qingdao University, Qingdao, China;

³Department of Cell Biology, New York University Grossman School of Medicine, New York, New York, USA.

SUMMARY Gaucher disease (GD), one of the most common lysosomal storage diseases, is caused by *GBA1* mutations resulting in defective glucocerebrosidase (GCase) and consequent accumulation of its substrates β -glucosylceramide (β -GlcCer). We reported progranulin (PGRN), a secretory growth factor-like molecule and an intracellular lysosomal protein was a crucial co-factor of GCase. PGRN binds to GCase and recruits Heat Shock Protein 70 (Hsp70) to GCase through its C-terminal Granulin (*Grn*) E domain, termed as ND7. In addition, both PGRN and ND7 are therapeutic against GD. Herein we found that both PGRN and its derived ND7 still displayed significant protective effects against GD in Hsp70 deficient cells. To delineate the molecular mechanisms underlying PGRN's Hsp70-independent regulation of GD, we performed a biochemical co-purification and mass spectrometry with His-tagged PGRN and His-tagged ND7 in Hsp70 deficient cells, which led to the identification of ERp57, also referred to as protein disulfide isomerase A3 (PDIA3), as a protein that binds to both PGRN and ND7. Within type 2 neuropathic GD patient fibroblasts L444P, bearing *GBA1* L444P mutation, deletion of ERp57 largely abolished the therapeutic effects of PGRN and ND7, as manifested by loss of effects on lysosomal storage, GCase activity, and β -GlcCer accumulation. Additionally, recombinant ERp57 effectively restored the therapeutic effects of PGRN and ND7 in ERp57 knockout L444P fibroblasts. Collectively, this study reports ERp57 as a previously unrecognized binding partner of PGRN that contributes to PGRN regulation of GD.

Keywords progranulin, ERp57, granulin E, GCase, Gaucher disease

1. Introduction

Gaucher disease (GD), one of the most common lysosomal storage diseases (LSDs), is caused by mutations in *GBA1* encoding GCase, which is responsible for the degradation of its substrate glucosylceramide (GCase) (1,2). The accumulated substrates in lysosomes lead to dysfunction of lysosomes in indicative organs (3,4). GD is divided into three types based on its clinical presentations (5,6). Type 1 non-neuropathic GD accounts for over 90% of GD patients and mainly involves macrophages of peripheral systems; patients have symptoms of anemia, bleeding, osteoporosis, and bone pain, as well as hepatosplenomegaly. Type 2 and 3, which are rare neuropathic types accounting for less than 10% of patients, affect the central nervous system as well as peripheral symptoms. Type 2 is rapidly progressive, and patients usually die before 3 years-old, while type 3 patients live to adulthood with slowly progressive neurological involvement (7,8). Currently,

enzyme replacement therapy (ERT) is available as effective treatment for non-neuropathic GD. ERT offsets low levels of GCase enzyme with a modified version of the enzyme. However, ERT is very expensive (around \$350,000/year/patient) and not effective for all patients (9,10). In addition, substrate reduction therapy (SRT) drugs have similarly shown clinical improvement in visceral disease parameters but have no therapeutic utility for treating neuropathic GD, because they cannot penetrate the blood-brain barrier (BBB) and are ineffective for treating neuropathic GD (nGD) (11,12).

Clinical symptoms may have many variations among patients carrying the same *GBA1* mutations, ranging from a life-threatening manifestation to nearly asymptomatic manifestations (13,14), suggesting the presence of GCase co-factor(s) whose deficiency/mutations may contribute the diverse clinical manifestations of GD. Indeed, we previously reported that ovalbumin (OVA)-challenged progranulin (PGRN) deficient mice developed GD-like phenotypes, including Gaucher cells and tubular-like

lysosomes (15). PGRN is a multi-faceted glycoprotein with a unique "beads-on-a-string" structure (16-18). PGRN can function both extracellular as a growth factor like molecule and intracellular as a critical lysosomal protein (19-25). Growing evidence revealed the association of PGRN with several lysosomal storage diseases, such as GD and Tay-Sachs disease (15,26,27). We found that PGRN bound to GCase and recruited Hsp70 to GCase through its *Grn* E domain (15,28). In addition, PGRN deficiency impairs the autophagy in GD (29). Furthermore, PGRN and its derived ND7, the C-terminal 98 amino acid fragment of PGRN bearing *Grn* E domain, could ameliorate the GD phenotypes in OVA-challenged PGRN deficient mice and GD patient fibroblasts (28). In addition, ND7 could cross BBB and effectively ameliorated the nGD manifestations in GD mouse models (30).

In the current study, we found that PGRN and ND7 still exhibit therapeutic effects against GD in Hsp70 knockout (KO) cells. We then sought to investigate the underlying mechanisms of PGRN regulation of GD in Hsp70-independent manner. Through mass spectrum (MS) and co-immunoprecipitation screening, we identified ERp57, also called protein disulfide isomerase A3 (PDIA3), is a novel binding component for both PGRN and ND7. Additionally, ERp57 deficiency abolished the therapeutic effects of PGRN and ND7, and recombinant ERp57 rescued PGRN and ND7's effects in ERp57 deficient type 2 GD patient fibroblasts.

2. Materials and Methods

2.1. Cells and Antibodies

Fibroblasts of WT and type 2 GD patients were obtained from Cornell Cell Repositories (Camden, NJ, USA). Antibodies targeted for GFP (sc-9996), His-tag (sc-57598), and GAPDH (sc-25778) were all purchased from Santa Cruz Biotechnology (Dallas, TX USA). PCDGF antibody (40-3400) was procured from Invitrogen (Waltham, MA, USA). ERp57 antibody (G117) was procured from Cell Signaling Technology (Danvers, MA, USA). All fluorescence-labeled secondary antibodies used in these experiments were purchased from Jackson Immuno Research Laboratories (West Grove, PA, USA). The substrate 4-Methylumbelliferyl β -D-glucopyranoside (4-MUG, M3633) was acquired from Sigma-Aldrich (Natick, MA, USA). The dye, LysoTracker Red DND99 (L7528), and both resins, Pierce High-Capacity Endotoxin Removal Resin (2,162,373.3) and HisPur™ Ni-NTA Resin (88,221), were all purchased from Thermo Fisher Scientific (Bridgewater, NJ, USA). The fluorescent stain, DAPI (H-1200), was acquired from VECTOR Laboratories (Burlingame, CA, USA). As delineated previously, the purified recombinant His-tag-PGRN protein was collected from HEK293T stable cell lines (30). Fetal bovine serum (FBS, 16,000-044) as well

as the Dulbecco's modified Eagle's medium (DMEM; 11,965-118) were both acquired from Gibco-BRL (Waltham, MA, USA).

2.2. Cell culture

Type 2 patient fibroblasts (GM08760) with the *GBA1* genotype, L444P/L444P, were acquired from Cornell Cell Repositories (Camden, NJ, USA). HEK293T cells and L444P fibroblasts were both cultured within DMEM that is supplemented with 1% penicillin-streptomycin and 10% FBS.

2.3. Generation of ERp57 knockout cell lines using Clustered Regularly Interspaced Short Palindromic Repeats Cas-9 (CRISPR-Cas9)

The CRISPR-Cas9 genome editing technology was implemented for the deletion of ERp57 gene. The sgRNA (5'CCGACGTGCTAGAACTCACG3') targeting the human PDIA3 genomic sequence was sub-cloned into a lentiCRISPR lentiviral plasmid following the provided protocol (Addgene, 49,535; Dr. Feng Zhang's CRISPR Depositing Lab). Preparation of the lentivirus involved cloning human ERp57 small guided (sg) RNA into lentiCRISPR plasmids followed by their transfection into HEK293 cells, which were co-transfected with both psPAX3 and pMD2.G lentiviral packaging plasmids. Following its assembly in HEK293T cells, the lentivirus produced was used to infect GD fibroblasts L444P, and individual clones were generated with drug selection (Puromycin 0.5 μ g/mL) for 5-7 days. To analyze the ERp57 knockout deficiency within these selected cells, western blotting was utilized.

2.4. Western blotting

SDS-PAGE was used to separate protein samples. After gel electrophoresis, these samples were then transferred onto a nitrocellulose membrane. Upon completion of the transfer, the membrane was blocked with 5% nonfat milk for 1 h to prevent non-specific binding. After the hour, primary antibody was used to probe the membrane overnight at 4°C. The next day, Tris Buffered Saline, with Tween® 20, pH 8.0 (TBST) was used to wash the membrane before incubating the membrane with the secondary antibody. Incubation was for 1 h at room temperature with intermittent washing by TBST. In order to develop the bands on the membrane, ECL Prime Western Blotting Detection Reagent was used for visualization (Amersham, Pittsburg, PA, USA).

2.5. Preparation of lipid extraction

Mouse brain tissues were obtained and served as a source of a lipid mixture. Under sterile conditions, one mouse brain was briefly dissected. Next, 50 mL of Phosphate-

Buffered Saline (PBS) was used to homogenize the collected brain tissues. Finally, the protein level within in the brain lysates were determined using a bicinchoninic acid assay.

2.6. LysoTracker assay

WT or type 2 GD L444P patient fibroblasts were cultured on Black-clear bottom 96-well microplate and challenged with lipid lysis (50 $\mu\text{g}/\text{mL}$) plus PBS, ND7, or PGRN for 24 h. The next day, fresh medium containing 300 nM LysoTracker[®] Red was added for 1 h. The cells were washed with PBS. The fluorescence intensity was read by the plate reader at excitation/emission of 647/668 nm, or the live images were taken by fluorescence microscopy.

2.7. GCCase activity assay

GCCase enzyme activity in indicated cell lysate was determined fluorometrically with 4-methylumbelliferyl- β -D-glucopyranoside (4MU-Glc) in the presence of the GCCase irreversible inhibitor, Conduritol B epoxide (CBE, 2 mM, Millipore, Bedford, MD) as previously described (31). Briefly, cell pellets were lysed with lysis buffer and protein concentrations of cell lysate were determined by BCA assay using BSA for normalization. GCCase activity was determined by 4MU-Glc as substrate in 0.25%Tc/Tx diluted in 0.1 M citrate phosphate (CP) buffer (pH 5.6). The GCCase-specific activity was calculated by subtracting background activity (with CBE) from total activity (without CBE) and normalized to total protein.

2.8. Preparation of recombinant PGRN

Generation of our recombinant PGRN stable cell line and purification of recombinant PGRN has been described in our previous publication (24). In brief, stable cells were cultured in DMEM that contained 1 mg/mL G418. PGRN was affinity-purified from the medium of starved cells by using nickel nitrilotriacetic-agarose. The purity of recombinant PGRN was determined by SDS-PAGE.

2.9. Expression and purification of ND7

The sequence encoding ND7, the *Grn* E, was inserted into the pD444 expression vector with a 6xHis-tag (DNA2.0, Menlo Park, CA) as described (28). ND7 was expressed in the BL21(DE3) *Escherichia coli* strain. Three hours after induction by 1 mM IPTG, *E. coli* cells were pelleted and sonicated to release the fusion protein. 6xHis-tagged ND7 was purified using His-Select Nickel Affinity Gel (Sigma-Aldrich, Natick, MA, USA). Briefly, *E. coli* cell lysate was incubated with affinity beads overnight and washed with washing buffer (50 mM NaH_2PO_4 , 200 mM NaCl, 50 mM imidazole, pH 8.0) five times. ND7 was eluted from beads with elution

buffer (50 mM NaH_2PO_4 , 200 mM NaCl, 250 mM imidazole, pH 8.0). After dialysis with PBS, endotoxin removal using Pierce High-Capacity Endotoxin Removal Resin (Cat. No. 2162373.3) (Thermo Fisher Scientific, Bridgewater, NJ, USA), and 0.2- μm filter sterilization, recombinant ND7 protein was ready to use.

2.10. Construction of expression plasmids

cDNAs encoding either full-length human PGRN or its C-terminal *Grn* E domain were cloned into pEGFP-N1 vectors by using *EcoRI* and *BamHI* restriction sites. The construct were confirmed by DNA sequence.

2.11. Solid phase binding

First, 1 $\mu\text{g}/\text{mL}$ ERp57 or BSA was coated to the plate. Then biotin-labeled BSA, PGRN, or ND7 with differing doses (0, 1, 2, 5 $\mu\text{g}/\text{mL}$) were added as bait, or recombinant ERp57 with different dose (0.2, 0.5, 1, 2, 4 $\mu\text{g}/\text{mL}$) were used as bait and 1 $\mu\text{g}/\text{mL}$ recombinant PGRN or BSA was used as coating protein. These steps were followed by the addition of HRP-labeled Streptavidin and its substrates. After washing to remove the unbound streptavidin-HRP, 100 μL TMB was added to each well for 30 min in the dark followed by adding 100 μL stop solution to each well. The plate was read using an automatic plate reader at 450 nm.

2.12. Immunoprecipitation

Plasmids of GFP-tagged PGRN, its C-terminal *Grn* E domain, or GFP-vector, were transfected in HEK293T cells over 48 h. Cells were lysed by RIPA lysis, and a total of 1 mg protein was used to conduct co-immunoprecipitation (Co-IP) in each sample. Anti-GFP antibody was used to perform immunoprecipitation, and ERp57 antibody was used to probe the protein complex.

2.13. Immunofluorescence staining and confocal microscope

Fixation of culture cells was performed using 4% paraformaldehyde for 10 min, which was followed by PBS wash. Next, 0.1% Triton X-100 was used for permeabilization, then 2% normal BSA was used to block the cells for 1 h, and finally, the cells were incubated with primary antibodies overnight at 4°C. On following day, PBS was used to wash cell coverslips, which were then incubated with the indicated fluorescence-labeled secondary antibodies at room temperature for 1 hour. Soon after washing with PBS, the cell coverslips were secured onto anti-fade medium that contained DAPI. A Leica TCS SP5 confocal system was used to capture images, and Image J application was used to analyze the quantification. Briefly, to analysis the mean fluorescence intensity of the indicative color of the

whole image, the image was gray scaled to 8 bit prior to measurement. In gray scale mode, pixels are associated with a value between 1 to 255, which represents their "lightness" and corresponds to the intensity of the fluorescent signal. Next after setting desired parameters, including Area, Integrated density and Mean Grey Value et. al., the measurement can be performed. By default, measurements are made over the en-tire area of the currently-selected 2D image slice. The grey value of the measurement can be export and analyzed.

2.14. Statistical analyses

All statistical analysis was performed using GraphPad Prism 7 Software. If the data met normal distribution and the variances were equal, one-way ANOVA was used for comparison among the multiple treatment. Post-hoc analysis was performed to determine which groups are significantly different to one another. Unpaired *t*-test was also performed where appropriate. Data are shown as mean ± SD, **p* < 0.05, ***p* < 0.01, ****p* < 0.001.

3. Results

3.1. PGRN and ND7 effectively reduced lysosomal storages in Hsp70 knockout cells

We previously reported that PGRN recruited Hsp70 to GCcase and formed a ternary complex when delivering

GCcase to the lysosome through its C-terminal *Grn* E domain, termed as ND7 (28). Both PGRN and ND7 are therapeutic against GD (28). Herein, we treated Hsp70 KO lung epithelium cells (Figure 1A) with lipid, or lipid plus recombinant PGRN (Figure 1B, C) or ND7 (Figure 1D). The lipid stimulation markedly enhanced the lysosomal storage in Hsp70 KO cells. To our surprise, both PGRN and ND7 protein still effectively reduced lysosomal storage to a basal level without Hsp70 (Figure 1E, F), indicating that Hsp70-independent molecular mechanisms also play an important role in PGRN/ND7's therapeutic effects against GD.

3.2. ERp57 was identified as an Hsp70-independent PGRN- and ND7-binding molecule

Exploring the molecular mechanisms of PGRN's regulation of GD in an Hsp70-independent manner promoted us to identify the novel components involved in PGRN- and ND7-mediated therapeutic effects against GD. Given that both PGRN and ND7 effectively prevented lysosomal storage in Hsp70 KO cells (Figure 1), we hypothesized that key protein partners should be able to bind to both PGRN and ND7 in Hsp70-independent manner. After adding His-tagged PGRN and ND7 (5 µg/mL) to Hsp70 KO cells for 24 hours, the cell lysates were immunoprecipitated by anti-His antibody (Figure 2A). The bound proteins were identified by mass spectrum (MS) analysis. Totally, 16 hits were identified

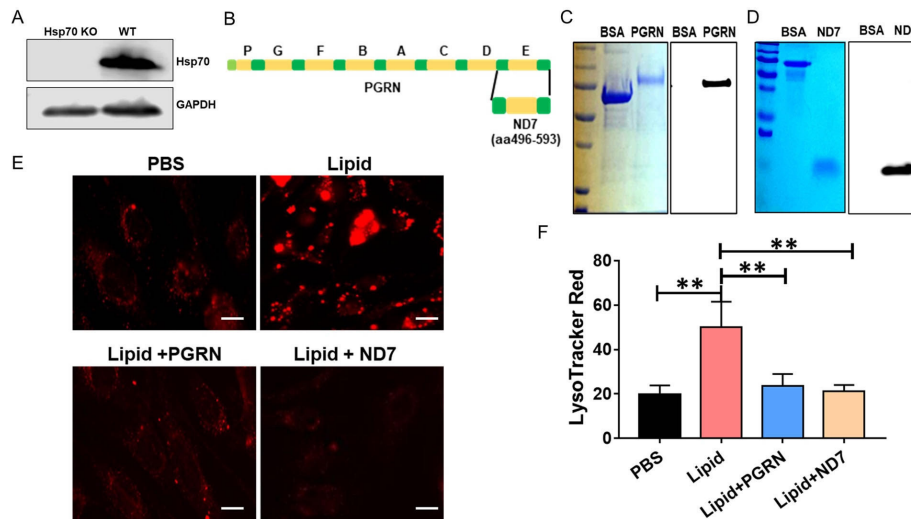


Figure 1: The effects of PGRN and ND7 on GD fibroblasts is Hsp70-independent. (A) The protein level of Hsp70 in mouse lung epithelium cells, assayed by western blotting. (B) Diagram of PGRN and ND7 (the 7th N-terminal deletion). PGRN regions were highlighted in yellow, which include seven and half granulin unit (P, G, F, B, A, C, D, E). The full regions linkers were highlighted in green, and half region (P) linker was highlighted in light blue, respectively. (C) Expression and characterization of recombinant His tagged-PGRN. His-tagged PGRN protein was purified from the HEK293 cells expressing His-PGRN using His-Select Nickel Affinity Gel. Purified PGRN was analyzed by Coomassie blue staining (left) and western blotting with PGRN antibody (right). (D) Expression and characterization of recombinant His tagged-ND7. Purified ND7 was analyzed by Coomassie blue staining (left) and western blotting with PGRN antibody (right). (E) PGRN and ND7 effectively reduce lysosomal storage in Hsp70 knockout cells. Hsp70 KO lung epithelium cells were stimulated with lipid lysis and treated with recombinant ND7 (5 µg/mL) or PGRN (10 µg/mL) for 24 h, PBS served as control. The cells were stained with LysoTracker Red. The live fluorescence microscopy imaging was taken using fluorescence microscope. (F) The quantification analysis of the mean fluorescence intensity E. Data are shown as mean ± SD of 3 independent experiments. One-way ANOVA tests. *, *p* < 0.05, **, *p* < 0.01. Scale bar=100 µm.

that specifically bound to both PGRN and ND7. Among the 16 hits, 7 hits were sequences related to the antibody; only 9 hits are functional proteins (Figure 2B). Among these 9 hits, identification of TCP-1 and Arpc4, two known PGRN-binding proteins (28), validated the technique. In addition, several RNA-binding proteins, including Sfpq, eif-4, Luc71, Alyref, Tufm, and Arglu1 were also identified as co-binding partners for PGRN and ND7 (Figure 2B). First within the protein ranking was PDIA3, which is also known as ERp57, an isomerase known to be critical for protein folding by promoting formation of disulfide bonds (32).

Solid phase binding assay demonstrated saturation of ERp57 binding to PGRN and ND7 (Figure 3A, B). Co-immunoprecipitation (Co-IP) further demonstrated the interaction between endogenous PGRN and ERp57 in L444P (Figure 3C). In addition, we used Nickel beads to pull down His-tagged PGRN, and then the precipitated His-tagged PGRN complex was immunoblotted onto a nitrocellulose membrane followed by detection with antibodies against ERp57. As shown in Figure 3D, ERp57 was co-purified with PGRN, further revealing the physical interaction between PGRN and ERp57.

3.3. Loss of ERp57 abolished PGRN- and its derivative ND7-mediated therapeutic effects in type 2 GD fibroblasts

Given that ERp57 is critical for promoting the formation of disulfide bonds in their glycoprotein substrates, both PGRN and ND7 are very rich in cysteine, and that ERp57 binds to both PGRN and ND7, these facts led us to hypothesize that ERp57 is important for PGRN and ND7's activities through regulating their cysteine disulfide bonds and conformation. To test

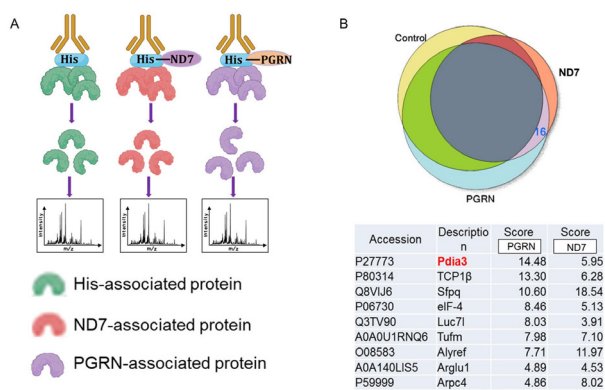


Figure 2: ERp57 was identified as an Hsp70-independent PGRN- and ND7-binding molecule. (A) The scheme of the method used to identify potential molecules involved in PGRN- and ND7-mediated regulation of GD in Hsp70-independent manner. Immunoprecipitation was performed with His antibody from His-tagged PGRN and His-tagged ND7 treated Hsp70 KO mouse lung epithelium cells, followed by mass spectrometry. PBS treatment was used as a control. (B) Summary of the mass spectrometry hits that specifically bound to both PGRN and ND7.

this hypothesis, we deleted the ERp57 gene in type 2 GD fibroblast line *GBA1*^{L444P} (L444P) using CRISPR/Cas9 technology (Figure 4A), a powerful genome-editing approach (33,34). The knockout efficiency of ERp57 was confirmed using Western blot with anti-ERp57 antibody (Figure 4B). PGRN and ND7 displayed significant therapeutic effects in type 2 GD fibroblasts L444P, including reduced lysosomal storage (Figure 4C, D) and reduced accumulation of GCcase substrate β -GlcCer (Figure 4E, F). However, the deletion of ERp57 abolished PGRN and ND7-mediated reduction in lysosomal storage and rescue of GCcase activity in GD patient fibroblasts compared to the significant reduction of lysosomal storage and increased GCcase activity after PGRN or ND7 treatment in control L444P fibroblasts (Figure 4G and H). These data indicated that loss of ERp57 abolished, at least largely, PGRN- and its derivative ND7-mediated therapeutic effect in GD fibroblasts.

3.4. Recombinant ERp57 restored the therapeutic effect of PGRN and ND7 in ERp57 deficient type 2 GD fibroblasts

Since ERp57 was identified as a binding partner of PGRN and ND7, and ERp57 deficiency ablated the therapeutic effects of PGRN and ND7 in type 2 GD patient fibroblasts L444P, including abolished their effects on lysosomal storage and GCcase activity, we next examined whether addition of ERp57 in ERp57

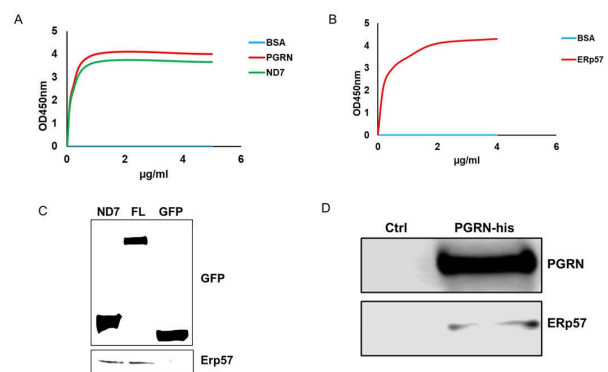


Figure 3. The identification of interaction between ERp57 and PGRN/ND7. (A) The interactions between ERp57 and PGRN/ND7, assayed by solid phase binding. Briefly, 1 μ g/mL ERp57 or BSA was coated to the plate. Then biotin-labeled BSA, PGRN, or ND7 with differing doses (0, 1, 2, 5 μ g/mL) were added as bait. (B) The interactions between ERp57 and PGRN by solid phase binding using recombinant ERp57 with different dose (0.2, 0.5, 1, 2, 4 μ g/mL) as bait, and 1 μ g/mL recombinant PGRN or BSA was used as coating protein. (C) Co-IP assay was used to examine the binding between PGRN and ERp57 in vivo. HEK293 cells were transfected with plasmids encoding GFP-fused full-length PGRN or ND7. The cell lysates were immunoprecipitated with GFP antibody. The complex was probed with ERp57 antibody. GFP-fused vector was used as a control. (D) Examination of the binding between PGRN and ERp57. Proteins co-purified with His-tagged PGRN were probed with ERp57 antibody. HEK293 cells transfected with His-tag vector was used as control.

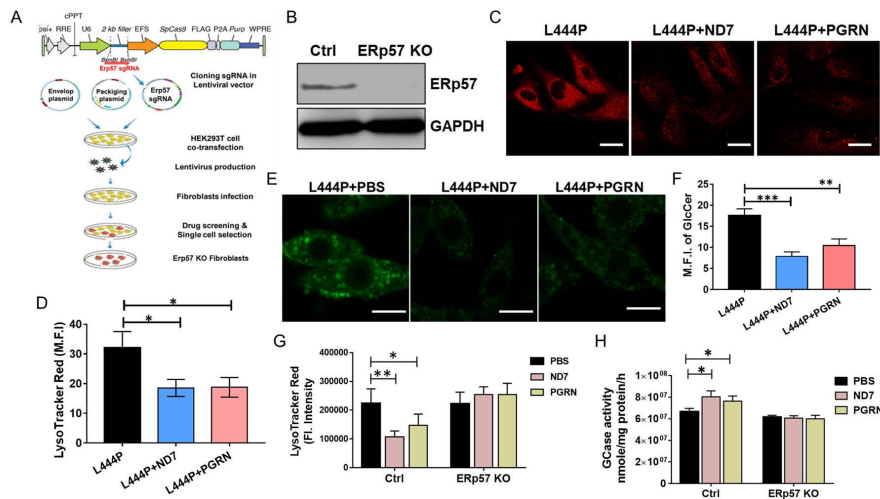


Figure 4. Deletion of ERp57 blunted the therapeutic effects of ND7 and PGRN in GD patient fibroblasts. (A) Diagram of the CRISPR/Cas9 technique for construction of human ERp57 KO GD type 2 fibroblasts L444P. (B) The levels of ERp57 in ERp57 KO L444P and control L444P fibroblasts, as-sayed by Western Blotting. (C) The lysosomal content in L444P with or without ND7 and PGRN treatment. L444P fibroblasts were stimulated with lipid lysis and treated with recombinant ND7 (5 µg/mL) or PGRN (10 µg/mL) for 24 hours. PBS used as control. The cells were stained with LysoTracker Red. The fluorescence intensity of the LysoTracker Red was determined by the live fluorescence microscopy imaging. (D) Quantification of mean fluorescence intensity of C analyzed using Image J. (E) The accumulation of β-glucosylceramide (β-GlcCer, green) in L444P fibroblasts with or without PGRN or ND7 treatment was analyzed by immunofluorescence staining with antibody against β-GlcCer. (F) Quantification of mean fluorescence intensity of E. (G) The lysosomal content in control or ERp57 KO L444P with or without ND7 and PGRN treatment. L444P fibroblasts were stimulated with lipid lysis and treated with recombinant ND7 (5 µg/mL) or PGRN (10 µg/mL) for 24 hours. PBS used as control. The cells were stained with LysoTracker Red. The fluorescence intensity of the LysoTracker Red was determined using SpectraMax i3x plate reader at excitation/emission of 647/668 nm. (H) The GCase activity in control or ERp57 KO L444P fibroblasts with or without ND7 and PGRN treatment were assayed by released 4MU-Glc. Data are shown as mean ± SD of 3 independent experiments. One-way ANOVA tests. *, $p < 0.05$, **, $p < 0.01$, *** $p < 0.001$. Scale bar=100 µm.

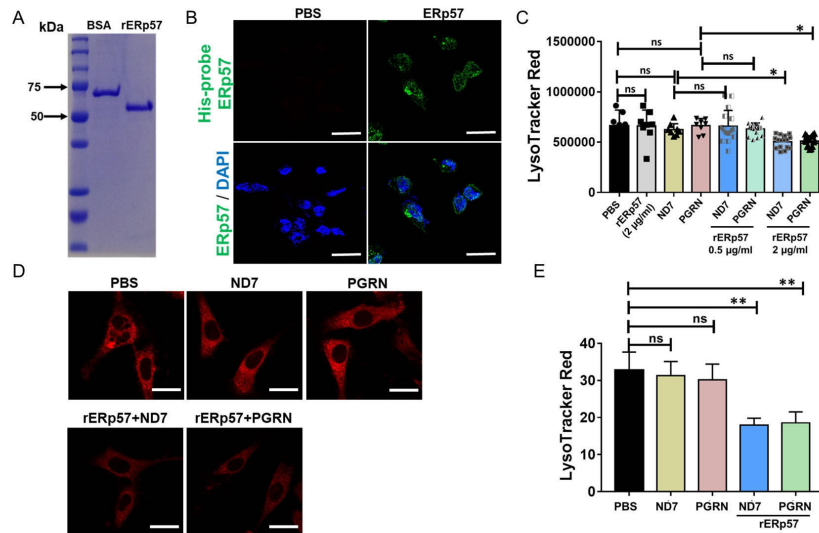


Figure 5. Recombinant ERp57 restored the effects of PGRN and ND7 on lysosomal storage in ERp57 KO L444P fibroblasts. (A) The characterization of recombinant ERp57 (rERp57) by Coomassie blue staining. (B) The endocytosis of rERp57. L444P fibroblasts were treated with His-tagged rERp57 (2 µg/mL) for 8 hours. The endocytosis of rERp57 was analyzed by immunofluorescence staining with antibody against His-probe. PBS was used as control. DAPI was used to stain the nuclei. (C) The lysosomal storage in ERp57 KO L444P. ERp57 KO L444P fibroblasts were treated with ND7 (5 µg/mL), or PGRN (10 µg/mL), or ND7/PGRN plus rERp57 (0.5 µg/mL or 2 µg/mL) for 24 hours. PBS and ERp57 (2 µg/mL) were used as controls. The fluorescence intensity of the LysoTracker Red was read using SpectraMax i3x plate reader at excitation/emission of 647/668 nm. (D) The live fluorescence imaging of lysosomal storage in ERp57 KO L444P fibroblasts with or without PGRN (10 µg/mL), ND7 (5 µg/mL), PGRN plus rERp57 (2 µg/mL), or ND7 plus rERp57 (2 µg/mL), measured by LysoTracker Red. PBS used as control. (E) Quantification of mean fluorescence intensity of D. Data are shown as mean ± SD of 3 independent experiments. One-way ANOVA tests. *, $p < 0.05$, **, $p < 0.01$. ns: not significant. Scale bar=100 µm.

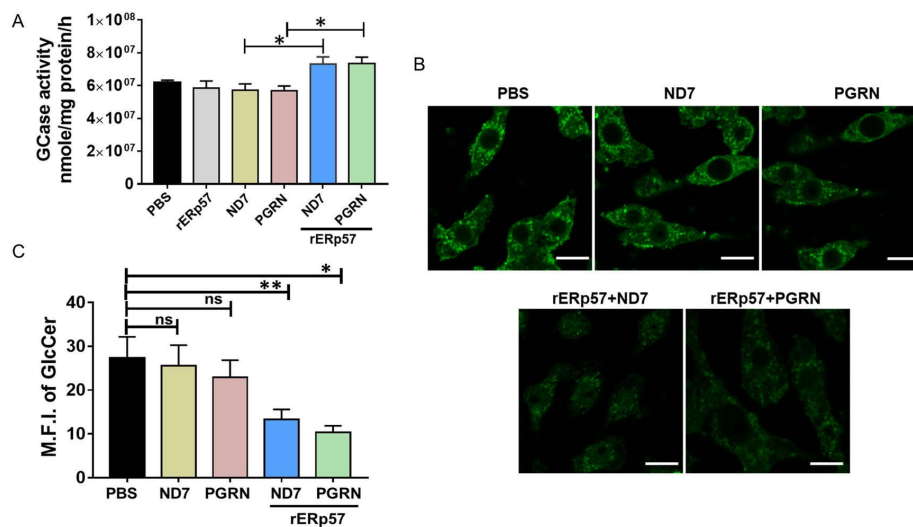


Figure 6. Recombinant ERp57 restored PGRN- and ND7-mediated increase of GCCase activity and decrease of β -GlcCer accumulation in ERp57 KO L444P fibroblasts. (A) The GCCase activity in ERp57 KO L444P with or without ND7 (5 μ g/mL) and PGRN (10 μ g/mL), or ND7 and PGRN plus rERp57 (2 μ g/mL) for 24 hours. PBS and rERp57 (2 μ g/mL) were used as controls. The cell lysate was used to measure the GCCase activity, assayed by released 4MU-Glc. (B) β -GlcCer accumulation in ERp57 KO L444P with or without ND7 (5 μ g/mL) and PGRN (10 μ g/mL), or ND7 and PGRN plus rERp57 (2 μ g/mL) for 24 hours, analyzed by immunofluorescence staining with antibody against β -GlcCer. (C) Quantification of mean fluorescence intensity of B. Data are shown as mean \pm SD of 3 independent experiments. One-way ANOVA tests. *, $p < 0.05$, **, $p < 0.01$. ns: not significant. Scale bar=100 μ m.

KO L444P fibroblasts could restore PGRN/ND7's therapeutic effects. For this purpose, recombinant ERp57 (rERp57) (Figure 5A) was used to treated ERp57 KO L444P fibroblasts. To test if rERp57 could be taken up by the cells, ERp57 KO L444P fibroblasts were treated with His-tagged rERp57 (2 μ g/mL) for 8 hours and then immunofluorescence staining was performed with His-probe to determine the endocytosis of ERp57. PBS was used as a control. Figure 5B clearly showed that rERp57 could be taken up by the cells, indicated by the green signals. In order to determine the optimum working dose of rERp57, ERp57 KO L444P fibroblasts were treated with PGRN and ND7, or PGRN- and ND7- plus rERp57 at different doses, 0.5 μ g/mL and 2 μ g/mL, respectively. We found that PGRN- or ND7- plus high dose of ERp57 (2 μ g/mL) significantly decreased the lysosomal storage in ERp57 KO L444P fibroblasts, while PGRN or ND7 plus the low dose of ERp57 did not show significant changes compared with PGRN or ND7 treatment groups (Figure 5C). The high dose of ERp57 (2 μ g/mL) is thus selected as the effective working dose for the further experiments.

Consequently, 2 μ g/mL ERp57 was used to evaluate its mediation on the therapeutic effects of PGRN and ND7 in GD fibroblasts. In Figure 5D and E, PGRN and ND7 treatment could not rescue the lysosomal storage in ERp57 KO L444P fibroblasts, however, in the presence of ERp57 (2 μ g/mL), both PGRN and ND7 significantly decreased the lysosomal content indicated by the fluorescence intensity of LysoTracker Red (Figure 5D and E). Furthermore, the GCCase activity of

ERp57 KO L444P fibroblasts after the treatment with PGRN or ND7 in the presence or absence of ERp57 was determined. GCCase activity was not restored with PGRN or ND7 treatment in ERp57 KO L444P fibroblasts in comparison with that of the PBS control group, while it was increased significantly with PGRN or ND7 treatment in the presence of ERp57 (2 μ g/mL), measured by the mean fluorescence intensity (MFI) of released 4-methylumbelliferone (Figure 6A). Accordingly, in the presence of ERp57 (2 μ g/mL), PGRN or ND7 treatment reduced the β -GlcCer accumulation by approximately 50% (Figure 6B and C). Collectively, these data suggested that ERp57 is crucial for PGRN/ND7's therapeutic effects in GD fibroblast.

4. Discussion

We previously reported that PGRN is a novel modifier of GCCase in GD (15). OVA-challenged PGRN deficiency mice developed typical GD phenotypes (28). Serum levels of PGRN was significantly lower in GD patients than in healthy controls (15). Further study showed that PGRN directly bound to GCCase through its *Grn* E domain, acting as a co-chaperone of Hsp70, recruited Hsp70 to GCCase and forms a ternary complex in the delivery of GCCase to lysosome (28). Moreover, recombinant PGRN and its derived biologic ND7, which includes the full region of the *Grn* E domain, could ameliorate the GD phenotypes in OVA-challenged PGRN deficient mice and GD patient fibroblasts (28). Although PGRN bound to GCCase through its *Grn* E

domain (ND7) and formed a complex with Hsp70, we unexpectedly found that PGRN and ND7 still displayed significant protective effects against GD in Hsp70 deficient cells. The molecular mechanisms underlying Hsp70-independent promoted us to identify the new binding partners that may mediate PGRN's and ND7's therapeutic effects against GD. Through MS and co-immunoprecipitation analysis *et al.*, ERp57, an enzyme known to be important in promoting the formation of disulfide bonds and the protein folding, was identified as a novel binding partner of both PGRN and its derivative ND7 (Figure 2 and 3).

ERp57, also known as PDIA3, is a pleiotropic member of the protein disulfide isomerase (PDI) family that has attracted significant attention from researchers (35). ERp57 is dominantly located in the endoplasmic reticulum (ER) (36) as well as other cellular compartments, such as the nucleus and the cell membrane (37,38). ERp57 is associated with various of diseases, such as neurological disease (39), cancer (40), and infectious disease (41). To determine whether ERp57 could mediate PGRN/ND7's therapeutic effect in GD, we measured the GD phenotypes after PGRN and ND7 treatment in type 2 GD patient fibroblasts L444P with or without ERp57. We found that both recombinant PGRN and ND7 could ameliorate GD phenotypes in L444P fibroblast (Figure 4), consistent with the previous report (28). However, these therapeutic effects of PGRN and ND7 were compromised in ERp57 KO L444P fibroblasts compared with those of control L444P fibroblast (Figure 4G, H). ERp57 is an isomerase enzyme, involved in protein folding, catalyzing the formation, and critical for remodeling of disulfide bonds in their glycoprotein substrates (42,43). Both PGRN and ND7 are rich in cysteine; ERp57 might play a critical role in PGRN and ND7's activities by regulating their cysteine disulfide bonds and functional conformation in GD.

To prove our hypothesis, we analyzed the GD phenotypes after PGRN/ND7 treatment in the presence or absence of recombinant ERp57 in ERp57 KO L444P fibroblast. From Figure 5B, it clearly showed that rERp57 could be taken up by the cells, accordingly, the GD phenotypes in ERp57 KO fibroblasts were rescued after PGRN or ND7 plus rERp57 in comparison with no ERp57 (Figure 5 and Figure 6). These data supported our hypothesis that ERp57 play a critical role in mediating PGRN and ND7's therapeutic effects against GD.

Currently, ERT is mainly available as an effective treatment for non-neuropathic type 1 GD in clinics. However, ERT is very expensive and not effective for all patients, and especially ineffective for treating neuropathic type 2 and 3 GD patients. Approved SRT drugs have shown similar clinical improvement in visceral disease parameters but have no therapeutic utility for neuropathic GD (9-12). Developing an alternative treatment for GD, specifically for nGD

is an urgent and unmet medical need. PGRN was identified as a novel modifier of GCase and involved in various lysosomal storage disease by previous studies, especially our recent published paper showed that PGRN derivative ND7 could penetrate BBB and protect GD and nGD pathologies in *Grn* and *Gba1* double mutant mice, another new GD mouse mode showing more severer GD phenotypes compared with the traditional GD model (27,28,30). Furthermore, PGRN and ND7 also ameliorated the GD phenotypes in both type 1 and type 2 GD patient fibroblasts (31). The previous study indicated the promising therapeutic potentials of PGRN derivative ND7 against GD. Compared with the ERT and SRT treatment for GD, ND7 showed unique functions, including BBB penetration, ameliorated GD and nGD phenotypes, and prevention of the neurodegenerative markers (30). In addition, the development of peptide-based drug has more advantages, including high potency, low cost and potential low toxicity, *et al.*(44,45). Our study showed that ERp57 plays an important role in the regulation of both PGRN and its derivative ND7, in type 2 neuropathic GD patient fibroblasts. Given that ND7 showed therapeutic effect in different GD animal models, and type 1 and type 2 GD patient fibroblast, ERp57, the identification and manipulation of this novel PGRN/ND7 binding partner may lead to innovative therapeutic for GD and other lysosomal storage diseases.

However, a few limitations to the current study were also noted. First, ERp57 mediate-therapeutic effect of PGRN or ND7 was studied only in type 2 GD patient fibroblasts, whether this meditation effect is universal need further study in other types of GD. Second, multiple doses of recombinant ERp57 should be tested to find out the best working efficiency of ERp57 to rescue the therapeutic effect of PGRN and ND7 in GD. Eventually, how ERp57 exert its role once endocytosed to the cells is unclear in the study. Several hypotheses can be considered, ERp57 might escape from the endosomes and interact with PGRN to play the role, or ERp57 released to lysosome once endosome fused with lysosome and interact with PGRN in lysosomes. Having pointed out these issues, the subsequent studies, such as determine the ERp57 meditation effect of PGRN/ND7 in type 1 and type 3 GD patient fibroblast. In addition, the localization of ERp57 after endocytosed where it might exert its role is also need investigation.

In conclusion, this study reports ERp57 as a novel binding component for PGRN. ERp57 deficiency abolished the therapeutic effects of PGRN and its derivative ND7. However, the addition of recombinant ERp57 reinstated the effects of PGRN and ND7 in type 2 GD patient fibroblasts deficient in ERp57. With the consideration that ERp57 is involved in a plethora of disease processes, the identification and manipulation of this novel PGRN/ND7 binding partner may lead to innovative therapeutic for GD and other lysosomal storage diseases.

Acknowledgements

The authors would like to acknowledge all lab members for insightful discussions and critical reading. We thank Dr. Yan Deng at NYU Medical School OCS Microscopy Core for their assistance with confocal and electron microscope imaging.

Funding: This work is supported partly by NIH research grants R01NS103931, R01AR062207, R01AR061484, R01AR076900, R01AR078035, and R21OD033660.

Conflict of Interest: The authors have no conflicts of interest to disclose.

References

- Stone DL, Tayebi N, Orvisky E, Stubblefield B, Madike V, Sidransky E. Glucocerebrosidase gene mutations in patients with type 2 Gaucher disease. *Hum Mutat.* 2000; 15:181-188.
- Ankleshwaria C, Mistri M, Bavdekar A, Muranjan M, Dave U, Tamhankar P, Khanna V, Jasinge E, Nampoothiri S, Edayankara Kadangot S, Sheth F, Gupta S, Sheth J. Novel mutations in the glucocerebrosidase gene of Indian patients with Gaucher disease. *J Hum Genet.* 2015; 60:285.
- Platt FM. Sphingolipid lysosomal storage disorders. *Nature.* 2014; 510:68-75.
- Chen Y, Sud N, Hettinghouse A, Liu CJ. Molecular regulations and therapeutic targets of Gaucher disease. *Cytokine Growth Factor Rev.* 2018; 41:65-74.
- Mistry PK, Lopez G, Schiffmann R, Barton NW, Weinreb NJ, Sidransky E. Gaucher disease: Progress and ongoing challenges. *Mol Genet Metab.* 2017; 120:8-21.
- Nair S, Branagan AR, Liu J, Boddupalli CS, Mistry PK, Dhodapkar MV. Clonal Immunoglobulin against Lysolipids in the Origin of Myeloma. *N Engl J Med.* 2016; 374(6):555-561.
- Stirneemann J, Belmatoug N, Camou F, Serratrice C, Froissart R, Caillaud C, Levade T, Astudillo L, Serratrice J, Brassier A, Rose C, Billette de Villemeur T, Berger MG. A Review of Gaucher Disease Pathophysiology, Clinical Presentation and Treatments. *Int J Mol Sci.* 2017; 18:441.
- Desnick RJ, Barton NW, Furbish S, Grabowski GA, Karlsson S, Kolodny EH, Medin JA, Murray GJ, Mistry PK, Patterson MC, Schiffmann R, Weinreb NJ, Roscoe Owen Brady, MD: Remembrances of co-investigators and colleagues. *Mol Genet Metab.* 2017; 120:1-7.
- Kirkegaard T, Gray J, Priestman DA, *et al.* Heat shock protein-based therapy as a potential candidate for treating the sphingolipidoses. *Sci Transl Med.* 2016; 8:355ra118.
- Lukina E, Watman N, Dragosky M, Pastores GM, Arreguin EA, Rosenbaum H, Zimran A, Angell J, Ross L, Puga AC, Peterschmitt JM. Eliglustat, an investigational oral therapy for Gaucher disease type 1: Phase 2 trial results after 4 years of treatment. *Blood Cells Mol Dis.* 2014; 53:274-276.
- Kuter DJ, Mehta A, Hollak CE, Giraldo P, Hughes D, Belmatoug N, Brand M, Muller A, Schaaf B, Giorgino R, Zimran A. Miglustat therapy in type 1 Gaucher disease: clinical and safety outcomes in a multicenter retrospective cohort study. *Blood Cells Mol Dis.* 2013; 51:116-124.
- Bennett LL, Mohan D. Gaucher disease and its treatment options. *Ann Pharmacother.* 2013; 47:1182-1193.
- Weiss K, Gonzalez A, Lopez G, Pedoeim L, Groden C, Sidransky E. The clinical management of Type 2 Gaucher disease. *Mol Genet Metab.* 2015; 114:110-122.
- Staretz-Chacham O, Choi JH, Wakabayashi K, Lopez G, Sidransky E. Psychiatric and behavioral manifestations of lysosomal storage disorders. *Am J Med Genet B Neuropsychiatr Genet.* 2010; 153B:1253-1265.
- Jian J, Zhao S, Tian QY, *et al.* Association Between Progranulin and Gaucher Disease. *EBioMedicine.* 2016; 11:127-137.
- Hrabal R, Chen Z, James S, Bennett HP, Ni F. The hairpin stack fold, a novel protein architecture for a new family of protein growth factors. *Nat Struct Biol.* 1996; 3:747-752.
- Palfree RG, Bennett HP, Bateman A. The Evolution of the Secreted Regulatory Protein Progranulin. *PLoS One.* 2015; 10:e0133749.
- Tolkatchev D, Malik S, Vinogradova A, Wang P, Chen Z, Xu P, Bennett HP, Bateman A, Ni F. Structure dissection of human progranulin identifies well-folded granulin/epithelin modules with unique functional activities. *Protein Sci.* 2008; 17:711-724.
- Li SS, Zhang MX, Wang Y, Wang W, Zhao CM, Sun XM, Dong GK, Li ZR, Yin WJ, Zhu B, Cai HX. Reduction of PGRN increased fibrosis during skin wound healing in mice. *Histol Histopathol.* 2019; 34:765-774.
- Jian J, Konopka J, Liu C. Insights into the role of progranulin in immunity, infection, and inflammation. *J Leukoc Biol.* 2013; 93:199-208.
- Bateman A, Bennett HP. The granulin gene family: from cancer to dementia. *Bioessays.* 2009; 31:1245-1254
- Kao AW, McKay A, Singh PP, Brunet A, Huang EJ. Progranulin, lysosomal regulation and neurodegenerative disease. *Nat Rev Neurosci.* 2017; 18:325-333.
- Cui Y, Hettinghouse A, Liu CJ. Progranulin: A conductor of receptors orchestra, a chaperone of lysosomal enzymes and a therapeutic target for multiple diseases. *Cytokine Growth Factor Rev.* 2019; 45:53-64.
- Tang W, Lu Y, Tian QY, *et al.* The growth factor progranulin binds to TNF receptors and is therapeutic against inflammatory arthritis in mice. *Science.* 2011; 332:478-484.
- Zhao X, Hasan S, Liou B, Lin Y, Sun Y, Liu C. Analysis of the Biomarkers for Neurodegenerative Diseases in Aged Progranulin Deficient Mice. *Int J Mol Sci.* 2022; 23:629.
- Jian J, Hettinghouse A, Liu CJ. Progranulin acts as a shared chaperone and regulates multiple lysosomal enzymes. *Genes Dis.* 2017; 4:125-126.
- Chen Y, Jian J, Hettinghouse A, Zhao X, Setchell KDR, Sun Y, Liu CJ. Progranulin associates with hexosaminidase A and ameliorates GM2 ganglioside accumulation and lysosomal storage in Tay-Sachs disease. *J Mol Med (Berl).* 2018; 96:1359-1373.
- Jian J, Tian QY, Hettinghouse A, Zhao S, Liu H, Wei J, Grunig G, Zhang W, Setchell KDR, Sun Y, Overkleeft HS, Chan GL, Liu CJ. Progranulin Recruits HSP70 to β -Glucocerebrosidase and Is Therapeutic Against Gaucher Disease. *EBioMedicine.* 2016; 13:212-224.
- Zhao X, Liberti R, Jian J, Fu W, Hettinghouse A, Sun Y, Liu CJ. Progranulin associates with Rab2 and is involved in autophagosome-lysosome fusion in Gaucher disease. *J Mol Med (Berl).* 2021; 99:1639-1654.

30. Zhao X, Lin Y, Liou B, Fu W, Jian J, Fannie V, Zhang W, Setchell KDR, Grabowski GA, Sun Y, Liu CJ. PGRN deficiency exacerbates, whereas a brain penetrant PGRN derivative protects, GBA1 mutation-associated pathologies and diseases. *Proc Natl Acad Sci U S A*. 2023; 120:e2210442120.
31. Liou B, Zhang W, Fannin V, Quinn B, Ran H, Xu K, Setchell KDR, Witte D, Grabowski GA, Sun Y. Combination of acid β -glucosidase mutation and Saposin C deficiency in mice reveals Gba1 mutation dependent and tissue-specific disease phenotype. *Sci Rep*. 2019; 9:5571.
32. Hirano N, Shibasaki F, Sakai R, Tanaka T, Nishida J, Yazaki Y, Takenawa T, Hirai H. Molecular cloning of the human glucose-regulated protein ERp57/GRP58, a thiol-dependent reductase. Identification of its secretory form and inducible expression by the oncogenic transformation. *Eur J Biochem*. 1995; 234:336-342.
33. Long C, McAnally JR, Shelton JM, Mireault AA, Bassel-Duby R, Olson EN. Prevention of muscular dystrophy in mice by CRISPR/Cas9-mediated editing of germline DNA. *Science*. 2014; 345:1184-1188.
34. Maddalo D, Manchado E, Concepcion CP, Bonetti C, Vidigal JA, Han YC, Ogorowski P, Crippa A, Rekhman N, de Stanchina E, Lowe SW, Ventura A. *In vivo* engineering of oncogenic chromosomal rearrangements with the CRISPR/Cas9 system. *Nature*. 2014; 516:423-427.
35. Hettinghouse A, Liu R, Liu CJ. Multifunctional molecule ERp57: From cancer to neurodegenerative diseases. *Pharmacol Ther*. 2018; 181:34-48.
36. Grillo C, D'Ambrosio C, Scaloni A, Maceroni M, Merluzzi S, Turano C, Altieri F. Cooperative activity of Ref-1/APE and ERp57 in reductive activation of transcription factors. *Free Radic Biol Med*. 2006; 41:1113-23.
37. Grindel BJ, Rohe B, Safford SE, Bennett JJ, Farach-Carson MC. Tumor necrosis factor- α treatment of HepG2 cells mobilizes a cytoplasmic pool of ERp57/1,25D₃-MARRS to the nucleus. *J Cell Biochem*. 2011; 112:2606-2615.
38. Chichiarelli S, Altieri F, Paglia G, Rubini E, Minacori M, Eufemi M. ERp57/PDIA3: new insight. *Cell Mol Biol Lett*. 2022; 27:12.
39. Bargsted L, Hetz C, Matus S. ERp57 in neurodegeneration and regeneration. *Neural Regen Res*. 2016; 11:232-233.
40. Powell LE, Foster PA. Protein disulphide isomerase inhibition as a potential cancer therapeutic strategy. *Cancer Med*. 2021; 10:2812-2825.
41. Wu J, Wang Y, Wei Y, Xu Z, Tan X, Wu Z, Zheng J, Liu GD, Cao Y, Xue C. Disulfide isomerase ERp57 improves the stability and immunogenicity of H3N2 influenza virus hemagglutinin. *Virol J*. 2020; 17:55.
42. Turano C, Gaucci E, Grillo C, Chichiarelli S. ERp57/GRP58: a protein with multiple functions. *Cell Mol Biol Lett*. 2011; 16:539-563.
43. Bechtel TJ, Weerapana E. From structure to redox: The diverse functional roles of disulfides and implications in disease. *Proteomics*. 2017; 17:10.1002/pmic.201600391.
44. Craik DJ, Fairlie DP, Liras S, Price D. The future of peptide-based drugs. *Chem Biol Drug Des*. 2013; 81:136-147.
45. Luo X, Chen H, Song Y, Qin Z, Xu L, He N, Tan Y, Dessie W. Advancements, challenges and future perspectives on peptide-based drugs: Focus on antimicrobial peptides. *Eur J Pharm Sci*. 2023; 181:106363.

Received February 6, 2023; Revised March 1, 2023; Accepted March 6, 2023.

§These authors contributed equally to this work.

*Address correspondence to:

Chuanju Liu, Department of Orthopaedic Surgery, NYU Grossman School of Medicine, 301 East 17th Street, New York, NY 10003, USA.

E-mail: chuanju.liu@nyulangone.org

Released online in J-STAGE as advance publication March 9, 2023.

FOXA2 plays a critical role in hepatocellular carcinoma progression and lenvatinib-associated drug resistance

Zhengxia Wang^{1,2,§}, Junyi Shen^{1,3,4,§}, Chuwen Chen^{1,§}, Tianfu Wen^{1,4}, Chuan Li^{1,*}

¹Department of Liver Surgery, West China Hospital, Sichuan University, Chengdu, Sichuan, China;

²Department of Hepatobiliary Pancreatic Surgery, Chengdu Second People's Hospital, Chengdu, China;

³Institute of Clinical Pathology, West China Hospital, Sichuan University, Chengdu, Sichuan, China;

⁴Laboratory of Liver Transplantation, Frontiers Science Center for Disease-related Molecular Network, West China Hospital, Sichuan University, Chengdu, Sichuan, China.

SUMMARY Hepatic forkhead box protein A2 (FOXA2) is a crucial transcription factor for liver development and metabolic homeostasis. However, its role in hepatocellular carcinoma (HCC) progression and lenvatinib-related drug resistance remains unknown. In this study, the level of FOXA2 expression was found to be lower in HCC tissues than in paired adjacent tumor tissues. A low level of FOXA2 expression was associated with aggressive tumor characteristics (vascular invasion and poor differentiation). A low level of FOXA2 expression was found to be an independent risk factor for tumor recurrence (hazard ratio (HR): 1.899, $P < 0.001$) and long-term survival (HR: 2.011, $P = 0.003$) in HCC patients after hepatectomy. In xenograft animal models, FOXA2 overexpression significantly inhibited tumor growth. Moreover, FOXA2 overexpression was found to enhance the inhibitory effect of lenvatinib on HCC cells by upregulating the adenosine monophosphate-activated protein kinase-mechanistic target of rapamycin (AMPK-mTOR) pathway. Conversely, inhibition of adenosine monophosphate-activated protein kinase (AMPK) or stimulation of mechanistic target of rapamycin (mTOR) attenuated the sensitization of cells overexpressing FOXA2 to lenvatinib. Similarly, FOXA2 overexpression augmented the antitumor effect of lenvatinib in animal models with xenograft tumors. FOXA2 overexpression increased autophagy in HCC cells treated with lenvatinib. Lenvatinib treatment activated the platelet-derived growth factor receptor-extracellular regulated protein kinase (PDGFR-ERK) pathway in HCC. FOXA2 overexpression further downregulated the PDGFR-ERK pathway through the activation of the AMPK-mTOR axis. In conclusion, FOXA2 was identified as an independent risk factor for HCC after hepatectomy. FOXA2 was found to be closely associated with the biological progression of HCC. By modulating the AMPK-mTOR-autophagy signaling pathway, FOX2 significantly augmented antitumor effect of lenvatinib in HCC.

Keywords hepatocellular carcinoma, FOXA2, lenvatinib, AMPK-mTOR pathway, drug resistance

1. Introduction

Hepatocellular carcinoma (HCC) is the most common liver malignancy, with an incidence of 42.5% in China (1). Overall, the 5-year survival rate of HCC patients in China is only 11.7-14.1% (2). Therefore, elucidating the mechanisms underlying HCC development is important. The hepatocyte nuclear factor 3 (HNF3) family, which includes the transcription factors hepatic forkhead box protein A1 (FOXA1), hepatic forkhead box protein A2 (FOXA2), and hepatic forkhead box protein A3 (FOXA3), was first identified in the liver (3). The HNF3 family regulates the expression of over 50% of functional genes in the liver, including those involved

in liver development, glucose and lipid metabolism, and bile metabolism (4-6). Unlike FOXA1 and FOXA3, FOXA2 knockout in the endoderm resulted in immediate postnatal death in mice. Approximately 43.5% of genes are reported to interact with FOXA2. Its knockdown can affect the transcription of the bile acid transporter gene, leading to intrahepatic cholestasis (7). FOXA2 has also been found to be downregulated in many solid tumors, such as pancreatic cancer, prostate cancer, breast cancer, and colon cancer. The expression of FOXA2 has been linked to tumor invasion and metastasis, as well as a poor prognosis. For instance, Smith *et al.* (8) found that FOXA2 had a high number of mutations in endometrial cancer tissues and was closely related

to tumor progression. Vorvis *et al.* (9) reported that FOXA2 knockdown in prostate cancer cells significantly inhibited cell growth. McDaniel *et al.* (10) found that FOXA2 regulated the development and differentiation of biliary progenitor cells. Similarly, a previous study by the current authors indicated that downregulation of FOXA2 promoted intrahepatic cholangiocarcinoma development (11). A number of studies have investigated the role of FOXA2 in HCC. The inactivation of FOXA2 has been found to regulate the Notch pathway, thereby promoting the progression of HCC (12). FOXA2 also regulated the transcription of p53 and p21, thereby affecting the proliferation of HCC cells (13,14). FOXA2 was found to be associated with the epithelial-mesenchymal transition (EMT) by downregulating the expression of E-cadherin (15). All of the aforementioned findings indicate that FOXA2 plays a critical role in both liver development and liver tumors.

Lenvatinib, a small-molecule inhibitor of multiple receptor tyrosine kinases, was approved for the first-line treatment of patients with unresectable HCC (16). Despite the high objective response rate in the treatment of HCC, drug resistance was inevitable. Because lenvatinib's potent antiangiogenic ability depended on various tyrosine kinase inhibitors, the mechanisms of lenvatinib resistance were complex. Previous studies have indicated that neurofibromin 1 (NF1), dual-specificity phosphatase 9 (DUSP9), and dual-specificity phosphatase 4 (DUSP4) were critical drivers of lenvatinib resistance in HCC (17,18). Inhibition of epidermal growth factor receptor (EGFR) might enhance the sensitivity of HCC to lenvatinib (19). The activation of signal transducers and activators of transcription 3 (STAT3) / ATP binding cassette subfamily B member 1 (ABCB1) signaling contributed to lenvatinib resistance, whereas the inhibition of EGFR reversed this process (20). Targeting pathways, such as the Integrin beta 8 (ITGB8) / heat shock protein 90 (HSP90) / protein kinase B (AKT) axis or the AKT/mechanistic target of rapamycin (mTOR) and extracellular regulated protein kinase (ERK) signaling pathways, might enhance the sensitivity of lenvatinib in HCC patients (21,22). Further understanding the mechanism of lenvatinib resistance to HCC could provide a potential treatment strategy in the event of unsatisfactory clinical benefits from lenvatinib. Since FOXA2 interacts with numerous genes in HCC, the effect of FOXA2 on lenvatinib resistance in HCC required investigation.

2. Materials and Methods

2.1. Human tumor tissues and follow-up

In total, 290 HCC patients with complete clinical data who underwent surgical resection at the West China Hospital of Sichuan University between January 2010 and December 2016 were included in this study. Overall

survival (OS) was defined as the duration between the initial surgery and the patient's death. Recurrence-free survival (RFS) was defined as the duration between the date of curative surgery and the date of relapse. Tissue microarray (TMA) cores (1.5 mm in diameter) were derived from formalin-fixed, paraffin-embedded samples. Immunohistochemical (IHC) staining was performed on the TMA slides, and the results were interpreted by three pathologists using a blinded method. The level of FOXA2 expression was scored based on the distribution and intensity of the signal. At least five areas were examined under 400x magnification and scored based on their signal distribution as follows: 1, $\leq 25\%$ stained; 2, 26-50% stained; 3, 51-75% stained; and 4, $> 75\%$ stained. The staining intensity was scored as follows: 0, negative; 1, weakly positive (light yellow); 2, positive (brownish yellow); and 3, intensely positive (brown). Tissues with an IHC score of less than or equal to 7 were designated as having a low level of expression, while those with a score of more than seven were designated as having a high level of expression. To investigate the relationship between FOXA2 expression and HCC, classic clinical characteristics, such as age, alpha fetoprotein (AFP) level, hepatitis B virus (HBV) infection status, albumin, total bilirubin, degree of differentiation, tumor size, satellite lesion, vascular invasion, and cirrhosis of the liver, were included. This study was approved by the Ethics Committee of West China Hospital, Sichuan University, and written informed consent was obtained from each participant.

2.2. Animals and treatments

Subcutaneously, 5×10^6 cells infected with Lenti-FOXA2 or Lenti-GFP were inoculated into the right forelimb of nude mice ($n = 15$). HCC tumors were successfully grafted to the majority of mice after three weeks. Lenvatinib (Selleck Chemicals, USA, cat# S1164) was dissolved in 100% dimethyl sulfoxide (DMSO; Sigma-Aldrich, USA) according to the manufacturer's instructions to produce a 20-mM stock solution. The 20-mM stock solution was diluted to 1 mM in a 0.3% sodium carboxymethyl cellulose solution. Mice were administered either DMSO or lenvatinib (200 μ L). DMSO (diluted in 0.3% sodium carboxymethyl cellulose solution) was used as an untreated control. Mice were randomly assigned to one of four groups: green fluorescent protein (GFP)-vehicle ($n = 5$), a GFP-lenvatinib ($n = 5$), a FOXA2-vehicle ($n = 5$), and FOXA2-lenvatinib ($n = 5$). The tumor size was recorded every 5 days. The tumor weight was recorded at sacrifice. Animal experiments were conducted in accordance with national and international laws and policies, and they were approved by the Department of Animal Care and Use Committee of Sichuan University.

2.3. Western blotting and immunohistochemistry

Western blotting was performed in accordance with the standard protocols. Proteins were extracted from cells or tissues using RIPA buffer containing a protease inhibitor cocktail, separated by sodium dodecyl sulfate-polyacrylamide gel electrophoresis, and transferred to a nitrocellulose membrane (Millipore). The antibodies used in this study were as follows: FOXA2 (1:1000; Abcam, UK, cat# EPR22919-71), FLAG-tag (1:1500; Proteintech, USA, cat# 80010-1-RR), Actin (1:1500; Proteintech, USA, cat# 66009-1-Ig), PDGFR: platelet-derived growth factor receptor (1:1000; Abcam, UK, cat# ab215978), p-PDGFR (1:1000; Abcam, UK, cat# ab134048), p-ERK1/2 (1:500; Abcam, UK, cat# ab76299), ERK1/2: extracellular regulated protein kinases 1/2 (1:1000; Abcam, UK, cat# ab184699), p-AMPK (T172) (1:500; Abcam, UK, cat# ab133448), adenosine monophosphate-activated protein kinase (AMPK) (1:500; Abcam, UK, cat# ab32047), p-mTOR (S2448) (1:500; Abcam, UK, cat# ab109268), ribosomal protein S6 kinase (S6K) (1:500; Abcam, UK, cat# ab186753), p-S6K (1:500; Abcam, UK, cat# ab60948), cleaved-caspase 3 (1:500; Abcam, UK, cat# ab32042), cleaved-PARP1 (1:500; Abcam, UK, cat# ab32561), microtubule-associated protein light chain 3II (LC3II) (1:500; Abcam, UK, cat# ab192890), and glyceraldehyde-3-phosphate dehydrogenase (GAPDH) (1:1500; Proteintech, USA, cat# 60004-1-Ig). Immunohistochemistry (IHC) was performed as previously described (11).

2.4. Cell culture, transfection, cell proliferation, and invasion

The HCC cell lines Hep3B and Huh7 were obtained from the Institute of Biochemistry and Cell Biology (Chinese Academy of Sciences, Shanghai, China). The cells were cultured in Dulbecco's Modified Eagle Medium supplemented with 10% heat-inactivated fetal calf serum. The small interfering RNA (siRNA) against FoxA2 (target sequence: CCATGAACATGTCGTCGTA) was synthesized by RiboBio Co., Ltd. (Shanghai, China). A FOXA2 overexpression plasmid (pcDNA3.1-FLAG-FOXA2) and the plvx-FOXA2 lentivirus were obtained from Tsingke Biotechnology Co., Ltd. (Beijing, China). Tumor cells (3×10^3 cells/well) were seeded in 96-well plates and grown for 24 h. Hep3B and Huh7 cells were transfected with the siRNA or FOXA2 overexpression plasmid and incubated for 72 h. A cell proliferation assay (CCK-8 kit, BD Biosciences, USA) was performed to assess Hep3B and Huh7 cell proliferation. A wound healing assay was performed to evaluate tumor cell invasion. The scratch wound healing assay and the transwell migration assay (BD Bioscience) were used to assess the migration of tumor cells. The results were analyzed using the mean number of cells in three fields for each sample.

2.5. Statistical analysis

The software R (3.6.1 Windows version) was used for statistical analyses. The continuous variables were expressed as the median \pm interquartile range (IQR), and the difference between groups was tested using the Mann-Whitney *U* test. Categorical variables were expressed as percentages, and statistical analyses were performed using the χ^2 test or Fisher's exact test. The Kaplan-Meier test was used for survival analysis and the log-rank test was used for difference analysis. The risk factors were analyzed using a stepwise Cox regression model. The potential risk factors ($P < 0.1$) were selected in univariate analysis and then included in multivariate analysis. The gray values of protein bands in Western blots were measured and analyzed using the software ImageJ (LOCI, University of Wisconsin, USA). $P < 0.05$ was considered statistically significant.

3. Results

3.1. FOXA2-associated tumor features and the prognosis for HCC patients

Western blotting (WB) revealed that FOXA2 was significantly downregulated in tumor tissue compared to adjacent tumor tissue (Figure 1A). Based on the IHC score (Figure 1B), 150 patients had a high level of FOXA2 expression and 140 had a low level of FOXA2 expression. The study included 290 patients with HCC after hepatectomy, as shown in Supplementary Table S1 (<http://www.biosciencetrends.com/action/getSupplementalData.php?ID=137>). There were significant differences in portal vein tumor thrombus (PVTT), poorly differentiated tumors, and serum alpha-fetoprotein (AFP) levels ($P < 0.05$). In comparison to the group with a high level of FOXA2 expression, the group with a low level of FOXA2 expression had a higher incidence of PVTT (12.9% vs. 5.3%), a higher proportion of poorly differentiated tumors (8.6% vs. 34.0%), and higher AFP levels (> 400 ng/mL). Based on survival analysis, the 1-year, 3-year, and 5-year recurrence-free survival (RFS) in the group with a low level of FOXA2 expression was 48.6%, 28.7%, and 17.0%, respectively, whereas the 1-year, 3-year, and 5-year RFS in the group with a high level of FOXA2 expression was 70.6%, 45.8%, and 34.6%, respectively ($P < 0.001$). The 1-year, 3-year, and 5-year OS in the group with a low level of FOXA2 expression was 92.7%, 76.7%, and 49.1%, respectively, whereas the 1-year, 3-year, and 5-year OS in the group with a high level of FOXA2 expression was 72.9%, 47.7%, and 25.9%, respectively ($P < 0.001$) (Figure 1C). A low level of FOXA2 expression was an independent risk factor for tumor recurrence (hazard ratio (HR): 1.899, $P < 0.001$) and long-term survival (HR: 2.011, $P = 0.003$) in HCC patients after hepatectomy (Figure 1D). Therefore, a low level of FOXA2 expression in HCC indicated aggressive tumors.

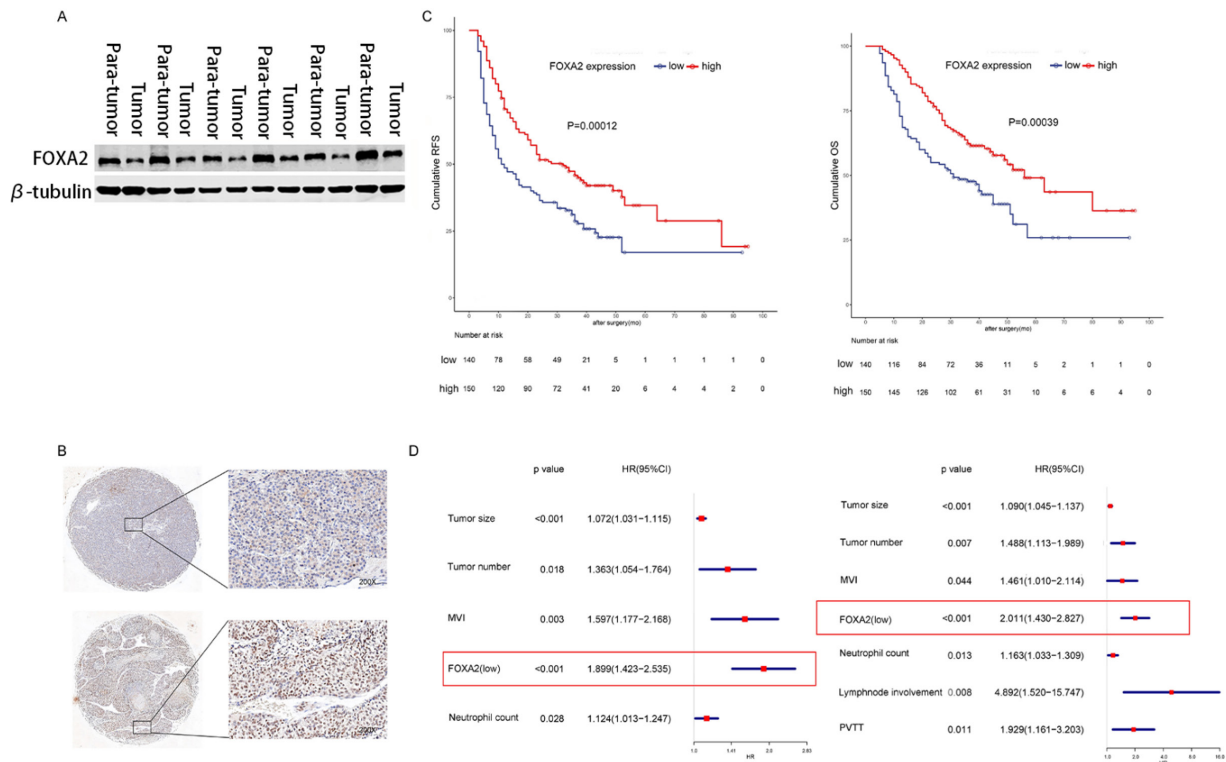


Figure 1. Clinicopathological features correlated with the expression of FOXA2. A: Western blots indicating FOXA2 expression in paired tumor and para-tumor tissue ($n = 6$). B: Representative images of low and high levels of FOXA2 expression in HCCs. C: survival analysis of HCC patients with a high or low level of FOXA2 expression; D: Multivariate analysis of recurrence-free survival (left) and overall survival (right) after HCC resection.

3.2. FOXA2 expression influenced HCC cell proliferation and invasion

FOXA2 was overexpressed and knocked down in Hep3B by plasmid transfection and in Huh7 cells by siRNA transfection (Supplementary Figure S1, <http://www.biosciencetrends.com/action/getSupplementalData.php?ID=137>). The cell cloning assay revealed that the proliferation of Hep3B and Huh7 cells was significantly enhanced after FOXA2 knockdown but inhibited when FOXA2 was overexpressed (Figure 2G and 2H). The scratch wound healing and transwell migration assays revealed that the knockdown of FOXA2 increased the invasion of Hep3B and Huh7 cells while the overexpression of FOXA2 inhibited it (Figure A-F). These findings suggest that a low level of FOXA2 expression might promote HCC progression.

3.3. Effects of FOXA2 expression on the cytotoxicity of lenvatinib in HCC cells

Hep3B and Huh7 cells were divided into two groups, with one group transfected with an empty plasmid and the other group transfected with a FLAG-FOXA2 plasmid. Both groups received varying concentrations of lenvatinib (0 μ M, 1 μ M, 2.5 μ M, 5 μ M, 10 μ M, and 20 μ M). Cell death occurred at 5 μ M, 10 μ M, and 20 μ M and the number of dead cells increased with an

increase in the lenvatinib concentration (Figure 3A and 3B). FOXA2 overexpression was found to increase the sensitivity of HCC cells to lenvatinib. Hep3B and Huh7 cells were transfected with FLAG-FOXA2 and treated with lenvatinib (200 nM); clone proliferation decreased significantly compared to that in the FOXA2 overexpression + lenvatinib group (Figure 3C and 3D). These findings suggest that FOXA2 overexpression augmented the ability of lenvatinib to promote cell death.

3.4. FOXA2 increased the antitumor effect of lenvatinib via the AMPK-mTOR pathway

Stemness and drug resistance were found to be closely related to the AMPK-mediated pathway (23,24). WB revealed that FOXA2 overexpression and lenvatinib treatment upregulated p-APMK expression in a synergistic manner (Figure 4A and 4B). Lenvatinib has been found to effectively inhibit HCC cell invasion. Following lenvatinib treatment, Hep3B and Huh7 cells overexpressing or not overexpressing FOXA2 were treated with AMPK inhibitor compound C (2 μ M). Their ability to invade cells was significantly restored, with no significant differences between the groups (Figure 4C). When the mTOR activator MHY1485 (5 μ M) was added to Hep3B/Huh7 cells overexpressing FOXA2 after treatment with lenvatinib (10 μ M), the antitumor effect of lenvatinib that was enhanced by FOXA2 was attenuated

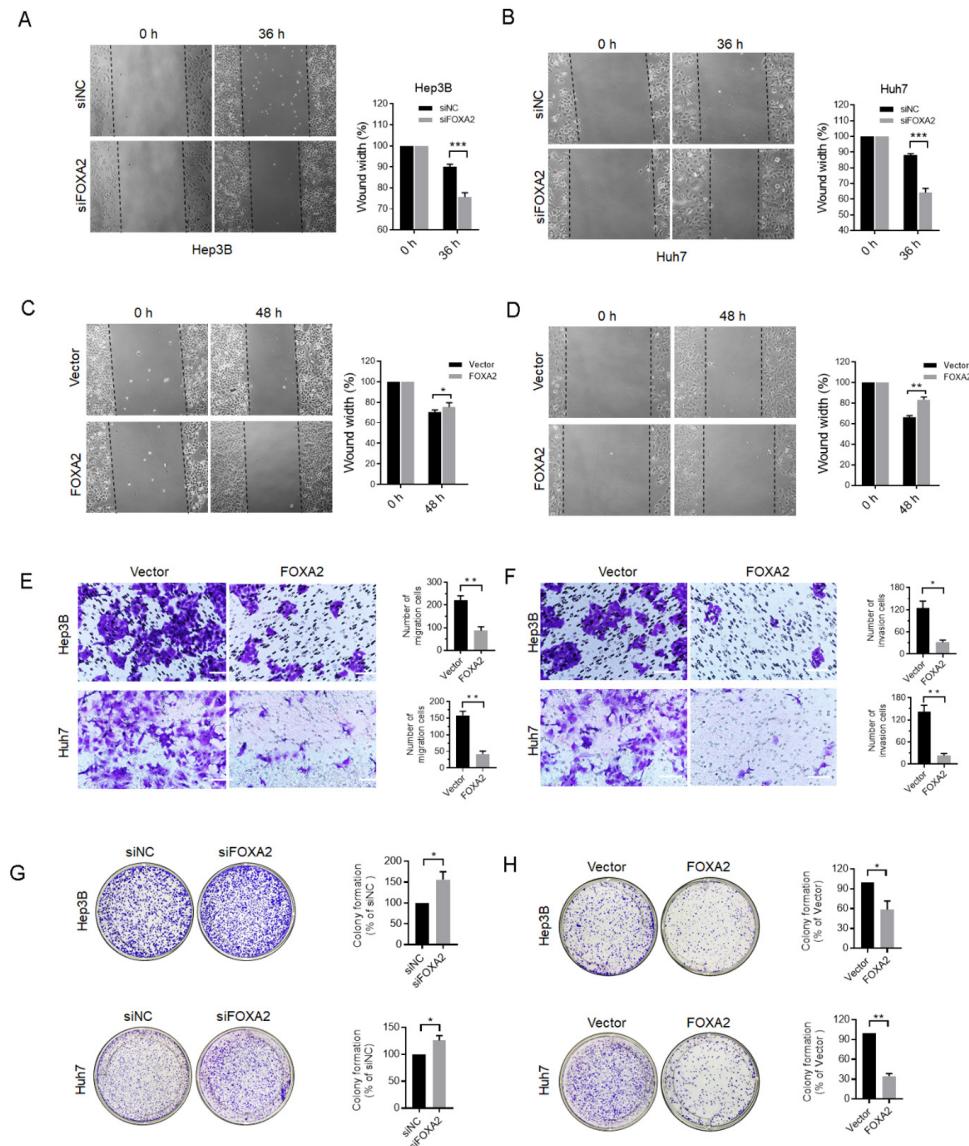


Figure 2. FOXA2 inhibited HCC cell (Huh7/Hep3B) invasion. Scratch wound and transwell assay suggested that FOXA2 inhibited or promoted HCC cell migration after FOXA2 overexpression or knockdown (A-F); Clonal formation assays indicated that cell proliferation decreased after FOXA2 overexpression and increased after FOXA2 knockdown (G and H).

(Figure 4G). Similar results have been observed in cloning assay (Figure 4 E-F). This suggested that the inhibitory effect of FOXA2 on HCC was associated with AMPK activation and mTOR inhibition. The levels of p-mTOR and p-S6K expression decreased, while the level of p-AMPK expression increased. Mammalian target of rapamycin C1 (mTORC1) is an important AMPK substrate. FOXA2 overexpression combined with lenvatinib inhibited mTORC1 activation, whereas AMPK inhibitor compound C (2 μ M) significantly restored p-mTOR expression (Figure 4H). These findings indicated that FOXA2 overexpression inhibited the mTOR pathway by activating AMPK (Figure 9).

3.5. Lenvatinib combined with FOXA2 overexpression upregulated the STRAD α - LKB1 axis

Activation of AMPK or inhibition of mTOR in HCC

may enhance the antitumor effect of lenvatinib (25,26). Lenvatinib combined with FOXA2 overexpression was found to activate AMPK. Moreover, metformin activated AMPK in HCC cell lines and indeed enhanced the antitumor effect of lenvatinib in HCC cell lines. LKB1 is an important upstream regulator of AMPK (Supplementary Figure S2, <http://www.biosciencetrends.com/action/getSupplementalData.php?ID=137>). A previous study reported that the nuclear residence of LKB1 in HCC cells attenuated activation of AMPK (27). Ste20-related adaptor alpha (STRAD α) may promote the nuclear - cytoplasmic translocation of liver kinase B1(LKB1) (28). Compared to lenvatinib treatment alone, lenvatinib combined with FOXA2 overexpression lead to significantly increased LKB1 phosphorylation. The expression of the LKB1 regulator STRAD α was up-regulated (Figure 5A). After FOXA2 overexpression, the levels of LKB1 and STRAD α protein in the

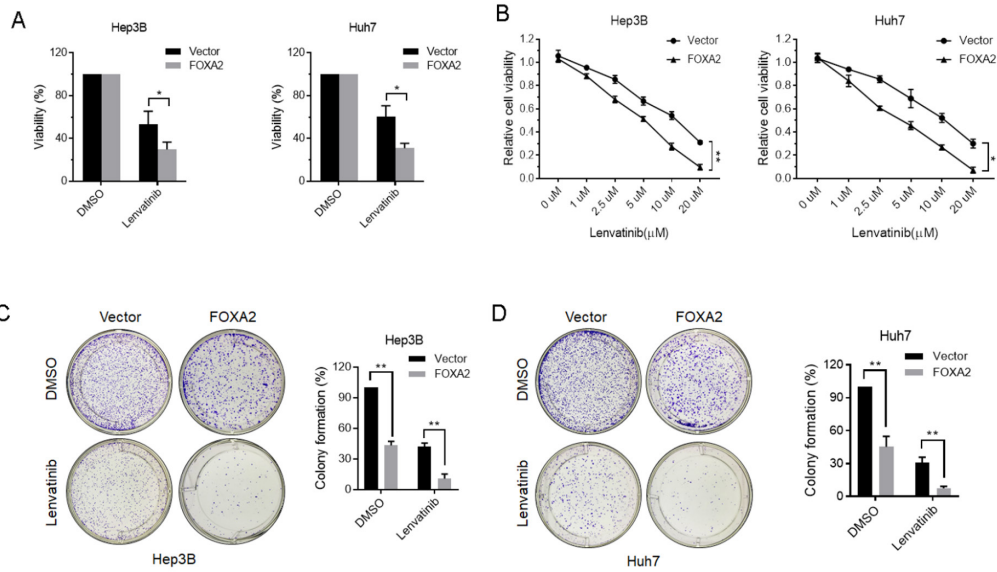


Figure 3. FOXA2 increased HCC cell (Hep3B/Huh7) sensitivity to lenvatinib. The viability of HCC cell lines was significantly reduced by lenvatinib and further inhibited after FOXA2 overexpression (A and B). Clonal formation assays suggested that FOXA2 overexpression further inhibited HCC cell proliferation (C and D).

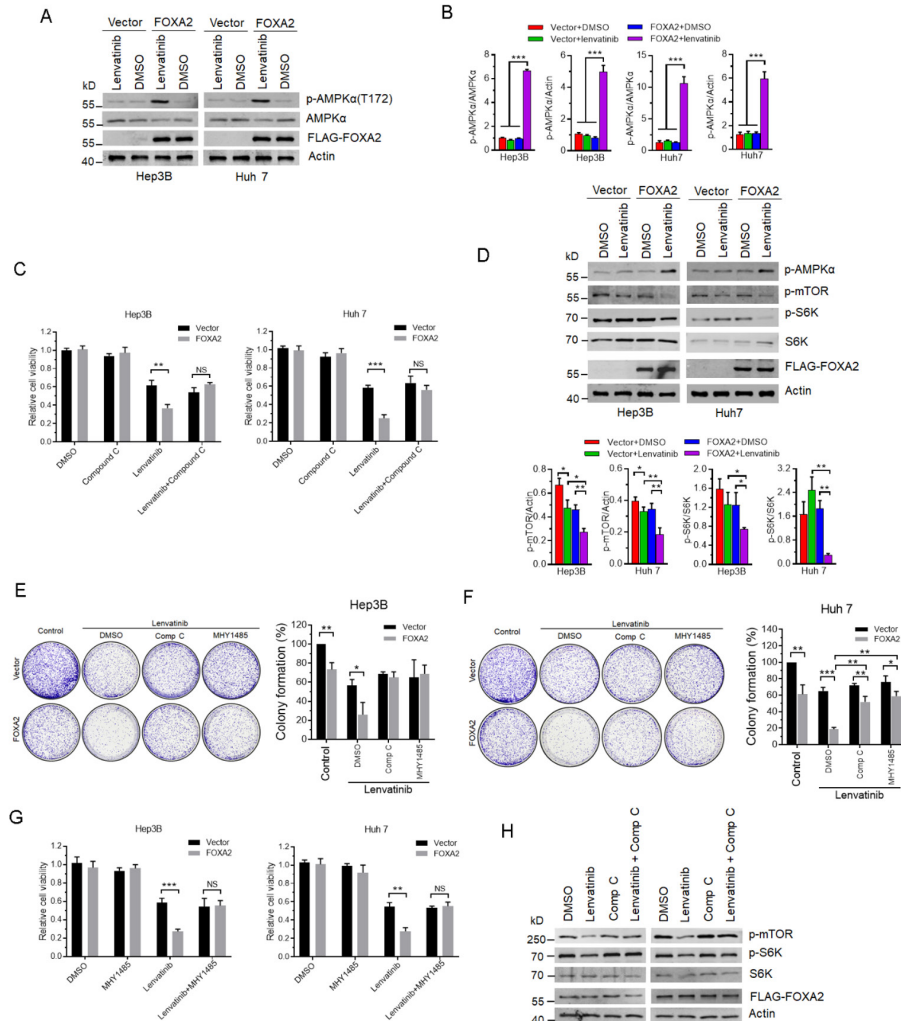


Figure 4. FOXA2 increased HCC cell (Hep3B/Huh7) sensitivity to lenvatinib via the AMPK signaling pathway. p-AMPK significantly was up-regulated in HCC cell lines overexpressing FOXA2 after treatment with lenvatinib (A and B). After adding AMPK inhibitor Compound C (2 μM) for 48 h, a CCK-8 assay indicated that the cell viability was restored by treatment with lenvatinib (C). The levels of p-mTOR and p-S6K protein were significantly down-regulated in HCC cell lines overexpressing FOXA2 after treatment with lenvatinib (D). Colony assay and CCK-8 indicated that inhibition of AMPK or activation of mTOR impaired HCC cell line sensitivity to lenvatinib by FOXA2 (E-G). Inhibition of AMPK upregulated the levels of p-mTOR or p-S6K protein in HCC cell lines treating with lenvatinib and FOXA2 overexpression (H).

cytoplasm were up-regulated, while the levels of LKB1 and STRAD α protein in the nucleus were down-regulated (Figure 5B). This suggested that lenvatinib combined with FOXA2 overexpression further promoted LKB1 cytoplasmic residence and activated AMPK by upregulating the level of STRAD α expression (Figure 9).

3.6. Autophagy increased with a high level of FOXA2 expression and lenvatinib treatment

The AMPK-mTOR pathway plays an important role in autophagy. To determine whether FOXA2-induced

lenvatinib sensitization occurs *via* AMPK-mediated autophagy, the level of expression of LC3-II, a key molecule of autophagy, was measured. When cells overexpressing FOXA2 were treated with lenvatinib, the level of LC3-II expression increased. When the cells overexpressing FOXA2 were treated with an autophagy inhibitor (bafilomycin A1) after lenvatinib treatment, the level of LC3-II expression continued to increase (Figure 6A). These results revealed that LC3-II accumulation was caused by an increase in autophagy rather than inhibition of autophagy clearance. Hep3B cells were co-transfected with GFP-LC3 and FLAG-FOXA2

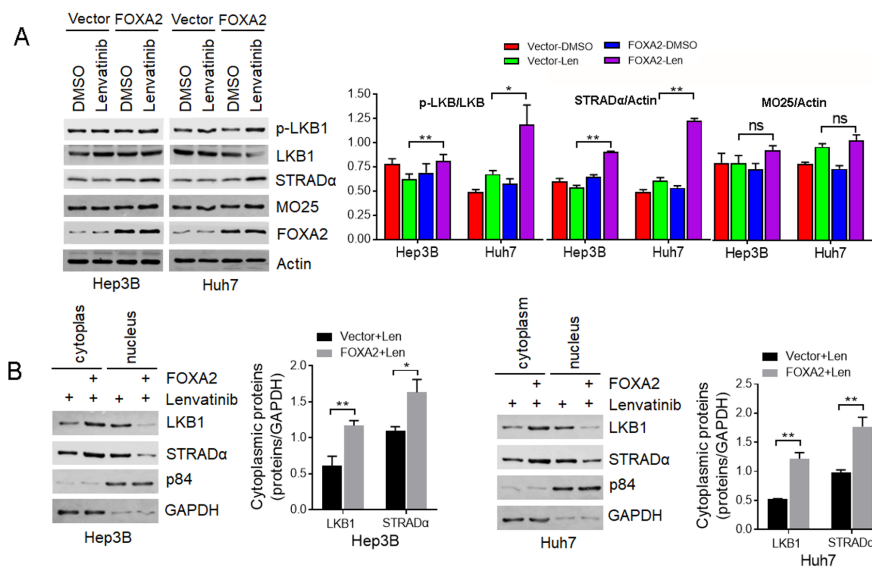


Figure 5. Lenvatinib combined with FOXA2 overexpression upregulated p-LKB1 and the STRAD α -LKB1 axis. The level of LKB1 phosphorylation increased and the level of expression of the LKB1 regulator STRAD α was up-regulated (A). After FOXA2 overexpression, the levels of LKB1 and STRAD α protein in the cytoplasm were up-regulated, and the levels of LKB1 and STRAD α protein in the nucleus were down-regulated (B). MO25: Liver kinase B1 (LKB1, also known as STK11), MO25, and STRAD. p84: Nuclear matrix protein p84.

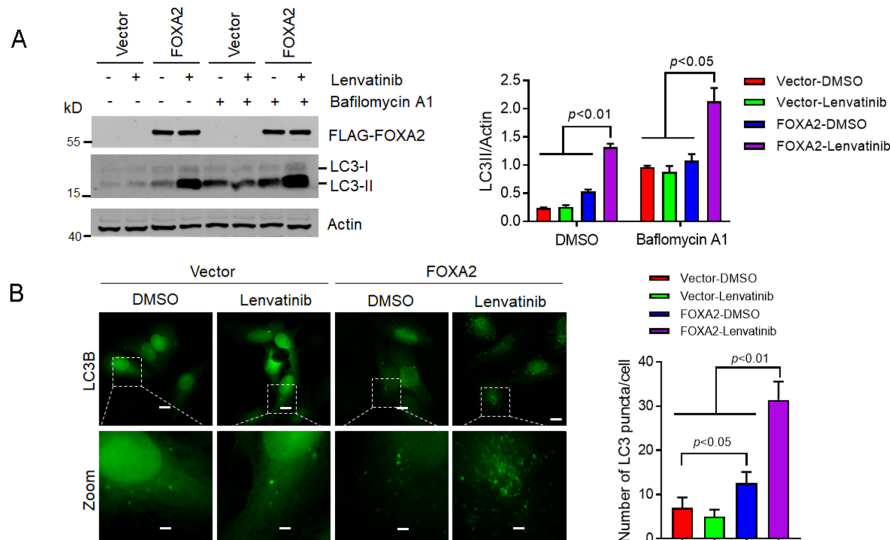


Figure 6. Lenvatinib combined with FOXA2 overexpression promoted autophagy. Microtubule-associated protein light chain 3II (LC3II) was significantly up-regulated in HCC cells overexpressing FOXA2 after lenvatinib treatment. After adding bafilomycin A1, LC3II was further up-regulated (A). The number of LC3 puncta/cell was highest in the FOXA2+lenvatinib group. This suggested that autophagy was enhanced (B). LC3-I: microtubule-associated protein light chain 3 I.

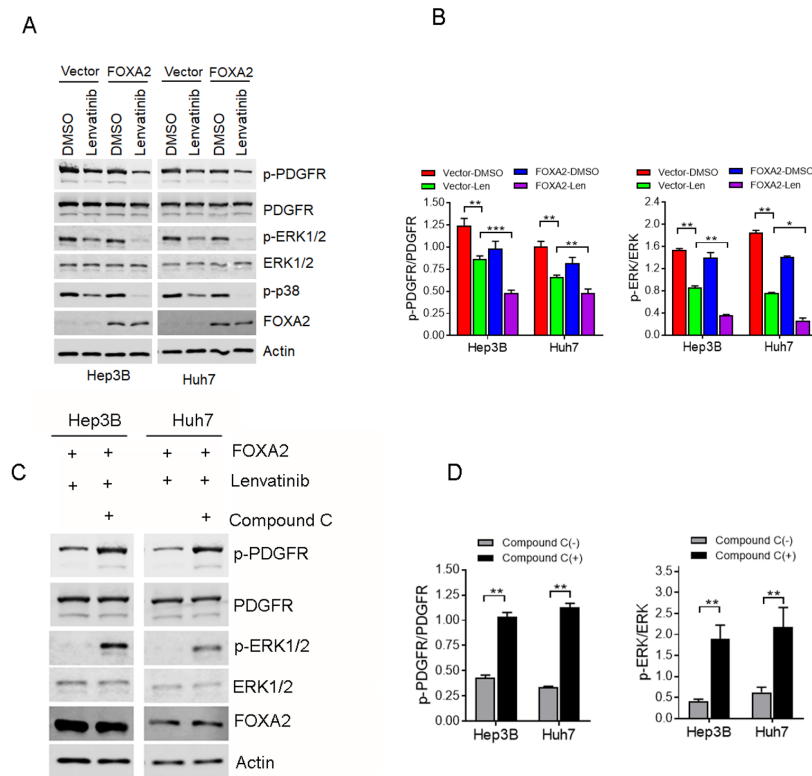


Figure 7. Lenvatinib combined with FOXA2 overexpression inhibits the PDGFR-ERK pathway via the AMPK signaling pathway. After HCC cell lines were transfected with FOXA2 for 24 hours, they were treated with lenvatinib (10 μ M) and AMPK inhibitor Compound C (2 μ M) for 48 hours. Western blotting indicated that the levels of p-PDGFR and p-ERK1/2 protein were significantly down-regulated compared to lenvatinib or FOXA2 overexpression alone (A and B). After adding AMPK inhibitor Compound C, the levels of p-PDGFR and p-ERK1/2 protein were up-regulated (C and D).

vectors and incubated for 24 h, followed by treatment with lenvatinib (10 μ M) for 24 h. The results suggested that FOXA2 overexpression combined with lenvatinib treatment caused a significant increase in autophagy (Figure 6B).

3.7. Lenvatinib treatment combined with FOXA2 overexpression inhibited the PDGFR-ERK pathway

PDGFR plays a significant role in anti-tumor drug resistance. Lenvatinib inhibits tumor progression by targeting PDGFR. Results indicated that FOXA2 overexpression significantly inhibited the expression of p-PDGFR, implying that the enhanced antitumor effect of lenvatinib by forced FOXA2 expression may depend on modification of PDGFR (Figure 7A-B). When the AMPK pathway was inhibited, the effect of forced FOXA2 expression on the sensitivity of HCC cells to lenvatinib was diminished. Interestingly, expression of p-PDGFR and p-ERK1/2 was reversed (Figure 7C-D). These results suggested that FOXA2 may regulate the PDGFR-ERK pathway *via* the AMPK signaling axis and contribute to the antitumor effect of lenvatinib (Figure 9).

3.8. FOXA2 further inhibited the growth of HCC treated with lenvatinib *via* the AMPK signaling pathway

Hep3B cells were divided into two groups; one group was transfected with lentivirus-green fluorescent protein (Lenti-GFP), and the other group was transfected with lentivirus-FOXA2 (Lenti-FOXA2). Two group cells were seeded in nude mice and observed for 4 weeks. The results indicated that the tumorigenic ability diminished significantly in the group overexpressing FOXA2. Then, two groups were treated with lenvatinib. The weakest tumorigenicity and very slow tumor growth were observed in the group overexpressing FOXA2 (Figure 8A-C). Protein detection in tumor tissues indicated that the level of p-AMPK expression increased significantly in the group overexpressing FOXA2 (Figure 8D-E). This confirmed that FOXA2 enhanced the antitumor effect of lenvatinib *via* the AMPK-mTOR pathway.

4. Discussion

Results indicated that the expression of FOXA2 in tumor tissue was downregulated compared to that in adjacent tumor tissue. Consistent with the current findings, data from high-throughput sequencing expression profiling suggested that the content of FOXA2 mRNA in tumor samples was significantly lower than that in paired non-cancer tissues (GSE119336, by Cao Peng and Li Yong). The level of FOXA2 expression in a variety of human

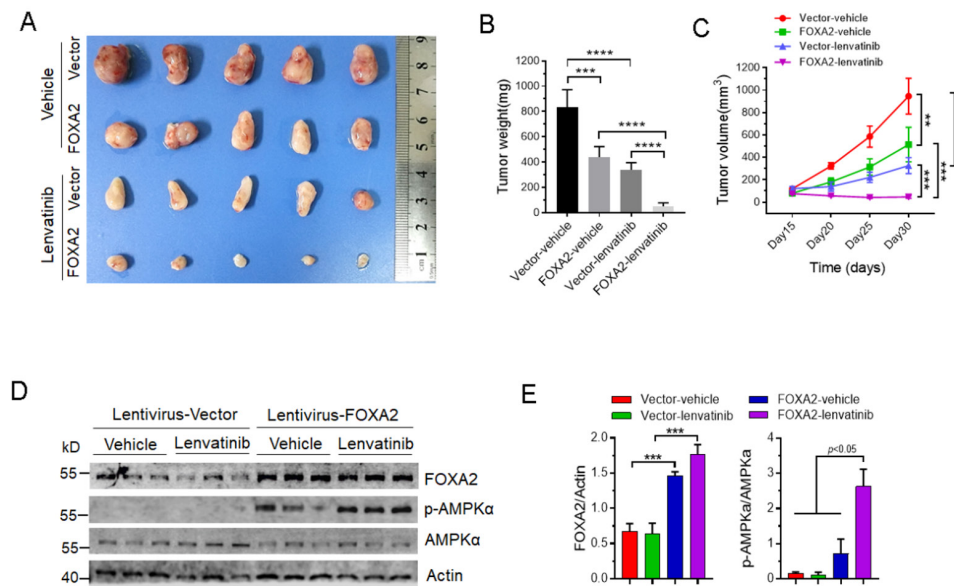


Figure 8. FOXA2 further inhibited the growth of HCC treated with lenvatinib via the AMPK signaling pathway. FOXA2 overexpression enhanced the antitumor effect of lenvatinib (A). Tumor weight (B) and volume (C) of subcutaneous implant models in nude mice produced by injecting HCC cells stably expressing FOXA2 ($n = 10$, lenvatinib: $n = 5$; control: $n = 5$) and an empty vector ($n = 10$, lenvatinib: $n = 5$; control: $n = 5$); FOXA2 overexpression combined with lenvatinib up-regulated p-AMPK (D and E).

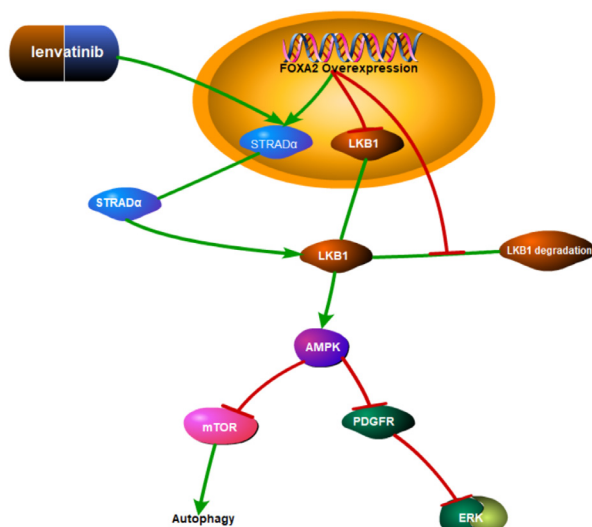


Figure 9. FOXA2 overexpression increased the antitumor effect of lenvatinib via the AMPK-mTOR-Autophagy pathway. Lenvatinib treatment combined with FOXA2 overexpression inhibited the PDGFR-ERK pathway via activation of AMPK. The levels of LKB1 and STRAD α protein in the nucleus were down-regulated. FOXA2: forkhead box protein A2; STRAD α : ste20-related adaptor alpha; LKB1: liver kinase B1; AMPK: adenosine monophosphate-activated protein kinase; mTOR: mechanistic target of rapamycin; PDGFR: platelet-derived growth factor receptor; ERK: extracellular regulated protein kinases.

HCC cell lines has been reported to be significantly lower than that in normal human fetal hepatocytes (LO-2) (29). According to IHC, 48.3% of patients had a low level of FOXA2 expression. Patients with a low level of FOXA2 expression had a higher incidence of portal vein invasion and poorly differentiated tumors. This suggested

that the expression of FOXA2 was associated with tumor aggressiveness. In terms of prognosis, patients with a high level of FOXA2 expression had a significantly higher 5-year RFS and OS than patients with a low level of FOXA2 expression. A low level of FOXA2 expression was identified as an independent risk factor for tumor recurrence. In addition, tumor size, the number of tumors, MVI, PVTT, and lymph node status have been found to be independent risk factors for patients with HCC (30). This indicates that a low level of FOXA2 expression was associated with a highly invasive tumor.

The proliferation and invasion capacity of HCC cells were found to be significantly enhanced by a decrease in FOXA2 expression but increased after forced FOXA2 expression. Previous studies have found that patients with higher levels of FOXA2 expression have a better prognosis for breast carcinoma and gastric cancer (31,32). A study has also found that FOXA2 acted as a tumor suppressor and inhibited the invasion of various tumors (13). FOXA2 regulated tumor behavior by interacting with various genes, including the cadherin 1(CDH1) promoter, forkhead box protein P2 (FOXP2), and staphylococcal nuclease domain containing 1 (SND1) (29,33,34). The current authors previously reported that FOXA2 promotes intrahepatic cholesteatoma by activating the MAPK signaling pathway (11). According to preliminary findings and previous research (11), FOXA2 contributed to tumor progression in HCC cells. Lenvatinib is a small-molecule inhibitor of multiple receptor tyrosine kinases that is widely used to treat patients with unresectable HCC. However, this drug has only a limited clinical benefit. Numerous studies have been conducted to investigate potential targets to

improve prognosis (17-19,21). The current study found that overexpression of FOXA2 enhanced the ability of lenvatinib to promote cell death in lenvatinib-sensitive HCC cells.

FOXA2 mutations have been reported to be associated with the AMPK signaling pathway (35). The AMPK pathway is closely involved in cancer drug resistance *via* several mechanisms of antitumor drug resistance (24,36). An AMPK activator enhanced the antitumor effect of cisplatin in meningiomas *via* the AMPK/mTOR signaling pathway (37). AMPK/mTOR-mediated autophagy was found to contribute to docetaxel resistance in castration-resistant prostate cancer (38). These findings suggest that the contribution of FOXA2 to lenvatinib sensitivity in HCC might be dependent on the AMPK signaling pathway. The enhanced antitumor effect of lenvatinib by forced overexpression of FOXA2 was found to be attenuated when AMPK was inhibited. AMPK phosphorylation increased significantly in HCC cells following lenvatinib treatment and overexpression of FOXA2; however, the levels of p-mTOR and p-S6K expression decreased. These findings indicate that the AMPK/mTOR signaling pathway played a critical role in increasing lenvatinib sensitization by FOXA2 in HCC cells. The AMPK enzyme is a critical energy and nutrient sensor in cells. AMPK activation might regulate the metabolic reprogramming and self-regeneration of cancer stem cells. Therefore, targeting the AMPK signaling pathway is a potential strategy for overcoming cancer drug resistance (24,39). The current study found that FOXA2 might be a key target for overcoming lenvatinib resistance.

Autophagy is a physiological cell survival mechanism utilized by tumor cells to prevent cell death and induce drug resistance. FOXA2 has been found to be closely related to autophagy (40). mTOR-mediated cancer drug resistance inhibits autophagy and generates a druggable metabolic vulnerability (41). AMPK phosphorylation has a critical role in mediating autophagy (39). Chloroquine is an autophagy inducer that increases microtubule-associated protein light chain 3B-II protein expression. Cisplatin induced autophagy and contributed to drug resistance by activating the AMPK/mTOR signaling pathway. Cisplatin in combination with chloroquine decreased the level of p-AMPK expression and increased the level of p-mTOR expression, which inhibited the activation of autophagy (42). Cisplatin in combination with chloroquine was also found to increase the cisplatin-induced apoptosis and growth of lung adenocarcinoma cells. This indicates that the AMPK-mTOR pathway plays an important role in autophagy. The current study indicated that FOXA2 in combination with lenvatinib activated the AMPK signaling pathway and enhanced autophagy. PDGFR is one of the key targets of lenvatinib (43,44). In the current study, lenvatinib and FOXA2 overexpression significantly reduced the expression of p-PDGFR

compared to lenvatinib alone or overexpressed FOXA2 alone. However, this phenomenon was reversed by an AMPK inhibitor. This may be why FOXA2 overexpression promotes lenvatinib sensitivity in HCC. However, the current study had several limitations. First, lenvatinib inhibits HCC *via* many targets. This study focused on the PDGFR-ERK pathway in drug resistance. Second, the relationship between the AMPK signaling pathway and autophagy has been well-established, but autophagy in lenvatinib-related drug resistance was not fully investigated. Therefore, the hope is that additional quality research will delve into this issue.

In conclusion, results indicated that a low level of FOXA2 expression is significantly associated with poor tumor biology. Results also revealed that overexpressed FOXA2 enhanced HCC susceptibility to lenvatinib, which was mediated by the AMPK/PDGFR signaling pathway. These findings indicate that FOXA2 may be a promising target to treat lenvatinib-associated drug resistance.

Funding: This work was supported by grants from the Scientific and Technological Support Project of Sichuan Province (2022YFS0257 and 2022YFS0255).

Conflict of Interest: The authors have no conflicts of interest to disclose.

Ethics approval and consent to participate: The experimental protocol was established according to the ethical guidelines of the Helsinki Declaration and was approved by the Human Ethics Committee of West China Hospital, Sichuan University. Written informed consent was obtained from individual participants or their guardian. Animal experiments were conducted in accordance with national and international laws and policies and were approved by the Department of Animal Care and Use Committee of Sichuan University.

Availability of data and materials: The datasets used and/or analyzed during the current study are available from the corresponding author on reasonable request.

References

1. Qiu H, Cao S, Xu R. Cancer incidence, mortality, and burden in China: A time-trend analysis and comparison with the United States and United Kingdom based on the global epidemiological data released in 2020. *Cancer Commun (Lond)*. 2021; 41:1037-1048.
2. Park JW, Chen M, Colombo M, Roberts LR, Schwartz M, Chen PJ, Kudo M, Johnson P, Wagner S, Orsini LS, Sherman M. Global patterns of hepatocellular carcinoma management from diagnosis to death: The BRIDGE Study. *Liver Int*. 2015; 35:2155-2166.
3. Wederell ED, Bilenky M, Cullum R, *et al*. Global analysis of *in vivo* Foxa2-binding sites in mouse adult liver using massively parallel sequencing. *Nucleic Acids Res*. 2008; 36:4549-4564.

4. Li Z, White P, Tuteja G, Rubins N, Sackett S, Kaestner KH. Foxa1 and Foxa2 regulate bile duct development in mice. *J Clin Invest.* 2009; 119:1537-1545.
5. Lee CS, Friedman JR, Fulmer JT, Kaestner KH. The initiation of liver development is dependent on Foxa transcription factors. *Nature.* 2005; 435:944-947.
6. Liu M, Lee DF, Chen CT, *et al.* IKK α activation of NOTCH links tumorigenesis *via* FOXA2 suppression. *Mol Cell.* 2012; 45:171-184.
7. Wang W, Yao LJ, Shen W, Ding K, Shi PM, Chen F, He J, Ding J, Zhang X, Xie WF. FOXA2 alleviates CCl₄-induced liver fibrosis by protecting hepatocytes in mice. *Sci Rep.* 2017; 7:15532.
8. Smith B, Neff R, Cohn DE, Backes FJ, Suarez AA, Mutch DG, Rush CM, Walker CJ, Goodfellow PJ. The mutational spectrum of FOXA2 in endometrioid endometrial cancer points to a tumor suppressor role. *Gynecol Oncol.* 2016; 143:398-405.
9. Vorvis C, Hatzia Apostolou M, Mahurkar-Joshi S, Koutsoumpa M, Williams J, Donahue TR, Poultsides GA, Eibl G, Iliopoulos D. Transcriptomic and CRISPR/Cas9 technologies reveal FOXA2 as a tumor suppressor gene in pancreatic cancer. *Am J Physiol Gastrointest Liver Physiol.* 2016; 310:G1124-1137.
10. McDaniel K, Meng F, Wu N, *et al.* Forkhead box A2 regulates biliary heterogeneity and senescence during cholestatic liver injury in mice. *Hepatology.* 2017; 65:544-559.
11. Shen J, Zhou Y, Zhang X, Peng W, Peng C, Zhou Q, Li C, Wen T, Shi Y. Loss of FoxA2 accelerates neoplastic changes in the intrahepatic bile duct partly *via* the MAPK signaling pathway. *Aging (Albany NY).* 2019; 11:9280-9294.
12. Li Z, Tuteja G, Schug J, Kaestner KH. Foxa1 and Foxa2 are essential for sexual dimorphism in liver cancer. *Cell.* 2012; 148:72-83.
13. Shang H, Shi L, Jiang X, Zhou P, Wei Y. Correlation between high expression of FOXA2 and improved overall survival in ovarian cancer patients. *Medical Sci Monitor.* 2021; 27:e928763.
14. Xie W, Xue Y, Zhang H, Wang Y, Meng M, Chang G, Shen X. A high-concentrate diet provokes inflammatory responses by downregulating Forkhead box protein A2 (FOXA2) through epigenetic modifications in the liver of dairy cows. *Gene.* 2022; 837:146703.
15. Kondratyeva LG, Sveshnikova AA, Grankina EV, Chernov IP, Kopantseva MR, Kopantzev EP, Sverdlov ED. Downregulation of expression of mater genes SOX9, FOXA2, and GATA4 in pancreatic cancer cells stimulated with TGF β 1 epithelial-mesenchymal transition. *Dokl Biochem Biophys.* 2016; 469:257-259.
16. Kudo M, Finn RS, Qin S, *et al.* Lenvatinib versus sorafenib in first-line treatment of patients with unresectable hepatocellular carcinoma: A randomised phase 3 non-inferiority trial. *Lancet (London, England).* 2018; 391:1163-1173.
17. Lu Y, Shen H, Huang W, He S, Chen J, Zhang D, Shen Y, Sun Y. Genome-scale CRISPR-Cas9 knockout screening in hepatocellular carcinoma with lenvatinib resistance. *Cell Death Discov.* 2021; 7:359.
18. Huang S, Ma Z, Zhou Q, Wang A, Gong Y, Li Z, Wang S, Yan Q, Wang D, Hou B, Zhang C. Genome-wide CRISPR/Cas9 library screening identified that DUSP4 deficiency induces lenvatinib resistance in hepatocellular carcinoma. *Int J Bio Sci.* 2022; 18:4357-4371.
19. Jin H, Shi Y, Lv Y, *et al.* EGFR activation limits the response of liver cancer to lenvatinib. *Nature.* 2021; 595:730-734.
20. Hu B, Zou T, Qin W, *et al.* Inhibition of EGFR overcomes acquired lenvatinib resistance driven by STAT3-ABCB1 signaling in hepatocellular carcinoma. *Cancer Res.* 2022; 82:3845-3857.
21. Hou W, Bridgeman B, Malnassy G, Ding X, Cotler SJ, Dhanarajan A, Qiu W. Integrin subunit beta 8 contributes to lenvatinib resistance in HCC. *Hepatol Commun.* 2022; 6:1786-1802.
22. Zhao Z, Song J, Zhang D, Wu F, Tu J, Ji J. Oxysophocarpine suppresses FGFR1-overexpressed hepatocellular carcinoma growth and sensitizes the therapeutic effect of lenvatinib. *Life Sci.* 2021; 264:118642.
23. Wu H, Liu B, Chen Z, Li G, Zhang Z. MSC-induced lncRNA HCP5 drove fatty acid oxidation through miR-3619-5p/AMPK/PGC1 α /CEBPB axis to promote stemness and chemo-resistance of gastric cancer. *Cell Death Dis.* 2020; 11:233.
24. Tan W, Zhong Z, Carney RP, Men Y, Li J, Pan T, Wang Y. Deciphering the metabolic role of AMPK in cancer multi-drug resistance. *Seminars Cancer Bio.* 2019; 56:56-71.
25. Ma X, Qiu Y, Sun Y, Zhu L, Zhao Y, Li T, Lin Y, Ma D, Qin Z, Sun C, Han L. NOD2 inhibits tumorigenesis and increases chemosensitivity of hepatocellular carcinoma by targeting AMPK pathway. *Cell Death Dis.* 2020; 11:174.
26. Roberts JL, Poklepovic A, Booth L, Dent P. The multi-kinase inhibitor lenvatinib interacts with the HDAC inhibitor entinostat to kill liver cancer cells. *Cellular Signalling.* 2020; 70:109573.
27. Wang L, Li H, Zhen Z, Ma X, Yu W, Zeng H, Li L. CXCL17 promotes cell metastasis and inhibits autophagy *via* the LKB1-AMPK pathway in hepatocellular carcinoma. *Gene.* 2019; 690:129-136.
28. Dorfman J, Macara IG. STRAD α regulates LKB1 localization by blocking access to importin- α , and by association with Crm1 and exportin-7. *Molec Bio Cell.* 2008; 19:1614-1626.
29. Zhan F, Zhong Y, Qin Y, Li L, Wu W, Yao M. SND1 facilitates the invasion and migration of cervical cancer cells by Smurf1-mediated degradation of FOXA2. *Exper Cell Res.* 2020; 388:111809.
30. Llovet JM, Bru C, Bruix J. Prognosis of hepatocellular carcinoma: The BCLC staging classification. *Seminars Liver Dis.* 1999; 19:329-338.
31. Yang Z, Jiang X, Zhang Z, Zhao Z, Xing W, Liu Y, Jiang X, Zhao H. HDAC3-dependent transcriptional repression of FOXA2 regulates FTO/m6A/MYC signaling to contribute to the development of gastric cancer. *Cancer Gene Ther.* 2021; 28:141-155.
32. Zhang Z, Yang C, Gao W, Chen T, Qian T, Hu J, Tan Y. FOXA2 attenuates the epithelial to mesenchymal transition by regulating the transcription of E-cadherin and ZEB2 in human breast cancer. *Cancer Lett.* 2015; 361:240-250.
33. Bow YD, Wang YY, Chen YK, Su CW, Hsu CW, Xiao LY, Yuan SS, Li RN. Silencing of FOXA2 decreases E-cadherin expression and is associated with lymph node metastasis in oral cancer. *Oral Dis.* 2020; 26:756-765.
34. Liu Y, Chen T, Guo M, Li Y, Zhang Q, Tan G, Yu L, Tan Y. FOXA2-interacting FOXP2 prevents epithelial-mesenchymal transition of breast cancer cells by stimulating E-cadherin and PHF2 transcription. *Front*

- Oncol. 2021; 11:605025.
35. Roelands J, Hendrickx W, Zoppoli G, *et al.* Oncogenic states dictate the prognostic and predictive connotations of intratumoral immune response. *J Immunother Cancer.* 2020; 8:e000617.
 36. Wang Z, Wang N, Liu P, Xie X. AMPK and cancer. *Exp Suppl.* 2016; 107:203-226.
 37. Guo L, Cui J, Wang H, Medina R, Zhang S, Zhang X, Zhuang Z, Lin Y. Metformin enhances anti-cancer effects of cisplatin in meningioma through AMPK-mTOR signaling pathways. *Mol Ther Oncolytics.* 2021; 20:119-131.
 38. Lin JZ, Wang WW, Hu TT, Zhu GY, Li LN, Zhang CY, Xu Z, Yu HB, Wu HF, Zhu JG. FOXM1 contributes to docetaxel resistance in castration-resistant prostate cancer by inducing AMPK/mTOR-mediated autophagy. *Cancer Lett.* 2020; 469:481-489.
 39. Wang Z, Liu P, Chen Q, Deng S, Liu X, Situ H, Zhong S, Hann S, Lin Y.. Targeting AMPK signaling pathway to overcome drug resistance for cancer therapy. *Current Drug Targets.* 2016; 17:853-864.
 40. Peng Q, Qin J, Zhang Y, Cheng X, Wang X, Lu W, Xie X, Zhang S. Autophagy maintains the stemness of ovarian cancer stem cells by FOXA2. *J Exper Clin Cancer Res.* 2017; 36:171.
 41. Gremke N, Polo P, Dort A, Schneikert J, Elmshäuser S, Brehm C, Klingmüller U, Schmitt A, Reinhardt HC, Timofeev O, Wanzel M, Stiewe T. mTOR-mediated cancer drug resistance suppresses autophagy and generates a druggable metabolic vulnerability. *Nature Comm.* 2020; 11:4684.
 42. Wu T, Wang MC, Jing L, Liu ZY, Guo H, Liu Y, Bai YY, Cheng YZ, Nan KJ, Liang X.. Autophagy facilitates lung adenocarcinoma resistance to cisplatin treatment by activation of AMPK/mTOR signaling pathway. *Drug Design, Dev Ther.* 2015; 9:6421-6431.
 43. Iesato A, Li S, Roti G, Hacker MR, Fischer AH, Nucera C. lenvatinib targets PDGFR- β pericytes and inhibits synergy with thyroid carcinoma cells: Novel translational insights. *J Clin Endo Metab.* 2021; 106:3569-3590.
 44. Scott LJ. Lenvatinib: First global approval. *Drugs.* 2015; 75:553-560.

Received December 27, 2022; Revised February 13, 2023; Accepted February 21, 2023.

[§]These authors contributed equally to this work.

*Address correspondence to:

Chuan Li, Department of Liver Surgery, West China Hospital, Sichuan University, Chengdu 610041, China.

E-mail: lichuan@scu.edu.cn

Released online in J-STAGE as advance publication February 24, 2023.

Optimized concurrent hearing and genetic screening in Beijing, China: A cross-sectional study

Cheng Wen^{1,2,3,8}, Xiaozhe Yang^{1,2,3,8}, Xiaohua Cheng^{1,2,3}, Wei Zhang^{1,2,3}, Yichen Li⁴, Jing Wang⁴, Chuan Wang⁵, Yu Ruan^{1,2,3}, Liping Zhao^{1,2,3}, Hongli Lu⁶, Yingxin Li⁶, Yue Bai⁶, Yiding Yu^{1,2,3}, Yue Li^{1,2,3}, Jinge Xie^{1,2,3}, Bei-er Qi^{1,2,3}, Hui En^{1,2,3}, Hui Liu^{1,2,3}, Xinxing Fu^{1,2,3}, Lihui Huang^{1,2,3,*}, Demin Han^{1,2,3,*}

¹Otolaryngology-Head and Neck Surgery, Beijing Tongren Hospital, Capital Medical University, Beijing, China;

²Beijing Institute of Otolaryngology, Beijing, China;

³Key Laboratory of Otolaryngology Head and Neck Surgery, Ministry of Education, Beijing, China;

⁴Maternal and Child Health, Beijing Obstetrics and Gynecology Hospital, Capital Medical University. Beijing Maternal and Child Health Care Hospital, Beijing, China;

⁵Maternal and Child Health Hospital of Chao Yang District, Beijing, China;

⁶CapitalBio Corporation & National Engineering Research Center for Beijing Biochip Technology, Beijing, China.

SUMMARY Concurrent screening has been proven to provide a comprehensive approach for management of congenital deafness and prevention of ototoxicity. The *SLC26A4* gene is associated with late-onset hearing loss and is of great clinical concern. For much earlier detection of newborns with deafness-causing mutations in the *SLC26A4* gene, the Beijing Municipal Government launched a chip for optimized genetic screening of 15 variants of 4 genes causing deafness based on a chip to screen for 9 variants of 4 genes, and 6 variants of the *SLC26A4* gene have now been added. To ascertain the advantage of a screening chip including 15 variants of 4 genes, the trends in concurrent hearing and genetic screening were analyzed in 2019 and 2020. Subjects were 76,460 newborns who underwent concurrent hearing and genetic screening at 24 maternal and child care centers in Beijing from January 2019 to December 2020. Hearing screening was conducted using transiently evoked otoacoustic emissions (TEOAEs), distortion product otoacoustic emissions (DPOAE), or the automated auditory brainstem response (AABR). Dried blood spots were collected for genetic testing and 15 variants of 4 genes, namely *GJB2*, *SLC26A4*, mtDNA *12S rRNA*, and *GJB3*, were screened for using a DNA microarray platform. The initial referral rate for hearing screening decreased from 3.60% (1,502/41,690) in 2019 to 3.23% (1,124/34,770) in 2020, and the total referral rate for hearing screening dropped from 0.57% (236/41,690) in 2019 to 0.54% (187/34,770) in 2020, indicating the reduced false positive rate of newborn hearing screening and policies to prevent hearing loss conducted by the Beijing Municipal Government have had a significant effect. Positivity according to genetic screening was similar in 2019 (4.970%, 2,072/41,690) and 2020 (4.863%, 1,691/34,770), and the most frequent mutant alleles were c.235 del C in the *GJB2* gene, followed by c.919-2 A > G in the *SLC26A4* gene, and c.299 del AT in the *GJB2* gene. In this cohort study, 71.43% (5/7) of newborns with 2 variants of the *SLC26A4* gene were screened for newly added mutations, and 28.57% (2/7) of newborns with 2 variants of the *SLC26A4* gene passed hearing screening, suggesting that a screening chip including 15 variants of 4 genes was superior at early detection of hearing loss, and especially in early identification of newborns with deafness-causing mutations in the *SLC26A4* gene. These findings have clinical significance.

Keywords Deafness-related genes, Newborn genetic screening, Newborn hearing screening, Concurrent screening, Hearing loss

1. Introduction

Hearing loss is the most common human neurosensory disorder. The World Report on Hearing published by

the World Health Organization (WHO) indicates that > 1.5 billion people currently experience some degree of hearing loss, which could grow to 2.5 billion by 2050 (1). The WHO estimates that over 400 million people,

including 34 million children, live with disabling hearing loss, which affects their health and quality of life (1). The reported incidence of hearing loss ranges from 1 to 2 per 1,000 newborns; in more than half of these newborns, it has a genetic etiology (2,3). A universal newborn hearing screening (UNHS) program has been implemented in China since the 1990s and has contributed to early hearing loss detection, diagnosis, and interventions, with good social benefits (4,5). The UNHS program is considered to be an extraordinarily successful public health program worldwide, but it has some limitations. The conventional UNHS is limited by its ability to detect children with late-onset or progressive sensorineural hearing loss after birth, and these children may not benefit from improved outcomes conferred from early identification and intervention by UNHS alone (6).

In 2006, Morton *et al.* pointed out the limitations of traditional newborn hearing screening and proposed the concept of combined newborn hearing screening and genetic screening for deafness for the first time (7). In 2007, Chinese scholars Wang *et al.* preliminarily discussed the protocol and strategy for concurrent newborn hearing and genetic screening and proposed that hearing screening and genetic screening should be conducted for prelingual hearing loss, delayed-onset high-risk children, or carriers of deafness-related genes and combined with regular follow-up and monitoring; they also advocated for extensive simultaneous newborn hearing screening and genetic screening; this has become a highly powerful screening strategy (8). In 2011, the Beijing Municipal Health Bureau conducted a successful pilot project on genetic screening of newborns for deafness at Beijing Tongren Hospital and the Chinese People's Liberation Army General Hospital. In 2012, with the support of the Beijing Municipal Government, the former Beijing Municipal Health Bureau initiated a project for genetic screening of newborns for deafness. The project screened for 9 mutations in 4 common deafness-related genes, including c.235delC (p.Leu79Cysfs*3), c.299_300delAT (p.His100Argfs*14), c.176_191del16 (p.Gly59Alafs*18), and c.35delG (p.Gly12Valfs*2) in *GJB2* (MIM: 121011); c.919-2A>G and c.2168A>G (p.His723Arg) in *SLC26A4* (MIM: 605646); and m.1555A>G and m.1494C>T of mtDNA *12SrRNA* (MIM: 561000); c.538C>T (p.Arg180*) in *GJB3* (MIM: 603324). The genetic screening project was led by Beijing Tongren Hospital, in collaboration with 5 facilities conducting genetic screening of newborns for deafness in Beijing, thus making Beijing the first city in China to genetically screen newborns for deafness. Based on the demonstrated effectiveness in Beijing, other cities like Chengdu, Changzhi, Zhengzhou, and Nantong in about 20 provinces, municipalities, and autonomous regions started including this project in their livelihood projects and they began genetically screening newborns for deafness for free (9). After more than 10 years in practice, the concurrent hearing and genetic screening of

newborns in China had entered a phase of rapid progress.

In 2019, the current authors' group conducted concurrent hearing and genetic screening of 180,469 neonates with follow-up in Beijing, China. For genetic testing, dried blood spots were collected and 9 variants of 4 genes, namely *GJB2*, *SLC26A4*, mtDNA *12SrRNA*, and *GJB3*, were screened for using a DNA microarray platform (10). Results revealed that 25% of infants with pathogenic combinations of *GJB2* or *SLC26A4* variants and 99% of infants with an m.1555A>G or m.1494C>T variant passed routine newborn hearing screening¹⁰. In 2020, the current status of genetic screening of newborns for deafness was analyzed from 2016 to 2017 in multiple regions of China, and results revealed that the genetic screening of newborns for deafness is more extensive in the eastern region of China than in the central and western regions (9). In 2021, the China Clinical Multicenter Collaborative Research Group for Genetic Screening and Diagnosis of Deafness and the National Technical Guidance Group for Prevention and Treatment of Deafness promulgated the "Specifications for Genetic Screening for Deafness," which focus on the principles, process, technical methods, interpretation of results, and genetic counseling for deafness, with the aim of providing guidance for professionals engaged in this work and standardizing the workflow of genetic screening for deafness and post-screening in China (11). It makes genetic screening for deafness more effective for early diagnosis, treatment and prevention of deafness. Above all, it indicates that after 15 years of clinical practice, concurrent newborn hearing and genetic screening is superior to traditional hearing screening, especially in identifying infants with deafness-gene-caused hearing loss.

Data in China have indicated that *SLC26A4* is the second most common gene that causes non-syndromic hearing loss (NSHL), accounting for 14.5% (12). Individuals with mutations in the *SLC26A4* gene may have hearing loss, as well as an enlarged vestibular aqueduct (EVA). In 2017, the current authors' research team retrospectively analyzed 582 subjects with genetic mutations causing deafness, results indicated that *SLC26A4* gene mutations were mainly associated with high-frequency hearing loss and profound-severe hearing loss (13). In addition, some patients with *SLC26A4* mutations may develop delayed-onset hearing loss (14). For earlier detection of newborns with deafness-causing mutations in the *SLC26A4* gene, the Beijing Municipal Government launched a new chip to genetically screen for 15 variants of 4 genes based on a screening chip including 9 variants of 4 genes. The new chip added 6 variants of the *SLC26A4* gene: c.1975G>C (p.Val659Leu), c.1707+5G>A, c.1229C>T (p.Thr410Met), c.1226G>A (p.Arg409His), c.2027T>A (p.Leu676Gln), and c.1174A>T (p.Asn392Tyr). To ascertain the advantage of screening for 15 mutations of 4 genes over screening for 9 mutations of 4 genes, the

current study first analyzed trends in concurrent hearing and genetic screening and differences across 2 years. This study also reported the sex-specific and gestational age-specific results of hearing and genetic screening, indicating the sex differences and gestational age differences in concurrent hearing and genetic screening. These findings might provide a reference for the promotion and implementation of hearing and genetic screening.

2. Material and Methods

2.1. Clinical data

Subjects were 76,460 infants born at 24 maternal and child care centers in Beijing who underwent concurrent hearing and genetic screening between January 2019 to December 2020. The clinical data on newborns who were screened for pathogenic deafness-associated variants were followed up systematically (Table S1, <http://www.biosciencetrends.com/action/getSupplementalData.php?ID=142>). Conventional newborn hearing screening and concurrent genetic screening were both conducted within 72 h after birth for all neonates at no charge.

2.2. Hearing screening

According to the "Technical Specifications for Newborn Hearing Screening (2010 Edition)," initial screening was conducted using transiently evoked otoacoustic emission (TEOAE) or distortion product otoacoustic emission (DPOAE) testing for normal infants 48-72 h after birth. For high-risk infants, the automated auditory brainstem response (AABR) test was completed prior to discharge from the hospital (15). For those referred after initial testing, a repeat otoacoustic emission (OAE) test or OAE test combined with AABR analysis was conducted by the age of 42 days. The relevant test parameters were as follows: TEOAE: acoustic stimulation – click; stimulus intensity – 70-75 dB; sound pressure level (SPL); signal superposition – 500-2,080 times; background noise \leq 45 dB (A); passing criteria – total reaction intensity \geq 10 dB SPL; repetition rate \geq 50%; and signal-to-noise ratio (SNR) (at least 3 frequencies) \geq 3 dB; DPOAE: acoustic stimulation – two consecutive pure tones f_1 and f_2 ; stimulus intensity – 65 dB and 55/50 dB; SPL; and frequency ratio – 1.1-1.5 (at least 6 frequencies); AABR: acoustic stimulation – click; stimulus intensity – 35 dB n HL; stimulation rate – 93 times/sec; sampling rate – 16 kHz; signal superposition – up to 15,000 times; spectrum range – 700/750 -5,000 Hz; and background noise: \leq 45 dB (A). The TEOAE, DPOAE and AABR results were automatically determined by the screening device and displayed as "PASS" or "REFER." Those who failed rescreening would be referred to Beijing Tongren Hospital for diagnostic hearing testing within 3 months.

2.3. Genetic screening

The Deafness Gene Variant Detection Array Kit (Capital Bio) was used to identify 15 variants of 4 genes in newborns born between January 2019 to December 2020, including c.235delC (p.Leu79Cysfs*3), c.299_300delAT (p.His100Argfs*14), c.176_191del16 (p.Gly59Alafs*18), and c.35delG (p.Gly12Valfs*2) in *GJB2*; c.919-2A>G, c.2168A>G (p.His723Arg), c.1975G>C (p.Val659Leu), c.1707+5G>A, c.1229C>T (p.Thr410Met), c.1226G>A (p.Arg409His), c.2027T>A (p.Leu676Gln), and c.1174A>T (p.Asn392Tyr) in *SLC26A4*; c.538C>T (p.Arg180*) in *GJB3*; and m.1555A>G and m.1494C>T in mtDNA *12S rRNA* (Table S2, <http://www.biosciencetrends.com/action/getSupplementalData.php?ID=142>, Figure S1, <http://www.biosciencetrends.com/action/getSupplementalData.php?ID=142>) (16). Dried blood spots from all newborn infants were collected from all 24 maternal and child care centers in Beijing where hearing screening is routinely conducted. Genetic screening was conducted at Beijing Tongren Hospital, which has genetic screening laboratories that were authorized by the Beijing Municipal Health Commission (10). Results were recorded in a report card (Table S3, <http://www.biosciencetrends.com/action/getSupplementalData.php?ID=142>) as pass (wild-type genotypes), refer (homozygote or compound heterozygote of *GJB2* or *SLC26A4*, mtDNA *12SrRNA* variants), or carrier (heterozygote of *GJB2* or *SLC26A4* and heterozygote or homozygote of *GJB3*). Genotypes with homozygous and compound heterozygous variants of *GJB2* or *SLC26A4* were diagnosed as deafness-causing genotypes, and those with mtDNA *12SrRNA* variants were diagnosed as drug-susceptible.

2.4. Statistical analysis

In the current study, the cohort consisted of 54,359 neonates in 2019 and 39,106 neonates in 2020. Analyses included all participants for whom the variables of interest were available. Missing data were not imputed. Ultimately, this study involved a cohort of 41,690 neonates in 2019 and 34,770 neonates in 2020 (Table S4, <http://www.biosciencetrends.com/action/getSupplementalData.php?ID=142>). The significance of differences was assessed using the χ^2 test for categorical variables and the *t* test or ANOVA for continuous variables. All data analyses were performed using SAS (version 9.4) (SAS Institute, Cary, NC, USA).

2.5. Ethics statement

This study was approved by the Ethics Committee of the Beijing Institute of Otolaryngology. Fully informed written consent was obtained from the parents of all neonates for evaluation and publication of their clinical data.

3. Results

3.1. Baseline characteristics of hearing loss in the 2 years studied

In the current study, 41,690 infants born in 2019 and 34,770 infants born in 2020 underwent concurrent hearing and genetic screening within 72 h after birth and before hospital discharge. Demographic characteristics are shown in Table 1. The mean gestational age was 38.71 weeks in 2019 and 38.67 weeks in 2020. The mean birth weight was 3,294 grams in 2019 and 3,285 grams in 2020. Seven-point-one percent of newborns were born prematurely in 2019 and 7.31% were born prematurely in 2020. In this cohort of newborns, there were more males than females, with a total sex ratio of 1.083:1.000. In 2019, 96.07% of newborns were singleton pregnancies and 96.39% were singleton pregnancies in 2020, 3.93% were multiple pregnancies in 2019, and 3.61% were multiple pregnancies in 2020.

3.2. Hearing screening results in the 2 years studied

Table 1. The baseline characteristics of hearing and genetic screening in different years

Characteristics	Year group	
	2019 (N = 41,690)	2020 (N = 34,770)
Gestational age, weeks, mean (SD)	38.71 ± 1.66	38.67 ± 1.67
Premature, %	2,961 (7.10)	2,542 (7.31)
Sex, %		
Female	20,014 (48.01)	16,693 (48.01)
Male	21,676 (51.99)	18,075 (51.98)
Unspecified	0 (0.00)	2 (0.01)
Birth weight, g, mean (SD)	3,294.59 ± 488.76	3,285.62 ± 490.21
Fetus		
Single birth	40,052 (96.07)	33,514 (96.39)
Multiple births	1,638 (3.93)	1,256 (3.61)

N, number of newborns.

The initial referral rate for hearing screening decreased in the 2 years studied, from 3.60% (1,502/41,690) to 3.23% (1,124/34,770) (Table 2). Those newborns who were referred were screened again at the age of 42 days; 0.57% (236/41,690) did not pass the second hearing screening either bilaterally or unilaterally in 2019 and 0.54% (187/34,770) did not pass in 2020, so the percentage tended to decline. There were significant differences in trends for both initial screening and second screening between 2020 and 2019 ($P = 0.0057$).

3.3. Genetic screening results in the 2 years studied

Forty-one thousand six hundred and ninety newborns underwent genetic screening in 2019 and 34,770 did so in 2020, and genetic screening data are shown in Table 3. Four-point-nine-seven percent of neonates (2,072/41,690) screened positive for deafness-associated variants in 2019 and 4.863% (1,691/34,770) did so in 2020. The percentages were similar in the 2 years studied. There were no significant differences between 2020 and 2019 ($P = 0.4973$).

Trends in allele frequency in genetic screening are shown in Table 4. The most frequent mutant alleles were those of the *GJB2* gene, *SLC26A4* gene, and *GJB3* gene in the 2 years studied, in descending order. The frequency of mutant alleles in the *GJB2* gene, in descending order over the 2 years studied, was 1.229% (1,025/83,380) in 2019 and 1.150% (800/69,540) in 2020. The frequency of mutant alleles in the *SLC26A4* gene, in descending order over the 2 years studied, was 1.015% (705/69,540) in 2020 and 1.013% (844/83,380) in 2019. The frequency of mutant alleles in the *GJB3* gene, from high to low, was 0.168% (117/69,540) in 2020 and 0.156% (130/83,380) in 2019.

The most frequent mutant alleles were c.235 del C in the *GJB2* gene, followed by c.919-2 A > G in the *SLC26A4* gene, and c.299 del AT in the *GJB2* gene in both years studied. The frequency of the mutant

Table 2. Trends in results of hearing screening

Results	Year group				P values for total referrals (%)
	2019		2020		
	N	Percentage (%)	N	Percentage (%)	
Initial hearing screening					
Passed	40,188	96.40	33,646	96.77	
Unilateral referral	903	2.16	685	1.97	
Bilateral referral	599	1.44	439	1.26	$P = 0.0057$
Total referrals (%)	1,502	3.60	1,124	3.23	
Second hearing screening					
Passed	41,454	99.43	34,583	99.46	
Unilateral referral	98	0.24	99	0.29	
Bilateral referral	138	0.33	88	0.25	
Total referrals (%)	236	0.57	187	0.54	
Total	41,690	100	34,770	100	

N, number of newborns.

Table 3. Trends in results of genetic screening

Genotypes	Group by year				<i>P</i> value for the positive genotype (%)
	2019		2020		
	<i>N</i>	Percentage (%)	<i>N</i>	Percentage (%)	
Wild type	39,618	95.030	33,079	95.137	<i>P</i> = 0.4973
Positive	2,072	4.970	1,691	4.863	
Total	41,690	100	34,770	100	

N, number of newborns. * Newborns born from April 2013 to March 2014.

Table 4. Trends in allele frequency in genetic screening

Variants	Group by year					
	2019 (15-site chip)			2020 (15-site chip)		
	Heterozygotes (<i>N</i>)	Homozygotes (<i>N</i>)	Allele frequency (%)	Heterozygotes (<i>N</i>)	Homozygotes (<i>N</i>)	Allele frequency (%)
<i>GJB2</i> c.35 del G	6	0	0.007	6	0	0.009
<i>GJB2</i> c.176 del 16	40	0	0.048	39	0	0.056
<i>GJB2</i> c.235 del C	761	3	0.920	599	1	0.864
<i>GJB2</i> c.299 del AT	212	0	0.254	154	0	0.221
<i>GJB3</i> c.538 C > T	130	0	0.156	117	0	0.168
<i>SLC26A4</i> c.2168 A > G	109	0	0.131	100	0	0.144
<i>SLC26A4</i> c.919-2 A > G	567	0	0.680	427	2	0.620
<i>SLC26A4</i> c.1174 A > T	28	0	0.034	33	0	0.047
<i>SLC26A4</i> c.1226 G > A	22	0	0.026	29	0	0.042
<i>SLC26A4</i> c.1229 C > T	23	0	0.028	36	0	0.052
<i>SLC26A4</i> c.1975 G > C	61	0	0.073	40	0	0.058
<i>SLC26A4</i> c.2027 T > A	24	0	0.029	22	1	0.035
<i>SLC26A4</i> c.1707+5 G > A	10	0	0.012	12	0	0.017

N, number of newborns.

allele c.235 del C in the *GJB2* gene in 2019 (0.920%, 767/83,380) was higher than in 2020 (0.864%, 601/69,540). The frequency of the mutant allele c.919-2 A > G in the *SLC26A4* gene in 2019 (0.680%, 567/83,380) was also higher than in 2020 (0.620%, 431/69,540). The frequency of the mutant allele c.299 del AT in the *GJB2* gene in 2019 (0.254%, 212/83,380) was higher than in 2020 (0.221%, 154/69,540).

3.4. Concurrent hearing and genetic screening in the 2 years studied

Associations between hearing and genetic screening are summarized in Table 5. In the 2 years studied, 63 of the 423 neonates who did not pass hearing screening, either bilaterally or unilaterally, were also referred for genetic screening. Moreover, 3,700 neonates who passed hearing screening were positive according to genetic screening. Among infants referred for genetic screening, 4 (0.0052%) had 2 variants of the *GJB2* gene, 7 (0.0091%) had 2 variants of the *SLC26A4* gene, and 222 (0.2903%) carried mtDNA *12SrRNA* variants. Among the deafness-associated variant carriers, 1,817 (2.3764%) were heterozygous carriers of *GJB2*, 1,535 (2.0076%) were heterozygous carriers of *SLC26A4*, and 247 (0.3230%) had the *GJB3* heterozygous or homozygous variant. A

point worth noting is that 71.43% (5/7) of newborns with 2 variants of the *SLC26A4* gene were screened for newly added mutations, and as shown in Table S5 (<http://www.biosciencetrends.com/action/getSupplementalData.php?ID=142>), 28.57% (2/7) of newborns with 2 variants of the *SLC26A4* gene passed hearing screening.

In 2019, 35 (14.83%) of 236 neonates who did not pass hearing screening, either bilaterally or unilaterally, were also referred for genetic screening. In 2020, 28 (14.97%) of 187 neonates who did not pass hearing screening, either bilaterally or unilaterally, were also referred for genetic screening. In addition, 2,037 (4.91%, 2,037/41,454) of the neonates who passed hearing screening were positive according to genetic screening in 2019, and 1,663 (4.81%, 1,663/34,583) were positive according to genetic screening in 2020. Among the deafness-associated variant carriers, 31 (1.54%) of 2,017 heterozygous mutation carriers were referred for additional hearing screening in 2019, and 24 (1.47%) of 1,632 heterozygous mutation carriers were referred for additional hearing screening in 2020. In addition, 99.19% (123/124) of infants with a m.1555A>G or m.1494C>T variant in 2019 and 98.98% (97/98) of those newborns in 2020 passed newborn hearing screening.

3.5. Sex-specific results of hearing and genetic screening

Table 5. Associations between hearing and genetic screening

Genotypes	Group by year				Total number (%)
	2019		2020		
	Passed hearing screening <i>N</i> (%)	Referred for hearing screening <i>N</i> (%)	Passed hearing screening <i>N</i> (%)	Referred for hearing screening <i>N</i> (%)	
Carrier					
<i>GJB2</i> heterozygote	998 (2.3939)	21 (0.0504)	779 (2.2404)	19 (0.0546)	1,817 (2.3764)
<i>SLC26A4</i> heterozygote	830 (1.9909)	8 (0.0192)	694 (1.9960)	3 (0.0086)	1,535 (2.0076)
<i>GJB3</i> heterozygote	129 (0.3094)	1 (0.0024)	115 (0.3307)	2 (0.0058)	247 (0.3230)
<i>GJB2</i> heterozygote with <i>SLC26A4</i> heterozygote	23 (0.0552)	1 (0.0024)	15 (0.0431)	0 (0.00)	39 (0.0510)
<i>GJB2</i> heterozygote with <i>GJB3</i> heterozygote	0 (0.00)	0 (0.00)	0 (0.00)	0 (0.00)	24 (0.0093)
<i>SLC26A4</i> heterozygote with <i>GJB3</i> heterozygote	6 (0.0144)	(0.00)	5 (0.0144)	0 (0.00)	11 (0.0144)
Pathogenic variants					
<i>GJB2</i> homozygote	0 (0.00)	3 (0.0072)	0 (0.00)	1 (0.0029)	4 (0.0052)
<i>SLC26A4</i> homozygote	0 (0.00)	0 (0.00)	1 (0.0029)	2 (0.0058)	3 (0.0039)
<i>SLC26A4</i> compound Heterozygote	1 (0.0024)	2 (0.0048)	0 (0.00)	1 (0.0029)	4 (0.0052)
Mitochondrial variants					
m.1494 C>T homoplasmy	10 (0.0240)	0 (0.00)	7 (0.0201)	0 (0.00)	17 (0.0222)
m.1555A>G homoplasmy	66 (0.1583)	1 (0.0024)	56 (0.1611)	0 (0.00)	123 (0.1609)
m.1555A>G heteroplasmy	47 (0.1127)	0 (0.00)	34 (0.0978)	1 (0.0029)	82 (0.1072)
Non-wild type (n)	2,037 (4.8861)	35 (0.0840)	1,663 (4.7829)	28 (0.0805)	3,763 (4.9215)
Wild type (n)	39,417 (94.5479)	201 (0.4821)	32,920 (94.6793)	159 (0.4573)	72,697 (95.0785)
Total for all screened	41,454 (99.4339)	236 (0.5661)	34,583 (99.4622)	187 (0.5378)	76,460 (100.00)

N, number of newborns.

The sex-specific results of hearing and genetic screening in 2019 and 2020 were analyzed in Table 6. Of the screened newborns, 51.99% were males and 48.01% were females in both 2019 and 2020. In 2019, 4.97% of newborns were referred for genetic screening and 0.57% were referred for hearing screening. In 2020, 4.86% newborns were referred for genetic screening and 0.54% were referred for hearing screening. The referral rates for genetic screening for females in 2019 (5.07%) and 2020 (4.97%) were higher than the referral rates for males (4.88% in 2019 and 4.76% in 2020) but not significantly so ($P = 0.384$, $P = 0.354$, respectively). The referral rates for hearing screening for females in 2019 and 2020 were 0.47% and 0.44%, both of which were lower than referral rates for males (0.66% in 2019 and 0.63% in 2020), and the rates differed significantly ($P = 0.0117$ and $P = 0.0138$, respectively). Taken together, there were significant differences between females and males only in hearing screening results.

3.6. Gestational age-specific results of hearing and genetic screening

The gestational age-specific and gestational age-standardized results of hearing and genetic screening in 2019 and 2020 were analyzed in Table 7. In 2019, non-premature babies accounted for 92.90% of the 41,690 neonates, and the remaining 7.10% were premature neonates. In 2020, non-premature babies accounted for 92.69% of the 34,770 neonates and 7.31% were

premature ones. The referral rate for genetic screening for non-premature newborns was 5.02% in 2019, which was higher than the rate for premature newborns (4.36%) but not significantly so ($P = 0.111$). However, positivity according to genetic screening for nonpreterm newborns was 4.83% in 2020, which was lower than the positivity for premature newborns (5.31%) but not significantly so ($P = 0.276$). The referral rate for hearing screening for nonpreterm newborns was 0.57% in 2019 and 0.54% in 2020, both of which were higher than the referral rates for premature newborns (0.51% in both 2019 and 2020) but not significantly so ($P = 0.6544$, $P = 0.850$, respectively).

4. Discussion

This study analyzed concurrent newborn hearing and genetic screening results for 76,460 neonates in total. This study also reported the sex-specific and gestational age-specific hearing and genetic screening results in the 2 years studied. Here, the trends in hearing screening, genetic screening, and concurrent screening in the years studied are discussed. Also discussed is the association between sex, gestational age, and concurrent hearing and genetic screening.

4.1. Hearing screening during the 2 years studied

In 2004, the former Ministry of Health issued the "Technical Specifications for Newborn Hearing

Table 6. Sex-specific results of hearing and genetic screening in Beijing

		Group by year							
		2019			2020				
		Male	Female	Total	Male	Female	Total		
Genetic screening	Passed	<i>N</i>	20,618	19,000	39,618	17,215	15,863	33,078	
		(%)	49.46	45.57	95.03	49.51	45.63	95.14	
		Row (%)	52.04	47.96		52.04	47.96		
	Column (%)	95.12	94.93		95.24	95.03			
	Referred	<i>N</i>	1,058	1,014	2,072	860	830	1,690	
		(%)	2.54	2.43	4.97	2.47	2.39	4.86	
		Row (%)	51.06	48.94		50.89	49.11		
	Column (%)	4.88	5.07		4.76	4.97			
	Total	21,676	20,014	41,690	18,075	16,693	34,768		
		51.99	48.01	100	51.99	48.01	100		
		2019			2020				
Hear screening	Passed	<i>N</i>	21,534	19,920	41,454	17,961	16,620	34,581	
		(%)	51.65	47.78	99.43	51.66	47.80	99.46	
		Row (%)	51.95	48.05		51.94	48.06		
	Column (%)	99.34	99.53		99.37	99.56			
	Referred	<i>N</i>	142	94	236	114	73	187	
		(%)	0.34	0.23	0.57	0.33	0.21	0.54	
		Row (%)	60.17	39.83		60.96	39.04		
	Column (%)	0.66	0.47		0.63	0.44			
	Total	21,676	20,014	41,690	18,075	16,693	34,768		
		51.99	48.01	100	51.99	48.01	100		

N, number of newborns; two newborns of an unspecified sex in the 2020 cohort were excluded from the analysis.

Table 7. Gestational age-specific and gestational age-standardized results of hearing and genetic screening in Beijing

		Group by year							
		2019			2020				
		Non-premature	Premature	Total	Non-premature	Premature	Total		
Genetic screening	Passed	<i>N</i>	36,786	2,832	39,618	30,672	2,407	33,079	
		(%)	88.24	6.79	95.03	88.21	6.92	95.14	
		Row (%)	92.85	7.15		92.72	7.28		
	Column (%)	94.98	95.64		95.17	94.69			
	Referred	<i>N</i>	1,943	129	2,072	1,556	135	1,691	
		(%)	4.66	0.31	4.97	4.48	0.39	4.86	
		Row (%)	93.77	6.23		92.02	7.98		
	Column (%)	5.02	4.36		4.83	5.31			
	Total	38,729	2,961	41,690	32,228	2,542	34,770		
		92.90	7.10	100	92.69	7.31	100		
		2019			2020				
Hearing screening	Passed	<i>N</i>	38,508	2,946	41,454	32,054	2,529	34,583	
		(%)	92.37	7.07	99.43	92.19	7.27	99.46	
		Row (%)	92.89	7.11		92.69	7.31		
	Column (%)	99.43	99.49		99.46	99.49			
	Referred	<i>N</i>	221	15	236	174	13	187	
		(%)	0.53	0.04	0.57	0.5	0.04	0.54	
		Row (%)	93.64	6.36		93.05	6.95		
	Column (%)	0.57	0.51		0.54	0.51			
	Total	38,729	2,961	41,690	32,228	2,542	34,770		
		92.90	7.10	100	92.69	7.31	100		

N, number of newborns.

Screening (2004 Edition)," which set clear requirements for institutional settings, personnel, housing and equipment, as well as clear regulations for hearing screening, diagnosis, interventions, and quality control (17). In 2005, the Beijing Children's Hearing Care Expert Steering Group summarized early hearing detection and interventions for children ages 0-6 years in Beijing and it further standardized the hearing screening and diagnosis for children ages 0-6 years (18). At this point, newborn hearing screening and diagnosis constitutes a system that is being widely implemented and gradually standardized in all regions. In 2010, the former Ministry of Health promulgated the "Technical Specifications for Newborn Hearing Screening (2010 Edition)," which further promoted the standardization of the program. The World Health Organization has paid increasing attention to the Chinese UNHS program and reported in 2017 that the UNHS program is effective in high-income countries, including China, at identifying serious problems promptly (19).

In 2020, Wen *et al.* (20) studied the current status of the UNHS program at 26 facilities in China, and results revealed that the total referral rate for initial screening in 2017 (9.21%) was lower than that in 2016 (10.26%). In the current study, the initial referral rate for hearing screening decreased in the 2 years studied, from 3.60% to 3.23%; these rates are lower than those reported by Wen *et al.* The reason may be that the newborns included in the study by Wen *et al.* were from different regions in east, central, and west China, while the newborns included in the current study were all from Beijing. The UK's Newborn Hearing Screening Programme Standards 2016 to 2017 mentioned that a referral rate within 15% at initial screening in a community program was acceptable, that a rate within 13.5% was achievable, and that the rate is a negative polarity standard, meaning that a lower percentage is considered better (21). The initial referral rate for hearing screening was 3.60% and 3.23% in the 2 years studied, both of which were within the 13.5% recommended by the UK's UNHS guidelines and which were in line with international recommendations. In 2019, Dai *et al.* reported that 6.54% neonates were referred at initial screening and 1.061% of 180,469 neonates were referred bilaterally or unilaterally for hearing screening (10). Wang *et al.* (22) reported an initial screening referral rate of 6.87% and an overall failure rate in newborn hearing screening of 0.748% in 9,755 newborns born in Beijing from January 2017 to December 2017. The initial referral rate in the current study was lower than 6.54% and 6.87%; the reason may be due to the quality control of newborn hearing screening by the Beijing expert group in recent years and the Beijing Municipal Government's emphasis on concurrent newborn hearing screening and genetic screening for deafness, which improved the quality of screening in 2019 and 2020 compared to 2013. The overall failure rate of newborn hearing

screening in the current study was 0.57% in 2019 and 0.54% in 2020, both of which were much lower than the 1.061% reported by Dai *et al.* and the 0.748% reported by Wang *et al.* (10,22) In the current study, after follow-up, all newborns who failed the initial screening were rescreened at the age of 42 days, and the decrease in the overall failure rate of newborn hearing screening was associated with a decrease in the initial screening failure rate.

4.2. Trends in genetic screening during the 2 years studied

Genetic screening of newborns for deafness has been implemented in China for more than 10 years. In 2011, Wang *et al.* (23) reported genetic screening for 3 common genes, mtDNA 12S rRNA, GJB2, and SLC26A4, and positivity was 2.05% (306/14,913). In 2013, Zhang *et al.* analyzed the concurrent hearing and genetic screening results of 58,397 neonates born in Tianjin. Twenty common hearing loss-associated mutations of GJB2, GJB3, SLC26A4, and mtDNA 12S rRNA were screened for, and they found that 5.52% of infants carried at least one mutant allele (24). Wu *et al.* conducted simultaneous hearing screening and genetic screening for 4 common deafness-related mutations in 5,173 newborns and found that 1.6% had conclusive genotypes and 16.2% had a GJB2 or SLC26A4 mutation (25). Later in 2017, Lu *et al.* reported that 1.2% of 1,716 newborns had conclusively positive genotypes on genetic screening and 20.10% had a GJB2 or SLC26A4 mutation (26). In 2019, Dai *et al.* reported that 4.508% of 180,469 neonates born from April 2013 to March 2014 were positive according to genetic screening (10). Positivity in genetic screening for deafness was higher in both 2019 (4.970%) and 2020 (4.863%) than the rate reported previously (4.508%), and this is probably because screening included 6 more mutations in 2019 and 2020 than in 2013. Positivity in genetic screening in the current study was higher than the 2.05% reported by Wang *et al.* in 2011 and lower than the 5.52% reported by Zhang *et al.* in 2013; this may be due to differences in genes and mutations that were screened for. Similarly, positivity in genetic screening for deafness in the current study was lower than that reported by Taiwanese researchers; this is probably due to their genetic screening targeting four common deafness mutations including p.V37I of GJB2 gene, which has a high allele frequency in Chinese population. In summary, the current study reported increasing positivity in genetic screening for deafness using more powerful gene microarray chips in 2019 and 2020 than in 2013. These findings may provide a reference for the development of genetic screening for deafness in the Chinese Han population in other regions.

The GJB2 gene is the most common gene that causes non-syndromic hearing loss (NSHL) (27). Researches have found that SLC26A4 is the second most common

gene that causes NSHL and is related to an EVA (12). The most frequent mutant alleles were those of the *GJB2* gene, *SLC26A4* gene, and *GJB3* gene in the 2 years studied, in descending order, and this finding was consistent with the results of previous studies. In 2019 and 2020, 6 mutations of the *SLC26A4* gene were added to a chip screening for 9 variants of 4 genes. Therefore, the frequency of mutant alleles in the *SLC26A4* gene in 2019 (1.013%) and 2020 (1.015%) was higher than in 2013 (0.809%), suggesting that a microarray to screen for 15 variants of 4 genes can screen more newborns for an EVA and may yield better societal benefits.

Early in 2007, Dai *et al.* conducted a study on the prevalence of the c.235delC mutation in *GJB2* in the Chinese deaf population, and they found that the c.235delC mutation in the *GJB2* gene caused NSHL in as much as 15% of patients in certain regions of China (28). Later in 2008, Dai *et al.* reported that the c.919-2A>G mutation in the *SLC26A4* gene alone would identify the molecular cause in up to 8–12% of individuals with sensorineural hearing loss in a few eastern and central regions of China (29). A large population-based cohort study by Zhang *et al.* also proved that the c.235delC mutation in the *GJB2* gene was the most common variant and that the second most common variant was the c.919-2A>G mutation in the *SLC26A4* gene in the Chinese population (30). The most frequent mutant allele was c.235 del C in the *GJB2* gene, followed by c.919-2 A > G in the *SLC26A4* gene in the 2 years studied, and this finding was consistent with the results of previous research.

4.3. Concurrent hearing and genetic screening during the 2 years studied

Genetic screening of newborns for deafness makes up the deficiency of the conventional UNHS program and allows for early detection of congenital hereditary hearing loss, drug-sensitive newborns, and carriers of common deafness-related genes. In 2011, Schuelke *et al.* (31) conducted two-step DPOAE screening and newborn genetic screening for deafness among 1,017 newborns, who were screened for p.V37I and c.235delC in *GJB2*, c.919-2A>G in *SLC26A4*, and mitochondrial m.1555A>G. They found that 27.27% (3/11) of babies who were homozygous for p.V37I, 83.33% (5/6) who were compound heterozygous for p.V37I and c.235delC, and 100% (1/1) who were homoplasmic for m.1555A>G passed hearing screening at birth. Later in 2017, Wu *et al.* reported that 56.1% (46/82) of 5,173 newborns with conclusive genotypes passed hearing screening at birth and that long-term follow-up identified progressive hearing loss in children with the *GJB2* p.V37I/p.V37I and p.V37I/c.235delC genotypes (25). Dai *et al.* reported that among 4.508% newborns who were born between 2013 and 2014 and who were positive according to genetic screening, 4.375% passed hearing screening,

25% of infants with pathogenic combinations of *GJB2* or *SLC26A4* variants, and 99% of infants with an m.1555A>G or m.1494C>T variant passed routine newborn hearing screening (10).

Significantly, 71.43% of newborns with 2 variants of the *SLC26A4* gene were identified by genetic screening for the newly added mutations, and 28.57% of newborns with 2 variants of the *SLC26A4* gene passed hearing screening. This indicates that the chip to screen for 15 variants of 4 genes is superior for concurrent hearing and newborn screening, and particularly in the early identification of newborns with deafness-causing mutations in the *SLC26A4* gene because of the 6 newly added *SLC26A4* gene mutations. In the current study, 2 newborns with c.2168 A > G/c.2027 T > A compound heterozygous mutations in the *SLC26A4* gene in 2019 and a newborn with a c.919-2A > G/ c.1229 C > T compound heterozygous mutation in the *SLC26A4* gene in 2020 failed the newborn hearing screening bilaterally and were later diagnosed with an EVA bilaterally; they underwent hearing management at the age of three months. Of note, there was a newborn with c.2168 A > G/c.1975 G > C compound heterozygous mutation in 2019 who passed the newborn hearing screening bilaterally and who was later diagnosed with moderately severe hearing loss in the left ear. In addition, there was a newborn with a c.2027 T > A homozygous mutation in 2020. According to the Deafness Variation Database (<http://deafnessvariationdatabase.org/>), c.2027 T > A is pathogenic and is associated with deafness. However, the newborn with a c.2027 T > A homozygous mutation passed the newborn hearing screening bilaterally and was later diagnosed with normal hearing at the age of 11 months. Computed tomography of the temporal bone revealed no enlargement of the vestibular aqueduct bilaterally and poor medial parietal morphology of the cochlea bilaterally. This case is currently being followed further. The mutations c.2027 T > A, c.1229 C > T, and c.1975 G > C, which were newly added to genetic screening in 2019, were identified, which allowed these families to directly benefit from early etiological diagnosis and early intervention.

Moreover, 4.91% and 4.81% of neonates who passed hearing screening but were positive according to genetic screening in the 2 years studied and 28.57% of newborns with 2 variants of the *SLC26A4* gene passed hearing screening. After hearing follow-up, a newborn with 2 pathogenic combinations of *SLC26A4* variants was found to exhibit sensorineural hearing loss, implying that the baby's hearing at birth might have been normal or near normal and could not have been detected by newborn hearing screening. Wang *et al.* also reported that genetic screening identified 13% more hearing-impaired infants than hearing screening alone and that it identified 0.23% of newborns predisposed to preventable ototoxicity undetectable by hearing screening (32). In 2020, Zhang *et al.* analyzed 22 studies related to concurrent hearing

and genetic screening in neonates in China and reported a pooled prevalence of passing the UNHS while failing genetic screening of 0.22%, while the pooled prevalence of passing the UNHS with the MT-RNR1 variant was 0.20% (33). The range of variation in this rate of neonates passing hearing screening but testing positive according to genetic screening was small and relatively stable over the 2 years studied. However, the wide range of variation in the rate of newborns with 2 pathogenic combinations of *GJB2* or *SLC26A4* variants who passed newborn hearing screening may be due to differences in the sample size of the 2-year period studied and few newborns carrying the pathogenic mutations. Six newborns screened positive for pathogenic mutations in 2019 and 5 screened positive in 2020. The rates in the current study were all lower than the 83.33% and 56.1% reported by Wu *et al.* (25, 31); the reason might be the differences in the screened population and the variants screened for. The screened population reported by Wu *et al.* was the Taiwanese population and the mutations screened for were p.V37I and c.235delC in *GJB2*, c.919-2A>G in *SLC26A4*, and mitochondrial m.1555A>G, whereas p.V37I was mainly associated with mild to moderate hearing loss (34). In addition, 98.98% and 99.19% of infants with a m.1555A>G or m.1494C>T variant passed newborn hearing screening in the current study, and this finding was consistent with the 100% reported by Schuelke *et al.* (31). These newborns are all potentially sensitive to aminoglycoside antibiotics, and their hearing may be compromised by even small amounts of such drugs (10). This indicates that genetic screening for deafness can identify such newborns early, guide medication, and minimize the incidence of drug-related deafness.

4.4. Association between sex and gestational age and hearing loss

According to the World Report on Hearing published by the World Health Organization in 2021, causative factors that lead to hearing loss across the course of one's life include genetic factors and intrauterine infections during the prenatal period, hypoxia or birth asphyxia, hyperbilirubinemia, a low birth weight, perinatal infections, and receiving ototoxic medicines during the perinatal period (1). The 12 separate factors of hearing loss were listed by the Joint Committee on Infant Hearing in 2019 and included 9 predominantly perinatal risk factors and 3 postnatal risk factors, including family members being deaf or hard of hearing with onset in childhood, infants requiring care in the NICU or special care nursery for more than 5 days, hyperbilirubinemia, aminoglycoside administration for more than 5 days, perinatal asphyxia, and in-utero infections (35).

Nie *et al.* explored the risk indicators of newborn hearing loss and found that there were 3 high-risk indicators associated with newborn hearing loss: a family

history of hearing loss, craniofacial anomalies, and receiving care in the NICU (36). Yu *et al.* investigated the correlation between genetic abnormalities causing deafness and high-risk factors for hearing loss, and they reported that detection of gene mutations causing deafness was highest among children with a family history of congenital hearing loss (37). The referral rates for genetic screening for females and males in the 2 years studied did not differ significantly, suggesting that sex may not be directly associated with the results of genetic screening for deafness, but a family history of deafness that may be relevant was not included in the analysis in the current study. Studies have reported that passing rates on the UNHS were higher for female infants than for male infants (38,39). Fitzgibbons *et al.* predicted hearing loss from 10 years of universal newborn hearing screening results and risk factors, and they found that factors significantly associated with permanent childhood hearing loss included being female and bilateral referral as a result of screening (40). The finding that the referral rate for hearing screening was lower for females than for males in the 2 years studied was consistent with results reported by Yan *et al.* and Li *et al.* but was inconsistent with the results reported by Fitzgibbons *et al.* This may be due to differences in newborn hearing screening protocols, with the TEOAE or DPOAE technique being used for initial screening in this study, whereas Fitzgibbons *et al.* used a two-stage AABR screening protocol.

There were no significant differences in referral rates after the results of genetic and hearing screening were stratified by prematurity, suggesting that there may not necessarily be an association between prematurity and positivity in genetic screening for deafness. Sabbagh *et al.* reported that the main risk factors for hearing loss included a low gestational age (<35 weeks) (41). In the current study, preterm delivery was defined as less than 37 weeks of gestation. The current results indicated that preterm birth may not be a risk factor for hearing loss. Further study is warranted to investigate a more detailed definition of preterm delivery specifically for hearing and genetic screening.

5. Conclusions

In summary, the highlights and strengths of the current study lies in its analysis of the trends in concurrent newborn hearing and deafness genetic screening in different years. For the first time, a study has analyzed the advantages of a chip to screen for 15 variants of 4 genes. Findings suggest that the quality of newborn hearing screening improved in 2019 and 2020 and that a chip to screen for 15 variants of 4 genes has advantages in early identification of newborns with deafness-causing mutations in the *SLC26A4* gene. This chip can screen more newborns for large vestibular aqueduct syndrome at an early stage. These findings provided a reference

for other regions where genetic screening for deafness is proposed.

Acknowledgements

The authors wish to sincerely thank all of the subjects and family members for their participation in this study.

Funding: This work was supported by the National Research and Development Program of China (grant number 2018YFC1002200), the Capital's Funds for Health Improvement and Research (grant number, CFH 2022-2-1092), and the National Natural Science Foundation of China (grant numbers 82071064, 81870730, and 82101190).

Conflict of Interest: The authors have no conflicts of interest to disclose.

References

- World Health Organization. World Report on Hearing. Available from: <https://www.who.int/teams/noncommunicable-diseases/sensory-functions-disability-and-rehabilitation/highlighting-priorities-for-ear-and-hearing-care.2021> (accessed March 8, 2023)
- Fortnum HM, Summerfield AQ, Marshall DH, Davis AC, Bamford JM. Prevalence of permanent childhood hearing impairment in the United Kingdom and implications for universal neonatal hearing screening: Questionnaire based ascertainment study. *BMJ*. 2001; 323:536-540.
- Kennedy C, McCann D. Universal neonatal hearing screening moving from evidence to practice. *Arch Dis Child Fetal Neonatal Ed*. 2004; 89:F378-383.
- Tobe RG, Mori R, Huang L, Xu L, Han D, Shibuya K. Cost-effectiveness analysis of a national neonatal hearing screening program in China: Conditions for the scale-up. *PLoS One*. 2013; 8:e51990.
- Huang LH, Zhang L, Tobe RY, *et al*. Cost-effectiveness analysis of neonatal hearing screening program in China: Should universal screening be prioritized? *BMC Health Serv Res*. 2012; 12:97.
- Young NM, Reilly BK, Burke L. Limitations of universal newborn hearing screening in early identification of pediatric cochlear implant candidates. *Arch Otolaryngol Head Neck Surg*. 2011; 137:230-234.
- Morton CC, Nance WE. Newborn hearing screening - A silent revolution. *N Engl J Med*. 2006; 354: 2151-2164.
- Wang QJ, Zhao YL, Lan L, Zhao C, Han M, Han DY. Studies of the strategy for newborn gene screening. *Chin J Otorhinolaryngol Head Neck Surg*. 2007; 42:809-813. (in Chinese w/English abstract)
- Wen C, Huang LH, Xie ST, Zhao XL, Yu YD, Cheng XH, Guo L, Nie WY, Ge F, Wang C, Liu QM, Hu SJ, Chen YQ, Gao M, Han JN. Current status of genetic screening for deafness in newborns in parts of China. *J Clin Otorhinolaryngol Head Neck Surg (China)*. 2020; 34:972-976. (in Chinese)
- Dai P, Huang LH, Wang GJ, *et al*. Concurrent hearing and genetic screening of 180,469 neonates with follow-up in Beijing, China. *Am J Hum Genet*. 2019; 105:803-812.
- The China Clinical Multicenter Collaborative Research Group for Genetic Screening and Diagnosis of Deafness, the National Technical Guidance Group for Prevention and Treatment of Deafness. Specifications for genetic screening for deafness. *Natl Med J China*. 2021; 101:97-102. (in Chinese)
- Azaiez H, Yang T, Prasad S, Sorensen JL, Nishimura CJ, Kimberling WJ, Smith RJ. Genotype-phenotype correlations for SLC26A4-related deafness. *Hum Genet*. 2007; 122:451-457.
- Du Y, Huang L, Wang X, Cui Q, Cheng X, Zhao L, Ni T. Clinical data analysis of genotypes and phenotypes of deafness gene mutations in newborns: A retrospective study. *Biosci Trends*. 2017; 11:460-468.
- Wen C, Wang SJ, Zhao XL, Wang XL, Wang XY, Cheng XH, Huang LH. Mutation analysis of the *SLC26A4* gene in three Chinese families. *Biosci Trends*. 2019; 13:441-447.
- Ministry of Health of the People's Republic of China. Technical specifications for newborn hearing screening [2010 edition, No. 96]. *Chin J Child Health*. 2011; 19:574-575. (in Chinese)
- Wang GJ, Zhang GB, Yuan YY, Huang SS, Li YY, Kang DY, Cheng J, Dai P. Clinical application of DNA microarray in rapid genetic diagnosis of non-syndromic hearing loss. *Chin J Otol*. 2014; 12:6-10. (in Chinese w/ English abstract)
- Ministry of Health of the People's Republic of China. Technical specifications for newborn hearing screening. Maternal and Child Health Care of China. 2004-12-15. <http://www.nhc.gov.cn/bgt/pw/10501/200503/1f8c09206e9a42bf838882d1f2e4610shtml> (accessed March 8, 2023)
- Beijing Children's Hearing Care Expert Steering Group. Progress of early hearing detection and intervention for children aged 0-6 years in Beijing. *Chin J Otorhinolaryngol Head Neck Surg*. 2005; 40:79-80.
- Wilson BS, Tucci DL, Merson MH, O'Donoghue GM. Global hearing health care: New findings and perspectives. *Lancet*. 2017; 390:2503-2515.
- Wen C, Li X, Huang L, *et al*. Current status of universal newborn hearing screening program at 26 institutions in China. *Int J Pediatr Otorhinolaryngol*. 2020; 138:110131.
- Public Health England. NHS newborn hearing screening programme standards 2016 to 2017. <https://phescreening.blog.gov.uk/2016/04/06/nhs-newborn-hearing-programme-2016-to-2017-standards-published/> (accessed March 8, 2023)
- Wang C, Shang Y. Retrospective analysis of combined hearing and deafness gene screening in 9,755 newborns. *J Audiol Speech Pathol*. 2019; 27:16-19.
- Wang QJ, Zhao YL, Rao SQ, Guo YF, He Y, Lan L, Yang WY, Zheng QY, Ruben RJ, Han DY, Shen Y. Newborn hearing concurrent gene screening can improve care for hearing loss: A study on 14,913 Chinese newborns. *Int J Pediatr Otorhinolaryngol*. 2011; 75:535-542.
- Zhang J, Wang P, Han B, *et al*. Newborn hearing concurrent genetic screening for hearing impairment-a clinical practice in 58,397 neonates in Tianjin, China. *Int J Pediatr Otorhinolaryngol*. 2013; 77: 1929-1935.
- Wu CC, Tsai CH, Hung CC, Lin YH, Lin YH, Huang FL, Tsao PN, Su YN, Lee YL, Hsieh WS, Hsu CJ. Newborn genetic screening for hearing impairment: A population-based longitudinal study. *Genetics in Medicine*. 2017; 19:6-12.
- Lu CY, Tsao PN, Ke YY, Lin YH, Lin YH, Hung CC, Su YN, Hsu WC, Hsieh WS, Huang LM, Wu CC, Hsu

- CJ. Concurrent hearing, genetic, and cytomegalovirus screening in newborns, Taiwan. *J Pediat.* 2018; 199:144-150.
27. Kenneson A, Van Naarden Braun K, Boyle C. GJB2 (connexin 26) variants and nonsyndromic sensorineural hearing loss: A HuGE review. *Genet Med.* 2002; 4:258-274.
 28. Dai P, Yu F, Han B, Yuan Y, Li Q, Wang G, Liu X, He J, Huang D, Kang D, Zhang X, Yuan HJ, Schmitt E, Han DY, Wong LJ. The prevalence of the 235delC GJB2 mutation in a Chinese deaf population. *Genet Med.* 2007; 9:283-289.
 29. Dai P, Li Q, Huang D, Yuan Y, *et al.* SLC26A4 c.919-2A>G varies among Chinese ethnic groups as a cause of hearing loss. *Genet Med.* 2008; 10:586-592.
 30. Zhang J, Wang HY, Yan CB, Guan J, Yin LW, Lan L, Li J, Zhao LJ, Wang Q J. (2022). The frequency of common deafness-associated variants among 3,555,336 newborns in China and 141,456 individuals across seven populations worldwide. *Ear & Hearing.* 2023; 44:232-241.
 31. Schuelke M, Wu CC, Hung CC, Lin SY, Hsieh WS, Tsao PN, Lee CN, Su YN, Hsu CJ. Newborn genetic screening for hearing impairment: A preliminary study at a tertiary center. *PLoS One.* 2011; 6:e22314.
 32. Wang Q, Xiang J, Sun J, *et al.* Nationwide population genetic screening improves outcomes of newborn screening for hearing loss in China. *Genet Med.* 2019; 21:2231-2238.
 33. Zhang J, Wang DY, Han B, Zhou CY, Wang QJ. Newborn concurrent hearing and genetic screening: A systematic review and meta-analysis. *Chin J Otol.* 2020; 18:216-224.
 34. Huang SS, Huang BQ, Wang GJ, Yuan YY, Dai P. The relationship between the p.V37I mutation in GJB2 and hearing phenotypes in Chinese individuals. *PLoS One.* 2015; 10:e0129662.
 35. The Joint Committee on Infant Hearing. Position statement: Principles and guidelines for early hearing detection and intervention programs. *J Early Hear Detect Interv.* 2019; 4:1-44.
 36. Nie WY, Gong LX, Liu YJ, Lin Q, Liu XX, Qi YS, Xiang LL. A study on the risk indicators of newborn hearing loss. *Natl Med J China.* 2003; 83:1399-1401.
 37. Yu FC, Liu Y, Tan YN, Kuang XF, He QQ. Correlation between high-risk factors of hearing loss and deafness genes in 95 children. *Chin J Woman and Child Health Res.* 2021; 32:1855-1860.
 38. Yan M, Zhang B, Chen DS, Zeng FQ, Peng ZM, Xiong XL, Ke ZY. Hearing screening results analysis of 919 newborns. *J Audiol Speech Pathol.* 2021; 29:691-694.
 39. Li ZX, Zhou WS, Chen YH, Yang XR, Xiao X, Zhang J, Jiang HQ. Analysis of transient evoked otoacoustic emission hearing screening results in 9971 newborns. *J Audiol Speech Pathol.* 2009; 17:587-588.
 40. Fitzgibbons EJ, Driscoll C, Myers J, Nicholls K, Beswick R. Predicting hearing loss from 10 years of universal newborn hearing screening results and risk factors. *Int J Audiol.* 2021; 60:1030-1038.
 41. Sabbagh S, Amiri M, Khorramizadeh M, Iranpoumobarake Z, Nickbakht M. Neonatal hearing screening: Prevalence of unilateral and bilateral hearing loss and associated risk factors *Cureus.* 2021; 13:e15947.
- Received March 9, 2023; Revised April 7, 2023; Accepted April 12, 2023.
- [§]These authors contributed equally to this work.
- *Address correspondence to:
Lihui Huang and Demin Han, Otolaryngology-Head and Neck Surgery, Beijing Tongren Hospital, Capital Medical University, Beijing 100730, China; Beijing Institute of Otolaryngology, Beijing 100005, China; Key Laboratory of Otolaryngology Head and Neck Surgery, Ministry of Education, Beijing 100005, China.
E-mail: huanglihui@ccmu.edu.cn; deminhan_ent@hotmail.com
- Released online in J-STAGE as advance publication April 14, 2023.

2-4 weeks is the optimal time to operate on colorectal liver metastasis after neoadjuvant chemotherapy

Yurun Huang^{1,2,§}, Hang Jiang^{1,2,§}, Linwei Xu¹, Xitian Wu^{1,2}, Jia Wu^{1,*}, Yuhua Zhang^{1,*}

¹Department of Hepatobiliary and Pancreatic Surgery, Zhejiang Cancer Hospital, Institute of Basic Medicine and Cancer (IBMC) Chinese Academy of Sciences, Hangzhou, Zhejiang, China;

²Zhejiang Chinese Medical University, Hangzhou, Zhejiang, China.

SUMMARY Neoadjuvant chemotherapy (NAC) is generally accepted for treatment of liver metastasis of colorectal cancer (CRLM), but what is a reasonable interval between the latest NAC and surgery is still unknown. The aim of the current study was to investigate the proper timing of surgery after NAC. Subjects were 141 patients with CRLM who underwent NAC and then surgery were retrospectively identified from 2008 to 2020. They were divided into a short interval group (SIG, ≤ 4 weeks) and long interval group (LIG, > 4 weeks) using the software X-tile. The SIG was subclassified group into 3 time periods (1-2 weeks, 2-3 weeks, and 3-4 weeks) to assess the incidence of complications. Patients in the SIG were more likely to have significantly better recurrence-free survival (RFS) (3-year RFS of 47.4% vs. 20.5%, $P = 0.043$) and no difference in overall survival (OS) (3-year OS 76.1% vs. 79.9%, $P = 0.635$). The postoperative complication rate was 23.5% in the SIG and 14.0% in the LIG ($P = 0.198$). The postoperative complication rate in the 1-2 weeks subgroup was marginally higher than that in the > 4 weeks subgroup (35% vs. 14.3% $P = 0.055$). Multivariate analysis revealed that chemotherapy-free intervals of 1-2 weeks were an independent predictor of increased postoperative complications (OR = 0.263, 95% CI 0.7-0.985 $P = 0.048$). Patients who underwent surgery within 4 weeks of NAC had better RFS. In addition, 1-2 weeks was an independent factor influencing the development of more complications. For patients with CRLM, performing surgery within 2-4 weeks of NAC was feasible and safe, and it did not increase the incidence of postoperative complications but it did prolong RFS.

Keywords colorectal cancer, liver metastasis, neoadjuvant chemotherapy, chemotherapy-free interval

1. Introduction

Colorectal cancer (CRC) is the world's most common tumor of the digestive tract, with more than 550,000 deaths each year (1,2). The liver is the most frequent metastatic site of CRC and liver metastasis of colorectal cancer has a worse prognosis. Due to its anatomical characteristics, liver metastasis will be detected in up to 30-50% of patients as the disease progresses (3,4). Surgery plays a dominant role in radical therapy (5). However, about a quarter of people with CRLM are candidates for radical liver resection (6). For patients with resectable CRLM, NAC combined with surgical resection is increasingly being advocated and has been proven to prolong patients' recurrence-free survival (RFS) (7,8). Although NAC is recommended for those who were diagnosed with CRLM with a high clinical risk score (CRS) according to the guidelines of the Chinese Society of Clinical

Oncology (CSCO), the National Comprehensive Cancer Network (NCCN), and the European Society for Medical Oncology (ESMO), a consensus on the proper interval between NAC and surgery has yet to be reached (9-12). Related studies have analyzed the effect of the interval length on efficacy. Sutton *et al.* (13) concluded that intervals longer than 2 months lead to worse RFS and OS. Chen *et al.* (14) in 2020 noted better oncology outcomes with intervals of less than 5 weeks. However, adverse effects of neoadjuvant chemotherapy (NAC) can worsen intraoperative bleeding, such as oxaliplatin-induced hepatic sinusoidal dilatation and irinotecan-induced fatty liver (15,16). Welsh *et al.* (17) found that patients who had liver resection within 4 weeks of NAC had the highest incidence of postoperative complications. A long duration of systemic therapy may promote the progression of disease. The most appropriate timing for surgery needs to be investigated.

2. Materials and Methods

2.1. Patient selection

Patients with CRLM who underwent hepatectomy after NAC between 2008 and 2020 at Zhejiang Cancer Hospital were retrospectively studied. All patients were confirmed to be potential candidates for resection before receiving NAC. Patients who had received preoperative radiotherapy or transcatheter arterial chemoembolization (TACE) or who had extrahepatic metastases or positive surgical margins were excluded. CRLM was verified by pathology and immunohistochemistry. The baseline characteristics, perioperative data, and NAC regimens were acquired from the electronic medical record system of Zhejiang Cancer Hospital. In compliance with the declaration of Helsinki, this study was conducted with the approval of the medical ethics committee of Zhejiang Cancer Hospital.

Surgery was selected for appropriate patients after NAC based on tumor resectability and the physical condition of the patient. The majority of patients underwent less than 6 cycles of NAC in this 3-month period. The regimens of NAC consisted of capecitabine, 5-fluorouracil, oxaliplatin, and irinotecan. Patients who received NAC along with bevacizumab all underwent surgery after stopping the drug for more than six weeks.

2.2. Procedure

For the patients who underwent liver and colorectal resection simultaneously, colon or rectal radical resection was performed by the surgeon of the department of colorectal surgery. A resection of less than 3 Couinaud segments was defined as minor liver resection; otherwise, it was defined as major liver resection. The low central venous pressure (CVP) technique was used to reduce intraoperative bleeding. The Pringle maneuver was used to block hepatic inflow, which was limited to 15 min, and the interval between blocking was more than 5 min. An ultrasonic scalpel was used to transect liver parenchyma.

2.3. Definitions

Multiple metastases refer to more than 1 lesion in the liver. RFS was defined as the period of time from surgery to the first diagnosis of tumor recurrence. OS was defined as the duration from surgery to the time of death or the last follow-up. The chemotherapy-free interval (CFI) was defined as the interval from the end of the last NAC to surgery. Postoperative complications included bleeding, liver-related complications, and infectious complications. Liver-related complications included a bile leak, ascites, or postoperative liver dysfunction (international normalized ratio (INR)

elevated more than 1.8-fold the normal upper limit or total bilirubin elevated more than 3-fold the normal upper limit) (18). A surgical site infection, urinary tract infection, or pneumonia were all considered infectious complications. The Clavien-Dindo classification was used to classify the severity of each postoperative complication.

2.4. Data collection and follow-up

The baseline characteristics of the patients included their age, sex, comorbidities, carcinoembryonic antigen (CEA), the maximum tumor size, and TNM stage. Chemotherapy-related variables included NAC cycles and targeted therapy. Surgery-related variables included the procedure (open or endoscopic), range of hepatectomy (minor or major), intraoperative blood loss, and operating time. The follow-up cut-off date was set at January 31, 2022. Follow-up examinations should consist of a serology based on tumor markers, as well as contrast-enhanced CT or MRI scans. These evaluations should be conducted every 3 months in the first 2 years, and then every 6 months for up to 5 years. If recurrence is detected, the subsequent treatment can be determined based on the effectiveness of preoperative NAC, or other treatments such as radiofrequency ablation or TACE were available.

2.5. Statistical analysis

The statistical software SPSS (IBM SPSS, version 25.0) was used for statistical analysis. Continuous variables were expressed as the median and interquartile range (IQR), while categorical variables were expressed as numbers with percentages. The Mann-Whitney *U* test was used to compare continuous variables between groups, while Pearson's chi-squared test was used to compare categorical variables. A *P* value of < 0.05 was considered to be significant. An analysis of differences in OS and RFS was performed using the Kaplan-Meier method. X-tile (Yale University School of Medicine, New Haven, Connecticut, USA) (19) was used to analyze the survival data to determine the appropriate cut-off value for grouping. Logistic regression was used for univariate analysis, and multivariate analysis was performed with factors with a *P* value < 0.1 from univariate analysis. Multivariate analysis using logistic regression included a number of variables, and variables with a *P* < 0.05 were considered independent predictors of postoperative complications.

3. Results

3.1. Clinical characteristics

A total of 141 patients with CRLM consisted of 104 males and 37 females, and the median age was 58.0

years (IQR: 50-66). Sixty-five patients (46.1%) had primary tumors located in the colon. Forty-five tumors were in the left colon and 20 were in the right colon. Synchronous liver metastases were diagnosed in 110 patients (78.0%). Multiple liver metastases were noted in 97 patients (68.8%). Oxaliplatin-based regimens were used in 103 patients (73.0%). Moreover, 45 patients (31.9%) received targeted drugs (22 bevacizumab and 23 cetuximab) as well. All details are listed in Table 1.

3.2. The best cut-off value for the timing of surgery

X-tile analysis was used to determine the best cut-off value for CFI based on patients' RFS (Figure 1). The optimal point of CFI was 4 weeks, which was determined to be the best cut-off point for the interval for predicting recurrence. Thus, all patients were divided into two groups: a short interval group (SIG, ≤ 4 weeks, $n = 98$) and a long interval group (LIG, > 4 weeks, $n = 43$). The clinicopathologic characteristics are summarized in Table S1 (<http://www.biosciencetrends.com/action/getSupplementalData.php?ID=143>). There were no significant differences between the two groups in albumin levels, body mass index (BMI), comorbidities, preoperative CEA levels, the diameter of metastases, whether liver resection was major or minor, or other factors.

3.3. Clinical characteristics of subgroups

Table 1. Baseline characteristics of patients

Items	$n = 141$ (%)
Patient-related variables	
Age > 60 years	63 (44.7)
Male	104 (73.8)
BMI > 24	43 (30.5)
Comorbidity	46 (32.6)
ALB > 40 g/L	109 (77.3)
Child-Pugh A classification	140 (99.3)
Tumor-related variables	
CEA > 30 ng/mL	37 (26.2)
Synchronous liver metastasis	110 (78.0)
Colon	65 (46.1)
Multiple liver metastasis	97 (68.8)
Diameter of metastases > 5 cm	27 (19.1)
T3-4	134 (95.0)
Node-positive primary tumor	104 (73.8)
Poor differentiation	36 (25.5)
Chemotherapy-related variables	
OX-based regimens	103 (73.0)
NAC toxicity	22 (15.6)
NAC cycle > 6	33 (23.4)
Targeted therapy	45 (31.9)
Procedure-related variables	
Simultaneous resection	7 (5.0)
Major liver resection	58 (41.1)
Open surgery	41 (29.1)

BMI: body mass index; ALB: albumin; CEA: carcinoembryonic antigen; T3-4: The TNM staging of colorectal cancer primary tumor is stage 3 or 4; OX: oxaliplatin; NAC: neoadjuvant chemotherapy.

Subgroup analysis was performed to determine the incidence of postoperative complications in different CFI. To further analyze the incidence of complications within 4 weeks, the SIG group was divided into three subgroups: a CFI of 1-2 weeks, a CFI of 2-3 weeks, and a CFI of 3-4 weeks. Doing so allowed investigation of the incidence of postoperative complications that occurred within a 4-week period in each of these subgroups. The clinicopathologic characteristics of subclassification are shown in Table 2. There were no marked differences in clinicopathologic characteristics between subgroups, except for the albumin level, chemotherapy regimen, and targeted therapy. In addition, there were no significant differences in the albumin level and chemotherapy regimen between the SIG and LIG.

3.4. Short-term outcomes in subgroups

Intraoperative findings in the 4 groups are shown in Table 3. No intraoperative mortality occurred. Intraoperative bleeding, the operating time, and the duration of postoperative hospitalization did not differ significantly among the 4 groups.

A total of 29 patients developed postoperative complications, which occurred in 23 patients (23.5%) in the SIG and 6 patients (14.0%) in the LIG ($P =$

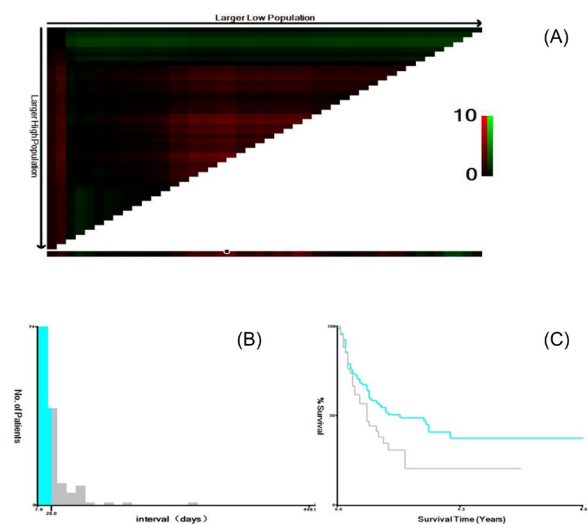


Figure 1. X-tile plots of the interval between finishing neoadjuvant chemotherapy and liver resection. X-tile plots show log-rank values with cut points, with the data divided into low and high groups. (A), The X-axis represents all potential cut-off values from low to high that define a low subset, whereas the Y-axis represents cut-off values from high to low that define a high subset. Red coloration of cut-off values indicates an inverse correlation with time to recurrence, and green coloration represents direct associations. The optimal cut-off value occurs at the brightest pixel according to a chi-square test. (B), A histogram of the entire cohort divided into low and high subgroups depending on the optimal cut-off value (4 weeks). (C), A Kaplan-Meier plot of RFS produced by the optimal cut-off value of CFI. Blue represents the SIG, and gray represents the LIG.

Table 2. Baseline characteristics in subgroups

Items	1-2 weeks <i>n</i> = 20 (%)	2-3 weeks <i>n</i> = 41 (%)	3-4 weeks <i>n</i> = 36 (%)	> 4weeks <i>n</i> = 43 (%)	<i>P</i>
Patient-related variables					
Age > 60 years	5 (25)	22 (53.7)	16 (44.4)	20 (46.5)	0.211
Male	12 (60)	33 (80.5)	23 (63.9)	36 (83.7)	0.072
BMI > 24	5 (25)	10 (24.4)	16 (44.4)	12 (27.9)	0.219
Comorbidity	7 (35)	13 (31.7)	10 (27.8)	15 (34.9)	0.910
ALB > 40g/L	15 (75)	26 (63.4)	33 (91.7)	35 (81.4)	0.025
Child-Pugh A classification	20 (100)	40 (97.6)	36 (100)	43 (100)	0.488
Tumor-related variables					
CEA > 30 ng/mL	6 (30)	9 (22)	12 (33.3)	10 (23.3)	0.646
Synchronous liver metastasis	18 (90.0)	30 (73.2)	29 (80.6)	32 (74.4)	0.444
Colon	10 (50)	21 (51.2)	14 (38.9)	19 (44.2)	0.714
Multiple liver metastasis	13 (65.0)	30 (73.2)	24 (66.7)	30 (69.8)	0.900
Diameter of metastases > 5 cm	5 (25)	7 (17.1)	8 (22.2)	7 (16.3)	0.802
T3-4	20 (100)	36 (87.8)	35 (97.2)	42 (97.7)	0.088
Node-positive primary tumor	17 (85.0)	29 (70.7)	26 (72.2)	31 (72.1)	0.660
Poor differentiation	4 (20)	10 (24.4)	8 (22.2)	14 (32.6)	0.645
Chemotherapy-related variables					
OX-based regimens	19 (95.0)	34 (82.9)	22 (61.1)	28 (65.1)	0.012
NAC toxicity	2 (10)	10 (24.4)	3 (8.3)	7 (16.3)	0.229
NAC cycle > 6	5 (25.0)	10 (24.4)	8 (22.2)	10 (23.3)	0.994
Targeted therapy	5 (25.0)	8 (19.5)	9 (25.0)	23 (53.5)	0.004
Procedure-related variables					
Simultaneous resection	1 (5.0)	1 (2.4)	4 (11.1)	1 (2.3)	0.257
Major liver resection	7 (35.0)	18 (43.9)	16 (44.4)	17 (39.5)	0.887
Open surgery	16 (80.0)	32 (78.0)	23 (63.9)	29 (67.4)	0.401

BMI: body mass index; ALB: albumin; CEA: carcinoembryonic antigen; T3-4: The TNM staging of colorectal cancer primary tumor is stage 3 or 4; OX: oxalipatin; NAC: neoadjuvant chemotherapy.

Table 3. Short-term outcomes in subgroups

Items	1-2 weeks (<i>n</i> = 19)	2-3 weeks (<i>n</i> = 40)	3-4 weeks (<i>n</i> = 33)	> 4 weeks (<i>n</i> = 41)	<i>P</i>
Intraoperative bleeding (mL); median (IQR)	200 (100-400)	350 (100-575)	200 (100-400)	300 (150-400)	0.453
Operating time (min); median (IQR)	152 (104-186)	148 (123.25-203)	142 (113-231.5)	166 (130-202)	0.535
Duration of postoperative hospitalization (days); median (IQR)	8 (6.25-11.75)	7 (6-10)	7 (5-10.5)	8 (6-10)	0.626

IQR: inter-quartile range

Table 4. Postoperative complications in subgroups

Complications	1-2 weeks <i>n</i> = 20 (%)	2-3 weeks <i>n</i> = 41 (%)	3-4 weeks <i>n</i> = 36 (%)	> 4 weeks <i>n</i> = 42 (%)	<i>P</i>
Overall	7 (35.0)	8 (19.5)	8 (22.2)	6 (14.3)	0.288
Abdominal infection	2 (10.0)	4 (9.8)	2 (5.6)	1 (2.4)	
Surgical site infection	1 (5.0)	0 (0.0)	1 (2.8)	1 (2.4)	
Urinary tract infection	0 (0.0)	1 (2.4)	0 (0.0)	0 (0.0)	
Postoperative bleeding	1 (5.0)	2 (4.9)	0 (0.0)	3 (7.1)	
Bile leak	0 (0.0)	1 (2.4)	1 (2.8)	0 (0.0)	
Hepatic insufficiency	0 (0.0)	1 (2.4)	1 (2.8)	0 (0.0)	
Pleural effusion	3 (15.0)	0 (0.0)	3 (8.3)	2 (4.8)	
Ileus	0 (0.0)	0 (0.0)	0 (0.0)	1 (2.4)	

0.198). All postoperative complications were mild. No mortality was reported within 30 days postoperatively. Although the incidence of postoperative complications in the CFI of 1-2 weeks group was higher than that in the CFI of > 4 weeks group (35% vs. 14.3%, *P* = 0.055), the difference was not significant. The complications that occurred are shown in Table 4.

The association between postoperative complications and baseline characteristics is shown in Table 5. In univariate analyses, a CFI of 1-2 weeks (*P* = 0.062) and ALB ≤ 40 g/L (*P* = 0.025) were associated with complications. In multivariate analyses, a CFI of 1-2 weeks (OR = 0.263, 95% CI:2.70-0.985, *P* = 0.048) and ALB > 40 g/L (OR = 0.341, 95% CI:0.124-0.945,

Table 5. Prognostic factors for postoperative complications

Items	Univariate OR (95% CI)	P	Multivariate OR (95% CI)	P
interval > 4 weeks	<i>ref</i>		<i>ref</i>	
interval of 3-4 weeks	0.568 (0.177-1.823)	0.341	0.516 (0.148-1.799)	0.299
interval of 2-3 weeks	0.669 (0.210-2.129)	0.496	1.154 (0.319-4.167)	0.827
interval of 1-2 weeks	0.301 (0.085-1.062)	0.062	0.263 (0.70-0.985)	0.048
Age > 60 years	1.406 (0.620-3.191)	0.415		
Male	1.111 (0.430-2.874)	0.827		
BMI > 24	0.663 (0.259-1.695)	0.391		
Comorbidity	0.611 (0.240-1.559)	0.303		
ALB > 40 g/L	0.360 (0.147-0.878)	0.025	0.341 (0.124-0.945)	0.038
CEA > 30 ng/mL	1.077 (0.430-2.697)	0.874		
Synchronous liver metastasis	2.009 (0.642-6.288)	0.231		
Colon	1.615 (0.710-3.677)	0.253		
Multiple metastasis	0.663 (0.259-1.695)	0.391		
Simultaneous resection	3.087 (0.650-14.645)	0.156		
Diameter of metastases > 5cm	1.845 (0.712-4.781)	0.208		
Major liver resection	1.192 (0.523-2.717)	0.677		
T3-4	1.600 (0.185-13.841)	0.669		
Node-positive primary tumor	0.501 (0.210-1.194)	0.119		
Targeted therapy	1.384 (0.590-3.244)	0.455		
Child-Pugh A classification	/	/		
NAC toxicity	2.639 (0.982-7.093)	0.054	2.640 (0.849-8.215)	0.094
NAC cycle > 6	1.040 (0.399-2.709)	0.936		
Poor differentiation	1.129 (0.450-2.834)	0.796		
Open surgery	0.591 (0.221-1.582)	0.295		

BMI: body mass index; ALB: albumin; CEA: carcinoembryonic antigen; T3-4: The TNM staging of colorectal cancer primary tumor is stage 3 or 4; OX: oxaliplatin; NAC: neoadjuvant chemotherapy.

$P = 0.038$) were definitely independent indicators for postoperative complications.

3.5. Survival analysis

Seventy-nine patients (56%) experienced tumor recurrence, and 31.2% of patients had died before the cut-off time. Median OS was 35 months (IQR:26-55), and median RFS was 13 months (IQR:5-26). Patients in the SIG were more likely to have significantly better RFS (3-year RFS 47.4% vs. 20.5%, $P = 0.043$) (Figure 2A). There were no significant differences in RFS among the 4 subgroups ($P = 0.103$). However, the median RFS of patients with a CFI of 3-4 weeks was 17 months (IQR: 22.35-38.75) vs. 12 months (IQR:4.5-18.5) for patients with a CFI of > 4 weeks ($P = 0.01$) (Figure 2B). There were no significant differences in OS among the 4 subgroups (Figure 2C).

4. Discussion

To the extent known, the proper timing for patients with CRLM to undergo hepatectomy after their last chemotherapy had never been defined. Published guidelines and consensus opinions were consulted for this study, but none recommended a proper interval between the last NAC and surgery. Two aspects of the interval need to be taken into account.

Initially, anti-cancer drugs can result in varying degrees of hepatocellular injuries, such as oxaliplatin-induced hepatic sinusoidal dilatation and irinotecan-

induced fatty liver (20,21). The primary concern with reducing the preoperative CFI was that liver injury caused by chemotherapy drugs may affect the surgical process and postoperative recovery (including increased intraoperative bleeding and a longer operating time) (22). However, Takeshi *et al.* (23) reported that liver function will return to normal after more than 2-4 weeks following the cessation of chemotherapy. Welsh *et al.* (17) found that patients who had liver resection within 4 weeks of NAC had the highest incidence of postoperative complications. This is consistent with the finding of the current study that an increase in postoperative complications in patients with a CFI of up to 4 weeks mainly occurred in patients with a CFI of up to 2 weeks.

In addition, NAC was considered to be the standard treatment for CRLM before surgery based on published studies (24-27). However, a prolonged CFI may increase the chances of recurrence and worsen prognosis (28). Adam *et al.* (29) found that disease progressed in about 25% of patients during the interval between NAC and surgery. Another study found that the cohort of patients who underwent resection more than 5 weeks after NAC, compared to the group that underwent less than 5 weeks after, had a worse pathological reaction and worse RFS (30). Thomas *et al.* (13) concluded that surgery within 2 months of NAC improved long-term outcomes.

In the current study, 4 weeks was the appropriate cut-off point for the assignment of patients to the SIG or LIG by X-tile analysis. In terms of short-term outcomes, there were no significant differences

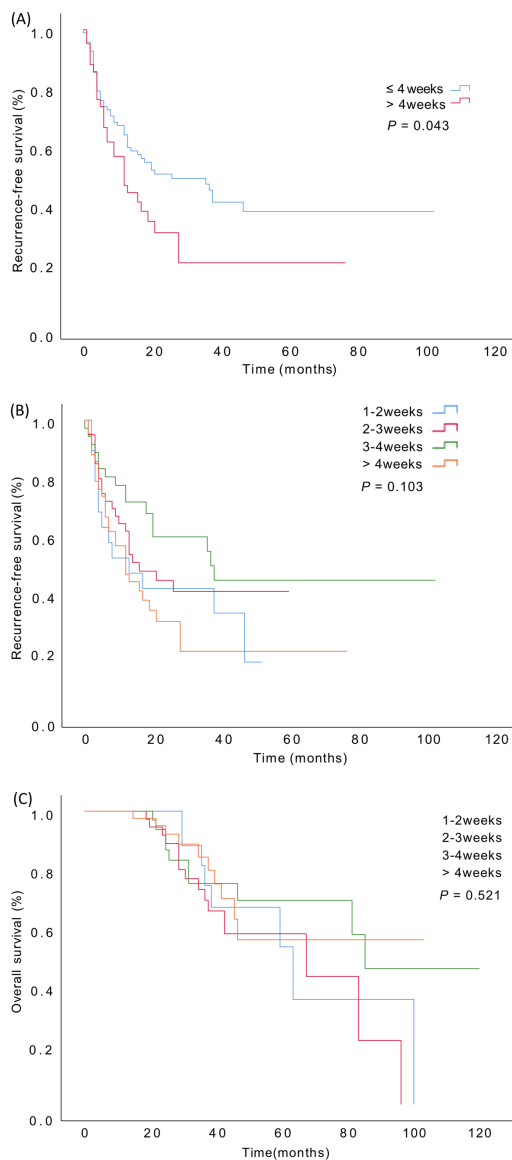


Figure 2. (A), Kaplan-Meier survival curve for RFS of the SIG and LIG. (B), Kaplan-Meier survival curve for RFS of subgroups. (3-4weeks vs. > 4weeks $p = 0.01$). (C), Kaplan-Meier survival curve for OS of subgroups.

between subgroups, including intraoperative bleeding, operating time, and the duration of postoperative hospitalization. Outcomes revealed that short intervals after NAC did not worsen perioperative data. However, the postoperative complication rate in the 1-2 weeks subgroup was marginally higher than that in the > 4 weeks subgroup (35% vs. 14.3% $P = 0.055$) according to subgroup analyses. In addition, 1-2 weeks was an independent indicator for postoperative complications according to multivariate analyses.

The current study found that patients in the SIG had a better 3-year RFS (47.4% vs. 20.5%, $P = 0.043$). However, the 3-year OS was not correlated with the length of the interval (76.1% in the SIG vs. 79.9% in the LIG, $P = 0.635$). Differences between RFS and OS might be explained by several factors. To start with,

recurrence of colorectal cancer after hepatic resection was caused by the unique biological characteristics of the disease, since liver metastasis will be detected in about half of patients as the disease progresses. RFS does not intuitively reflect the OS (31,32). Oba *et al.* argued that the time to recurrence of an unresectable tumor is strongly associated with the OS (33). The OS is a composite endpoint that is heavily affected by treatment, whether conservative or surgical (24). Although tumor progression leading to patient death remains the primary cause of mortality, the prolonging of OS has resulted in an increase in non-tumor-related deaths. This is also a significant factor affecting the differences between the RFS and OS. More chemotherapy drugs and targeted drugs are often used during the first recurrence in patients electing to undergo surgery, and this could have affected the OS. The development and use of tumor immune targeted therapy has reduced the role of surgery in the patient's prognosis and significantly improved OS (34,35).

This study found that a CFI < 4 weeks is associated with better RFS, and 1-2 weeks was an independent factor influencing the development of complications. Having balanced postoperative complications and oncological outcomes, the best interval between NAC and surgery was 2-4 weeks. Other studies have also indicated that the appropriate timing of surgery after NAC improved patient prognosis. Although factors such as chemotherapy regimens and targeted drug use will affect the interval, the impact of other factors on the CFI should be minimized.

As a single-center retrospective study, the current study has several limitations. First, bias with respect to the determination of resectability by different doctors could not be completely ruled out. All of the current patients had resectable CRLM, the toxicity of NAC, whether targeted therapy was used or not, and the patient's performance status may have influenced the timing of surgery. Second, there were differences in the choice of chemotherapy regimens in the 2 groups, and the decision was generally reached through conversations between patients and their doctors. Targeted drugs such as bevacizumab need to be stopped for more than 6 weeks, which is also a factor affecting the operating time. Third, this study had a small sample size. Larger samples and multicenter randomized controlled trials are needed to confirm the current results.

Funding: None.

Conflict of Interest: The authors have no conflicts of interest to disclose.

References

1. Bray F, Ferlay J, Soerjomataram I, Siegel RL, Torre LA, Jemal A. Global cancer statistics 2018: GLOBOCAN

- estimates of incidence and mortality worldwide for 36 cancers in 185 countries. *CA Cancer J Clin.* 2018; 68:394-424.
2. Dekker E, Tanis PJ, Vleugels JLA, Kasi PM, Wallace MB. Colorectal cancer. *Lancet.* 2019; 394:1467-1480.
 3. Tsilimigras DI, Brodt P, Clavien P-A, Muschel RJ, D'Angelica MI, Endo I, Parks RW, Doyle M, de Santibañes E, Pawlik TM. Liver metastases. *Nat Rev Dis Primers.* 2021; 7:27.
 4. Riihimäki M, Hemminki A, Sundquist J, Hemminki K. Patterns of metastasis in colon and rectal cancer. *Sci Rep.* 2016; 6:29765.
 5. Rees M, Tekkis PP, Welsh FK, O'Rourke T, John TG. Evaluation of long-term survival after hepatic resection for metastatic colorectal cancer: A multifactorial model of 929 patients. *Ann Surg.* 2008; 247:125-135.
 6. Primrose J, Falk S, Finch-Jones M, *et al.* Systemic chemotherapy with or without cetuximab in patients with resectable colorectal liver metastasis: The New EPOC randomised controlled trial. *The Lancet Oncology.* 2014; 15:601-611.
 7. Nordlinger B, Sorbye H, Glimelius B, *et al.* Perioperative chemotherapy with FOLFOX4 and surgery versus surgery alone for resectable liver metastases from colorectal cancer (EORTC Intergroup trial 40983): A randomised controlled trial. *The Lancet.* 2008; 371:1007-1016.
 8. Kanemitsu Y, Shimizu Y, Mizusawa J, *et al.* Hepatectomy followed by mFOLFOX6 versus hepatectomy alone for liver-only metastatic colorectal cancer (JCOG0603): A phase II or III randomized controlled trial. *J Clin Oncol.* 2021; 39:3789-3799.
 9. Benson AB, Venook AP, Al-Hawary MM, *et al.* Colon Cancer, Version 2.2021, NCCN Clinical Practice Guidelines in Oncology. *J Natl Compr Canc Netw.* 2021; 19:329-359.
 10. Van Cutsem E, Cervantes A, Adam R, *et al.* ESMO consensus guidelines for the management of patients with metastatic colorectal cancer. *Ann Oncol.* 2016; 27:1386-1422.
 11. Diagnosis, Treatment Guidelines for Colorectal Cancer Working Group C. Chinese Society of Clinical Oncology (CSCO) diagnosis and treatment guidelines for colorectal cancer 2018 (English version). *Chin J Cancer Res.* 2019; 31:117-134.
 12. Ayez N, van der Stok EP, Grünhagen DJ, Rothbarth J, van Meerten E, Eggermont AM, Verhoef C. The use of neo-adjuvant chemotherapy in patients with resectable colorectal liver metastases: Clinical risk score as possible discriminator. *Eur J Surg Oncol.* 2015; 41:859-867.
 13. Sutton TL, Wong LH, Walker BS, Dewey EN, Eil RL, Ibewuiké U, Chen EY, Rocha FG, Billingsley KG, Mayo SC. Surgical timing after preoperative chemotherapy is associated with oncologic outcomes in resectable colorectal liver metastases. *J Surg Oncol.* 2022; 125:1260-1268.
 14. Chen EY, Mayo SC, Sutton T, Kearney MR, Kardosh A, Vaccaro GM, Billingsley KG, Lopez CD. Effect of time to surgery of colorectal liver metastases on survival. *J Gastrointest Cancer.* 2020; 52:169-176.
 15. Karoui M, Penna C, Amin-Hashem M, Mitry E, Benoist S, Franc B, Rougier P, Nordlinger B. Influence of preoperative chemotherapy on the risk of major hepatectomy for colorectal liver metastases. *Ann Surg.* 2006; 243:1-7.
 16. Robinson SM, Wilson CH, Burt AD, Manas DM, White SA. Chemotherapy-associated liver injury in patients with colorectal liver metastases: A systematic review and meta-analysis. *Ann Surg Oncol.* 2012; 19:4287-4299.
 17. Welsh FKS, Tilney HS, Tekkis PP, John TG, Rees M. Safe liver resection following chemotherapy for colorectal metastases is a matter of timing. *Br J Cancer.* 2007; 96:1037-1042.
 18. Wolf PS, Park JO, Bao F, Allen PJ, DeMatteo RP, Fong Y, Jarnagin WR, Kingham TP, Gönen M, Kemeny N, Shia J, D'Angelica MI. Preoperative chemotherapy and the risk of hepatotoxicity and morbidity after liver resection for metastatic colorectal cancer: A single institution experience. *J Am Coll Surg.* 2013; 216:41-49.
 19. Camp RL, Dolled-Filhart M, Rimm DL. X-tile: A new bio-informatics tool for biomarker assessment and outcome-based cut-point optimization. *Clin Cancer Res.* 2004; 10:7252-7259.
 20. Viganò L, Capussotti L, De Rosa G, De Saussure WO, Mentha G, Rubbia-Brandt L. Liver resection for colorectal metastases after chemotherapy: Impact of chemotherapy-related liver injuries, pathological tumor response, and micrometastases on long-term survival. *Ann Surg.* 2013; 258:731-740; discussion 741-732.
 21. Zhao J, van Mierlo KMC, Gómez-Ramírez J, *et al.* Systematic review of the influence of chemotherapy-associated liver injury on outcome after partial hepatectomy for colorectal liver metastases. *Br J Surg.* 2017; 104:990-1002.
 22. Viganò L, De Rosa G, Toso C, Andres A, Ferrero A, Roth A, Sperti E, Majno P, Rubbia-Brandt L. Reversibility of chemotherapy-related liver injury. *J Hepatol.* 2017; 67:84-91.
 23. Takamoto T, Hashimoto T, Sano K, Maruyama Y, Inoue K, Ogata S, Takemura T, Kokudo N, Makuuchi M. Recovery of liver function after the cessation of preoperative chemotherapy for colorectal liver metastasis. *Ann Surg Oncol.* 2010; 17:2747-2755.
 24. Nordlinger B, Sorbye H, Glimelius B, *et al.* Perioperative FOLFOX4 chemotherapy and surgery versus surgery alone for resectable liver metastases from colorectal cancer (EORTC 40983): Long-term results of a randomised, controlled, phase 3 trial. *Lancet Oncol.* 2013; 14:1208-1215.
 25. Mitry E, Fields AL, Bleiberg H, *et al.* Adjuvant chemotherapy after potentially curative resection of metastases from colorectal cancer: A pooled analysis of two randomized trials. *J Clin Oncol.* 2008; 26:4906-4911.
 26. Krishnamurthy A, Kankesan J, Wei X, Nanji S, Biagi JJ, Booth CM. Chemotherapy delivery for resected colorectal cancer liver metastases: Management and outcomes in routine clinical practice. *Eur J Surg Oncol.* 2017; 43:364-371.
 27. Lehmann K, Rickenbacher A, Weber A, Pestalozzi BC, Clavien PA. Chemotherapy before liver resection of colorectal metastases: Friend or foe? *Ann Surg.* 2012; 255:237-247.
 28. Kambakamba P, Linecker M, Alvarez FA, Samaras P, Reiner CS, Raptis DA, Kron P, de Santibanes E, Petrowsky H, Clavien PA, Lesurtel M. Short chemotherapy-free interval improves oncological outcome in patients undergoing two-stage hepatectomy for colorectal liver metastases. *Ann Surg Oncol.* 2016; 23:3915-3923.
 29. Adam R, Pascal G, Castaing D, Azoulay D, Delvart V, Paule B, Levi F, Bismuth H. Tumor progression while

- on chemotherapy: A contraindication to liver resection for multiple colorectal metastases? *Ann Surg.* 2004; 240:1052-1061; discussion 1061-1054.
30. Chen Q, Mao R, Zhao J, Bi X, Li Z, Huang Z, Zhang Y, Zhou J, Zhao H, Cai J. From the completion of neoadjuvant chemotherapy to surgery for colorectal cancer liver metastasis: What is the optimal timing? *Cancer Med.* 2020; 9:7849-7862.
 31. Höppener DJ, Nierop PMH, van Amerongen MJ, Olthof PB, Galjart B, van Gulik TM, de Wilt JHW, Grünhagen DJ, Rahbari NN, Verhoef C. The disease-free interval between resection of primary colorectal malignancy and the detection of hepatic metastases predicts disease recurrence but not overall survival. *Ann Surg Oncol.* 2019; 26:2812-2820.
 32. Ecker BL, Lee J, Saadat LV, *et al.* Recurrence-free survival versus overall survival as a primary endpoint for studies of resected colorectal liver metastasis: A retrospective study and meta-analysis. *Lancet Oncol.* 2022; 23:1332-1342.
 33. Oba M, Hasegawa K, Matsuyama Y, Shindoh J, Mise Y, Aoki T, Sakamoto Y, Sugawara Y, Makuuchi M, Kokudo N. Discrepancy between recurrence-free survival and overall survival in patients with resectable colorectal liver metastases: A potential surrogate endpoint for time to surgical failure. *Ann Surg Oncol.* 2014; 21:1817-1824.
 34. Ye LC, Liu TS, Ren L, Wei Y, Zhu DX, Zai SY, Ye QH, Yu Y, Xu B, Qin XY, Xu J. Randomized controlled trial of cetuximab plus chemotherapy for patients with KRAS wild-type unresectable colorectal liver-limited metastases. *J Clin Oncol.* 2013; 31:1931-1938.
 35. Hurwitz H, Fehrenbacher L, Novotny W, *et al.* Bevacizumab plus irinotecan, fluorouracil, and leucovorin for metastatic colorectal cancer. *N Engl J Med.* 2004; 350:2335-2342.
- Received October 11, 2022; Revised March 7, 2023; Re-revised April 8, 2023; Accepted April 18, 2023.
- [§]These authors contributed equally to this work.
**Address correspondence to:*
Jia Wu and Yuhua Zhang, Department of Hepatobiliary and Pancreatic Surgery, Zhejiang Cancer Hospital, Institute of Basic Medicine and Cancer (IBMC) Chinese Academy of Sciences, Hangzhou, Zhejiang 310022, China.
E-mail: hpb_wujia@163.com (JW); drzhangyuhua@126.com (YZ)
- Released online in J-STAGE as advance publication April 22, 2023.

Decrease in CD226 expression on CD4⁺ T cells in patients with endometriosis

Cui Li^{1,§}, Jing Zhou^{2,§}, Jun Shao³, Lei Yuan³, Qiang Cheng⁴, Ling Wang^{2,5,6,*}, Zhongliang Duan^{1,*}

¹ Clinical Laboratory Department, Obstetrics and Gynecology Hospital of Fudan University, Shanghai, China;

² Laboratory for Reproductive Immunology, Obstetrics and Gynecology Hospital of Fudan University, Shanghai, China;

³ Gynecology Department, Obstetrics and Gynecology Hospital of Fudan University, Shanghai, China;

⁴ Information Department, Obstetrics and Gynecology Hospital of Fudan University, Shanghai, China;

⁵ The Academy of Integrative Medicine, Fudan University, Shanghai, China;

⁶ Shanghai Key Laboratory of Female Reproductive Endocrine-related Diseases, Shanghai, China.

SUMMARY Endometriosis is a chronic inflammatory disease. The immune-checkpoint molecules CD226 and TIGIT play an important role in regulating T cells' function. However, little is known about the proportion and function of CD226 and TIGIT on CD4⁺ T cells in endometriosis. The current study found no significant differences in the TIGIT percentage on peripheral CD4⁺ T cells between patients with endometriosis and the control group. However, CD226 was lower in patients with endometriosis than that in the control group ($P < 0.01$). The cytokines TNF- α , IL10, and IFN- γ were significantly elevated in TIGIT⁺ CD4⁺ T cells compared to TIGIT⁻ CD4⁺ T cells. HLA-DR⁺ cells were more numerous among TIGIT⁺ CD4⁺ T cells than among the TIGIT⁻ subset ($P < 0.001$). Similarly, the cytokines TNF- α , IL10, and IFN- γ were significantly elevated in CD226⁺ CD4⁺ T cells compared to levels in CD226⁻ CD4⁺ T cells. The proportion of HLA-DR⁺ CD4⁺ T cells among CD226⁺ CD4⁺ T cells was also significantly higher than that among the CD226⁻ subset ($P < 0.001$). After TIGIT was blocked, the level of IL-10 in TIGIT⁺ CD4⁺ T cells was higher than that in cells with unblocked TIGIT. There were no differences in TNF- α and IFN- γ . After CD226 was blocked, TNF- α and IFN- γ were lower while IL-10 was higher. In conclusion, there is a diminution of CD226 in CD4⁺ T cells in patients with endometriosis. This is correlated with the effector function of CD4⁺ T cells, and blocking CD226 can suppress this function.

Keywords TIGIT, CD226, endometriosis, CD4⁺ T cells

Endometriosis is a chronic inflammatory disease in which proinflammatory factors and chemokines in the local immune microenvironment are involved in normal and pathologic immune regulation (1), and this abnormal immune status is also reflected in peripheral blood (2). The T-cell immunoglobulin and immunoreceptor tyrosine-based inhibitory motif domain (TIGIT) is an immunosuppressive molecule discovered in 2005 (3) that is associated with T-cell activation and suppression (4). This receptor molecule mediates inhibitory signals by interacting with the ligands CD155 and CD112. TIGIT has been proven to exist mainly on activated T cells (5) and to play a role in suppressing immune effects in tumors, immune-related physiology, or in various diseases (6). CD226 (DNAM-1) is a co-stimulatory molecule that interacts with CD155 to activate TCR, that promotes Th1-related signal transduction, that enhances the effector

function of NK cells, and that promotes CD4⁺T cells to produce the proinflammatory cytokine interferon γ (IFN- γ) (7).

Although abnormal expression of TIGIT/CD226 in some immune-related diseases has been reported, there are few existing reports concerning both molecules regarding their expression and possible role(s) in endometriosis. Thus, the current study evaluated the molecular expression, state of activation, and cytokine production of the two immune-checkpoint molecules on CD4⁺ T cells in endometriosis in order to provide data to elucidate the development and progression of endometriosis.

Subjects were patients and female controls who met the following inclusion criteria and exclusion criteria. Inclusion criteria: The patients were diagnosed by a gynecologist, through clinical manifestations, ultrasound

or some other imaging exam, laparoscopy, or the like. To reduce the influence of age, subjects between the ages of 20 and 45 were selected. Exclusion criteria: Patients with diseases that might cause serious changes in the immune system were excluded. Patients with chromosomal diseases were excluded. Patients with unavailable data were also excluded. The control group: Healthy women seen at this hospital for a pre-pregnancy checkup were included as healthy controls; these women were age-matched to patients, had no chromosomal or immune system-related diseases, and consented to participate in this study.

Venous blood was anticoagulated with EDTA, and peripheral blood mononuclear cells were extracted using Ficoll-Paque lymphocyte separation medium (Huaqing, Shanghai, China) and frozen in a -80°C freezer. When a particular number of patients was selected, the frozen cells were thawed and suspended in RPMI 1640 for subsequent use.

Antibodies were purchased from BD BioLegend (San Diego, California, USA) and included CD3 APC-CY7, CD4 BV510, CD25 PE, TIGIT FITC, CD226-BV785, HLA-DR APC, TNF- α PE-CY7, IFN- γ -PE-Cy5.5, and IL10 BV421. Intracellular cytokines were stimulated before testing. Leukocyte Activation Cocktail (BD Biosciences, Franklin Lakes, NJ, USA) was used to stimulate them in accordance with the manufacturer's instructions. Then, cytokine antibodies TNF- α PE-CY7, IFN- γ -PE-Cy5.5, and IL10 BV421 were added. Before stimulation, the cells were blocked or not blocked with anti-TIGIT or anti-CD226 antibodies.

The software GraphPad Prism Version 5.0 (GraphPad, San Diego, CA, USA) and SPSS 19 were used for statistical analysis and graphs. Variables with a normal distribution were expressed as the mean \pm standard deviation ($X \pm SD$), and variables with an abnormal distribution were expressed as a median and range. Differences between the 2 groups were analyzed using a *t*-test or chi-square test. The Mann-Whitney *U* test was

used for abnormally distributed variables.

As shown in Table 1, there were 23 patients with endometriosis in the endometriosis group and 24 healthy women in the control group. Their clinical and demographic data are shown in Table 1. To compare TIGIT/CD226 markers between the two groups and to identify clinical associations with CD226 in patients with endometriosis, the expression of TIGIT and CD226 was first determined without any stimulation or activation. There were no significant differences in the TIGIT percentage on CD4⁺ T cells between the 2 groups. However, CD226 was significantly lower in patients with endometriosis compared to that in the control group ($P < 0.01$, Figure 1A, 1B). When the CD226 proportion on

Table 1. Clinical data on subjects

Parameters	Control group (n = 24)	Patients with endometriosis (n = 23)
Age (years)	36 \pm 4.47	35 \pm 5.04
CA125 (U/mL)	27.92 (4.89 - 63.22)	27.43 (3.64 - 73.19)
HE4 (pmol/L)	39.11 (15.01 - 137.00)	54.83 (22.02 - 116.75)
CRP (mg/L)	3.40 (0.8 - 8.72)	1.84 (0.8 - 13.64)
SAA (mg/L)	6.34 (2.65 - 22.75)	7.00 (2.45 - 23.76)
WBCs ($\times 10^9/L$)	6.51 \pm 1.56	6.20 \pm 1.95
Neutrophils ($\times 10^9/L$)	3.36 (2.22 - 5.93)	4.00 (1.81 - 9.94)
Lymphocytes ($\times 10^9/L$)	2.35 (1.11 - 3.49)	1.42 (0.62 - 2.76) *
PLTs ($\times 10^9/L$)	245.13 \pm 46.24	233.48 \pm 66.44
PDW (fL)	11.97 \pm 1.45	12.53 \pm 1.79
Endometrial antibody	6/24	6/23
NLR	1.67 (0.70 - 3.44)	2.52 (1.10 - 16.03) *
D dimer (mg/L)	0.28 (0.03 - 1.02)	0.33 (0.0 - 1.14)

Data are exhibited as means \pm SD for continuous variables, or medians and ranges for non-normally distributed data. * represents $P < 0.05$.

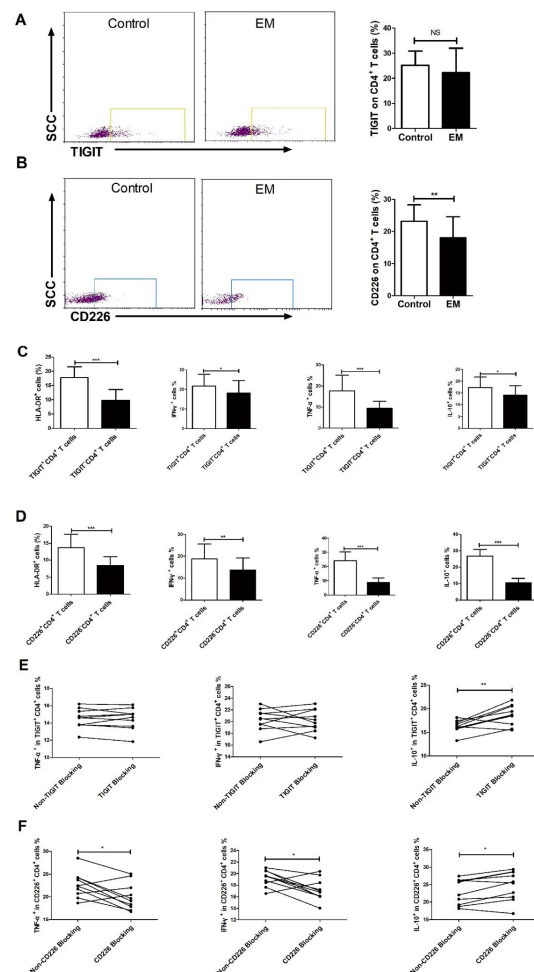


Figure 1. Characteristics of CD226 and TIGIT expressed on CD4⁺ T cells in patients with endometriosis and healthy controls. (A, B) Samples were examined using flow cytometry, and CD4-positive lymphocytes were gated for CD226 and TIGIT on the T cell surface. Data are expressed as the mean \pm SD, and a *t* test was used to compare patients with endometriosis ($n = 23$) and the control group ($n = 24$). **(C)** HLA-DR⁺ CD4⁺ T cells were more prevalent among TIGIT⁺ CD4⁺ T cells than the TIGIT⁻ subset. TNF- α , IFN- γ , and IL10 were significantly higher in TIGIT⁺ CD4⁺ T cells than in the TIGIT⁻ subset. **(D)** HLA-DR⁺ CD4⁺ T cells were more numerous among CD226⁺ CD4⁺ T than the CD226⁻ subset. **(E)** After TIGIT was blocked, there were no differences in TNF- α and IFN- γ in cells compared to cells with treated TIGIT and the IL-10 level was higher in TIGIT⁺ CD4⁺ T cells. **(F)** After CD226 was blocked, the levels of TNF- α , IFN- γ , and IL-10 were higher in TIGIT⁺ CD4⁺ T cells. * $P < 0.05$, ** $P < 0.01$, *** $P < 0.001$.

CD4⁺ T cells and the clinical data were analyzed, results revealed that the percentage of cells expressing CD226 was correlated with NLR ($r = 0.536$, $P = 0.008$). To evaluate the activation status and cytokine production of CD4⁺ T cells in endometriosis, their characteristics were analyzed using flow cytometry. After activation for 4 hours, the cytokines TNF- α , IFN- γ , and IL10 were significantly elevated in TIGIT⁺ CD4⁺ T cells compared to the TIGIT⁻ subset. HLA-DR⁺ CD4⁺ T cells were more numerous among TIGIT⁺ CD4⁺ T cells than among the TIGIT⁻ subset ($P < 0.001$). Similarly, the cytokines TNF- α , IL10, and IFN- γ were significantly elevated in CD226⁺ CD4⁺ T cells compared to levels in the CD226⁻ subset. The proportion of HLA-DR⁺ CD4⁺ T cells among CD226⁺ T cells was also significantly higher than that among the CD226⁻ subset ($P < 0.001$, Figures 1C, 1D).

The CD226 antibody can inhibit CD226 function in some diseases (8,9), so the current study sought to determine whether CD226 or TIGIT antibodies influenced their functioning in endometriosis. After CD226 or TIGIT was, cytokines were compared to those in cells with unblocked CD226 or TIGIT. There were no differences in TNF- α and IFN- γ after TIGIT was blocked, but the level of IL-10 was higher in TIGIT⁺ CD4⁺ T cells. After CD226 was blocked, TNF- α and IFN- γ were lower while IL-10 was higher (Figures 1E, 1F).

About 10% of women of childbearing age develop endometriosis; the condition especially affects infertile women, and women with chronic pelvic pain often exhibit endometriosis (10). The onset of endometriosis is related to sex hormones, immunity, inflammation, heredity, and other factors; and further research is required to elucidate its underlying pathogenesis. One of the most accepted views on the etiology of endometriosis is that abnormal immunity generates ectopic endometrial cells that invade unspecified locations and that are unable to be cleared. Immune-checkpoint molecules appear to regulate immunity in many diseases (11,12). For example, PD-1 regulates the actions of lymphocytes in endometriosis (13). There are no reports in the literature that mention TIGIT and CD226 in endometriosis, and the current study is thus the first to reveal abnormal expression of CD226 on peripheral CD4⁺ T cells. CD226 decreased in the current patients with endometriosis. This decrease may preclude CD4⁺ T cells from secreting enough cytokines to allow clearance of ectopic endometrial cells. Although TIGIT might produce an over-activated immune response (14), the current study found no difference in TIGIT between patients with endometriosis and the control group. The mildly negatively regulated molecule TIGIT is presumably replaced with PD-1 or another strongly negative immune-checkpoint molecule.

Results revealed that activated T cells expressed more TIGIT and CD226, a finding similar to that in several other studies (9,15). This may indicate that TIGIT and CD226 remain at a consistent level during health.

When endometrial cells invade ectopic sites such as the peritoneum or pelvic cavity, however, immune cells are then mobilized, and the immune-checkpoint molecules are activated.

Since the CD226 antibody inhibits CD226 function in some diseases, the current study sought to reveal whether CD226 or TIGIT influenced the functioning of CD226 and TIGIT in endometriosis. Thus, cytokine levels were examined when TIGIT or CD226 was blocked. There were no differences in TNF- α or IFN- γ levels in cells with blocked TIGIT, but after TIGIT was blocked the level of IL-10 was elevated in TIGIT⁺ CD4⁺ T cells. Thus, TIGIT did not inhibit CD4⁺ T cell function by reducing production of the cytokines TNF- α and IFN- γ . When CD226 was blocked before activating CD4⁺ T cells, TNF- α and IFN- γ decreased while IL-10 increased. CD226 presumably plays a positive role in the effector function of CD4⁺ T cells (8) since levels of the proinflammatory cytokines IFN- γ and TNF- α were consistent with levels of CD226, while levels of the anti-inflammatory cytokine IL-10 were negatively correlated. CD226 decreased significantly in patients with endometriosis, and this decrease may have reduced the secretion of enough TNF- α and IFN- γ effectors by CD4⁺ T cells to clear endometrial cells in the ectopic environment.

In summary, the current results indicated that there was a diminution of CD226 in CD4⁺ T cells in patients with endometriosis. CD226 was correlated with the effector role of CD4⁺ T cells in patients with endometriosis, and blocking CD226 suppressed this function. These results suggest that CD226 in CD4⁺ T cells has a potential role in diagnosing endometriosis.

Acknowledgments

This study was approved by the Ethics Committee of the Obstetrics and Gynecology Hospital of Fudan University.

Funding: This work was supported by grants from a project under the Scientific and Technological Innovation Action Plan of the Shanghai Natural Science Fund (grant no. 20ZR1409100 to L Wang), a project of the Chinese Association of Integration of Traditional and Western Medicine special foundation for Obstetrics and Gynecology-PuZheng Pharmaceutical Foundation (grant no. FCK-PZ-08 to L Wang), a project for hospital management of the Shanghai Hospital Association (grant no. X2021046 to L Wang), a clinical trial project of the Special Foundation for Healthcare Research of the Shanghai Municipal Health Commission (grant no. 202150042 to L Wang), and a project of the National Natural Science Foundation of China (grant no. 81971362 to Jun Shao).

Conflict of Interest: The authors no conflicts of interest to disclose.

References

1. Burney RO, Giudice LC. Pathogenesis and pathophysiology of endometriosis. *Fertil Steril.* 2012; 98:511-519.
2. Delbandi AA, Mahmoudi M, Shervin A, Moradi Z, Arablou T, Zarnani AH. Higher frequency of circulating, but not tissue regulatory T cells in patients with endometriosis. *J Reprod Immunol.* 2020; 139:103119.
3. Abbas AR, Baldwin D, Ma Y, Ouyang W, Gurney A, Martin F, Fong S, van Lookeren CM, Godowski P, Williams PM, Chan AC, Clark HF. Immune response in silico (IRIS): Immune-specific genes identified from a compendium of microarray expression data. *Genes Immun.* 2005; 6:319-331.
4. Yu X, Harden K, Gonzalez LC, Francesco M, Chiang E, Irving B, Tom I, Ivelja S, Refino CJ, Clark H, Eaton D, Grogan JL. The surface protein TIGIT suppresses T cell activation by promoting the generation of mature immunoregulatory dendritic cells. *Nat Immunol.* 2009; 10:48-57.
5. Joller N, Hafler JP, Brynedal B, Kassam N, Spoerl S, Levin SD, Sharpe AH, Kuchroo VK. Cutting edge: TIGIT has T cell-intrinsic inhibitory functions. *J Immunol.* 2011; 186:1338-1342.
6. Anderson AC, Joller N, Kuchroo VK. Lag-3, Tim-3, and TIGIT: Co-inhibitory receptors with specialized functions in immune regulation. *Immunity.* 2016; 44:989-1004.
7. Lozano E, Dominguez-Villar M, Kuchroo V, Hafler DA. The TIGIT/CD226 axis regulates human T cell function. *J Immunol.* 2012; 188:3869-3875.
8. Li W, Deng C, Yang H, Lu X, Li S, Liu X, Chen F, Chen L, Shu X, Zhang L, Liu Q, Wang G, Peng Q. Expansion of circulating peripheral TIGIT⁺CD226⁺ CD4 T cells with enhanced effector functions in dermatomyositis. *Arthritis Res Ther.* 2021; 23:15.
9. Deng C, Li W, Fei Y, Wang L, Chen Y, Zeng X, Zhang F, Li Y. Imbalance of the CD226/TIGIT immune checkpoint is involved in the pathogenesis of primary biliary cholangitis. *Front Immunol.* 2020; 11:1619.
10. Endometriosis Collaboration Group, Chinese Society of Obstetrics and Gynecology, Chinese Medical Association. Guidelines on the diagnosis and treatment of endometriosis (Third edition). *Zhonghua Fu Chan Ke Za Zhi.* 2021; 56:812-824. (in Chinese)
11. Tang H, Cao Y, Jian Y, Li X, Li J, Zhang W, Wan T, Liu Z, Tang W, Lu S. Conversion therapy with an immune checkpoint inhibitor and an antiangiogenic drug for advanced hepatocellular carcinoma: A review. *Biosci Trends.* 2022; 16:130-141.
12. Li C, Ying C, Duan Z. The imbalance of T-cell immunoglobulin and ITIM domain and CD226 on regulatory T cell in recurrent spontaneous abortion patients. *Reprod Dvlpmt Med.* 2022; 6:175-180.
13. Walankiewicz M, Grywalska E, Polak G, Korona-Glowniak I, Witt E, Surdacka A, Kotarski J, Rolinski J. The increase of circulating PD-1- and PD-L1-expressing lymphocytes in endometriosis: Correlation with clinical and laboratory parameters. *Mediators Inflamm.* 2018; 2018:7041342.
14. Ge Z, Peppelenbosch MP, Sprengers D, Kwekkeboom J. TIGIT, the next step towards successful combination immune checkpoint therapy in cancer. *Front Immunol.* 2021; 12:699895.
15. Deng C, Chen Y, Li W, Peng L, Luo X, Peng Y, Zhao L, Wu Q, Zhang W, Zhang X, Fei Y. Alteration of CD226/TIGIT immune checkpoint on T cells in the pathogenesis of primary Sjogren's syndrome. *J Autoimmun.* 2020; 113:102485.

Received December 1, 2022; Revised April 5, 2023; Accepted April 17, 2023.

[§]These authors contributed equally to this work.

*Address correspondence to:

Ling Wang and Zhongliang Duan, Obstetrics and Gynecology Hospital of Fudan University, 419 Fangxie Road, Shanghai 200011, China.

E-mail: dr.wangling@fudan.edu.cn (LW); zduan12@fudan.edu.cn (ZD)

Released online in J-STAGE as advance publication April 21, 2023.

Characteristics, scope of activity, and negative emotions in elderly women with urinary incontinence: Based on a longitudinal follow-up in Shanghai, China

Yunwei Zhang^{1,§}, Changying Wang^{1,§}, Xiaoyan Yu^{2,§}, Lingshan Wan¹, Wendi Cheng¹, Chunyan Xie¹, Duo Chen¹, Yifan Cao¹, Jia Xue¹, Yuhong Niu^{1,*}, Hansheng Ding^{1,*}

¹ Shanghai Health Development Research Center (Shanghai Medical Information Center), Shanghai, China;

² Jiangning Road Community Health Service Center of Jing'an District, Shanghai, China.

SUMMARY We conducted a study to assess the characteristics, scope of activity, and negative emotions in elderly women with urinary incontinence (UI) based on a longitudinal follow-up conducted in Shanghai, China from 2013 to 2019. A total of 3,531 elderly women were included in the final analysis, and 697 women who experienced UI during follow-up were included in the UI group. Subjects with UI were subdivided into those with partial UI (UI once a day or less) and UI (frequent UI). Two thousand eight hundred and thirty-four women who did not have UI during the same period served as the control group. The prevalence of UI was 19.74% in this study. Logistic regression analysis revealed that being older (> 80 years of age), having a high level of education (> 12 years; elderly people with a high level of education may pay more attention to their health and notice UI more readily), a low personal monthly income (\leq 3,000 RMB), more gravidity/parity, and having a chronic disease (chronic obstructive pulmonary disease (COPD), dementia, or Parkinson's disease) were risk factors for UI ($p < 0.05$). About 60% of women in the partial UI group engaged in daily activities outdoors, while this number decreased sharply to 3.6% in the UI group. Women in the UI group were more likely to have negative emotions, such as depression, anxiety, irritability, or feeling worthless ($p < 0.001$). Among elderly women with dementia, those with UI had defects in terms of judgment in everyday life, the ability of convey information, and the ability to understand information ($p < 0.05$). More attention needs to be paid to the adverse effects of UI on activities of daily living (ADL) and mental health in the future.

Keywords dementia, emotion, caregiving

Urinary incontinence (UI) is a common disease in the elderly, and a study had revealed that its prevalence in Chinese elderly women is 16.9% (1). Women with UI were more likely to have symptoms of anxiety and depression, as well as poor quality of life (QoL). There is a consensus that UI greatly affects QoL, and even mild urinary leakage significantly reduces QoL. UI also involves certain expenses. A study reported that women with UI used an average of 1.8 ± 2.1 incontinence products in 24 hours with a mean weekly cost of $\$5.42 \pm \8.59 (2). Some chronic conditions like COPD, dementia, and Parkinson's disease (PD) warrant attention in women with UI.

In summary, UI is one of the most common geriatric syndromes, influencing overall health, QoL, and financial circumstances in elderly people. The current large-scale population-based study sought to explore possible

factors related to UI, with a focus on women with UI and dementia. The study protocol was approved by the Ethics Committee of the Shanghai Health Development Research Center (No. 2022009), and all subjects signed a written informed consent form prior to commencing the study.

Study design

This study was designed based on a longitudinal follow-up conducted in Shanghai (China) from 2013 to 2021 (Supplemental Data, <http://www.biosciencetrends.com/action/getSupplementalData.php?ID=141>). The inclusion criteria were: *i*) women who age 60 and older; *ii*) individuals who were continuously followed; *iii*) women who did not have UI at the beginning of the study; and *iv*) women who responded "Yes" to the

question "Do you have UI?" during the study. Data from 2013 to 2015 were used because subjects with UI were relatively concentrated and follow-up was continuous during this period. A total of 3,531 elderly women were included in the final analysis, and 697 women who experienced UI during follow-up were included in the UI group. These women were subdivided into those with partial UI (UI once a day or less) and UI (frequent UI). Two thousand eight hundred and thirty-four women who did not have UI during the same period served as the control group. Demographic and disease characteristics, scope of activity, and emotion were obtained using the Unified Needs Assessment Form for Elderly Care, and cognitive function was assessed by community doctors.

Comparison of the characteristics of women with and without UI

Of 3,531 elderly women who participated in this study, 697 had UI (642 with partial UI and 55 with UI), so the prevalence of UI was 19.74% (Table 1). Women

with UI had a higher level of education, a higher rate of widowhood, lower personal income, and less gravidity/parity ($p < 0.05$). Women with UI were less likely to live in the community ($p < 0.001$) and live alone ($p = 0.002$) since they may need more assistance from caregivers. Women with UI had a higher prevalence of diabetes, COPD, dementia, PD, and worse performance in activities of daily living (ADL) ($p < 0.05$).

The prevalence of UI in this study was similar to that in another large sample cross-sectional study (3). A previous study focusing on Chinese women found that its prevalence was similar to that in Western countries (14.84%) (4). Studies have revealed that UI can be considered a possible consequence of metabolic syndrome. Obesity, diabetes, and, to a lesser extent, high blood pressure and cigarette smoking have been associated with UI in different settings. Thus, prevention programs aimed at losing weight, quitting smoking, a healthy diet, and increasing physical activity have resulted in a decreased incidence, prevalence, and severity of UI (5).

Table 1. Characteristics of subjects without UI, with partial UI, and with UI

Characteristic	Women without UI (n = 2,834)	Women in the partial UI group (n = 642)	Women in the UI group (n = 55)	p*
Demographic characteristics				
Age (years)				< 0.001
60-69	1,170 (41.28)	133 (20.71)	4 (7.27)	
70-79	780 (27.52)	148 (23.05)	6 (10.91)	
≥ 80	884 (31.20)	361 (56.24)	45 (81.82)	
BMI (kg/m ²)				< 0.001
< 18.5	145 (5.12)	38 (5.92)	9 (16.36)	
18.5-23.9	1,568 (55.33)	373 (58.10)	22 (40.0)	
24.0-27.9	968 (34.15)	190 (29.60)	22 (40.0)	
≥ 28	153 (5.40)	41 (6.38)	2 (3.64)	
Education				< 0.001
≤ 6years	1,112 (39.24)	258 (40.19)	40 (72.73)	
7-12 years	1,639 (57.83)	331 (51.56)	14 (25.45)	
> 12 years	83 (2.93)	53 (8.25)	1 (1.82)	
Widowhood				< 0.001
Yes	791 (27.91)	239 (37.23)	32 (58.18)	
No	2,043 (72.09)	403 (62.77)	23 (41.82)	
Living in the community	2,783 (98.20)	623 (97.04)	40 (72.73)	< 0.001
Residing				0.002
Alone	618 (21.81)	139 (21.65)	9 (16.36)	
With spouse or children	2,146 (75.72)	481 (74.92)	39 (70.91)	
With other people	70 (2.47)	22 (3.43)	7 (12.73)	
Personal monthly income (RMB)				< 0.001
≤ 3,000	1,086 (38.32)	340 (52.96)	26 (47.27)	
3,001-3,900	1,168 (41.21)	219 (34.11)	12 (21.82)	
> 3,900	580 (20.47)	83 (12.93)	17 (30.91)	
Gravidity/Parity				< 0.001
≤ 2	2,296 (81.02)	465 (72.43)	28 (50.91)	
> 2	538 (18.98)	177 (27.57)	27 (49.09)	
Disease characteristics				
Hypertension	2,040 (71.98)	484 (75.39)	41 (74.55)	0.33
Diabetes	615 (21.70)	151 (23.52)	20 (36.36)	0.03
COPD	45 (1.59)	19 (2.96)	3 (5.45)	0.01
Dementia	20 (0.71)	15 (2.34)	9 (16.36)	< 0.001
PD	18 (0.64)	10 (1.56)	3 (5.45)	< 0.001
ADL				
Normal	2,309 (81.47)	1 (0.16)	1 (1.82)	< 0.001
Mild disability	424 (14.96)	428 (66.67)	1 (1.82)	
Moderate disability	92 (3.25)	124 (19.31)	1 (1.82)	
Severe disability	9 (0.32)	89 (13.86)	52 (94.54)	

*p value of differences in subjects without UI, with partial UI, and with UI. BMI, body mass index; UI, urinary incontinence; COPD, chronic obstructive pulmonary disease; ADL, activities of daily living; PD, Parkinson's disease.

Table 2. Risk factors for elderly women with UI

Characteristic	n (%)	OR	95% CI	p
Diabetes (yes)	171 (24.53)	1.20	0.93-1.54	0.17
COPD (yes)	22 (3.16)	2.20	1.22-3.98	< 0.001
Dementia (yes)	24 (3.44)	4.77	2.15-10.56	< 0.001
Parkinson's disease (yes)	13 (1.87)	3.21	1.42-7.28	0.01
Age				
60-69	137 (19.66)	1.00	-	-
70-79	154 (22.09)	2.23	1.69-2.93	0.44
≥ 80	406 (58.25)	5.90	4.39-7.93	< 0.001
BMI				
< 18.5	47 (6.74)	0.92	0.63-1.35	0.64
18.5-23.9	395 (56.67)	1.00	-	-
24.0-27.9	212 (30.42)	0.93	0.76-1.13	0.49
≥ 28	43 (6.17)	1.11	0.76-1.64	0.43
Education				
≤ 6 years	298 (42.75)	1.00	-	-
7-12 years	345 (49.50)	2.56	2.00-3.29	0.26
> 12 years	54 (7.75)	8.81	5.57-13.94	< 0.001
Widowhood (Yes)	271 (38.89)	1.10	0.89-1.37	0.39
Living in the community (no)	34 (4.88)	1.58	0.93-2.67	0.09
Personal monthly income (RMB)				
≤ 3,000	366 (52.51)	2.36	1.77-3.15	< 0.001
3,001-3,900	231 (33.14)	1.39	1.04-1.87	0.37
> 3,900	100 (14.35)	1.00	-	-
Gravidity/Parity (> 2)	204 (29.27)	1.37	1.07-1.75	0.01

Level of education, personal income, gravidity/parity, and diseases were risk factors for UI

Results indicated that the risk factors for UI included advanced age (> 80 years) (OR = 5.90, 95% CI: 4.39-7.93), a high level of education (> 12 years) (OR = 8.81, 95% CI: 5.57-13.94), low personal monthly income (≤ 3,000 RMB) (OR = 2.36, 95% CI: 1.77-3.15), and more gravidity/parity (> 2) (OR = 1.37, 95% CI: 1.07-1.75) ($p < 0.05$, respectively). Moreover, a number of diseases, including COPD (OR = 2.20, 95% CI: 1.22-3.98), dementia (OR = 4.77, 95% CI: 2.15-10.56), and PD (OR = 3.21, 95% CI: 1.42-7.28), were also associated with a higher risk of UI ($p < 0.05$, respectively) (Table 2).

A study conducted in German and Danish populations found that age, BMI, and COPD were associated with UI (6). Multiple chronic conditions, diminished cognitive functioning, and less mobility were found to be associated with the incidence of UI (7,8). Moreover, a study conducted in Turkey indicated that risk factors may differ according to specific UI subtypes. The key risk factors for urge UI (UII) are hypertension and diabetes mellitus, and those are hypertension, multiparity, BMI, and low-level of education for stress UI (SUI) (9).

Studies have found that multiparity increased the risk of UI (10), which was consistent with the results of the current study. However, previous studies found that a low-level of education increased the risk of UI (11), which was inconsistent with the current findings. A possible explanation may be that elderly people with a high level education pay more attention to their health and notice UI more readily. A study revealed that elderly people with a higher level of education have more information about UI and feel less stigma than others, so they seek help in a timely manner (12).

Women with UI had a more limited scope of activity and negative emotions

Results revealed that women with partial UI or UI had a more limited scope of activity and that the scope decreased with the severity of UI. About 60% of women in the partial UI group engaged in daily activities outdoors, while this figured decreased sharply to 3.6% in the UI group. Moreover, over 80% of women in the UI group engaged in almost no outdoor activities and they could only sit in a wheelchair or lie in bed. Women in the UI group were more likely to have negative emotions, such as depression, anxiety, irritability, or feeling worthless ($p < 0.001$) (Table 3).

A study has indicated that UI has an impact on emotions. UI may be associated with depression among middle-aged and elderly women (13). Another study revealed that UI negatively influences ADL, physical and social activities, and emotional disposition (14). A previous study reported that the risk of stress and depression in older women with UI was approximately 2 and 1.5 times higher than that in regular women (15), which agreed with the current results. The reason may be that leakage of urine and odor leads to embarrassment, causing decreased self-esteem and depression as well as affecting emotions (16). Therefore, a holistic strategy is needed for elderly women with UI to alleviate negative emotions and manage depression.

Women with UI and dementia had less ability to convey and understand information

A total of 55 elderly women had no dementia at the beginning of study but had dementia at the end of study. These women consisted of 20 without UI, 15 with partial

Table 3. Scope of activity and negative emotion characteristics of women with UI

Characteristic	Women without UI (n = 2,834)	Women in the partial UI group (n = 642)	Women in the UI group (n = 55)	p
Scope of activity				< 0.001
Outdoor activities	2,276 (80.31)	396 (61.68)	2 (3.64)	
Indoor activities	448 (15.81)	144 (22.43)	7 (12.73)	
Almost no activities	110 (3.88)	102 (15.89)	46 (83.63)	
Depression				< 0.001
Never	2,136 (75.37)	390 (60.75)	14 (25.45)	
Sometimes	692 (24.42)	234 (36.45)	27 (49.10)	
Always	6 (0.21)	18 (2.80)	14 (25.45)	
Tendency to cry				< 0.001
Never	2,415 (85.22)	469 (73.05)	18 (32.73)	
Sometimes	417 (14.71)	165 (25.70)	28 (50.91)	
Always	2 (0.07)	8 (1.25)	9 (16.36)	
More easily angered				< 0.001
Never	2,032 (71.70)	404 (62.93)	15 (27.27)	
Sometimes	789 (27.84)	225 (35.05)	32 (58.18)	
Always	13 (0.46)	13 (2.02)	8 (14.55)	
More anxious				< 0.001
Never	2,230 (78.69)	380 (59.19)	18 (32.73)	
Sometimes	598 (21.10)	247 (38.47)	22 (40.00)	
Always	6 (0.21)	15 (2.34)	15 (27.27)	
Worried for no reason				< 0.001
Never	2,094 (73.89)	341 (53.12)	14 (25.45)	
Sometimes	727 (25.65)	283 (44.08)	30 (54.55)	
Always	13 (0.46)	18 (2.80)	11 (20.00)	
Feeling worthless				< 0.001
Never	778 (27.45)	106 (16.51)	3 (5.45)	
Sometimes	1,591 (56.14)	376 (58.57)	22 (40.00)	
Always	465 (16.41)	160 (24.92)	30 (54.55)	

Table 4. Cognitive characteristics of dementia women with UI

Characteristic	Women without UI (n = 20)	Women in the partial UI group (n = 15)	Women in the UI group (n = 9)	p
Judgment in everyday life				0.02
Yes	13 (65.00)	5 (33.33)	1 (11.11)	
No	7 (35.00)	10 (66.67)	8 (88.89)	
Ability to convey information				0.003
Yes	13 (65.00)	5 (33.33)	0	
No	7 (35.00)	10 (66.67)	9 (100.00)	
Ability to understand information				0.004
Yes	15 (75.00)	10 (66.67)	1 (11.11)	
No	5 (25.00)	5 (33.33)	8 (88.89)	

UI, and 9 with UI. Results revealed that judgment in everyday life, the ability to convey information, and the ability to understand information differed significantly depending on the severity of UI ($p < 0.05$) (Table 4). Women with partial UI and UI exercised less judgment in everyday life and had less ability to convey or understand information. Women in the UI group in particular had no ability to convey information.

To date, few studies have focused on individuals with dementia and UI, leading to heated debate on this topic. A study on patients with Alzheimer's disease (AD) patients indicated that they had a higher risk of suffering UI (17). Moreover, UI can be distressing for persons with dementia, so awareness of bladder and bowel services should be increased (18). However, a several scholars found that there was no significant correlation between age, cognitive function, depression, anxiety, and dementia and UI (19). A previous study found that dementia is associated with cognitive and functional deficits that may affect the urinary system, so they may

be risk factors for UI (20). Hence, one can conclude that individuals with dementia are at higher risk of developing UI, and a thorough assessment of a person with dementia experiencing incontinence needs to be conducted. Therefore, rapid diagnostic methods need to be explored to decrease the incidence of UI.

In conclusion, screening and early intervention in the population at risk of developing UI is highly necessary since these measures may reduce the impact of UI on the QoL of the elderly. Moreover, more attention needs to be paid to the adverse effects of UI on ADL and mental health due to a limited range of activity and negative emotions in the future.

Funding: This work was supported by a grant from the National Natural Science Foundation of China (General Program, Study on the Development of Automatic Generation Model of Personalized Long-term Care Plan Based on Care Needs Grade and Performance Evaluation and Popularization, no. 72074152).

Conflict of Interest: The authors have no conflicts of interest to disclose.

References

- Xue K, Palmer MH, Zhou F. Prevalence and associated factors of urinary incontinence in women living in China: A literature review. *BMC Urol.* 2020; 20:159.
- Chisholm LP, Sebesta EM, Gleicher S, Kaufman M, Dmochowski RR, Reynolds WS. The burdens of incontinence: Quantifying incontinence product usage and costs in women. *Neurourol Urodyn.* 2022; 41:1601-1611.
- Sumarsono B, Jong JJ, Wang JY, Liao L, Lee KS, Yoo TK, Liu SP, Chuang YC. The prevalence of urinary incontinence in men and women aged 40 years or over in China, Taiwan and South Korea: A cross-sectional, prevalence-based study. *Low Urin Tract Symptoms.* 2020; 12:223-234.
- Xu C, Chen M, Fu J, Meng Y, Qin S, Luo Y. Urinary incontinence status and risk factors in women aged 50-70 years: A cross-sectional study in Hunan, China. *Int Urogynecol J.* 2021; 32:95-102.
- John G. Urinary incontinence and cardiovascular disease: A narrative review. *Int Urogynecol J.* 2020; 31:857-863.
- Schreiber Pedersen L, Lose G, Høybye MT, Elsner S, Waldmann A, Rudnicki M. Prevalence of urinary incontinence among women and analysis of potential risk factors in Germany and Denmark. *Acta Obstet Gynecol Scand.* 2017; 96:939-948.
- Markland AD, Vaughan CP, Okosun IS, Goode PS, Burgio KL, Johnson TM 2nd. Cluster analysis of multiple chronic conditions associated with urinary incontinence among women in the USA. *BJU Int.* 2018; 122:1041-1048.
- Suhr R, Lahmann NA. Urinary incontinence in home care: A representative multicenter study on prevalence, severity, impact on quality of life, and risk factors. *Aging Clin Exp Res.* 2018; 30:589-594.
- Demir O, Sen V, Irer B, Bozkurt O, Esen A. Prevalence and possible risk factors for urinary incontinence: A cohort study in the city of Izmir. *Urol Int.* 2017; 99:84-90.
- Wuytack F, Moran P, Daly D, Begley C. Is there an association between parity and urinary incontinence in women during pregnancy and the first year postpartum?: A systematic review and meta-analysis. *Neurourol Urodyn.* 2022; 41:54-90.
- Saadia Z. Effect of age, educational status, parity and BMI on development of urinary incontinence-a cross sectional study in Saudi population. *Mater Sociomed.* 2015; 27:251-254.
- Concepcion K, Cheng Y, McGeechan K, Robertson S, Stewart M, Bateson D, Estoesta J, Chiarelli P. Prevalence and associated factors of urinary leakage among women participating in the 45 and up Study. *Neurourol Urodyn.* 2018; 37:2782-2791.
- Park GR, Park S, Kim J. Urinary incontinence and depressive symptoms: The mediating role of physical activity and social engagement. *J Gerontol B Psychol Soc Sci.* 2022; 77:1250-1258.
- Gascón MRP, Mellão MA, Mello SH, Negrão RM, Casseb J, Oliveira ACP. The impact of urinary incontinence on the quality of life and on the sexuality of patients with HAM/TSP. *Braz J Infect Dis.* 2018; 22:288-293.
- Kwak Y, Kwon H, Kim Y. Health-related quality of life and mental health in older women with urinary incontinence. *Aging Ment Health.* 2016; 20:719-726.
- Witkoś J, Wróbel P, Błońska-Fajfrowska B. Stress urinary incontinence in women as a medical, social, psychological and economic problem- Assessing the extent of knowledge of students graduating in medical fields. *Rehabilitacja Medyczna.* 2017; 21:1-10.
- Lee HY, Li CC, Juan YS, Chang YH, Yeh HC, Tsai CC, Chueh KS, Wu WJ, Yang YH. Urinary incontinence in Alzheimer's disease. *Am J Alzheimers Dis Other Demen.* 2017; 32:51-55.
- Juliebo-Jones P, Coulthard E, Mallam E, Archer H, Drake MJ. Understanding the impact of urinary incontinence in persons with dementia: Development of an interdisciplinary service model. *Adv Urol.* 2021; 2021:9988056.
- Li HC, Chen KM, Hsu HF. Modelling factors of urinary incontinence in institutional older adults with dementia. *J Clin Nurs.* 2019; 28:4504-4512.
- Yap P, Tan D. Urinary incontinence in dementia - A practical approach. *Aust Fam Physician.* 2006; 35:237-241.

Received December 2, 2022; Revised March 10, 2023; Accepted March 24, 2023.

§These authors contributed equally to this work.

*Address correspondence to:

Yuhong Niu and Hansheng Ding, Shanghai Health Development Research Center (Shanghai Medical Information Center), No. 602 Jianguo (W) Road, Xuhui District, Shanghai, China 200031.

E-mail: niuyuhong@126.com (YN), dinghansheng@hotmail.com (HD)

Released online in J-STAGE as advance publication March 31, 2023.

A cross-sectional study on the need for and utilization of assistive walking devices by people age 55 and older in Shanghai

Wendi Cheng^{1,§}, Yifan Cao^{1,§}, Hua Wang^{2,§}, Xin Peng^{3,§}, Chunyan Xie¹, Changying Wang¹, Duo Chen¹, Lingshan Wan¹, Jia Xue¹, Yunwei Zhang¹, Hongyun Xin¹, Wei Zhuang⁴, Hansheng Ding^{1,*}

¹Shanghai Health Development Research Center (Shanghai Medical Information Center), Shanghai, China;

²Siping Community Health Service Center of Yangpu District, Shanghai, China;

³Jiangning Road Community Health Service Center of Jing'an District, Shanghai, China;

⁴Shanghai University of Engineering Science, Shanghai, China.

SUMMARY We conducted a study to analyze the unmet needs of and risk factors for use of assistive walking devices by the elderly based on sample survey data from Shanghai, China from July to October 2019. Among a total sample size of 11,193 people age 55 and older, 1,947 people (17.39%) needed assistive walking devices, 829 (42.58%) of whom needed but did not use those devices. Multivariate analysis indicated that residence, living alone or cohabitating, indoor handrails, the number of diseases, and IADL were factors influencing the unmet need for assistive walking devices ($p < 0.05$, respectively). People who lived in community health centers ($p = 0.0104$, OR = 1.956, 95% CI: 1.171-3.267) and those who lived only with their spouse ($p = 0.0002$, OR = 2.901, 95% CI: 1.641-5.126) were more likely to have an unmet need for assistive walking devices. People without indoor handrails ($p = 0.0481$, OR = 0.718, 95% CI: 0.517-0.997), those with 3 or more diseases ($p = 0.0008$, OR = 0.577, 95% CI: 0.418-0.796), and those with severely impaired IADL ($p = 0.0002$, OR = 0.139, 95% CI: 0.05-0.386) were less likely to have an unmet need for assistive walking devices. Self-perceived needs of the elderly, the diversity and performance of assistive devices, and the accessibility and affordability of assistive walking devices may lead to unmet needs.

Keywords elderly, assistive walking devices, need, utilization, Shanghai

In recent years, China's aging population has continuously increased. The 2020 national population census indicated that the population age 65 and older accounted for 13.52% of the total population, or about 190 million people (1). Shanghai is one city with the earliest signs of aging in China (2). In 2020, the population age 65 and older in Shanghai accounted for 16.28% of the total population, or about 4.05 million people (1). The increase in the elderly population in China is accompanied by an increase in the proportion of disabled and semi-disabled people (3). The number of disabled or semi-disabled people in China was 48.09 million in 2020 and will be 120 million in 2050 (4). As the proportion of the elderly and disabled increase, the ability of the elderly to go out or walk safely may diminish (5), and their need for assistive walking devices is likely to grow (6-7).

Studies have indicated that the use of assistive walking devices differs among the elderly (8-14).

However, there are limited empirical studies on the need for and utilization of assistive walking devices by the elderly in China. Therefore, a study was conducted to analyze the unmet need for and risk factors for use of assistive walking devices by the elderly in Shanghai.

Study design

Subjects Data were collected in Shanghai, China on the elderly age 55 and older living in the community and nursing homes in 16 districts of Shanghai from July to October in 2019. Fifteen thousand copies of a questionnaires were sent out, and 14,944 copies were returned, for a return rate of 99.6%. Three thousand seven hundred and fifty-one subjects who were bedridden for a prolonged period, who had severe cognitive impairment, who were blind, or who lacked light perception were excluded, for a total of 11,193 subjects.

Methodology A matching analysis was performed

for the need for and utilization of assistive walking devices by the elderly. First, screening criteria were used to determine whether the elderly need to use assistive walking devices. Based on the collective standards of the Chinese Geriatrics Society and the Unified Elderly Care Needs Assessment, the Barthel Index scale, a simple psychiatric examination scale (MMSE), and several verification questions in the Unified Elderly Care Needs Assessment ("Do I need help changing from one sitting position to another?" and "Do I need help walking about 5 meters on flat ground?"), elderly people with a lower limb disorder, difficulty walking, or instability who needed to use walking aids were screened out (those who were bedridden for a prolonged period, who had severe cognitive impairment, who were blind, or who lacked light perception were excluded). Second, criteria were used to determine whether the elderly use assistive walking devices. Based on the question "What aids do you commonly use?" in the Unified Elderly Care Needs Assessment, whether the elderly use assistive walking devices and the type of device were determined. These assistive walking devices are crutches, wheelchairs, artificial limbs, or rollators.

Statistical analysis Descriptive statistics were used to analyze the need for and utilization of assistive walking devices by the elderly in Shanghai, and the quantitative data were described by frequency and component ratio. Logistic regression analysis was used for univariate and multivariate analysis. In a model of elderly people who need assistive walking devices, the dependent variable was whether assistive walking devices were used (0 = need and use (control group), 1 = need but do not use). The independent variables were sex, age, level of education, main source of income, residence, language use, living alone or cohabitating, physical care needs of the assessed subjects, elevators in one's residence, indoor steps, indoor handrails, number of diseases, IADL, and the self-rated health status of the elderly. A level of $\alpha = 0.05$ or $p < 0.05$ was considered statistically significant. The statistical software SAS9.4 was used to analyze data.

Comparison of characteristics of elderly with unmet needs and met needs for assistive walking devices

The total sample for this study was 11,193 subjects. Of those, 1,472 used assistive walking devices, accounting for 13.15%. Of the total, 1,947 subjects needed assistive walking devices, accounting for 17.39%, and of those, 829 needed but did not use assistive walking devices, accounting for 42.58%.

Compared to the elderly whose needs were met, the characteristics of the elderly with unmet need for assistive walking devices were as follows: 55-59 years of age (23 subjects, 60.53%), 60-69 years of age (159 subjects, 59.55%), a senior high school education (163 subjects, 52.24%), an unstable financial status

(16 subjects, 64.00%), living in a rented dwelling (79 subjects, 50.97%), living only with their spouses (227 subjects, 57.32%), with 0 diseases (69 subjects, 53.49%), normal ADL (184 subjects, 92.93%), self-reliant in IADL (149 subjects, 89.22%), and a very good self-rated health status (48 subjects, 67.61%) (Table 1).

Results indicated that assistive walking devices are underutilized (13.15%) by the elderly in Shanghai, and this figure is slightly higher than that in a previous study in three provinces in China (Sichuan, Chongqing, Inner Mongolia, assistive devices of an unspecified type, 10.9%) (13). This figure is also higher than that in a previous study in elderly with hearing loss (7.62%) (12). However, this figure is lower than that in a previous study that estimated that 16.6% of older adults use an assistive device outdoors in the US (6). Moreover, this figure is much lower than that in a previous study on use of assistive walking devices by disabled elderly (96%) (14).

Results also indicated that 42.58% of the elderly in Shanghai have an unmet need for assistive walking devices, which is slightly lower than the figure in a previous study in northern and southwestern China (the self-perceived need for assistive devices among the elderly was 46.1%) (13).

Residence, living alone or cohabitating, indoor handrails, number of diseases, and IADL were factors influencing the unmet need for assistive walking devices

Univariate analysis revealed significant differences in the use of assistive walking devices among the elderly who need them ($n = 1,947$) in terms of independent variables, such as age, level of education, financial status, residence, living alone or cohabitating, the physical need for care of the assessed subjects, an elevator in one's residence, the number of diseases, IADL, and self-rated health status. Multivariate analysis revealed that residence, living alone or cohabitating, indoor handrails, the number of diseases, and IADL were the factors influencing the unmet need for assistive walking devices ($p < 0.05$, respectively). People who lived in community health centers ($p = 0.0104$, OR = 1.956, 95% CI: 1.171-3.267) and those who lived only with their spouse ($p = 0.0002$, OR = 2.901, 95% CI: 1.641-5.126) were more likely to have an unmet need for assistive walking devices. Those without indoor handrails ($p = 0.0481$, OR = 0.718, 95% CI: 0.517-0.997), those with 3 or more diseases ($p = 0.0008$, OR = 0.577, 95% CI: 0.418-0.796), and those with severely impaired IADL ($p = 0.0002$, OR = 0.139, 95% CI: 0.050-0.386) were less likely to have an unmet need for assistive walking devices (Table 2).

Results indicated that the unmet need for assistive walking devices is higher among people who live in community health centers than those live in private

Table 1. Different variables for use of walking aids by the elderly who need them in Shanghai in 2019 [n (%)]

Variables	Needs a walking aid but has not used one (n = 829)	Needs a walking aid and has used one (n = 1,118)	p value
Sex, n (%)			0.4769
Male	347 (41.66%)	486 (58.34%)	
Female	482 (43.27%)	632 (56.73%)	
Age, n (%)			< 0.0001
55–60	23 (60.53%)	15 (39.47%)	
60–69	159 (59.55%)	108 (40.45%)	
70–79	179 (47.86%)	195 (52.14%)	
≥ 80	468 (36.91%)	800 (63.09%)	
Level of education, n (%)			0.0001
Primary School and below	316 (37.98%)	516 (62.02%)	
Junior high school	246 (42.49%)	333 (57.51%)	
Senior high school	163 (52.24%)	149 (47.76%)	
College and above	86 (47.51%)	95 (52.49%)	
Main source of income, n (%)			0.0038
Pension	732 (42.88%)	975 (57.12%)	
Help from relatives and friends	29 (29.90%)	68 (70.10%)	
Some other source	16 (64.00%)	9 (36.00%)	
Residence, n (%)			< 0.0001
Owner-occupied dwelling, private dwelling, etc.	313 (49.37%)	321 (50.63%)	
Rented dwelling	79 (50.97%)	76 (49.03%)	
Old age home or a similar facility	149 (31.43%)	325 (68.57%)	
Nursing home or a similar facility	142 (37.67%)	235 (62.33%)	
Community health service centers	88 (48.89%)	92 (51.11%)	
Hospital or a similar facility	48 (46.60%)	55 (53.40%)	
Language use, n (%)			0.4948
Mandarin	189 (44.68%)	234 (55.32%)	
Dialect	621 (41.73%)	867 (58.27%)	
Mute	5 (50.00%)	5 (50.00%)	
Living alone or cohabitating, n (%)			< 0.0001
Living alone	76 (38.97%)	119 (61.03%)	
Living with spouse	227 (57.32%)	169 (42.68%)	
Living with children	186 (37.58%)	309 (62.42%)	
Other	291 (38.70%)	461 (61.30%)	
Physical care needs of the assessed subjects, n (%)			0.0617
No need	17 (48.57%)	18 (51.43%)	
Care provided by the spouse	57 (41.91%)	79 (58.09%)	
Care provided by children or grandchildren	111 (31.90%)	237 (68.10%)	
Care provided by a professional caregiver	388 (37.34%)	651 (62.66%)	
Elevators in residential floors, n (%)			< 0.0001
Below the 6th floor, without an elevator	327 (47.88%)	356 (52.12%)	
Below the 6th floor, with an elevator	377 (38.91%)	592 (61.09%)	
The 7th floor, without an elevator	6 (46.15%)	7 (53.85%)	
The 7th floor, with an elevator	9 (17.65%)	42 (82.35%)	
The 8th floor and above	101 (48.79%)	106 (51.21%)	
Indoor steps, n (%)			0.2774
Yes	86 (39.27%)	133 (60.73%)	
No	731 (43.13%)	964 (56.87%)	
Indoor handrails, n (%)			0.0576
Yes	348 (40.23%)	517 (59.77%)	
No	469 (44.54%)	584 (55.46%)	
Number of diseases, n (%)			< 0.0001
1	276 (47.26%)	308 (52.74%)	
0	69 (53.49%)	60 (46.51%)	
2	310 (43.97%)	395 (56.03%)	
3 or more	174 (32.89%)	355 (67.11%)	
ADL, n (%)			< 0.0001
Normal	184 (92.93%)	14 (7.07%)	
Very severely impaired	80 (55.94%)	63 (44.06%)	
Severely impaired	205 (38.32%)	330 (61.68%)	
Moderately impaired	322 (32.46%)	670 (67.54%)	
IADL, n (%)			< 0.0001
Self-reliant	149 (89.22%)	18 (10.78%)	
Very severely impaired	361 (36.72%)	622 (63.28%)	
Severely impaired	124 (31.23%)	273 (68.77%)	
Moderately impaired	97 (41.45%)	137 (58.55%)	
Mildly impaired	98 (59.04%)	68 (40.96%)	
Self-rated health status of the elderly, n (%)			< 0.0001
Very good	48 (67.61%)	23 (32.39%)	
Good	88 (55.70%)	70 (44.30%)	
Average	547 (42.11%)	752 (57.89%)	
Bad	131 (33.76%)	257 (66.24%)	
Vary bad	12 (50.00%)	12 (50.00%)	

* p value for differences between elderly who need a walking aid but have not used one and who need a walking aid and have used one.

Table 2. Analysis of factors influencing the unmet need for walking aids for the elderly in Shanghai in 2019 (n = 1,947)

Variables	Single factor <i>p</i> value	OR	95% CI lower limit	95% CI upper limit	Multifactor <i>p</i> values	OR	95% CI lower limit	95% CI upper limit
Sex, male								
Female	0.4773	1.068	0.891	1.281	0.5839	1.075	0.830	1.392
Age, 55-60								
60-69	0.9087	0.96	0.479	1.924	0.6177	0.763	0.264	2.204
70-79	0.14	0.599	0.303	1.183	0.2668	0.557	0.198	1.566
≥ 80	0.0042	0.382**	0.197	0.738	0.4811	0.696	0.253	1.91
Level of education, Primary school and below								
Junior high school	0.0891	1.206	0.972	1.497	0.337	0.861	0.634	1.169
Senior high school	< 0.0001	1.786***	1.374	2.323	0.8282	1.044	0.710	1.533
College and above	0.0179	1.478*	1.07	2.043	0.8054	0.941	0.582	1.522
Main source of income, Pension								
Help from relatives and friends	0.0128	0.568*	0.364	0.887	0.2887	0.760	0.458	1.262
Some other source	0.0399	2.368*	1.041	5.389	0.4037	1.696	0.491	5.858
Residence, Owner-occupied dwelling, private dwelling, etc.								
Rented dwelling	0.7212	1.066	0.750	1.515	0.4904	0.818	0.463	1.447
Old age home or a similar facility	< 0.0001	0.47***	0.367	0.603	0.7152	1.086	0.698	1.689
Nursing home or a similar facility	0.0003	0.62***	0.478	0.804	0.2617	1.305	0.820	2.079
Community health service centers	0.9095	0.981	0.704	1.366	0.0104	1.956*	1.171	3.267
Hospital or a similar facility	0.6024	0.895	0.590	1.358	0.1159	1.652	0.884	3.089
Language use, Mandarin								
Dialect	0.2793	0.887	0.713	1.102	0.4891	1.111	0.824	1.499
Mute	0.7386	1.238	0.353	4.34	0.9942	0.994	0.207	4.779
Living alone or cohabitating, Living alone								
Living with spouse	< 0.0001	2.103***	1.482	2.984	0.0002	2.901***	1.641	5.126
Living with children	0.7332	0.943	0.671	1.325	0.3295	1.309	0.762	2.249
Other	0.9435	0.988	0.716	1.365	0.0258	1.843*	1.076	3.154
Physical care needs of the assessed subjects, No need								
Care provided by the spouse	0.4789	0.764	0.363	1.61	0.0703	0.439	0.180	1.071
Care provided by children and grandchildren	0.0496	0.496*	0.246	0.999	0.2104	0.577	0.244	1.364
Care provided by a professional caregiver	0.1811	0.631	0.321	1.239	0.0944	0.497	0.219	1.128
Elevators in residential floors, Below the 6 th floor, without an elevator								
Below the 6th floor, with an elevator	0.0003	0.693***	0.569	0.845	0.3302	0.827	0.564	1.212
The 7th floor, without an elevator	0.902	0.933	0.310	2.805	0.6022	0.544	0.055	5.376
The 7th floor, with an elevator	0.0001	0.233***	0.112	0.487	0.0084	0.184	0.052	0.648
The 8th floor and above	0.8174	1.037	0.760	1.416	0.8183	1.059	0.649	1.730
Indoor steps, Yes								
No	0.2778	1.173	0.879	1.564	0.749	1.067	0.717	1.588
Indoor handrails, Yes								
No	0.0577	1.193	0.994	1.432	0.0481	0.718*	0.517	0.997
Number of diseases, 1								
0	0.2008	1.283	0.876	0.0427	0.0427	1.684*	1.017	2.788
2	0.2379	0.876	0.703	0.1154	0.1154	0.790	0.590	1.059
3 or more	< 0.0001	0.547***	0.429	0.0008	0.0008	0.577***	0.418	0.796
IADL, Self-reliant								
Very severely impaired	< 0.0001	0.07***	0.042	0.0003	0.0003	0.153***	0.055	0.426
Severely impaired	< 0.0001	0.055***	0.032	0.0002	0.0002	0.139***	0.050	0.386
Moderately impaired	< 0.0001	0.086***	0.049	0.0077	0.0077	0.247**	0.089	0.691
Mildly impaired	< 0.0001	0.174***	0.098	0.0369	0.0369	0.318*	0.108	0.933
Self-rated health status of the elderly, Very good								
Good	0.0911	0.602	0.335	0.3073	0.3073	0.637	0.268	1.515
Average	< 0.0001	0.349	0.209	0.345	0.345	0.703	0.339	1.461
Bad	< 0.0001	0.244	0.142	0.2193	0.2193	0.615	0.283	1.335
Very bad	0.1258	0.479	0.187	0.555	0.555	1.431	0.435	4.701

*indicates $p < 0.05$, **indicates $p < 0.01$, ***indicates $p < 0.001$.

dwellings. A previous study indicated that 78% of elderly adults receiving community-based home care in Beijing used assistive devices (15), and that figure is quite high. However, little attention has been paid to research on the need for and utilization of assistive devices among people who live in community health centers.

The current results indicated that the unmet need

for assistive walking devices was higher among people living only with their spouses than among those living alone, which is consistent with previous studies. The use of assistive walking devices was lowest among married people and highest among widowed ones. Being married was negatively associated with the use of aids, while living alone was positively associated with their use

(3,16-19). This is possibly because the spouse plays the role of caregiver.

Self-perceived needs of the elderly, the diversity and performance of assistive devices, and the accessibility and affordability of assistive walking devices may lead to unmet needs

There may be various reasons why assistive walking devices needs were unmet, such as lack of self-awareness of one's need on the part of the elderly and a lack of diversity and poor performance of assistive devices and poor accessibility and affordability on the part of manufacturers.

First, the low level of self-perceived need and the lack of confidence in the diversity and performance of assistive devices may lead to their underutilization. On the one hand, the elderly had insufficient self-awareness of their need for assistive devices. On the other hand, only 37.6% of the elderly agreed that "assistive devices are of significant help to the safety and health of the elderly" (13).

Therefore, the lack of diversity and poor performance of assistive devices may also lead to their underutilization. On the one hand, aids are not sufficiently diverse. Most of the domestic assistive devices for the elderly are imitations of foreign products, with considerable homogeneity, few varieties, low quality, limited brand recognition, and a small high-end market. On the other hand, the performance of assistive devices is not fully guaranteed. The quality and performance of domestic accessories for the elderly need to be improved, and the reliability of middle and low-end products should be fully guaranteed (20).

In addition, the accessibility of assistive devices needs to be further improved, since this a key reason for their underutilization. On the one hand, there are not enough personnel in the evaluation stage. At present, there is a shortage of qualified personnel to evaluate suitable aids for the elderly in China. On the other hand, there is excessive marketing and a domestic emphasis in the product supply stage, and a mature service delivery mechanism has not yet to be created (20,21).

Last but not least, the affordability of assistive devices needs to be further improved, since this is another key reason for their underutilization. At present, insurance does not cover assistive devices for the elderly in China, and they need to be paid for by individuals. Some elderly people with an unstable financial situation cannot afford expensive assistive devices (20).

In conclusion, the following efforts need to be made to improve the utilization of assistive devices for the elderly: the self-awareness of need must be heightened among the elderly, the elderly need to be informed and educated about assistive devices, the diversity and performance of assistive devices needs to be enhanced,

and the accessibility and affordability of those devices needs to be enhanced.

Acknowledgements

The authors would like to thank the Community Health Service Center of Jiangning Road, Jing 'an District, Shanghai, and the elderly care facilities and nursing homes in 16 districts of Shanghai for their contributions to this research.

Funding: This research was supported by the National Natural Science Foundation of China (no.72074152).

Conflict of Interest: The authors have no conflicts of interest to disclose.

References

1. National Bureau of Statistics. Data from the seventh National Census. <https://data.stats.gov.cn/easyquery.htm?cn=C01&zb=A0305&sj=2020> (accessed November 15, 2022). (in Chinese)
2. Wang CY, Li F, Wang LN, Zhou WT, Zhu BF, Zhang XX, Ding LL, He ZM, Song PP, Jin CL. The impact of population aging on medical expenses: A big data study based on the life table. *Biosci Trends*. 2018; 11:619-631.
3. Ishigami Y, Jutai J, Kirkland S. Assistive device use among community-dwelling older adults: A profile of Canadians using hearing, vision, and mobility devices in the Canadian longitudinal study on aging. *Can J Aging*. 2021; 40:23-38.
4. Development Research Center, State Council. Healthy aging: Driven by policy and industrial development. China Development Press, China, Beijing, 2019. (in Chinese)
5. Niu YH, Li N, Jin CL, Chen D, Yang YT, Ding HS. Activity outside the home, environmental barriers, and healthy aging for community-dwelling elderly individuals in China. *Biosci Trends*. 2017; 11:603-605.
6. West BA, Bhat G, Stevens J, Bergen G. Assistive device use and mobility-related factors among adults aged ≥ 65 years. *J Safety Res*. 2015; 55:147-150.
7. The Social Welfare Department. 108 Annual Assistive Services Aggregation Analysis Report. 2020. <https://newrepat.sfaa.gov.tw/home/download?conditions%5bcategory.id%5d=2c90e4c76705ab7f01671535b6e40d29> (accessed August 31, 2022). (in Chinese)
8. Peterson LJ, Meng H, Dobbs D, Hyer K. Gender differences in mobility device use among U.S. older adults. *J Gerontol B Psychol Sci Soc Sci*. 2017; 72:827-835.
9. Zhang X, Chen G. Use and needs of assistive devices in the background of aging: Current situation and research progress. *Zhongguo Kangfu Lilun Yu Shijian*. 2016; 22:1350-1353. (in Chinese)
10. Zhang WJ, Tan WJ. An analysis on using behavior of assistive devices of Chinese elderly. *Population & Development*. 2016; 22:100-112+70. (in Chinese)
11. Jiang MD, Dai FM, Xu JJ, Jia WW, Li D, Liu SY. Current status of mobility devices usage in the elderly and influencing factors. *J Nursing Science*. 2019; 34:23-27. (in

- Chinese)
12. Gao JM, Zheng XY. Use of hearing aids and assistive listening devices and its influencing factors among the elderly with disabling hearing loss in China. *Chin J Public Health*. 2021; 37:1261-1266. (in Chinese)
 13. Yu S, Luo D, Zhu Y, Yang L, Li H, Luo J, Gu K, Wu D, Zhao Q, Bai D, Xiao M. Factors influencing utilisation of assistive devices by the elderly in China: A community-based cross-sectional study. *Public Health*. 2022; 213:12-18.
 14. Zhu XC, Wan WJ, Li Y, Chen XH. Analysis of the current status and factors influencing the use of mobile assistive devices by disabled elderly in pension institutions in Shanghai. *Modern Nurse*. 2022; 29:104-107. (in Chinese)
 15. Lai Q, Ouyang Q, Tu QL, Long H, Zhang XL. Survey on assistive devices utilization for old adults supported by community-based homecare in Dongcheng, Beijing. *Chin J Rehabil Theory Pract*. 2019; 25:234-238. (in Chinese)
 16. Agree EM, Freedman VA, Sengupta M. Factors influencing the use of mobility technology in community-based long-term care. *J Aging Health*. 2004; 16:267-307.
 17. Agree EM, Freedman VA, Cornman JC, Wolf DA, Marcotte JE. Reconsidering substitution in long-term care: When does assistive technology take the place of personal care? *J Gerontol B Psychol Sci Soc Sci*. 2005; 60:S272-S280.
 18. Pressler KA, Ferraro KF. Assistive device use as a dynamic acquisition process in later life. *Gerontologist*. 2010; 50:371-381.
 19. Tomita MR, Mann WC, Fraas LF, Stanton KM. Predictors of the use of assistive devices that address physical impairments among community-based frail elders. *Journal of Applied Gerontology*. 2004; 23:141-155.
 20. Luo YM. An examination of the establishment of a national system of assistive aids for the elderly. *Standard Science*. 2018; 3:61-65. (in Chinese)
 21. Wei CJ, Li GF. Status of and suggestions for a welfare policy on assistive technology in China. *Social Welfare*. 2021; 05:3-6. (in Chinese)

Received December 9, 2022; Revised March 10, 2023; Accepted March 24, 2023.

§These authors contributed equally to this work.

*Address correspondence to:

Hansheng Ding, Shanghai Health Development Research Center (Shanghai Medical Information Center), No. 602 Jianguo (W) Road, Xuhui District, Shanghai 200031, China.
E-mail: dinghansheng@hotmail.com

Released online in J-STAGE as advance publication March 31, 2023.

Poor emotional status increases the risk of attempted suicide for the elderly age 55 and older in Shanghai, China: A longitudinal follow-up study

Lingshan Wan^{1,§}, Tingting Zhu^{1,§}, Jing Zhang^{2,§}, Wendi Cheng¹, Duo Chen¹, Hansheng Ding^{1,*}

¹ Shanghai Health Development Research Center (Shanghai Medical Information Center), Shanghai, China;

² Jiangning Road Community Health Service Center of Jing'an District, Shanghai, China.

SUMMARY We conducted a study to explore how one's emotional state affects attempted suicide among the elderly in Shanghai, China. Random sampling was used to select people age 55 and older in Shanghai from 2013 to 2019. A questionnaire was used to collect relevant data, including attempted suicide and emotional status. Subjects were a total of 783 elderly people who participated in this study for two years and more, and they consisted of 569 elderly people did not commit suicide during the study period and 214 elderly people who attempted suicide. Cumulative logistic regression indicated that feeling less interested than usual in hobbies ($p < 0.001$, OR = 2.805, 95% CI: 0.941-8.360) and being more easily angered ($p < 0.0001$, OR = 11.972, 95% CI: 6.275-22.843) increase the risk of attempted suicide.

Keywords attempt suicide, risk factors, people age 55 and older, Shanghai

To the Editor,

Suicide has become a growing global public health concern. According to a report published by World Health Organization (WHO) in 2019, 703,000 people die by suicide every year, which is one person every 40 seconds (1). A prior suicide attempt is the single most significant risk factor for suicide in the general population. Based on data updated in July, 2021 the crude suicide rate for people age 65 and older is 129.42 per 100,000 population, three times that of the population under 64 years of age (2). About 25-30% of individuals who attempt suicide will continue to do so, and 22-44% will eventually die of suicide (3). Moreover, a 37-year longitudinal study has indicated that the risk of death due to attempted suicide remains over one's lifetime (4). Therefore, the study of attempted suicide and factors influencing it is significant to suicide prevention.

The characteristics of attempted suicide can help to explain the high suicide rate and unique characteristics of suicide (5). Attempted suicide is the stage of further behaviors after an individual's suicidal ideation but before successfully committing suicide (6). Therefore, identifying the risk factors for attempted suicides and preventing them among the elderly is significant. Research has indicated that the average annual suicide rate for urban elderly has increased significantly in the 21st century (7). The current study was conducted in

Shanghai, a typical urban area in China where over 35% of the population is elderly (60 years and older) (8). This study sought to explore the impact of emotional status on suicidal behavior by the elderly in Shanghai, China.

Study design This study obtained survey data from the Shanghai Unified Needs Assessment for Elderly Care. This study was a long-term survey organized by the Shanghai Health Development Research Center from March 2013 to October 2019. The Ethics Committee of the Shanghai Medical and Technology Information Institute approved this study (no. 2022009). Potential subjects age 55 and older were eligible for inclusion in this study if they participated in the survey for two years and more. As a result, there were 783 elderly subjects. All investigators receive standardized training. Subjects were then interviewed face to face after giving written informed consent.

The primary outcome measures in this study were subjects' suicidal behavior and emotional condition. *i)* The question to examine suicidal behavior was "How many times have you tried to commit suicide in the past 14 days?". Answers were collected in the form of "none", "once", "two or three times", "four to seven times", and "eight times or more". *ii)* Three questions were included in the section on emotional condition. The first question was "What do you think of your physical health over the last week?", and the options were: "excellent", "good",

Table 1. Risk factors associated with attempted suicide among elderly adults

Variables	Estimate	Standard Error	Wald Chi-square	Pr> ChiSq	OR	95% Wald Confidence Limits
Self-reported health status					1.000	
Same						
Worse	2.404	0.413	33.970	< 0.0001	13.756	3.964-47.738
Level of interest in hobbies						
Same						
Lower	1.310	0.351	13.927	0.000	2.805	0.941-8.360
More easily angered					1.000	
Same						
Worse	1.122	0.237	22.342	< 0.0001	11.972	6.275-22.843

"fair", "poor", and "very poor". The five possible answers to the question "How often do you spend engaged in your usual hobbies?" were "no or little time", "about once a month", "about once a week", "about once a day", and "multiple times a day". Similarly, the five possible answers to the question "Are you more easily angered than usual?" were "no or little time", "about once a month", "about once a week", "about once a day", and "multiple times a day".

Characteristics of study subjects A total of 783 subjects were divided into two groups depending on whether they had attempted suicide. The elderly who had not attempted suicide were designated the group who had not attempted suicide, and those who reported having attempted suicide one or more times were designated the group who had attempted suicide. Five hundred and sixty-nine subjects had not attempted suicide, but 214 subjects had attempted suicide during the study.

As mentioned, 214 subjects had not previously attempted suicide but attempted suicide during the study. Of these, 58 (27.10%) reported that their health had deteriorated, 63 (29.44%) reported that their health remained the same, and 93 (43.46%) reported that their health improved. Of the 214 subjects, 57 (26.64%) mentioned being less interested in their previous hobbies, 66 (30.84%) mentioned remaining interested in their previous hobbies, and 91 (42.52%) mentioned being more interested in their previous hobbies. Of the 214 subjects, 126 (58.88%) were more easily angered than usual, 47 (21.96%) remained the same, and 41 (19.16%) were less easily angered than usual.

Feeling less interested in previous hobbies was a risk factor associated with attempted suicide in the elderly Results of cumulative logistic regression analysis suggested that feeling less interested in previous hobbies ($p < 0.001$, OR = 2.805, 95% CI: 0.941-8.360) increased the risk of attempted suicide, indicating that elderly who have lost interest in hobbies are 2.805 times likelier to attempt suicide than elderly who remained interested. Results are shown in Table 1. A previous study noted a relationship between low positive affect and suicidal ideation (9) in the form of anhedonia. Anhedonia is one of the core symptoms of depression and represents a reduction in positive emotions such

as joy, enthusiasm, self-confidence, and interest. The previous study found that anhedonia is potentially associated with suicidal ideation, and this is similar to the current findings.

Being more easily angered was another risk factor that increases suicide attempts in the elderly Results of cumulative logistic regression analysis indicated that being more easily angered ($p < 0.0001$, OR = 11.972, 95% CI: 6.275-22.843,) also increased the risk of attempted suicide. The risk of attempted suicide among elderly who were more easily angered was 11.972 times higher than that in elderly with stable emotions. Results are shown in Table 1. Emerging research has indicated that higher levels of anger increase the risk of suicide (10).

The current study directly compares the situation of the same elderly before and after a suicide attempt. This can fully reflect changes in the specific situation of the elderly over time; therefore, the results are more accurate and persuasive. A limitation of this study is that it sought to explore factors influencing suicide attempts but it is based on responses to only two questions. More scientific and authoritative scales should be used for future studies.

In conclusion, the current results reveal ways to reduce attempted suicide by the elderly. Feeling less interested in previous hobbies and being more easily angered are risk factors for attempted suicide in the elderly. The emotional state of the elderly can be adjusted through specific interventions. Therefore, family members and society need to pay attention to the emotional status of the elderly, promptly detect emotional deterioration, and promptly intervene in order to effectively prevent suicide.

Funding: This work was supported by a grant from the National Natural Science Foundation of China (General Program, Study on the Development of Automatic Generation Model of Personalized Long-term Care Plan Based on Care Needs Grade and Performance Evaluation and Popularization, no. 72074152).

Conflict of Interest: The authors have no conflicts of interest to disclose.

References

1. World Health Organization (WHO). Suicide worldwide in 2019: Global health estimates. <https://www.who.int/publications/i/item/9789240026643> (accessed October 16, 2022).
2. World Health Organization (WHO). Suicide rates: Suicide rates, crude, 10-year age groups. <https://www.who.int/data/gho/data/themes/mental-health/suicide-rates> (accessed October 16, 2022).
3. Wu CZ, Rong S, Duan WT, Wang WX, Yu LX. Effect of negative life events on suicide attempt: the mediating roles of basic psychological needs and psychache. *Chin J Clin Psych.* 2020; 28:503-507. (in Chinese)
4. Suominen K, Isometsä E, Haukka J, Lönnqvist J. Substance use and male gender as risk factors for deaths and suicide--A 5-year follow-up study after deliberate self-harm. *Soc Psychiatry Psychiatr Epidemiol.* 2004; 39:720-724.
5. Fei LP. The present situation and future work direction of suicide in China. *Chin J Epidem.* 2004; 25:277-279. (in Chinese)
6. Luo M, Li J, He Y. Research on suicide ideation of elderly people. *Sci Res Aging.* 2015; 3:41-57. (in Chinese)
7. Jing J, Zhang J, Wu XY. Suicide among the elderly people in urban China. *Pop Res.* 2011; 35:84-96. (in Chinese)
8. Shanghai Municipal People's Government. Shanghai Statistical Yearbook 2021. <https://tjj.sh.gov.cn/tjnj/20220309/0e01088a76754b448de6d608c42dad0f.html> (accessed October 20, 2022). (in Chinese)
9. Bennardi M, Caballero FF, Miret M, Ayuso-Mateos JL, Haro JM, Lara E, Arensman E, Cabello M. Longitudinal relationships between positive affect, loneliness, and suicide ideation: Age-specific factors in a general population. *Suicide Life Threat Behav.* 2019; 49:90-103.
10. Wilks CR, Morland LA, Dillon KH, Mackintosh MA, Blakey SM, Wagner HR; VA Mid-Atlantic MIRECC Workgroup; Elbogen EB. Anger, social support, and suicide risk in U.S. military veterans. *J Psychiatr Res.* 2019; 109:139-144.

Received November 23, 2022; Revised March 10, 2023; Accepted March 24, 2023.

§These authors contributed equally to this work.

*Address correspondence to:

Hansheng Ding, Shanghai Health Development Research Center (Shanghai Medical Information Center), Shanghai No. 602, Jian Guo Road (West), Xuhui District, Shanghai, China 200031.

E-mail: dinghansheng@hotmail.com

Released online in J-STAGE as advance publication March 31, 2023.



Guide for Authors

1. Scope of Articles

BioScience Trends (Print ISSN 1881-7815, Online ISSN 1881-7823) is an international peer-reviewed journal. *BioScience Trends* devotes to publishing the latest and most exciting advances in scientific research. Articles cover fields of life science such as biochemistry, molecular biology, clinical research, public health, medical care system, and social science in order to encourage cooperation and exchange among scientists and clinical researchers.

2. Submission Types

Original Articles should be well-documented, novel, and significant to the field as a whole. An Original Article should be arranged into the following sections: Title page, Abstract, Introduction, Materials and Methods, Results, Discussion, Acknowledgments, and References. Original articles should not exceed 5,000 words in length (excluding references) and should be limited to a maximum of 50 references. Articles may contain a maximum of 10 figures and/or tables. Supplementary Data are permitted but should be limited to information that is not essential to the general understanding of the research presented in the main text, such as unaltered blots and source data as well as other file types.

Brief Reports definitively documenting either experimental results or informative clinical observations will be considered for publication in this category. Brief Reports are not intended for publication of incomplete or preliminary findings. Brief Reports should not exceed 3,000 words in length (excluding references) and should be limited to a maximum of 4 figures and/or tables and 30 references. A Brief Report contains the same sections as an Original Article, but the Results and Discussion sections should be combined.

Reviews should present a full and up-to-date account of recent developments within an area of research. Normally, reviews should not exceed 8,000 words in length (excluding references) and should be limited to a maximum of 10 figures and/or tables and 100 references. Mini reviews are also accepted, which should not exceed 4,000 words in length (excluding references) and should be limited to a maximum of 5 figures and/or tables and 50 references.

Policy Forum articles discuss research and policy issues in areas related to life science such as public health, the medical care system, and social science and may address governmental issues at district, national, and international levels of discourse. Policy Forum articles should not exceed 3,000 words in length (excluding references) and should be limited to a maximum of 5 figures and/or tables and 30 references.

Communications are short, timely pieces that spotlight new research findings or policy issues of interest to the field of global health and medical practice that are of immediate importance. Depending on their content, Communications will be published as "Comments" or "Correspondence". Communications should not exceed 1,500 words in length (excluding references) and should be limited to a maximum of 2 figures and/or tables and 20 references.

Editorials are short, invited opinion pieces that discuss an issue of immediate importance to the fields of global health, medical practice, and basic science oriented for clinical application. Editorials should not exceed 1,000 words in length (excluding references) and should be limited to a maximum of 10 references. Editorials may contain one figure or table.

News articles should report the latest events in health sciences and medical research from around the world. News should not exceed 500 words in length.

Letters should present considered opinions in response to articles published in *BioScience Trends* in the last 6 months or issues of general interest. Letters should not exceed 800 words in length and may contain a maximum of 10 references. Letters may contain one figure or table.

3. Editorial Policies

For publishing and ethical standards, *BioScience Trends* follows the Recommendations for the Conduct, Reporting, Editing, and Publication of Scholarly Work in Medical Journals issued by the International Committee of Medical Journal Editors (ICMJE, <https://icmje.org/recommendations>), and the Principles of Transparency and Best Practice in Scholarly Publishing jointly issued by the Committee on Publication Ethics (COPE, <https://publicationethics.org/resources/guidelines-new/principles-transparency-and-best-practice-scholarly-publishing>), the Directory of Open Access Journals (DOAJ, <https://doaj.org/apply/transparency>), the Open Access Scholarly Publishers Association (OASPA, <https://oaspa.org/principles-of-transparency-and-best-practice-in-scholarly-publishing-4>), and the World Association of Medical Editors (WAME, <https://wame.org/principles-of-transparency-and-best-practice-in-scholarly-publishing>).

BioScience Trends will perform an especially prompt review to encourage innovative work. All original research will be subjected to a rigorous standard of peer review and will be edited by experienced copy editors to the highest standards.

Ethical Approval of Studies and Informed Consent: For all manuscripts reporting data from studies involving human participants or animals, formal review and approval, or formal review and waiver, by an appropriate institutional review board or ethics committee is required and should be described in the Methods section. When your manuscript contains any case details, personal information and/or images of patients or other individuals, authors must obtain appropriate written consent, permission and release in order to comply with all applicable laws and regulations concerning privacy and/or security of personal information. The consent form needs to comply with the relevant legal requirements of your particular jurisdiction, and please do not send signed consent form to *BioScience Trends* to respect your patient's and any other individual's privacy. Please instead describe the information clearly in the Methods (patient consent) section of your manuscript while retaining copies of the signed forms in the event they should be needed. Authors should also state that the study conformed to the provisions of the Declaration of Helsinki (as revised in 2013, <https://wma.net/what-we-do/medical-ethics/declaration-of-helsinki>). When reporting experiments on animals, authors should indicate whether the institutional and national guide for the care and use of laboratory animals was followed.

Reporting Clinical Trials: The ICMJE (<https://icmje.org/recommendations/browse/publishing-and-editorial-issues/clinical-trial-registration.html>) defines a clinical trial as any research project that prospectively assigns people or a group of people to an intervention, with or without concurrent comparison or control groups, to study the relationship between a health-related intervention and a health outcome. Registration of clinical trials in a public trial registry at or before the time of first patient enrollment is a condition of consideration for publication in *BioScience Trends*, and the trial registration number will be published at the end of the Abstract. The registry must be independent of for-profit interest and publicly accessible. Reports of trials must conform to CONSORT 2010 guidelines (<https://consort-statement.org/consort-2010>). Articles reporting the results of randomized trials must include the CONSORT flow diagram showing the progress of patients throughout the trial.

Conflict of Interest: All authors are required to disclose any actual or potential conflict of interest including financial interests or relationships with other people or organizations that might raise questions of bias

in the work reported. If no conflict of interest exists for each author, please state "There is no conflict of interest to disclose".

Submission Declaration: When a manuscript is considered for submission to *BioScience Trends*, the authors should confirm that 1) no part of this manuscript is currently under consideration for publication elsewhere; 2) this manuscript does not contain the same information in whole or in part as manuscripts that have been published, accepted, or are under review elsewhere, except in the form of an abstract, a letter to the editor, or part of a published lecture or academic thesis; 3) authorization for publication has been obtained from the authors' employer or institution; and 4) all contributing authors have agreed to submit this manuscript.

Initial Editorial Check: Immediately after submission, the journal's managing editor will perform an initial check of the manuscript. A suitable academic editor will be notified of the submission and invited to check the manuscript and recommend reviewers. Academic editors will check for plagiarism and duplicate publication at this stage. The journal has a formal recusal process in place to help manage potential conflicts of interest of editors. In the event that an editor has a conflict of interest with a submitted manuscript or with the authors, the manuscript, review, and editorial decisions are managed by another designated editor without a conflict of interest related to the manuscript.

Peer Review: *BioScience Trends* operates a single-anonymized review process, which means that reviewers know the names of the authors, but the authors do not know who reviewed their manuscript. All articles are evaluated objectively based on academic content. External peer review of research articles is performed by at least two reviewers, and sometimes the opinions of more reviewers are sought. Peer reviewers are selected based on their expertise and ability to provide quality, constructive, and fair reviews. For research manuscripts, the editors may, in addition, seek the opinion of a statistical reviewer. Every reviewer is expected to evaluate the manuscript in a timely, transparent, and ethical manner, following the COPE guidelines (https://publicationethics.org/files/cope-ethical-guidelines-peer-reviewers-v2_0.pdf). We ask authors for sufficient revisions (with a second round of peer review, when necessary) before a final decision is made. Consideration for publication is based on the article's originality, novelty, and scientific soundness, and the appropriateness of its analysis.

Suggested Reviewers: A list of up to 3 reviewers who are qualified to assess the scientific merit of the study is welcomed. Reviewer information including names, affiliations, addresses, and e-mail should be provided at the same time the manuscript is submitted online. Please do not suggest reviewers with known conflicts of interest, including participants or anyone with a stake in the proposed research; anyone from the same institution; former students, advisors, or research collaborators (within the last three years); or close personal contacts. Please note that the Editor-in-Chief may accept one or more of the proposed reviewers or may request a review by other qualified persons.

Language Editing: Manuscripts prepared by authors whose native language is not English should have their work proofread by a native English speaker before submission. If not, this might delay the publication of your manuscript in *BioScience Trends*.

The Editing Support Organization can provide English proofreading, Japanese-English translation, and Chinese-English translation services to authors who want to publish in *BioScience Trends* and need assistance before submitting a manuscript. Authors can visit this organization directly at <https://www.iacmhr.com/iac-eso/support.php?lang=en>. IAC-ESO was established to facilitate manuscript preparation by researchers whose native language is not English and to help edit works intended for international academic journals.

Copyright and Reuse: Before a manuscript is accepted for publication in *BioScience Trends*, authors will be asked to sign a transfer of copyright agreement, which recognizes the common

interest that both the journal and author(s) have in the protection of copyright. We accept that some authors (e.g., government employees in some countries) are unable to transfer copyright. A JOURNAL PUBLISHING AGREEMENT (JPA) form will be e-mailed to the authors by the Editorial Office and must be returned by the authors by mail, fax, or as a scan. Only forms with a hand-written signature from the corresponding author are accepted. This copyright will ensure the widest possible dissemination of information. Please note that the manuscript will not proceed to the next step in publication until the JPA Form is received. In addition, if excerpts from other copyrighted works are included, the author(s) must obtain written permission from the copyright owners and credit the source(s) in the article.

4. Cover Letter

The manuscript must be accompanied by a cover letter prepared by the corresponding author on behalf of all authors. The letter should indicate the basic findings of the work and their significance. The letter should also include a statement affirming that all authors concur with the submission and that the material submitted for publication has not been published previously or is not under consideration for publication elsewhere. The cover letter should be submitted in PDF format. For an example of Cover Letter, please visit: <https://www.biosciencetrends.com/downcentre> (Download Centre).

5. Submission Checklist

The Submission Checklist should be submitted when submitting a manuscript through the Online Submission System. Please visit Download Centre (<https://www.biosciencetrends.com/downcentre>) and download the Submission Checklist file. We recommend that authors use this checklist when preparing your manuscript to check that all the necessary information is included in your article (if applicable), especially with regard to Ethics Statements.

6. Manuscript Preparation

Manuscripts are suggested to be prepared in accordance with the "Recommendations for the Conduct, Reporting, Editing, and Publication of Scholarly Work in Medical Journals", as presented at <https://www.ICMJE.org>.

Manuscripts should be written in clear, grammatically correct English and submitted as a Microsoft Word file in a single-column format. Manuscripts must be paginated and typed in 12-point Times New Roman font with 24-point line spacing. Please do not embed figures in the text. Abbreviations should be used as little as possible and should be explained at first mention unless the term is a well-known abbreviation (e.g. DNA). Single words should not be abbreviated.

Title page: The title page must include 1) the title of the paper (Please note the title should be short, informative, and contain the major key words); 2) full name(s) and affiliation(s) of the author(s), 3) abbreviated names of the author(s), 4) full name, mailing address, telephone/fax numbers, and e-mail address of the corresponding author; 5) author contribution statements to specify the individual contributions of all authors to this manuscript, and 6) conflicts of interest (if you have an actual or potential conflict of interest to disclose, it must be included as a footnote on the title page of the manuscript; if no conflict of interest exists for each author, please state "There is no conflict of interest to disclose").

Abstract: The abstract should briefly state the purpose of the study, methods, main findings, and conclusions. For articles that are Original Articles, Brief Reports, Reviews, or Policy Forum articles, a one-paragraph abstract consisting of no more than 250 words must be included in the manuscript. For Communications, Editorials, News, or Letters, a brief summary of main content in 150 words or fewer should be included in the manuscript. For articles reporting clinical trials, the trial registration number should be stated at the end of the Abstract. Abbreviations must be kept to a minimum and non-standard

abbreviations explained in brackets at first mention. References should be avoided in the abstract. Three to six key words or phrases that do not occur in the title should be included in the Abstract page.

Introduction: The introduction should provide sufficient background information to make the article intelligible to readers in other disciplines and sufficient context clarifying the significance of the experimental findings

Materials/Patients and Methods: The description should be brief but with sufficient detail to enable others to reproduce the experiments. Procedures that have been published previously should not be described in detail but appropriate references should simply be cited. Only new and significant modifications of previously published procedures require complete description. Names of products and manufacturers with their locations (city and state/country) should be given and sources of animals and cell lines should always be indicated. All clinical investigations must have been conducted in accordance Materials/Patients and Methods.

Results: The description of the experimental results should be succinct but in sufficient detail to allow the experiments to be analyzed and interpreted by an independent reader. If necessary, subheadings may be used for an orderly presentation. All Figures and Tables should be referred to in the text in order, including those in the Supplementary Data.

Discussion: The data should be interpreted concisely without repeating material already presented in the Results section. Speculation is permissible, but it must be well-founded, and discussion of the wider implications of the findings is encouraged. Conclusions derived from the study should be included in this section.

Acknowledgments: All funding sources (including grant identification) should be credited in the Acknowledgments section. Authors should also describe the role of the study sponsor(s), if any, in study design; in the collection, analysis, and interpretation of data; in the writing of the report; and in the decision to submit the paper for publication. If the funding source had no such involvement, the authors should so state.

In addition, people who contributed to the work but who do not meet the criteria for authors should be listed along with their contributions.

References: References should be numbered in the order in which they appear in the text. Citing of unpublished results, personal communications, conference abstracts, and theses in the reference list is not recommended but these sources may be mentioned in the text. In the reference list, cite the names of all authors when there are fifteen or fewer authors; if there are sixteen or more authors, list the first three followed by *et al.* Names of journals should be abbreviated in the style used in PubMed. Authors are responsible for the accuracy of the references. The EndNote Style of *BioScience Trends* could be downloaded at **EndNote** (https://ircabssagroup.com/examples/BioScience_Trends.ens).

Examples are given below:

Example 1 (Sample journal reference):

Inagaki Y, Tang W, Zhang L, Du GH, Xu WF, Kokudo N. Novel aminopeptidase N (APN/CD13) inhibitor 24F can suppress invasion of hepatocellular carcinoma cells as well as angiogenesis. *Biosci Trends*. 2010; 4:56-60.

Example 2 (Sample journal reference with more than 15 authors):

Darby S, Hill D, Auvinen A, *et al.* Radon in homes and risk of lung cancer: Collaborative analysis of individual data from 13 European case-control studies. *BMJ*. 2005; 330:223.

Example 3 (Sample book reference):

Shalev AY. Post-traumatic stress disorder: Diagnosis, history and life course. In: *Post-traumatic Stress Disorder, Diagnosis, Management and Treatment* (Nutt DJ, Davidson JR, Zohar J, eds.). Martin Dunitz, London, UK, 2000; pp. 1-15.

Example 4 (Sample web page reference):

World Health Organization. The World Health Report 2008 – primary health care: Now more than ever. http://www.who.int/whr/2008/whr08_en.pdf (accessed September 23, 2022).

Tables: All tables should be prepared in Microsoft Word or Excel and should be arranged at the end of the manuscript after the References section. Please note that tables should not in image format. All tables should have a concise title and should be numbered consecutively with Arabic numerals. If necessary, additional information should be given below the table.

Figure Legend: The figure legend should be typed on a separate page of the main manuscript and should include a short title and explanation. The legend should be concise but comprehensive and should be understood without referring to the text. Symbols used in figures must be explained. Any individually labeled figure parts or panels (A, B, *etc.*) should be specifically described by part name within the legend.

Figure Preparation: All figures should be clear and cited in numerical order in the text. Figures must fit a one- or two-column format on the journal page: 8.3 cm (3.3 in.) wide for a single column, 17.3 cm (6.8 in.) wide for a double column; maximum height: 24.0 cm (9.5 in.). Please make sure that the symbols and numbers appeared in the figures should be clear. Please make sure that artwork files are in an acceptable format (TIFF or JPEG) at minimum resolution (600 dpi for illustrations, graphs, and annotated artwork, and 300 dpi for micrographs and photographs). Please provide all figures as separate files. Please note that low-resolution images are one of the leading causes of article resubmission and schedule delays.

Units and Symbols: Units and symbols conforming to the International System of Units (SI) should be used for physicochemical quantities. Solidus notation (*e.g.* mg/kg, mg/mL, mol/mm²/min) should be used. Please refer to the SI Guide www.bipm.org/en/si/ for standard units.

Supplemental data: Supplemental data might be useful for supporting and enhancing your scientific research and *BioScience Trends* accepts the submission of these materials which will be only published online alongside the electronic version of your article. Supplemental files (figures, tables, and other text materials) should be prepared according to the above guidelines, numbered in Arabic numerals (*e.g.*, Figure S1, Figure S2, and Table S1, Table S2) and referred to in the text. All figures and tables should have titles and legends. All figure legends, tables and supplemental text materials should be placed at the end of the paper. Please note all of these supplemental data should be provided at the time of initial submission and note that the editors reserve the right to limit the size and length of Supplemental Data.

5. Submission Checklist

The Submission Checklist will be useful during the final checking of a manuscript prior to sending it to *BioScience Trends* for review. Please visit Download Centre and download the Submission Checklist file.

6. Online Submission

Manuscripts should be submitted to *BioScience Trends* online at <https://www.biosciencetrends.com/login>. Receipt of your manuscripts submitted online will be acknowledged by an e-mail from Editorial Office containing a reference number, which should be used in all future communications. If for any reason you are unable to submit a file online, please contact the Editorial Office by e-mail at office@biosciencetrends.com

8. Accepted Manuscripts

Page Charge: Page charges will be levied on all manuscripts accepted for publication in *BioScience Trends* (Original Articles / Brief Reports / Reviews / Policy Forum / Communications: \$140 per page for black white pages, \$340 per page for color pages; News / Letters: a total cost of \$600). Under exceptional circumstances, the author(s) may apply to the editorial office for a waiver of the publication charges by stating the reason in the Cover Letter when the manuscript online.

Misconduct: *BioScience Trends* takes seriously all allegations of potential misconduct and adhere to the ICMJE Guideline (<https://icmje.org/recommendations>) and COPE Guideline (https://publicationethics.org/files/Code_of_conduct_for_journal_editors.pdf). In cases of

suspected research or publication misconduct, it may be necessary for the Editor or Publisher to contact and share submission details with third parties including authors' institutions and ethics committees. The corrections, retractions, or editorial expressions of concern will be performed in line with above guidelines.

(As of December 2022)

BioScience Trends
Editorial and Head Office
Pearl City Koishikawa 603,
2-4-5 Kasuga, Bunkyo-ku,
Tokyo 112-0003, Japan.
E-mail: office@biosciencetrends.com

